BEHAVIOR OF WEB-TAPERED BUILT-UP I-SHAPED BEAMS

by

Bryan Scott Miller

B.S. in Civil Engineering, University of Pittsburgh, 2002

Submitted to the Graduate Faculty of

School of Engineering in partial fulfillment

of the requirements for the degree of

Master of Science in Civil Engineering

University of Pittsburgh

2003

UNIVERSITY OF PITTSBURGH

SCHOOL OF ENGINEERING

This thesis was presented

by

Bryan S. Miller

It was defended on

December 2, 2003

and approved by

Dr. Jeen-Shang Lin, Associate Professor, Department of
Civil and Environmental Engineering

Dr. Morteza A.M. Torkamani, Associate Professor, Department of
Civil and Environmental Engineering

Thesis Advisor: Dr. Christopher J. Earls, Associate Professor, Department of
Civil and Environmental Engineering

ABSTRACT

BEHAVIOR OF WEB-TAPERED BUILT-UP I-SHAPED BEAMS

Bryan S. Miller, M.S.

University of Pittsburgh, 2003

Appendix F of the AISC-LRFD Specification governs the design of web-tapered I-shaped beams. These design provisions are restricted to beams with equal flange areas and non-slender webs. However, the current practice in the low-rise metal building industry is to employ flanges of unequal area and slender webs; a time honored practice that has resulted in safe and economical structures. The current study utilizes validated nonlinear finite element analysis techniques to predict the flexural response and corresponding limit states associated with mild-carbon steel doubly-symmetric web-tapered I-shaped beams. A parametric study is performed to study the moment capacity and flexural ductility in the inelastic range of various beam geometries with length-to-depth ratios between two and three (i.e. what one normally encounters in the rafter sections of a low-rise metal building gable frame). Compactness criteria that ensure attainment of a rotation capacity equal to three are examined and results tabulated. A comparison is made between the Specification design provisions and the ultimate moment capacity and structural ductility predicted by the finite element method. Conclusions are made regarding the effects of plate slenderness on the behavior of the nonprismatic beam models. Recommendations are made for further research of singly-symmetric web-tapered beams.

TABLE OF CONTENTS

LIST OF TABLES

LIST OF FIGURES

ACKNOWLEDGEMENTS

I would like to thank my advisor, Dr. Christopher Earls, for everything he has done for me throughout my undergraduate and graduate studies. Also, I would like to thank my committee, Dr. Jeen-Shang Lin and Dr. Morteza Torkamani. It has been a pleasure working as a teaching assistant for both of them.

I would like to thank my parents, Charles and Pamela Miller, for all the support they have given me. Their encouragement and support means more to me than they could imagine.

I would like to thank my girlfriend Jessica Lyons for being so understanding and supportive throughout these past few years.

1.0 INTRODUCTION

Built-up web-tapered I-shaped beams are normally produced by welding flat plate stock together in a fashion very similar to what is done in the case of prismatic plate girders. While it is that prismatic plate girders are typically used in bridge construction, web-tapered built-up members are generally used in low-rise metal buildings. Through judicious specification of web tapering, the metal building industry has been able to strike a balance between fabrication expense and material cost so as to achieve very economical structural geometries for primary framing members. In low-rise metal buildings, both the columns and rafters are generally tapered to place the structural material where it is most needed. The column-to-rafter connections are typically designed as fully restrained moment end-plate connections using available design procedures (Sumner 1995).

The design of web-tapered I-shaped beams is governed by Appendix F of the American Institute of Steel Construction (AISC) Load and Resistance Factor Design (LRFD) Specification (Hereafter referred to as the "Specification"). However, Appendix F of the Specification restricts the designer to web-tapered beams having flanges of equal area and a web that is not slender (i.e. $\lambda_{web} < \lambda_r$). Interestingly, the current practice in the low-rise metal building industry is to employ flanges of unequal area and slender webs; a time honored practice that has resulted in safe and economical structures. To even be able to employ the current Specification provisions to tapered beams, the web slenderness ratio (h/t_w) from Table B5.1 in the

Specification must not exceed λ_r, calculated by the following equation for webs in flexural compression:

$$\lambda_r = 5.70\sqrt{E/F_y} \tag{1-1}$$

Since the webs of beams used in practice frequently possess a slenderness ratio greater than λ_r, the beams are considered as plate girders in the Specification. However, plate girder design in Appendix G of the Specification is limited to prismatic members and does not provide guidance for designs involving web-tapered geometries. Therefore, the Specification does not provide design equations for web-tapered I-shaped beam geometries of proportions that are consistent with what has been the industry standard for metal buildings for quite many years.

In the current study, behavior of mild-carbon steel web-tapered beam response, in the inelastic range, is studied using validated nonlinear finite element analysis methods. The nonlinear finite element modeling techniques employed herein are validated by: identifying relevant web-tapered member experimental programs from the literature that involved bending; constructing nonlinear finite element analogs of these tests; and then comparing results from both to ascertain to what degree the observed member responses agree. After the verification phase of the work is complete, a benchmark gable frame having web-tapered members typical of currently designed frames is analyzed to failure using the validated nonlinear finite element modeling techniques. The critical section within the gable frame model is then identified and subsequently modeled as a subassembly isolated from the rest of the benchmark frame. The subassembly model employs techniques that simulate the effects of the adjacent frame assemblies not explicitly considered. After obtaining similar results to those obtained in the critical section in the complete frame, the sub-assemblage beam is then used as the basis for a parametric study of web-tapered I-shaped beams. Such an approach is quite useful in reducing the computational expense associated with the modeling of the entire benchmark frame for the purposes of a parametric study possessing a similar scope. Observations and discussions related to prediction of ultimate moment capacity and structural ductility are given. Figure 1 is an illustration of a web-tapered I-shaped beam with nomenclature used throughout this study.

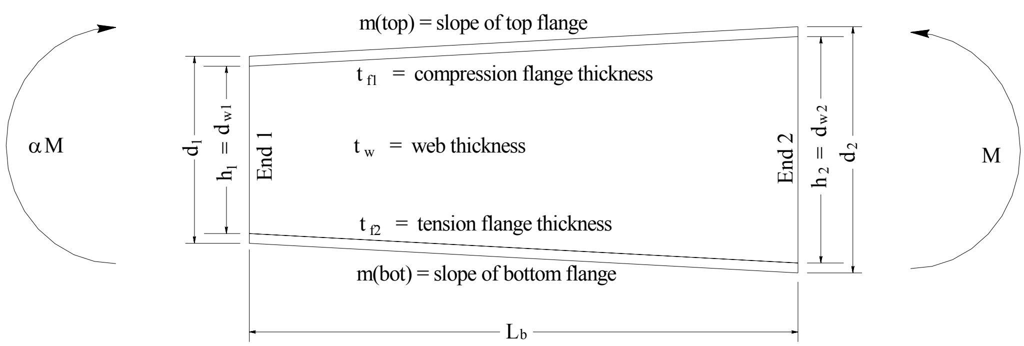

Figure 1 Web-tapered I-shaped Beam

1.1 GENERAL BEAM BEHAVIOR

The general behavior of a singly or doubly symmetric beam bent about the strong axis is illustrated in Figure 2. General beam behavior is classified as under one of three response categories: plastic, inelastic, and elastic. In the plastic range, the beam has the capability of reaching the plastic moment, M_p, and maintaining its strength through a rotation capacity, sufficient to ensure that moment redistribution may take place in indeterminate structures. In the inelastic range, a portion of the entire cross-section will yield with a small amount of inelastic deformation. In this range, the plastic moment, M_p, may or may not be reached before unloading. The unloading is due to instabilities occurring in the form of local or global buckling. In the elastic range, a beam will buckle while still fully elastic.

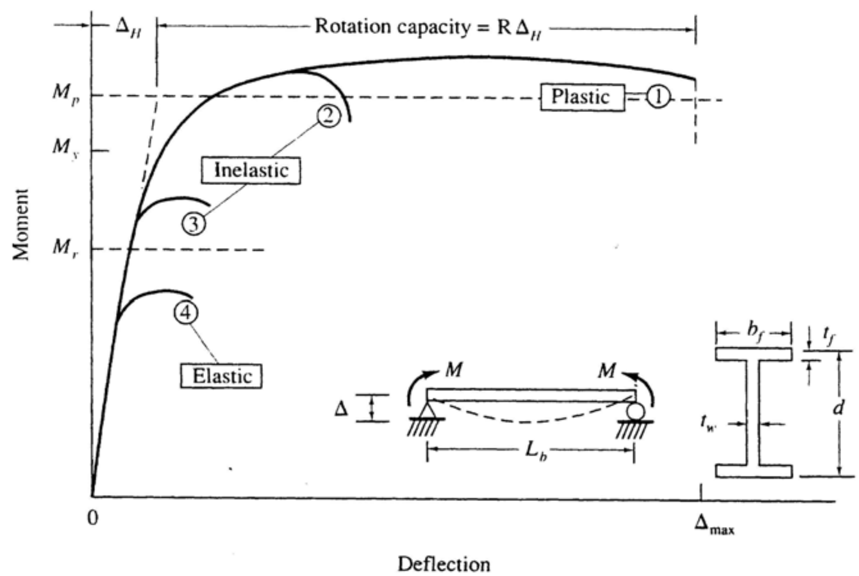

Figure 2 General Behavior of a Beam (Yura, Galambos, and Ravindra 1978)

Local and global buckling phenomenon in the flexural response of I-shaped beams and girders is rather complex. Three types of buckling may occur during pure flexure: lateral-torsional buckling, local buckling, and distortional buckling. Lateral-torsional buckling is the deflection and twisting of a beam simultaneously without distortion of the cross-section. This usually is the buckling mode for beams with larger length-to-depth ratios. Local buckling is the distortion of plates, either flange or web plates, without lateral deflection or twisting. Local buckling is generally limited to a small portion of a beam in flexure (i.e. a short wavelength mode). Distortional buckling possesses features of each of the previously mentioned modes. It is a medium wavelength mode displaying cross-sectional distortion of larger cross-sectional regions as compared with the local buckling case.

Structural ductility, or deformation capacity, may be measured by the rotation capacity of a beam. Rotation capacity is defined by ASCE (ASCE 1971) as Equation (1-2), where θ_u is the rotation when the moment capacity drops below M_p on the unloading portion of the M-θ plot and θ_p is the theoretical rotation at which the full plastic capacity is achieved based on elastic beam stiffness. This definition of rotation capacity is depicted graphically in Figure 3 where θ_1 and θ_2 correspond to θ_p and θ_u, respectively.

$$R = \frac{\theta_u}{\theta_p} - 1 \tag{1-2}$$

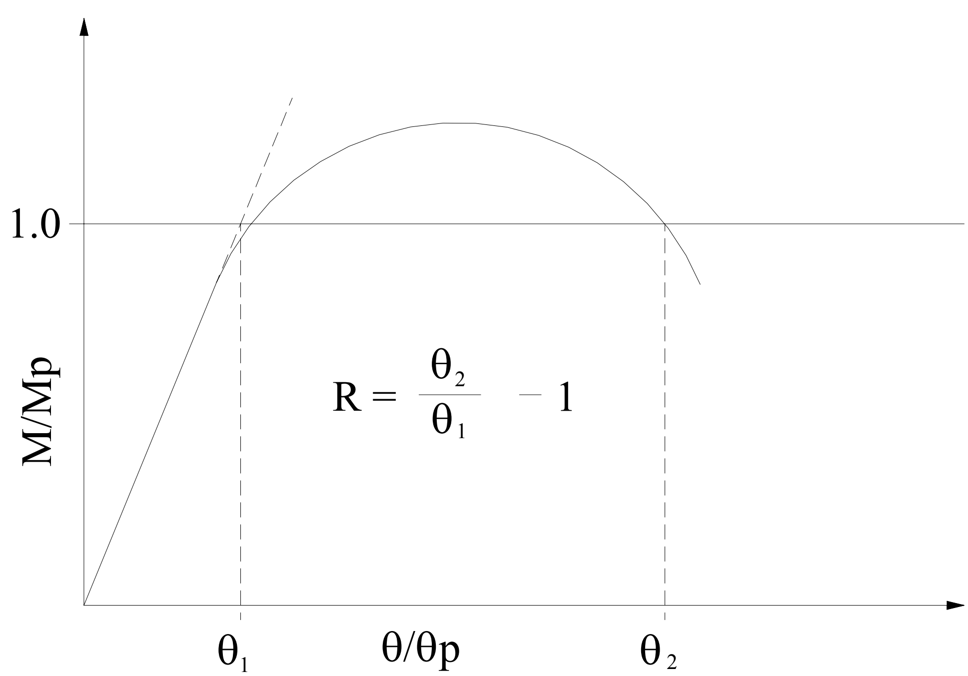

Figure 3 Rotation Capacity

1.2 SPECIFICATION PROVISIONS AND EARLY DESIGN RECOMMENDATIONS

A minimum rotation capacity of 3 is required for the purposes of employing plastic design and analysis according to the Specification. It is assumed that R = 3 is an adequate level of structural ductility to accommodate sufficient moment redistribution to allow formation of a collapse mechanism. The Specification lists compactness criteria for flanges and webs in flexure in Table B5.1. One of the goals of the AISC-LRFD compactness criteria shown in Table B5.1 of the Specification is to identify plate slenderness limits, λ_p, for cross-sectional plate components such that satisfaction of these limits will results in an overall flexural cross-section able to accommodate sufficient plastic hinge rotation to support system-wide moment redistribution as required for the development of a collapse mechanism. A section is considered compact if the plate slenderness ratio, $\lambda = b / t$, is less than the limiting value, λ_p.

For flanges of an I-beam in flexure, the following inequality must be true for the section to be considered compact:

$$\lambda_f = \frac{b_f}{2t_f} \leq \lambda_p = 0.38\sqrt{E/F_y} \tag{1-3}$$

For webs in flexural compression, the following inequality must be true for the section to be considered compact:

$$\lambda_w = \frac{h_w}{t_w} \leq \lambda_p = 3.76\sqrt{E/F_y} \tag{1-4}$$

If the slenderness ratios satisfy the inequalities (1-3) and (1-4), the section is considered to be compact and is theoretically able to accommodate sufficient flexural deformation, local buckling free, as required for collapse mechanism formation. Figure 4 illustrates the relationship between the slenderness ratio, λ, and the nominal moment strength, M_n. For a prismatic member, if the section is considered compact, plastic analysis is permitted by the Specification if L_{pd} is not exceeded.

$$L_{pd} = \left[0.12 + 0.076\left(\frac{M_1}{M_2}\right)\right]\left(\frac{E}{F_y}\right)r_y \tag{1-5}$$

where: F_y = specified minimum yield stress of the compression flange, ksi (MPa).

M_1 = smaller moment at end of unbraced length of beam, kip-in. (N-mm).

M_2 = larger moment at end of unbraced length of beam, kip-in. (N-mm).

r_y = radius of gyration about minor axis, in. (mm).

(M_1/M_2) is positive when moments cause reverse curvature and negative for single curvature.

Equation (1-5) is the complementary global buckling slenderness limit required to be able to accommodate sufficient flexural ductility for mechanism formation to occur without the attenuating effects of inelastic lateral-torsional buckling.

The main objective of the current research is to study the general behavior and governing limit states of web-tapered beams at ultimate loading. The results from the current research will be used to help decide if changes to the current AISC-LRFD design provisions, regarding web-tapered flexural response, should be proposed.

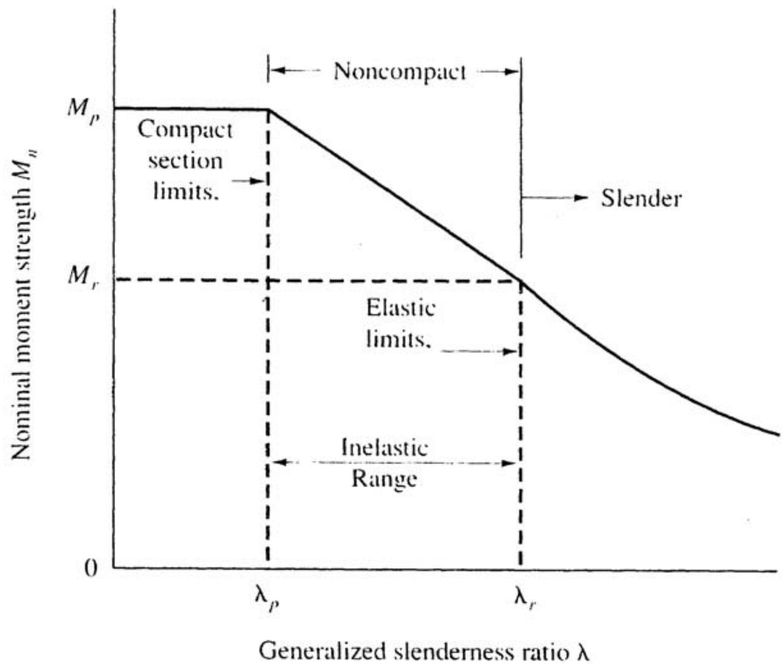

Figure 4 Nominal Strength M_n vs. Slenderness Ratio (Salmon and Johnson 1996)

1.3 LITERATURE REVIEW

The development of current AISC-LRFD Specification Appendix F web-tapered beam design provisions is based on research performed by Lee et al. and published in 1972. Morrell and Lee (1974) introduced improved flexural formulas that are used in the Specification as well. It has been suggested that web-tapered members ought to be considered capable of developing their full plastic cross-sectional capacity at any given position along the member longitudinal axis so long as compactness and bracing requirements are sufficient to exclude the possibility of significant erosion in ultimate capacity due to local and/or lateral-torsional buckling (Lee et al. 1981). Appendix F provides design equations for the lateral-torsional buckling limit state only. Therefore, it is reasonable to assume that the yielding limit state of Chapter F, based on the full cross-sectional plastic capacity, is a valid limit state of properly proportioned web-tapered beams since the provisions in Appendix F supplement the more general provisions provided in the main body of the Specification. However, the proem to Chapter F specifically states that the provisions therein apply only to prismatic members and therefore; implying that they may not be used for the design of web-tapered I-shaped beams.

The general design approach used in the Specification for the design of web-tapered beams is to apply modification factors to convert the tapered members into appropriately proportioned prismatic members in order that the prismatic LRFD beam equations may be applied. The strong axis bending design formulas in Appendix F were developed by adjusting the length of a prismatic beam (Sumner 1995) such that the ratio of the strength of a tapered member to the strength of a prismatic member, based on the smaller cross-section, is a function of the tapering ratio γ, the depth of the smaller end of the tapered member d_o, the flange width b, the flange thickness t_f, the web thickness t_w, and the member length (Lee et al. 1972). The development was restricted to doubly symmetric I-shaped beams due to the inability to uncouple the torsional and flexural deformations due to the varying location of the shear center for singly symmetric sections (Davis 1996). In addition, the development was limited to small tapering angles. Boley (1963) found that, using the Bernoulli-Euler theory, calculated normal stresses were accurate to within a few percent as long as the angle of taper was less than 15 degrees (Lee et al. 1972). The Specification adopted this restriction in Appendix F as equation (A-F3-1).

$$d = d_o(1 + \gamma \frac{z}{L}) \tag{1-6}$$

Where the limiting case for γ is then,

$$\gamma = \frac{d_L - d_o}{d_o} \leq 0.268\left(\frac{L}{d_o}\right) \tag{1-7}$$

where: d_L = depth at larger end of member, in. (mm).

d_o = depth at smaller end of member, in. (mm).

z = distance from the smaller end of member, in. (mm).

L = unbraced length of member measured between the center of gravity of the bracing members, in. (mm).

The limiting tapering ratio was also restricted to 6.0 for practical considerations (Lee et al. 1972). The development of the design equations was also restricted to flanges of equal and constant area and a constant web thickness.

The equations developed by Lee et al. (1972) and Morrell and Lee (1974) took into account the St. Venant's torsional and warping resistance of the tapered beams. Length modification factors were added to both St. Venant's and warping terms in the prismatic beam design equations so that they may be applied to tapered beams. The length modification factors create an equivalent prismatic beam that is analogous to the web-tapered I-shaped beam of a different length (Figure 5 depicts a web-tapered beam and the equivalent prismatic beam). The equivalent prismatic beam acquires the section properties of the smaller end of the tapered beam; the critical stress in the extreme fiber of a prismatic beam for elastic lateral torsional buckling may be expressed as:

$$\sigma_{cr} = \frac{1}{S_x}\sqrt{\frac{\pi^2 EI_y GK_T}{L^2} + \frac{\pi^2 EI_y EI_w}{L^4}} \tag{1-8}$$

where: σ_{cr} = elastic critical stress for a prismatic member, ksi.

S_x = elastic section modulus about strong axis, in.^{3}

E = modulus of elasticity, ksi.

I_y = weak-axis moment of inertia, in.^{4}

G = shear modulus, ksi.

K_T = torsional constant for the section, J, in.^{4}

L = unbraced length, in.

I_w = warping constant, C_w, in.^{6}

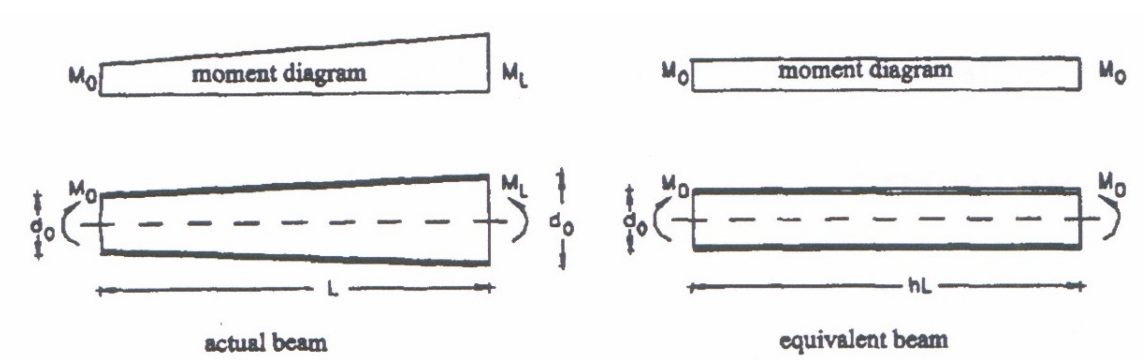

Figure 5 Tapered Beam and Equivalent Prismatic Beam (Polyzois and Raftoyiannis 1998)

When a length modification factor is introduced, equation (1-9) may be applicable to tapered members:

$$(\sigma_{cr})_\gamma = \frac{1}{S_{xo}}\sqrt{\frac{\pi^2 EI_{yo}GK_{To}}{(hL)^2} + \frac{\pi^2 EI_{yo}EI_{wo}}{(hL)^4}} \qquad (1\text{-}9)$$

where: $(\sigma_{cr})_\gamma$ = elastic critical stress for a tapered member, ksi.

S_{xo} = elastic section modulus of smaller end about strong axis, in.^{3}

I_{yo} = weak-axis moment of inertia of smaller end, in.^{4}

K_{To} = torsional constant for the section, J, in.^{4}

h = tapered member length modification factor.

I_{wo} = warping constant of smaller end, C_w, in.^{6}

The tapered member length modification factor, h, can then be solved for as follows:

$$h = \left[\frac{\pi^2 E I_{yo} G K_{To}}{L^2 (\sigma_{cr})_\gamma^2 S_{xo}^2} \left[1 + \sqrt{1 + \frac{\left[(\sigma_{cr})_\gamma S_{xo} d_o \right]^2}{(G K_{To})^2}} \right] \right]^{0.5} \tag{1-10}$$

In equation (1-10), all the unknowns are material or section properties that can be calculated with the exception of $(\sigma_{cr})_\gamma$, which must be calculated using the Rayleigh-Ritz method with the most severe end moment ratio (Lee et al. 1972, Davis 1996). The most severe end moment ratio is defined as the ratio between the end moments of a web-tapered beam that causes the maximum bending stress to be equal at both ends of the member.

In the spirit of modifying AISC specification equations for prismatic members for the case of tapered beams, Lee (1972) modified the then current allowable bending stress equations for prismatic members to account for the tapered geometry. The critical lateral-torsional buckling stress for warping resistance only, for a prismatic member, may be calculated by equation (1-11). A factor of safety of 5/3 is included in this formula.

$$F_w = \frac{170000 C_b}{(L/r_T)^2} \tag{1-11}$$

where: F_w = critical lateral-torsional buckling stress for a prismatic member considering warping resistance only, ksi.

C_b = moment gradient coefficient for prismatic members.

r_T = weak-axis radius of gyration considering the compression flange and one-third of the compression web, in.

The critical lateral-torsional buckling stress for pure torsional resistance only, for a prismatic member, may be calculated by equation (1-12). A factor of safety of 5/3 is included in this formula.

$$F_s = \frac{12000 C_b}{Ld/A_f} \tag{1-12}$$

where: F_s = critical lateral-torsional buckling stress for a prismatic member considering pure torsional resistance only, ksi.

d = depth of the section, in.

A_f = area of compression flange, in.^{2}

Lee et al. (1972) determined length modification factors for both warping resistance and pure torsional resistance by curve fitting equations for thin and deep sections (Equations (1-13) and (1-14)). The Specification adopted equations (1-13) and (1-14) as length modification factors:

$$h_w = 1.0 + 0.00385\gamma\sqrt{L/r_{To}} \tag{1-13}$$

$$h_s = 1.0 + 0.230\gamma\sqrt{Ld_o/A_f} \tag{1-14}$$

where: h_w = tapered member length modification factor, considering warping resistance only.

h_s = tapered member length modification factor, considering pure torsional resistance only.

The allowable flexural stress equations for a tapered beam can then be formulated as equations (1-15) and (1-16). The Specification modified these equations slightly as equations (A-F3-7) and (A-F3-6) in Appendix F. The modified equations are shown here as equations (1-17) and (1-18).

$$F_{w\gamma} = \frac{170000}{\left(h_w L/r_{To}\right)^2} \tag{1-15}$$

$$F_{s\gamma} = \frac{12000}{h_s L d_o/A_f} \tag{1-16}$$

$$F_{w\gamma} = \frac{5.9E}{\left(h_w L/r_{To}\right)^2} \tag{1-17}$$

$$F_{s\gamma} = \frac{0.41E}{h_s L d_o/A_f} \tag{1-18}$$

where: $F_{w\gamma}$ = critical lateral-torsional buckling stress considering warping torsional resistance only, ksi.

$F_{s\gamma}$ = critical lateral-torsional buckling stress considering pure torsional resistance only, ksi.

r_{To} = radius of gyration of a section at the smaller end, considering only the compression flange plus one-third of the compression web area, taken about an axis in the plane of the web, in. (mm).

The allowable bending stress equations were developed assuming a single unbraced length (i.e. the ends are assumed to be ideally flexurally and torsionally pinned), which rarely occurs in design. Tapered flexural members usually are continuous past several purlins or girts in low-rise metal buildings. Therefore, a modification factor, B, was introduced by Morrell and Lee (1974) to account for the effects of the moment gradient of sections past lateral braces and thus acts somewhat like a C_b term (i.e. moment gradient amplification factor). In addition, the modification factor accounts for the boundary conditions past the supports and hence also acts as an effective length factor (i.e. a k – factor). Morrell and Lee (1974) developed three modification equations that relate to three common cases in practice. The development of the modification factors was restricted to approximately equal adjacent segment unbraced lengths; a commonly encountered case in low-rise metal building design. Equations (1-19) through (1-21) were developed through the use of a finite element idealization involving meshes of prismatic beam elements approximating the web-tapered geometry in a piece-wise linear fashion by Morrell and Lee (1974). These finite element based results have been adopted by the Specification as equations (A-F3-8) through (A-F3-10). AISC-LRFD equation (A-F3-11) was also adopted as a special loading case. The four cases considered in the current Specification are illustrated in Figure 6. The following commentary is from the AISC-LRFD Appendix F Design Flexural Strength provisions:

Case I: When the maximum moment M_2 in three adjacent segments of approximately equal unbraced length is located within the central segment and M_1 is the larger moment at one end of the three-segment portion of a member:

$$B = 1.0 + 0.37\left(1.0 + \frac{M_1}{M_2}\right) + 0.50\gamma\left(1.0 + \frac{M_1}{M_2}\right) \geq 1.0 \qquad (1\text{-}19)$$

Case II: When the largest computed bending stress f_{b2} occurs at the larger end of two adjacent segments of approximately equal unbraced lengths and f_{b1} is the computed bending stress at the smaller end of the two-segment portion of a member:

$$B = 1.0 + 0.58\left(1.0 + \frac{f_{b1}}{f_{b2}}\right) - 0.70\gamma\left(1.0 + \frac{f_{b1}}{f_{b2}}\right) \geq 1.0 \qquad (1\text{-}20)$$

Case III: When the largest computed bending stress f_{b2} occurs at the smaller end of two adjacent segments of approximately equal unbraced length and f_{b1} is the computed bending stress at the larger end of the two-segment portion of the member:

$$B = 1.0 + 0.55\left(1.0 + \frac{f_{b1}}{f_{b2}}\right) + 2.20\gamma\left(1.0 + \frac{f_{b1}}{f_{b2}}\right) \geq 1.0 \qquad (1\text{-}21)$$

In the foregoing, $\gamma = (d_L - d_o)/d_o$ is calculated for the unbraced length that contains the maximum computed bending stress. M_1/M_2 is considered as negative when producing single curvature. In the rare case where M_1/M_2 is positive, it is recommended that it be taken as zero. f_{b1}/f_{b2} is considered as negative when producing single curvature. If a point of contraflexure occurs in one of two adjacent unbraced segments, f_{b1}/f_{b2} is considered positive. The ratio $f_{b1}/f_{b2} \neq 0$.

Case IV: When the computed bending stress at the smaller end of a tapered member or segment thereof is equal to zero:

$$B = \frac{1.75}{1.0 + 0.25\sqrt{\gamma}} \tag{1-22}$$

where: $\gamma = (d_L - d_o)/d_o$ and is calculated for the unbraced length adjacent to the point of zero bending stress.

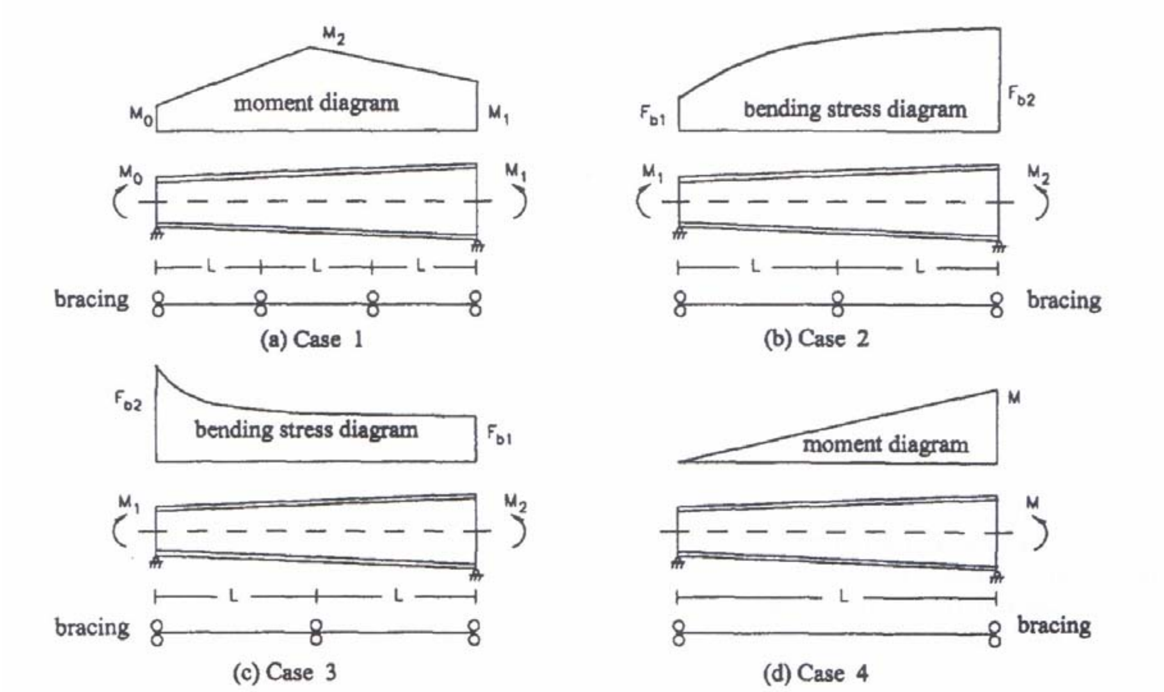

Figure 6 Four Cases Used in AISC-LRFD Specification (Polyzois and Raftoyiannis 1998)

After the continuity modification factor, B, has been calculated, the critical lateral-torsional buckling stress considering both warping torsional resistance and pure torsional resistance for the web-tapered members may be calculated. AISC-LRFD equations (A-F3-4) and (A-F3-5) are shown below as equations (1-23) and (1-24), respectively.

$$F_{b\gamma} = \frac{2}{3}\left[1.0 - \frac{F_y}{6B\sqrt{F_{s\gamma}^2 + F_{w\gamma}^2}}\right]F_y \leq 0.60F_y \qquad (1\text{-}23)$$

unless $F_{b\gamma} \leq F_y/3$, in which case

$$F_{b\gamma} = B\sqrt{F_{s\gamma}^2 + F_{w\gamma}^2} \qquad (1\text{-}24)$$

where: $F_{b\gamma}$ = critical lateral-torsional buckling stress considering both warping torsional resistance and pure torsional resistance for web-tapered members.

The design strength of tapered flexural members for the lateral-torsional buckling limit state is $\varphi_b M_n$, where φ_b = 0.90 and the nominal strength is calculated using AISC-LRFD equation (A-F3-3) as presented in equation (1-25):

$$M_n = (5/3) S'_x F_{b\gamma} \tag{1-25}$$

$$\varphi_b M_n = \varphi_b (5/3) S'_x F_{b\gamma} \tag{1-26}$$

where: S'_x = section modulus of the critical section of the unbraced beam length under consideration.

φ_b = resistance factor for flexure.

Polyzois and Raftoyiannis (1998) reexamined the modification factor, B, which accounts for both the stress gradient and the restraint provided by the adjacent spans of a continuous web-tapered beam. Use of the recommended AISC values of B factor implies that both parameters, stress gradient and continuity, are equally important (Polyzois and Raftoyiannis 1998). If lateral supports have insufficient stiffness or the supports are improperly applied to the tapered-member, the continuity effect of the modification factor, B, may need to be ignored. By using a finite element computer program, Polyzois and Raftoyiannis (1998) developed separate modification factor equations for stress gradient and continuity for various load cases. A general equation for the modification factor, B, can be expressed as equation (1-27). The variable R_γ

will be used in place of B to follow the nomenclature of Polyzois and Raftoyiannis (1998) and that of Lee et al. (1972).

$$R_\gamma = \frac{(\sigma_\gamma)_{LR}}{(\sigma_\lambda)_{SS}\big|_{\alpha=k}} \tag{1-27}$$

where: $(\sigma_\gamma)_{LR}$ = elastic buckling stress of a critical section in a laterally restrained tapered beam.

$(\sigma_\gamma)_{SS}$ = elastic buckling stress of a simply supported tapered beam the dimensions of which are identical to those of the critical section that is loaded with end moments producing a nearly uniform stress in the critical section.

The variable k, in equation (1-27), is the ratio of the smaller end section modulus to the larger end section modulus ($k = S_o/S_L$). The variable α, in equation (1-27), is the ratio of the end moment at the smaller end of the beam to the end moment at the larger end of the beam ($\alpha = M_o/M_L$). This implies that when $\alpha = k$, an approximately constant stress is present across the length of the beam and when $\alpha \neq k$, a stress gradient is present.

Polyzois and Raftoyiannis (1998) presented a general equation for the stress gradient in a similar fashion to the moment gradient coefficient C_b in prismatic members. This expression is shown with the factor B:

$$B = \frac{(\sigma_\gamma)_{SS}\big|_{\alpha\neq k}}{(\sigma_\gamma)_{SS}\big|_{\alpha=k}} \tag{1-28}$$

where: $(\sigma_\gamma)_{SS}\big|_{\alpha\neq k}$ = elastic critical buckling stress of a simply supported single span tapered member with stress gradient, i.e., unequal end stresses.

$(\sigma_\gamma)_{SS}\big|_{\alpha=k}$ = critical buckling stress of the same member without stress gradient, i.e., equal end stresses.

Polyzois and Raftoyiannis (1998) use the variable R as the restraint factor used to account for the restraining effect. The general equation is expressed as follows:

$$R = \frac{(\sigma_\gamma)_{LR}\big|_{\alpha=k}}{(\sigma_\gamma)_{SS}\big|_{\alpha=k}} \tag{1-29}$$

where: $(\sigma_\gamma)_{LR}\big|_{\alpha=k}$ = elastic critical buckling stress of the critical span in a laterally restrained tapered beam with zero stress gradient.

For brevity, the specialized equations for various loading conditions for the stress gradient factors and restraint factors will not be expressed in this report. The reader is directed to Polyzois and Raftoyiannis (1998) for the equations developed by regression methods and curve-fitting techniques for seven different cases.

1.4 PREVIOUS EXPERIMENTAL WORK

Experimental results by Prawel, Morrell, and Lee (1974) are used in a verification study of the nonlinear finite element analysis techniques discussed and employed herein. The research performed by Prawel et al. (1974), at the State University of New York at Buffalo tested several web-tapered beams to destruction in pure bending. The member lengths and conditions of support for the test beams were chosen so that failure of the members occurred in the inelastic range (Prawel et al. 1974). The results of the LB-3 test beam are presented using a load vs.

deflection plot. This data, along with other test data presented, is utilized to construct a finite element model of the beam as well as boundary and loading conditions in order that a comparison of results might be undertaken to assess agreement. The effects of residual stresses in the beams and the effects of various fabrication processes on the behavior of the beams were also discussed by Prawel et al. (1974). Due to the method of fabrication in the test specimens, an initial lateral deflection of the flanges was present. However, the response of the tapered members experimentally tested was very much the same as the response of prismatic members, in that large angles of twist were necessary before there was any significant loss in strength (Prawel et al. 1974).

Five different geometries of rafter-to-column sub-assemblages were experimentally tested at Virginia Polytechnic Institute and State University (Sumner 1995) in order to assess web-tapered beam shear capacity. A very detailed description of the specimen design, tested geometry, and specimen material properties were provided in the work of the investigators at Virginia Tech (Sumner 1995) and as a result of this, the tests are ideal subjects for the verification study described later in this report.

1.5 SCOPE

The main objective of the current study is to investigate the behavior and governing limit states exhibited by gently tapered I-shaped beams at their maximum load. Compactness criteria that ensure attainment of R = 3 are examined using experimentally verified nonlinear finite element modeling techniques. The commercial multipurpose finite element software package ABAQUS version 5.8-22 is employed in this research. A parametric study is conducted to determine the rotational capacity of web-tapered members in flexure possessing various cross-sections and beam geometries. The geometries of the tapered beams considered are of realistic dimensions vis-à-vis what one normally encounters within the rafter sections of metal buildings manufactured in the U.S. The current research acts as a pilot study in the pursuit of revisions to the web-tapered member flexural design provision contained in Appendix F of the AISC-LRFD Specification.

1.6 THESIS ORGANIZATION

Section 2 describes the finite element modeling methods and techniques used in the current research. Section 3 discusses the verification study to validate these same nonlinear finite element modeling techniques. This section also covers the analysis of a benchmark gable frame modeled using the commercial finite element program ABAQUS. A portion of the frame is then modeled in ABAQUS as a sub-assemblage from the complete frame; the analysis of the individual beam is discussed in Section 3. Section 4 describes, in detail, the parametric study and the results obtained from more than 200 finite element models. Conclusions for this study are provided, with recommendations, in Section 5. Appendix A includes example ABAQUS input files utilized during the parametric study. The results of the parametric study are included in Appendix B and representative rotation capacity plots for a number of the more practically useful parametric combinations resulting in compact beam response are illustrated in Appendix C.

2.0 FINITE ELEMENT METHOD

The current study utilizes the finite element method to study the behavior of web-tapered I-shaped beams in pure bending. The finite element method was originally developed to analyze complex airframe structures in the aircraft industry (Clough 1965). With use of early computers, aeronautical and structural engineers developed the method to analyze the complex airframes by improving on the Hrennikoff-McHenry 'lattice analogy' for analyzing plane stress systems. Later, this method was refined to be able to be used on any structural component. Clough defines the finite element method as "a generalization of standard structural analysis procedures which permits the calculation of stresses and deflections in two- and three-dimensional structures by the same techniques which are applied in the analysis of ordinary framed structures" (Clough 1965). The finite element method is a numerical method for solving complicated systems that may be impossible to be solved in the closed form. It acquired its name based the approach used within the technique; assembling a finite number of structural components or elements interconnected by a finite number of nodes. Any solid or structure may be idealized as a finite number of elements assembled together in a structural system (i.e. discretizing a continuous system). The analysis itself is an approximation to the actual structure since the original continuum is divided into an equivalent patchwork through the use of two- and three-dimensional structural elements. The material properties from the continuum are retained by the elements as part of the analysis methodology. This method is a powerful tool that can be used to analyze any two- or three-dimensional structural component. In the case of the current research, the commercial multipurpose software package ABAQUS is used to execute a nonlinear finite element parametric study.

2.1 THE FINITE ELEMENT PROCEDURE

The procedure of the finite element method can be summed up in three steps. The first step is the structural idealization, or discretization. This idealization is the subdivision of the original member into a number of equivalent finite elements. Great care must be given to this step because the assembled finite elements must satisfactorily simulate the behavior of the original continuum. Generally, better results are obtained by using a finer discretization scheme leading to a denser mesh of finite elements spanning the problem geometry. In theory, when the mesh size of properly formulated elements is successively reduced, the solution of the problem will converge to the exact solution (exact within the assumptions of any underlying classical theory). It is also important to select elements that are compatible in deformation with adjacent elements. If compatibility were not satisfied, the elements would distort independently from each other thus creating gaps or overlaps within the model (i.e. allowing for violation of the compatibility condition for a continuum). This would cause the idealization to be much more flexible than the actual continuum. In addition, if compatibility were not satisfied, large stress concentrations would develop at the nodal points. The stress concentrations would make the solution of the problem deviate even further from the actual solution.

The second step to the finite element method is the evaluation of the element properties. This implies developing the stiffness matrix for the given elements to form a force-displacement relationship for the original member. The force-displacement relationship encapsulates the characteristics of the elements by relating the forces applied at the nodes with the resulting deflections. This step is critical for obtaining accurate results from the analysis. The following equation relates the force vector {F} to the displacement vector {d} by the use of the stiffness matrix of the system [K]:

$$\{F\} = [K]\{d\} \tag{2-1}$$

The third and final step to the finite element method is the actual structural analysis of the element assemblage. Three requirements must be satisfied in order to analyze the structure. Equilibrium, compatibility, and the force-displacement relationship all must be satisfied. Two basic approaches can be used to satisfy the requirements. These approaches include the force method and the displacement method, which can be used for structural analysis of the elements. In each case, as long as the structural system or continuum is elastic, the governing system may be solved directly using any of a number of efficient solution algorithms (e.g. Gauss elimination, Cholesky Factorization, Frontal Solution, etc.). In a nonlinear analysis, this is not the case and hence the equilibrium path must be traced in an iterative and incremental fashion.

2.2 NONLINEAR FINITE ELEMENT ANALYSIS

Two nonlinearities may arise in structural analysis problems; these emanate from material and geometric nonlinear influences. These nonlinearities are associated with material deformation and stiffness variations. Material nonlinearity arises when the stress-strain behavior becomes nonlinear, as in the case of plasticity. The following equation for uniaxial loading, Hooke's Law, becomes invalid in the plastic range where material nonlinearity dominates:

$$\sigma = E\varepsilon \tag{2-2}$$

Geometric nonlinearity may be present when large deformations exist. The effect is precipitated by a nonlinear strain-displacement relationship (Sathyamoorthy 1998). As a result, equilibrium may not be formulated using the undeformed structure.

The finite element analysis program ABAQUS deals with both types of nonlinearities that may occur in modeled structures. ABAQUS traces the nonlinear equilibrium path through an iterative approach. In the context of the current research program, the program loads the beam in small increments; ABAQUS assumes the structural response to be linear within each increment. After each incremental loading, a new structural configuration is determined and a new ideal linearized structural response (i.e. tangent stiffness matrix) is calculated. Within each of these increments, the linearized structural problem is solved for displacement increments using load increment. The incremental displacement results are subsequently added to previous deformations (as obtained from earlier solution increments). In ABAQUS, the load increment is denoted by a load proportionality factor related to the applied load. For example, an initial load increment may be 0.001 times the applied load, where 0.001 is the load proportionality factor, and a second load increment may be 0.003 times the applied load. The load proportionality factor may increase in size if the solution convergence rate appears to be more and more favorable with each increment. However, as the ultimate load for the structure is approached, the load increments are reduced in size. After each converged increment is obtained a new tangent stiffness matrix is computed using the internal loads and the deformation of the structure at the beginning of the load increment. This tangent stiffness can be represented by the following equation:

$$[k_T] = [k_o] + [k_p] \tag{2-3}$$

where $[k_o]$ is the usual linear stiffness matrix and $[k_p]$ is the so called "stress matrix" arising out of the nonlinear strain-displacement relationship at the heart of geometric nonlinear analysis.

2.3 MODIFIED RIKS-WEMPNER METHOD

To track the nonlinear equilibrium path of a structural system in load control, ABAQUS utilizes either the Newton-Raphson Algorithm or the modified Riks-Wempner Algorithm. Both methods are powerful tools in determining nonlinear response of a system. ABAQUS uses a modified Newton-Raphson method as its default solution algorithm. The Newton-Raphson Algorithm traces the nonlinear equilibrium path by successively formulating linear tangent stiffness matrices at each load level. The tangent stiffness matrix changes at each load interval due to a difference in internal force and applied external load (i.e. as a direct effect of the stress softening effects of $[k_p]$). The Newton-Raphson method is advantageous because of its quadratic convergence rate when the approximation at a given iteration is within the radius of convergence (ABAQUS 2001). However, the Newton-Raphson method is unable to plot the unloading portion of a nonlinear equilibrium path because it is incapable of negotiating limit and bifurcation points (Earls 1995). Since this study focuses on the rotational capacity of web-tapered beams in pure bending in the presence of buckling influences, the algorithm of choice for this particular study is the modified Riks-Wempner method.

In simple cases, linear eigenvalue analysis may be sufficient for a design evaluation considering rudimentary effects of instability, but if there is concern over material nonlinearity, geometric nonlinearity prior to buckling, or unstable post-buckling response, a fully nonlinear iterative analysis must be performed to investigate the problem further (ABAQUS 2001). A representative highly nonlinear response including unstable static response is illustrated in Figure 7.

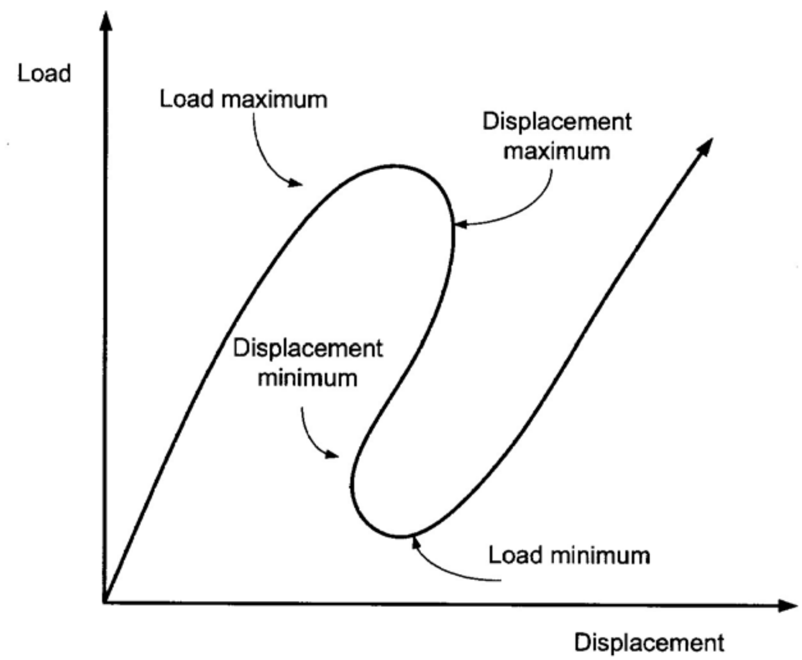

Figure 7 Representative Unstable Static Response (ABAQUS 2001)

The Riks-Wempner algorithm is a nonlinear solution strategy that utilizes the "arc length" method to trace the nonlinear equilibrium path through the unstable critical point, unlike the Newton-Raphson method, which cannot negotiate such a point. Therefore, within the context of the current research, the Riks-Wempner method allows the web-tapered beams to buckle and unload (as shown schematically in Figure 8).

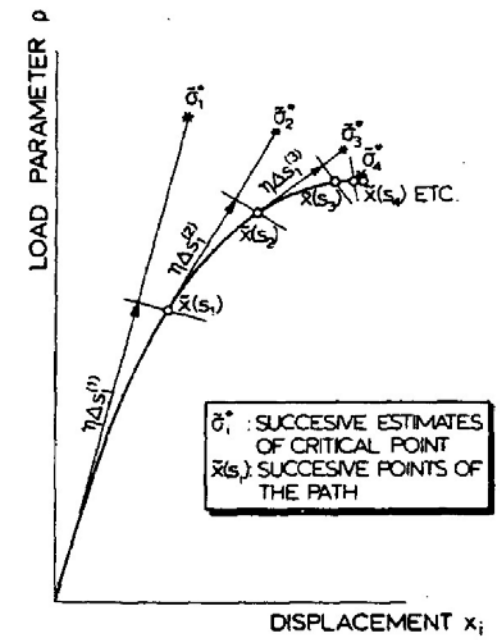

Figure 8 Riks "Arc Length" Method (Riks 1979)

The kinematical configurations of a structure are assumed to possess a finite set of generalized coordinates, also referred to as displacement variables or deformation parameters (Riks 1979):

$$\tilde{t} = [t_1, t_2, t_3, \ldots, t_N] \tag{2-4}$$

If the loading intensity parameter is denoted by ρ, the potential energy of the structure is expressed as follows:

$$P = P(\tilde{t}\,; \rho) \tag{2-5}$$

The configuration $[\rho;\tilde{t}]$ of the structure may be visualized as a point in a (N+1) dimensional Euclidean Space R_{N+1} (Riks 1979). Since more than one deformed structural configuration may exist at any one load ρ, and since the solutions vary when the load ρ varies, the equilibrium paths of the structure may be described in parametric form by the following equations where η is a suitably chosen path parameter:

$$\rho = \rho(\eta); \tilde{t} = \tilde{t}\,(\eta) \tag{2-6}$$

For the case of the modified Riks-Wempner algorithm, the mathematical model utilized takes the following form where η is defined as the arc length of the curve (2-6):

$$\left(\frac{d\rho}{d\eta}\right)^2 + \frac{dt_h}{d\eta}\frac{dt_h}{d\eta} = 1 \tag{2-7}$$

Equation 2-7 is a constraint equation involving both the displacement and load factor involved in the solution during the previous equilibrium iteration. The net effect of the constraint equation 2-7 is that as the solution becomes more difficult to converge on, the distance that the solution algorithm will venture out, into the given solution space, is reduced. Thus, as limit points in the equilibrium path of the system are approached, the solution algorithm detects the additional effort needed to converge on a solution and thus cuts back on the load proportionality factor.

2.4 YIELD SURFACE

A yield criterion for an elastic material may be expressed as a yield function $f(\sigma_{ij},Y)$ (Boresi 1993). The variable σ_{ij} represents a given multiaxial state of stress and Y is the uniaxial tensile or compressive yield strength. When the yield function, $f(\sigma_{ij},Y)$ is equal to zero, the yield criterion is satisfied and plastic flow becomes possible. The stress state is elastic when $f(\sigma_{ij},Y)$ is less than zero and undefined when greater than zero. The yield criterion is usually shown schematically through the use of a yield surface. An example of the von Mises yield surface is illustrated in Figure 9. This three-dimensional illustration of the yield function is plotted against the principal stresses σ_1, σ_2, and σ_3. As implied by Figure 9, the hydrostatic stress state does not influence the initiation of yielding. Only stresses that deviate from the hydrostatic stress state, referred to as deviatoric stresses, influence and cause yielding in a ductile metal (typically possessing a face-centered or body-centered crystal lattice structure at the atomic level – as in the case of aluminum, titanium, iron, and steel). Figure 10 is the von Mises yield surface for a biaxial stress state, where σ_3 is set equal to zero (i.e. a plane stress state). As a result of the plane stress state, the yield surface assumes the shape of an ellipse resulting from the projection of the intersection of the stress plane with the 3-D failure surface.

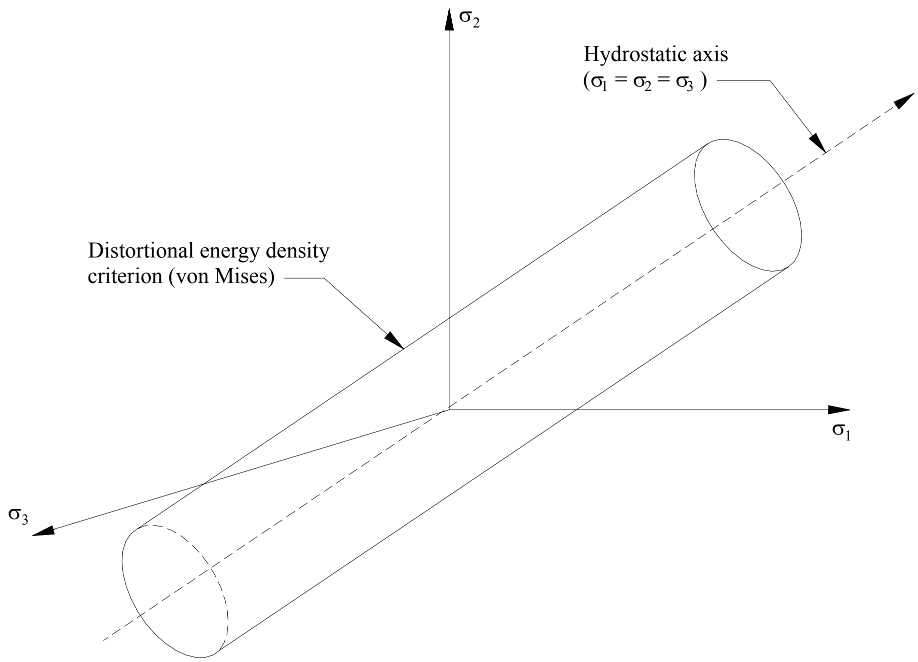

Figure 9 von Mises Yield Criterion

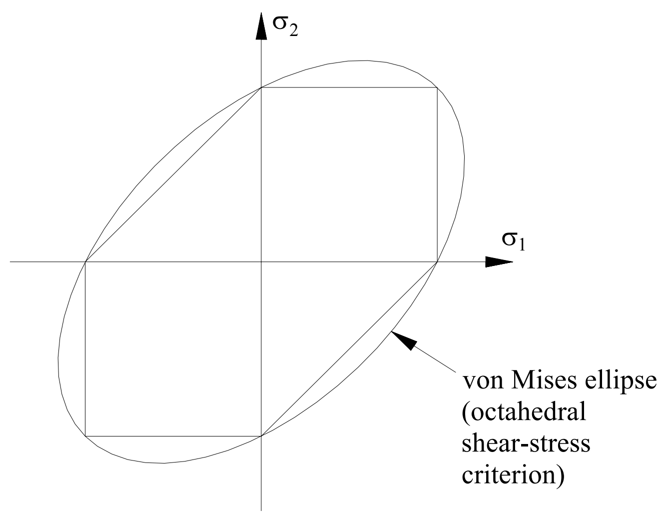

Figure 10 Biaxial Stress State ($\sigma_3 = 0$)

Several different yield criteria exist. For this study, the distortional energy density, or von Mises yield criterion is utilized. This criterion is also referred to as the maximum octahedral shear-stress criterion. The von Mises yield criterion states that yielding begins when the distortional strain energy density at a point equals the distortional strain energy density at yield in uniaxial tension or compression. The distortional strain energy density is that energy associated with a change in the shape of a body (Boresi 1993). The theory of strain energy density is used to develop the yield function. The total strain energy density is defined by the following equation:

$$U_O = \frac{(\sigma_1 + \sigma_2 + \sigma_3)^2}{18K} + \frac{(\sigma_1 - \sigma_2)^2 + (\sigma_2 - \sigma_3)^2 + (\sigma_3 - \sigma_1)^2}{12G} \tag{2-8}$$

where K = bulk modulus and is calculated using the following equation:

$$K = \frac{E}{[3(1-2\nu)]} \tag{2-9}$$

G = shear modulus and is calculated using the following equation from the Theory of Elasticity:

$$G = \frac{E}{[2(1+\nu)]} \tag{2-10}$$

The first term in equation (2-8) is the energy associated with volumetric change and the second term is the distortional strain energy density and is defined as follows:

$$U_D = \frac{(\sigma_1 - \sigma_2)^2 + (\sigma_2 - \sigma_3)^2 + (\sigma_3 - \sigma_1)^2}{12G} \tag{2-11}$$

Alternatively, the distortional energy density may be restated as follows:

$$U_D = \frac{1}{2G} J_2 \tag{2-12}$$

where: J_2 = second deviator stress invariant and is expressed as follows:

$$J_2 = \frac{1}{6}\left[(\sigma_1 - \sigma_2)^2 + (\sigma_2 - \sigma_3)^2 + (\sigma_3 - \sigma_1)^2\right] \tag{2-13}$$

Since at yield for uniaxial stress conditions $\sigma_1=\sigma$ and $\sigma_2=\sigma_3=0$, it can be shown that the yield function for the von Mises yield criterion is expressible as:

$$f(\sigma, Y) = \sigma_e^{\,2} - Y^2 \tag{2-14}$$

where: σ_e = effective stress and is expressed as:

$$\sigma_e = \sqrt{\frac{1}{2}\left[(\sigma_1 - \sigma_2)^2 + (\sigma_2 - \sigma_3)^2 + (\sigma_3 - \sigma_1)^2\right]} = \sqrt{3J_2} \tag{2-15}$$

2.5 STRESS-STRAIN RELATIONSHIPS

Two different stress-strain relationships are usually used when characterizing the plasticity of metals. The most common relationship in engineering practice is the engineering stress versus engineering strain. Engineering stress is calculated using the original, undeformed, cross-sectional area of a specimen. The engineering stress for a uniaxial tensile or compressive test has a magnitude $\sigma = P/A_o$, where P is the force applied and A_o is the original cross-sectional area. Engineering strain is the change or elongation of a sample over a specified gage length L. The engineering strain is equal to $\varepsilon = e/L$, where e is the elongation of the material over the gage length.

When employing nonlinear finite element modeling strategies considering material nonlinear effects, it is important to use true stress and its energy conjugate counterpart – logarithmic strain when characterizing the material response within the finite element environment. True stress and true strain is required by ABAQUS in cases of geometric nonlinearity because of the nature of the formulation used in the incremental form of the equilibrium equations in ABAQUS. The true stress may be presented conceptually by the following equation:

$$\sigma_t = \frac{P}{A_t} \tag{2-16}$$

where A_t = the actual cross-sectional area of the sample specimen when the load P is acting on it.

In terms of the engineering stress and engineering strain, true stress may be expressed as follows:

$$\sigma_t = \sigma_{eng}(1 + \varepsilon_{eng}) \tag{2-17}$$

True strain is different from engineering strain it that true strain is not linearly related to the elongation, e, of the original gage length L. Figure 11 depicts the true stress vs. true strain plot. The formulation of the engineering strain is shown by equation (2-18).

$$\varepsilon_t = \int_L^{L_t} d\varepsilon_t = \ln\left(\frac{L_t}{L}\right) = \ln\left(\frac{L+e}{L}\right) = \ln(1 + \varepsilon_{eng}) \tag{2-18}$$

The logarithmic plastic strain may be expressed as follows:

$$\varepsilon_{\ln}^{pl} = \ln(1 + \varepsilon_{eng}) - \frac{\sigma_t}{E} \tag{2-19}$$

Furthermore, Logarithmic strain is a more appropriate strain measure to use in geometrically nonlinear finite element problems as a result of its invariance under rigid body rotation.

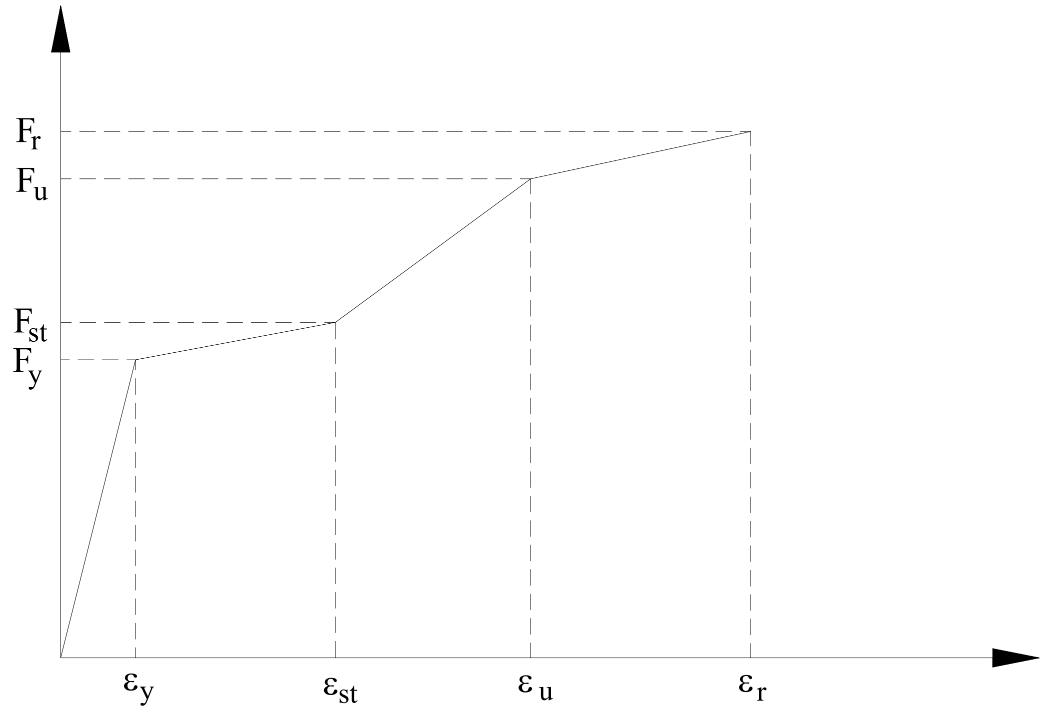

Figure 11 True Stress vs. True Strain

2.6 SHELL ELEMENT

Shell elements from the ABAQUS element library are utilized in this study due to the inherent ability of shell elements to economically model structures in which one dimension, the thickness, is much smaller than the other dimensions and the normal stresses through the thickness of the elements are considered negligible. The nonlinear shell element chosen for this study is the S4R shell element (ABAQUS 2001). The S4R element is defined by ABAQUS (2001) as a 4-node doubly curved general-purpose shell, with reduced integration, hourglass control, and finite membrane strains. The S4R element can be used in thick shell and thin shell formulations. This is important during the parametric study because the shell thicknesses are changed for each model to simulate various plate thicknesses. Six active degrees of freedom exist for each of the four nodes of the S4R shell element. These degrees of freedom are shown as follows:

$$1,2,3,4,5,6(u_x, u_y, u_z, \phi_x, \phi_y, \phi_z) \tag{2-20}$$

The S4R element uses a reduced order of integration when forming the element stiffness matrix of each individual element. Reduced integration usually provides results that are more accurate (as a means of overcoming some over stiffness effects in the shell), provided the elements are not distorted or loaded in in-plane bending, and it significantly reduces running time (ABAQUS 2001). Since the integration is performed at only one Gauss point per element, the S4R shell element is described as being computationally inexpensive. Figure 12 represents one S4R element with the one Gauss point shown as denoted by ABAQUS (2001).

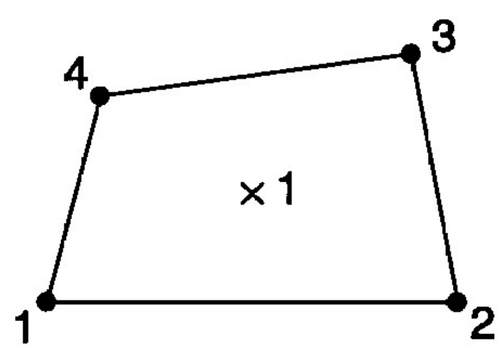

Figure 12 4-Node Reduced Integration Element (ABAQUS 2001)

3.0 FINITE ELEMENT MODELING

In order to use the finite element method with confidence, it must first be validated against previous experimental results directly related to the modeling problem under investigation. The experimental test that is utilized for a verification study related to the current research is the LB-3 test beam by Prawel et al. (1974). Figure 13 illustrates the tapered beam experimentally tested by Prawel and co-workers which is modeled in ABAQUS as part of the current research. The meshed surface planes are taken as the mid-depths of each plate as shown in Figure 14 (i.e. planes of the shell mesh surface coincide with the middle surface of the constituent plate elements in the cross-section). A dense mesh is utilized in the verification study and an aspect ratio approximately equal to one at the beam mid-span is imposed on the web. The aspect ratio for the web varies as the beam tapers to either side of the beam mid-span since a constant number of elements is used to make up the depth of the web. The aspect ratio for the flanges is held constant at one.

The beam is constructed by defining nodes and creating node sets between each node. The node sets are then used to define S4R shell elements as elements sets. Each element set is defined using a different set of material properties and shell thicknesses. Since the accuracy of the finite element results correlates with the mesh density, an extremely dense mesh is created for the verification study as well as the subsequent parametric studies. The computational time required for the solution of a given finite element model also tends to be related to the mesh density (i.e. the greater the density, the greater the solution times). However, since powerful, high-speed computers are used for the study, a dense mesh could be used in pursuit of the most accurate results possible. The dense mesh created for the verification study includes 12,516 nodes and 12,006 elements.

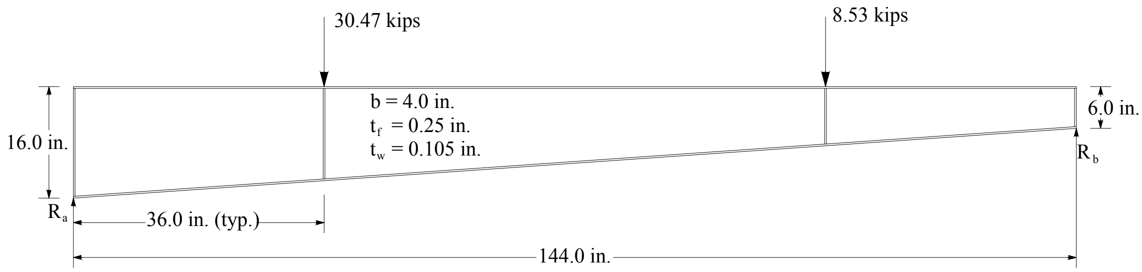

Figure 13 LB-3 Test Beam for Verification Study

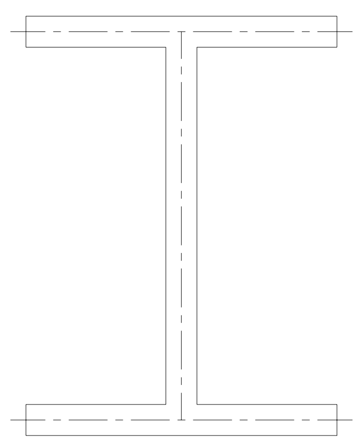

Figure 14 Meshed Surface Planes

3.1 IMPERFECTION SEED

In modeling studies where inelastic buckling is investigated, it is important that the evolution of the modeling solution be carefully monitored so that any indication of bifurcation in the equilibrium path is carefully assessed to guarantee that the equilibrium branch being followed corresponds to the lowest energy state of the system (Earls and Shah 2001). An imperfection seed is introduced into the finite element models in order for the models to ensure that the lowest energy equilibrium path be followed in the inelastic range. Several buckling modes are obtained from the linearized eigenvalue buckling analysis using ABAQUS. Each of these modes is subsequently evaluated to ensure that the "correct" buckling mode is used (meaning the mode possessing the dominant features noted as consistent with the governing failure mode). Figures 15 and 16 illustrate the imperfection used for the verification study of the LB-3 web-tapered beam. The displacement field associated with the given buckling mode is scaled and subsequently introduced into the model to create an initial perturbation in the geometry of the mesh. This perturbation is frequently necessary to accurately apply finite element modeling techniques to "real-world" beams, since in the "real-world" it is not possible to achieve perfect loading, i.e., beams are never perfectly straight, not perfectly homogeneous, and are usually not loaded in exactly the plane that is assumed for design and analysis (Salmon and Johnson 1996). The scale used in the benchmark frame, as discussed later, is $L_b/1000$. An imperfection scale factor of $L_b/500$ is used for the beam in the verification study, the sub-assemblage beam, and the parametric study beams. A scale factor of $L_b/500$ was suggested by Winter (1960) to obtain several of the design equations in the Load and Resistance Factor Design method (Salmon and Johnson 1996). A sensitivity study is performed on web-tapered beams with various imperfection scale factors and it is determined that the web-tapered beams are extremely insensitive to changes in the scale factor. The change in capacity of the beams is negligible between the scale factors of $L_b/1200$ and $L_b/100$. However, this is not the case for the frame. The frame is extremely sensitive to changes in the imperfection scale factor. Therefore, the normal out-of-straightness fabrication tolerance of $L_b/1000$ is utilized in the frame analysis work. Table 1 shows the results from the sensitivity study of various imperfection scale factors in determining the ultimate load proportionality factors for the frame as well as for the sub-assemblage beam. The mode of failure for each scale factor is identical between the frame and beam. The load proportionality factors shown in Table 1 represent the factors multiplied by the applied load at which unloading begins. For example, for an imperfection scale factor of $L_b/500$, the sub-assemblage beam will fail when the load reaches 1.11 times the applied loading.

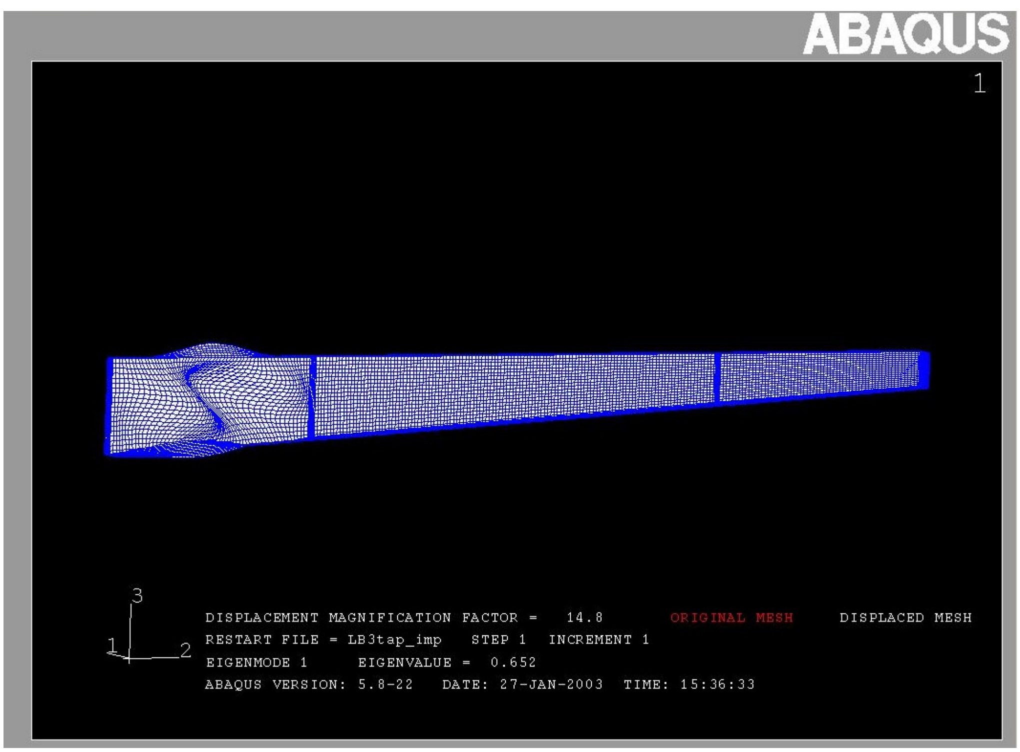

Figure 15 Imperfection Seed of Verification Beam LB-3

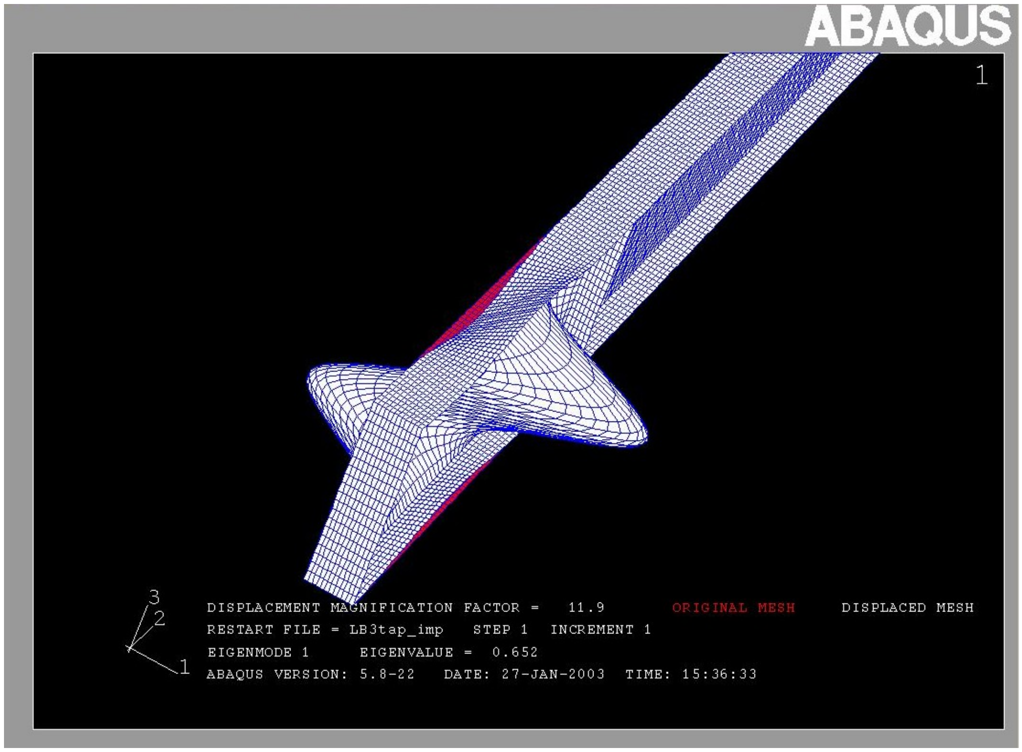

Figure 16 Imperfection Seed of Verification Beam LB-3

Table 1 Sensitivity Study Results of Various Imperfection Scale Factors using ABAQUS

	Lb/1200	Lb/1000	Lb/500
Frame	1.31	1.19	0.977
Sub-Assemblage Beam	1.11	1.11	1.11

3.2 VERIFICATION STUDY RESULTS

The initial focus of the verification study modeling is the web-tapered beam LB-3 experimentally tested by Prawel et al. (1974). The grade of steel used in the experimental beam is A242 steel; having a nominal yield strength of 51.5 ksi. Young's Modulus is set at 29000 ksi and Poisson's Ratio is set at 0.3. The beam tapers from a maximum depth of 16.0 inches to a minimum of 6.0 inches with an overall length of 144.0 inches. The flanges are 4 inches wide and 0.25 inches thick. The web varies in depth and is 0.105 inches thick. The values of $b/2t_f$ and h/t_w for this particular beam are higher than those permitted by the Specification for plastic design of prismatic members. The beam is braced against lateral displacements at each of the stiffeners. In the ABAQUS model, the stiffness of the lateral braces is set as infinite. The stiffeners are located at the ends of the beams and at the first and third quarter points, creating a maximum unbraced length of 72.0 inches. Point loads are placed at the first and third quarter point stiffeners to create the moment gradient over the middle portion of the beam. The beam is simply supported at the ends and its supports and loadings are illustrated in Figure 17. Figure 18 shows the von Mises stress distribution on the beam at maximum loading.

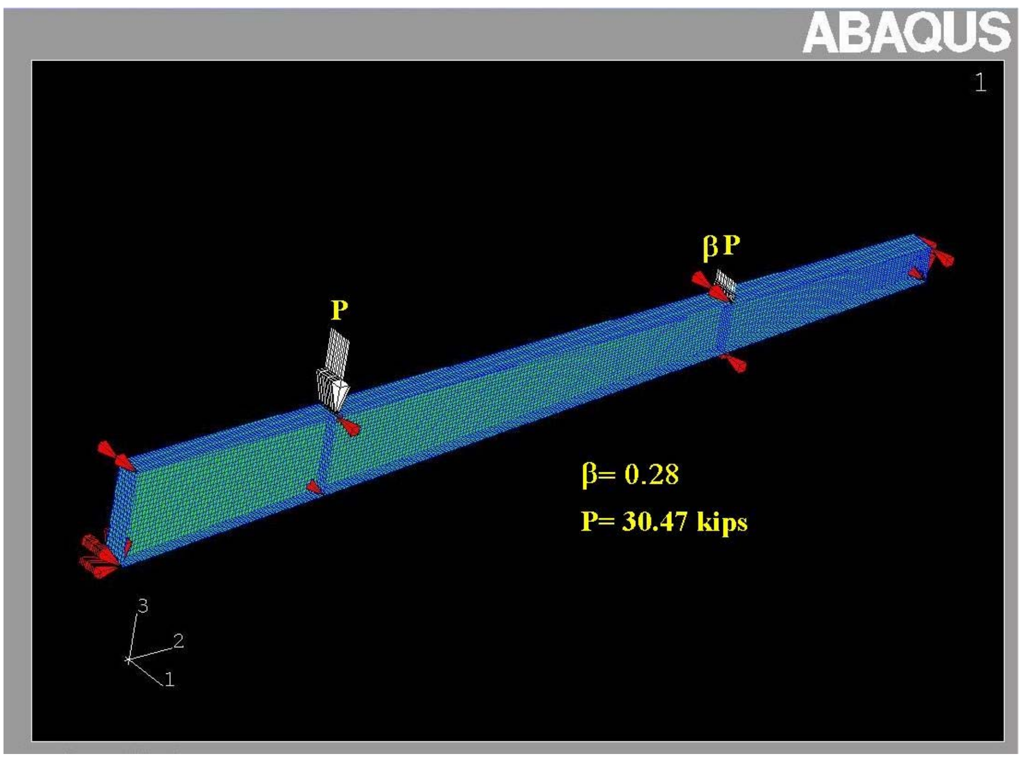

Figure 17 Verification Beam with Applied Loads and Reactions

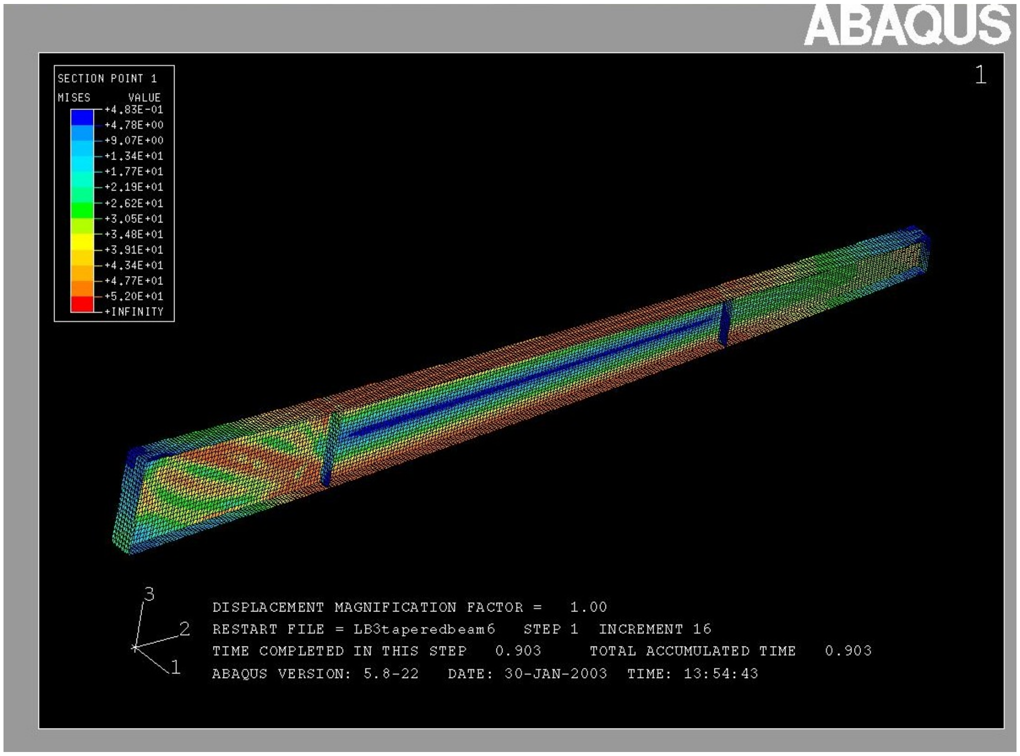

Figure 18 Verification Beam von Mises Stress Distribution

In Prawel's experiment, the tapered beam reached a total load of 39.0 kips (P = 30.47 kips and βP = 8.53 kips) before unloading and had a maximum vertical deflection at the beam mid-span of 1.04 inches. Using an imperfection seed scale factor of $L_b/500$, the ABAQUS model reaches a total load of 36.07 kips (P = 28.18 kips and βP = 7.89 kips) before unloading and deflects at the beam mid-span a total of 0.903 inches. The ABAQUS model also has a small amount of lateral movement as well. Figure 19 is a comparison of in-plane load vs. deflection between the experimental and analytical beams. The results of the two models are similar; as the two lines are approximately parallel throughout the tests. The experimental beam by Prawel et al. was not carried into the unloading portion of the equilibrium path far enough to compare unloading characteristics between the actual beam and the ABAQUS model. It is noted that the effects of residual stresses are not incorporated into the ABAQUS models and thus represents a slight deviation in the modeling of the LB-3 test beam. However, in an overall sense, the finite element model of the LB-3 beam in ABAQUS closely resembles the behavior of the experimental test results. Therefore, the nonlinear finite element modeling strategies using ABAQUS appear valid for the analysis of web-tapered I-shaped beams and will be used throughout the parametric study discussed herein.

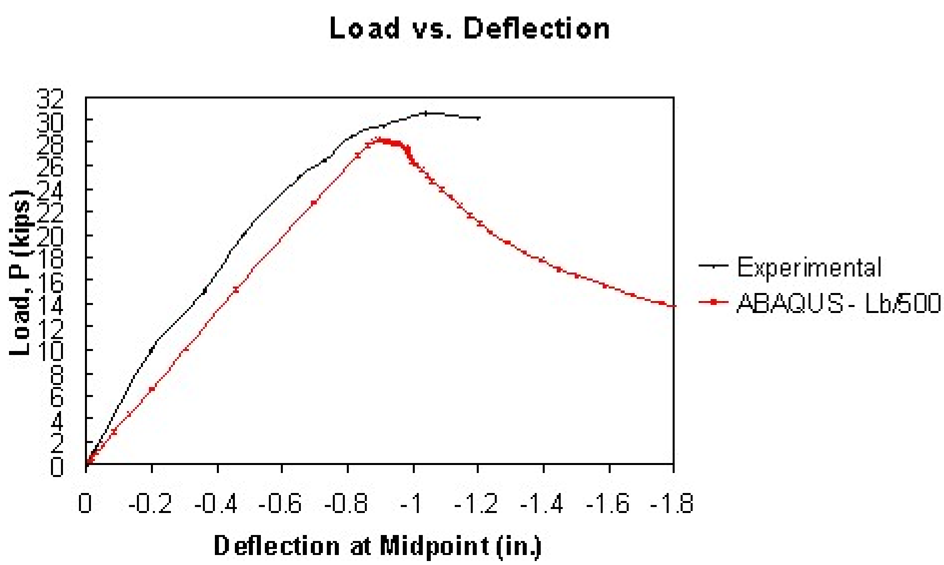

Figure 19 Verification Study LB-3 Beam Load vs. Deflection

In addition to the previous beam study, five different geometries of rafter-to-column sub-assemblages (designated as KNEE 1, 2, 3, & 5 by Sumner (1995)) are modeled after the experimental tests carried out by Sumner and Murray at Virginia Tech. Comparisons of the ABAQUS model response with the experimental results are presented in Figures 20 through 23. Figure 24 depicts the test setup used by Sumner and Murray. Table 2 gives the geometric data for each of the test specimens. For the tests of Knees 1, 2, and 3, a positive type of loading is applied, inducing a negative moment into the column – rafter section. For test specimen designated as Knee 5, a cyclic loading is applied, producing both positive and negative moments into the frame section. In the figure legends, the "k" percentages reference the bracing force used (i.e. the percentage of the force required to yield the compression flange)) acting through a displacement if L / 1000 (where L is the maximum unbraced length within the test specimen). Similarly, the "I" percentages represent the value of the scaling factor used in conjunction with the initial geometric imperfections obtained from a linearized eigenvalue buckling analysis.

Table 2 Cross-Sectional Data for Knee Test Specimens (Sumner 1995)

Test Designation	Depth at Connection (in.)	Flange Width (in.)	Column Web Thickness (in.)	Column Flange Thickness (in.)	Rafter Web Thickness (in.)	Rafter Flange Thickness (in.)
Knee 1	24	6	0.150	0.375	0.160	0.313
Knee 2	24	6	0.127	0.375	0.127	0.313
Knee 3	24	6	0.120	0.375	0.120	0.313
Knee 5	24	6	0.375	0.375	0.127	0.313

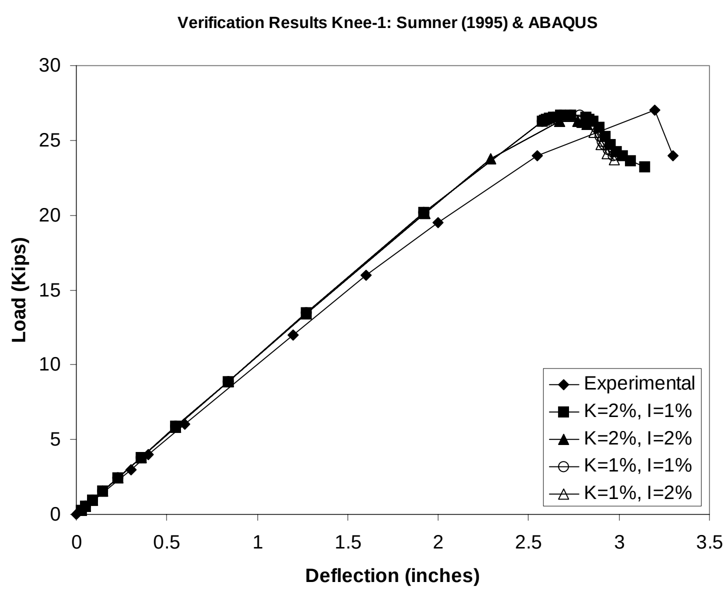

Figure 20 Test Specimen - Knee 1

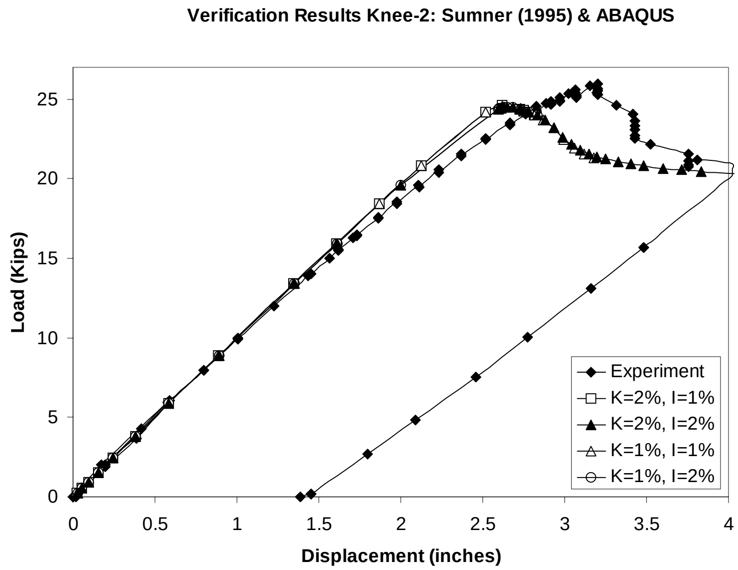

Figure 21 Test Specimen - Knee 2

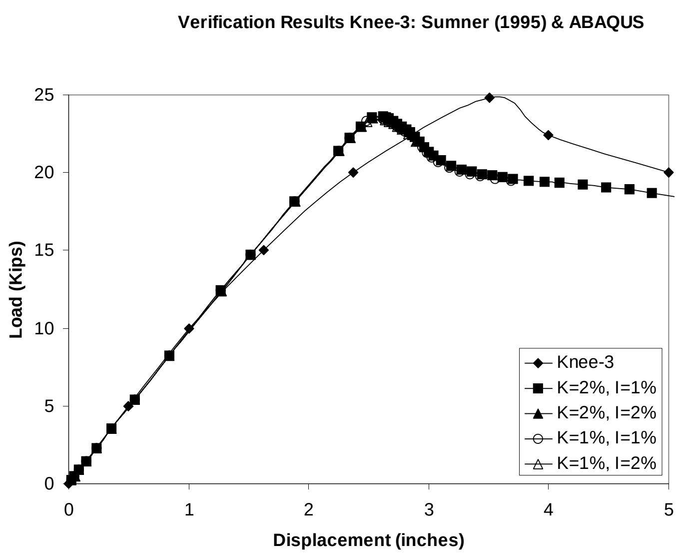

Figure 22 Test Specimen - Knee 3

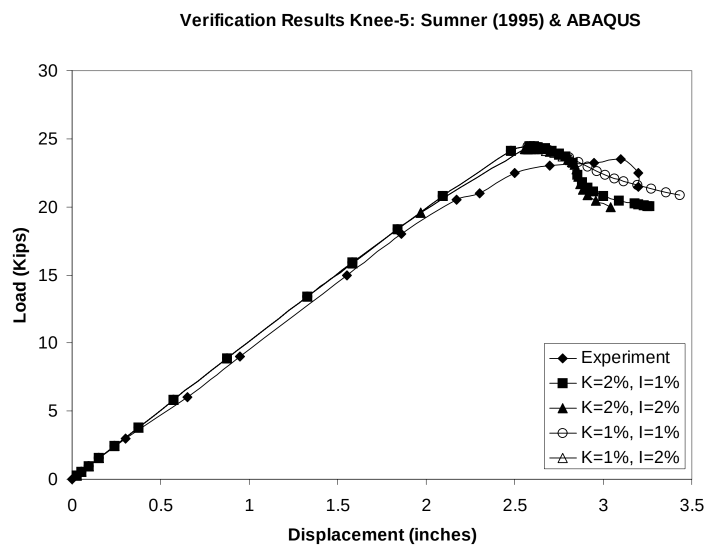

Figure 23 Test Specimen - Knee 5

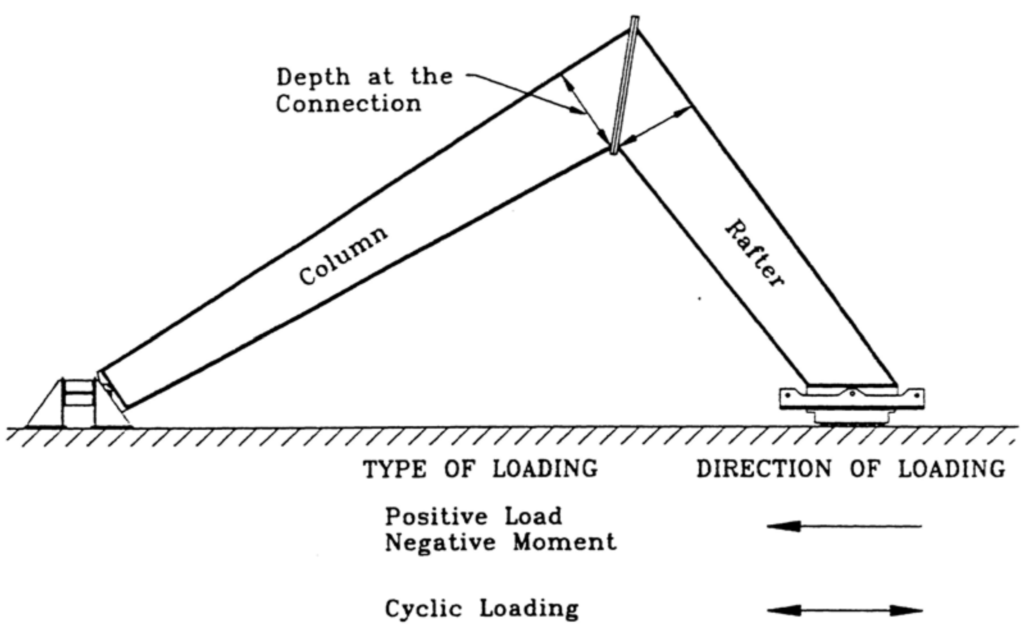

Figure 24 Rafter-to-Column Sub-Assemblages (Sumner 1995)

3.3 BENCHMARK FRAME

After obtaining good results in the verification study, the verified nonlinear finite element modeling strategies are used to model a benchmark tapered-member gable frame whose proportions are arrived at through consultation with the Metal Building Manufacturers Association (MBMA). The frame design provided possesses features that are typical of frame geometry common in low-rise metal buildings currently being constructed in the U.S. Figure 25 illustrates the dimensions and members sizes for the benchmark frame. The yield strength and modulus of elasticity of the steel used for the frame and subsequent parametric studies is 56.8 ksi and 29600 ksi, respectively. Poisson's ratio is set at 0.3 for steel. Spacing from centerline to centerline of frames is taken to be 25 feet (i.e. the interval between frame lines as measured into the page). The unbraced length of the tapered beams is equal to the spacing of the z-purlins. For the benchmark frame, this unbraced length is 4'-4 11/16" for the first 2 rafter segments and 5'-0" for the next 6 rafter segments, as measured along the rafter longitudinal axis heading from the eave to the ridge-line of the frame. In addition, the frame is braced against lateral movement on the columns at 7'-4" and 13'-4" above the ground. The bracing system for the frame consists of z-purlins to brace the top of the tapered members and angle members attached to the z-purlins and bottom flange of the tapered member to brace the bottom of the frame girder (e.g. the angles form knee bracing for the bottom flange of the rafters and interior flanges of the columns). Figure 26 is an illustration of the bracing system designed for the benchmark frame in the current study. Spring elements (SPRING1) are utilized in ABAQUS to simulate the stiffness of each lateral brace point. The stiffness of each spring is calculated as 2% of the axial force needed to yield the compression flange acting through a distance equal to $L_{b(max)}/500$. The equation used to calculate the stiffness at each z-purlin is as follows:

$$k = \frac{0.02P}{L_b/500} \quad (3\text{-}1)$$

Pinned boundary conditions are applied to the column bases. The load applied to the frame consists of point loads at the z-purlin locations and are calculated as the service, or unfactored, loads. The maximum dead load calculated for a tributary area of 125 square feet is 3.077 psf including frame self-weight and the live load calculated is 30 psf from the MBMA Low-Rise Building Systems Manual (1996). The frame analysis does not include wind loads or snow loads. The imperfection seed for the benchmark frame is illustrated in Figure 27. The first eigenmode is used as the superimposed imperfection seed in the frame analysis. The buckled portion of the frame, as indicated by the linearized eigenvalue analysis, is located adjacent to the ridge-line of the symmetric frame; a scale factor of $L_b/1000$ is utilized in the analysis.

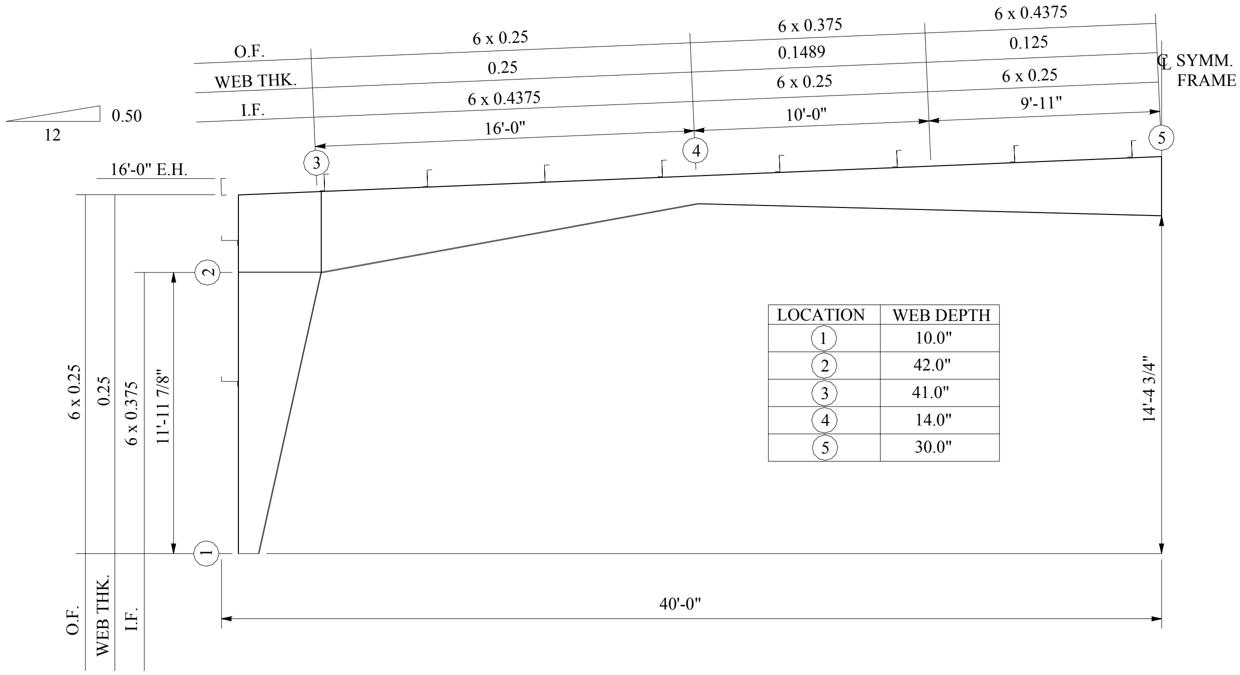

LOCATION	WEB DEPTH
1	10.0"
2	42.0"
3	41.0"
4	14.0"
5	30.0"

Figure 25 Benchmark Frame

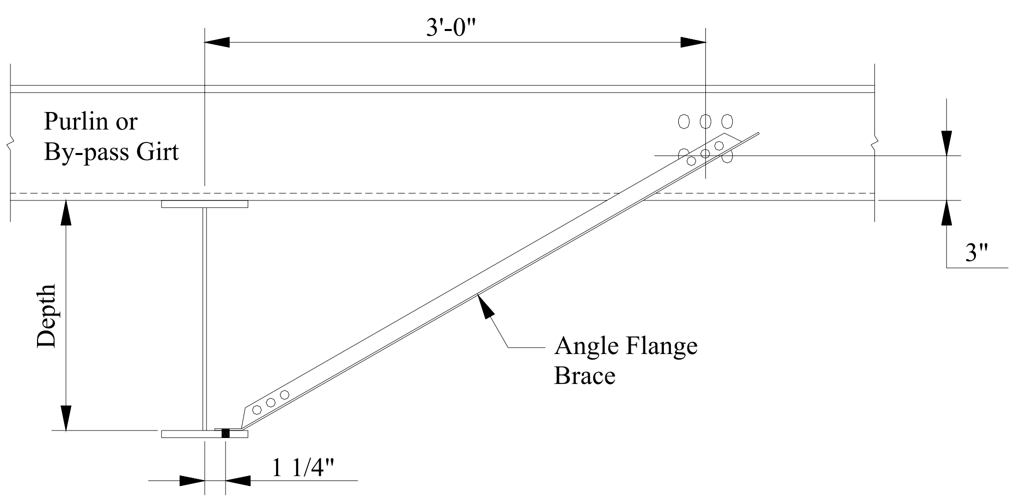

Figure 26 Typical Bracing Detail for Web-tapered Gable Frames

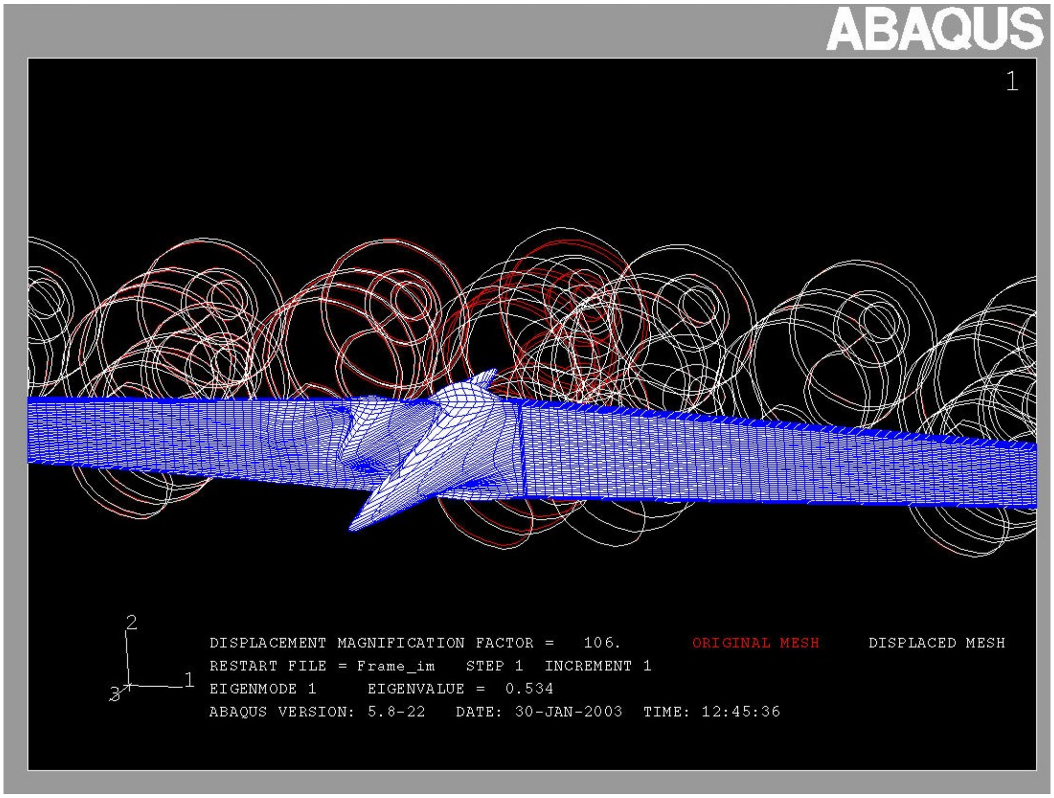

Figure 27 Imperfection Seed for Benchmark Frame

The ABAQUS analysis results for the benchmark frame yield a load proportionality factor of 1.19 at ultimate; meaning the frame will fail at 1.19 times the applied service loads (i.e. factor of safety = 1.19 against collapse). The failure mode of the benchmark frame involves primarily web local buckling near the centerline of the frame. Figures 28 and 29 illustrate the von Mises stresses in the frame at maximum loading and Figure 30 illustrates the von Mises stresses on the entire frame in the unloading portion of the equilibrium path.

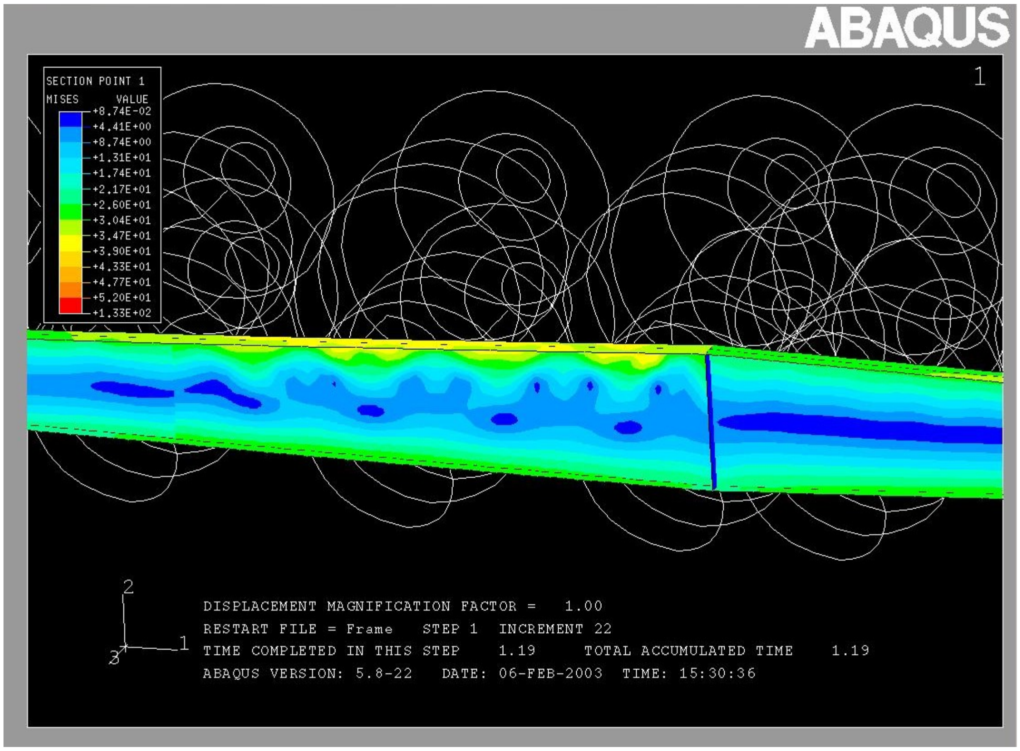

Figure 28 von Mises Stresses at Maximum Loading on Benchmark Frame

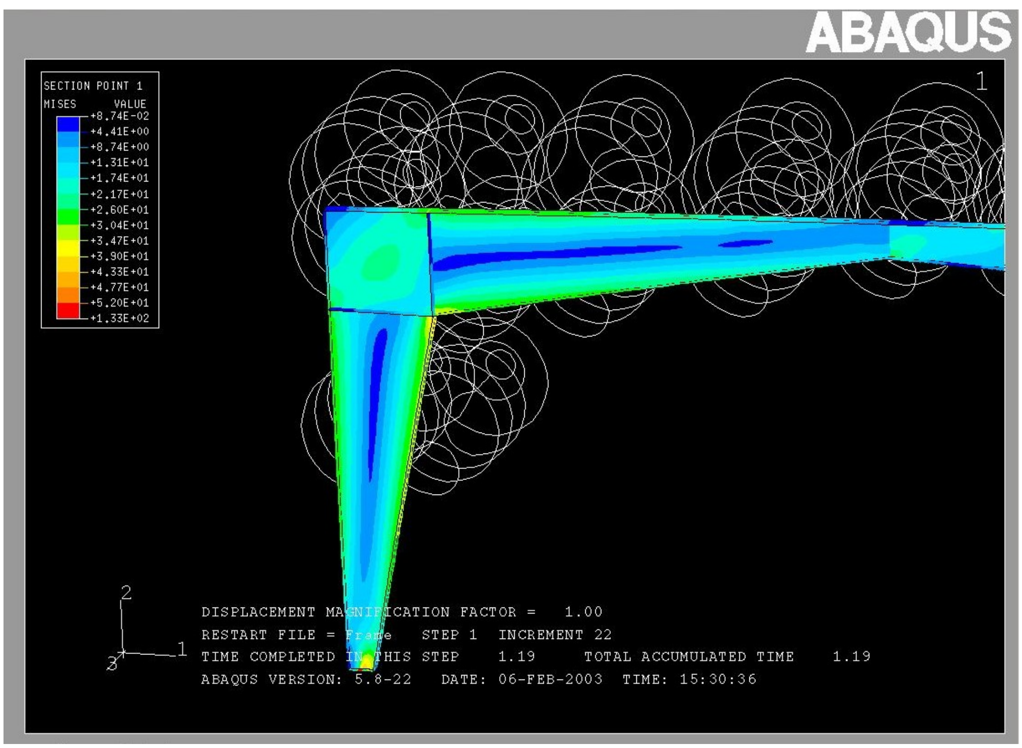

Figure 29 von Mises Stresses at Maximum Loading on Benchmark Frame

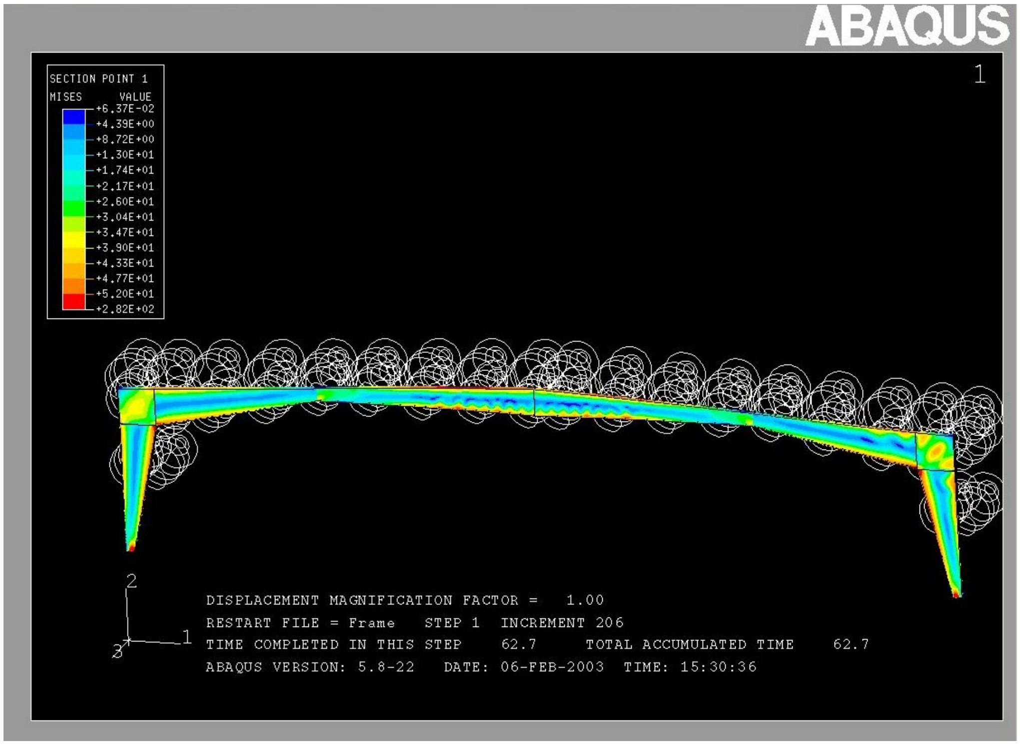

Figure 30 von Mises Stresses After Unloading Begins on Benchmark Frame

3.4 BEAM SUB-ASSEMBLAGE

Following the frame analysis in ABAQUS, the frame is modeled using the computer software package Algor to obtain the moment distribution over the entire frame: Figure 31 illustrates the moment distribution over the entire frame as obtained from Algor. The moments at the endpoints, or brace points, of the unbraced length of the critical section of the frame are determined as well. This critical section of the frame is then modeled as a simply supported beam, or sub-assemblage extracted from the entire frame, but with continuity effects retained. The critical section is modeled with an unbraced length of 60 inches and an additional 60-inch unbraced length to either side of the critical section. The critical section retains the same material properties and geometry as in the frame. The additional lengths on either side of the critical section retain the same geometry as in the frame but the modulus of elasticity is increased by a multiple of ten. By using a Young's Modulus of 290000 ksi for the end sections, the material will approach a rigid condition and the additional beam lengths will force compatibility and continuity at the critical section junction. Utilizing the additional beam sections will allow point loads to be applied at the beam ends. This, in turn, will allow the same moment gradient to be applied across the critical sub-assemblage section as that applied to the same section within the benchmark frame analysis; in this way, a computationally efficient and numerically accurate finite element base model is created for use in subsequent parametric studies. The applied moment at the shallow end of the critical beam section is 198.75 kip-ft. and the moment at the deep end of the beam section is 209.08 kip-ft. Reaction points are placed as pinned connections at the mid-height of the web to model the beam as simply supported. The pinned connections are placed one element into the rigid portion of the model so the affects of the reactions are not present in the critical section. The same spring stiffness values are used in the beam sub-assemblage model. Figure 32 depicts the modeled critical section. For this finite element model, 19,866 nodes and 19,500 shell elements are used to construct the beam. Figure 33 shows methodology of how the critical section is modeled in ABAQUS.

Developing the imperfection seed for the beam sub-assemblage of the frame critical section proves to be difficult. Analysis by ABAQUS results in unrealistic buckled configurations for each of the three eigenmodes developed. Therefore, the beam cross-section is changed slightly to obtain more realistic buckling modes (i.e. ones more consistent, in a phenomenological sense, with the governing modes displayed by the full benchmark frame model). Since the critical section in the frame fails due to local buckling of the web and compression flange, the average flange thickness is used for both the top and bottom flange thicknesses except for the compression flange over the critical section. The smaller of the two flange thicknesses is used for the compression flange over the critical section for the linearized eigenvalue buckling analysis in ABAQUS. This forces the beam to buckle in a realistic fashion. The buckled imperfection for the beam sub-assemblage is shown in Figure 34. An imperfection seed scale factor of $L_b/500$ is used in the sub-assemblage modeling.

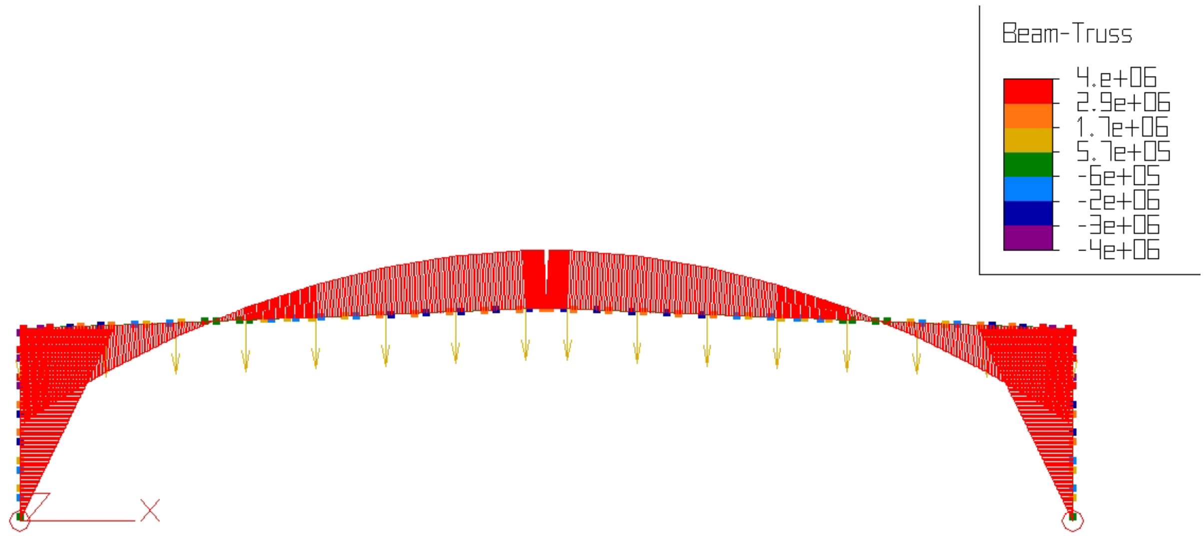

Figure 31 Moment Distribution Across Benchmark Frame

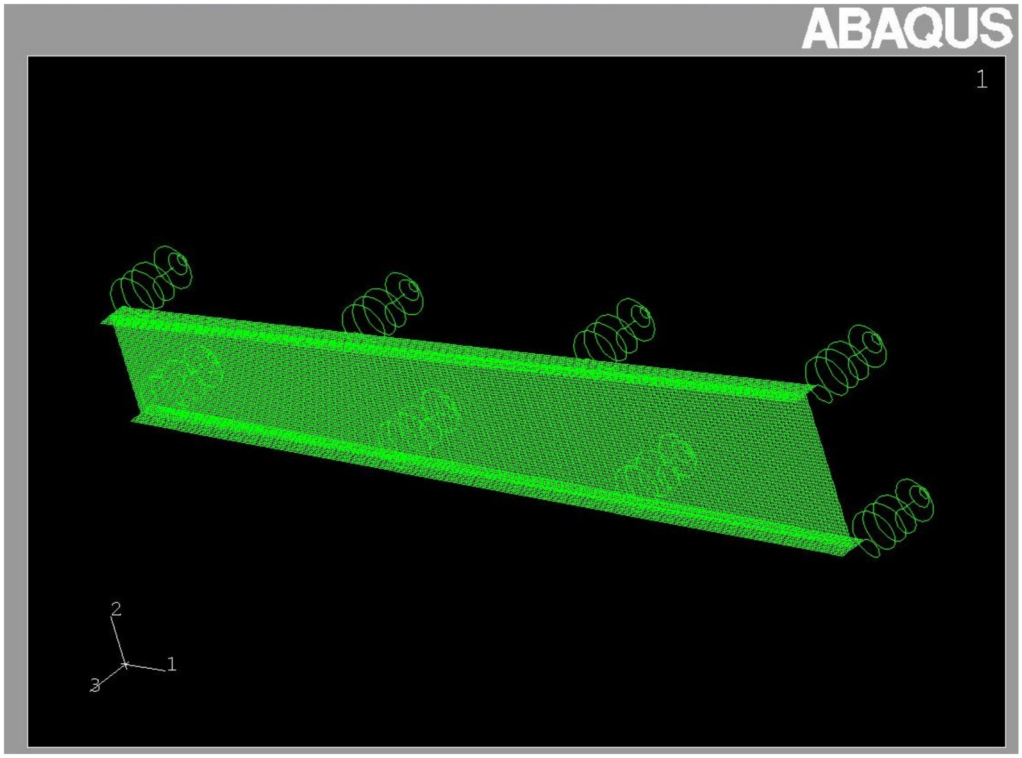

Figure 32 Sub-assemblage Mesh with Spring Braces

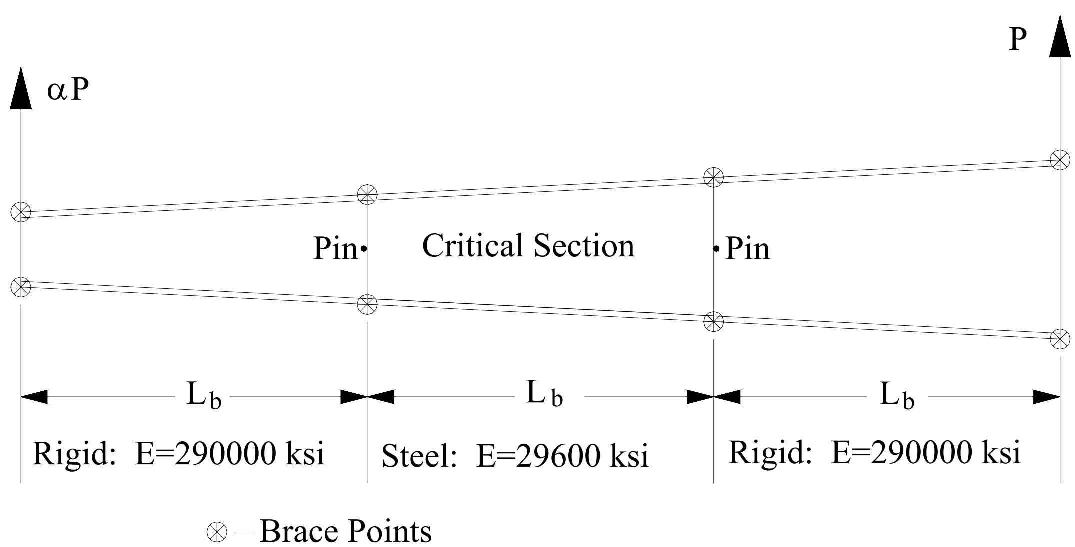

Figure 33 Modeling Methodology of Critical Section

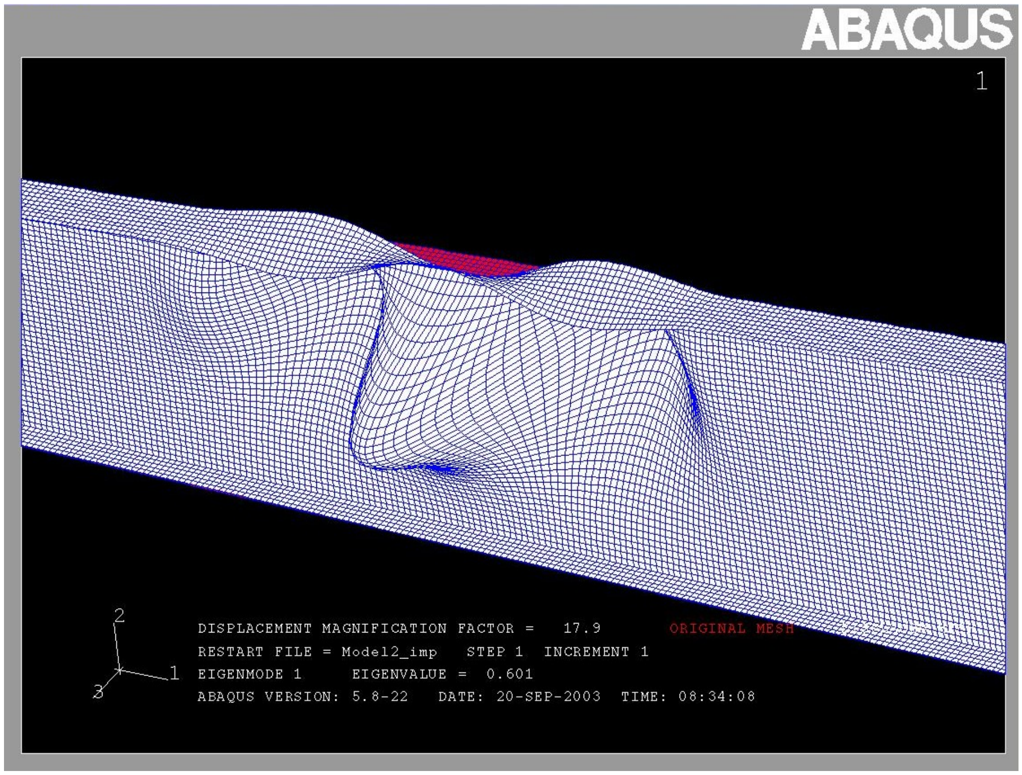

Figure 34 Sub-assemblage Imperfection Seed

The results of the sub-assemblage beam are very similar to the results for the critical section of the frame. The beam model fails at a load proportionality factor of 1.11 whereas the frame fails at 1.19. This indicates that the beam will fail at 1.11 times the applied service loading. Since the applied loadings in the frame and beam create the same moment gradient across the critical section, and since the modes of failure are quite similar, the modeled beam behavior is considered to be a close representation of the behavior of the same section in the benchmark frame. In addition, the modeled beam is slightly conservative since it fails at a lower level than the frame. Figure 35 and Figure 36 show the von Mises stress distribution at the ultimate load on the beam sub-assemblage. Note the similar von Mises stress patterns as in the critical section in the frame in Figure 28.

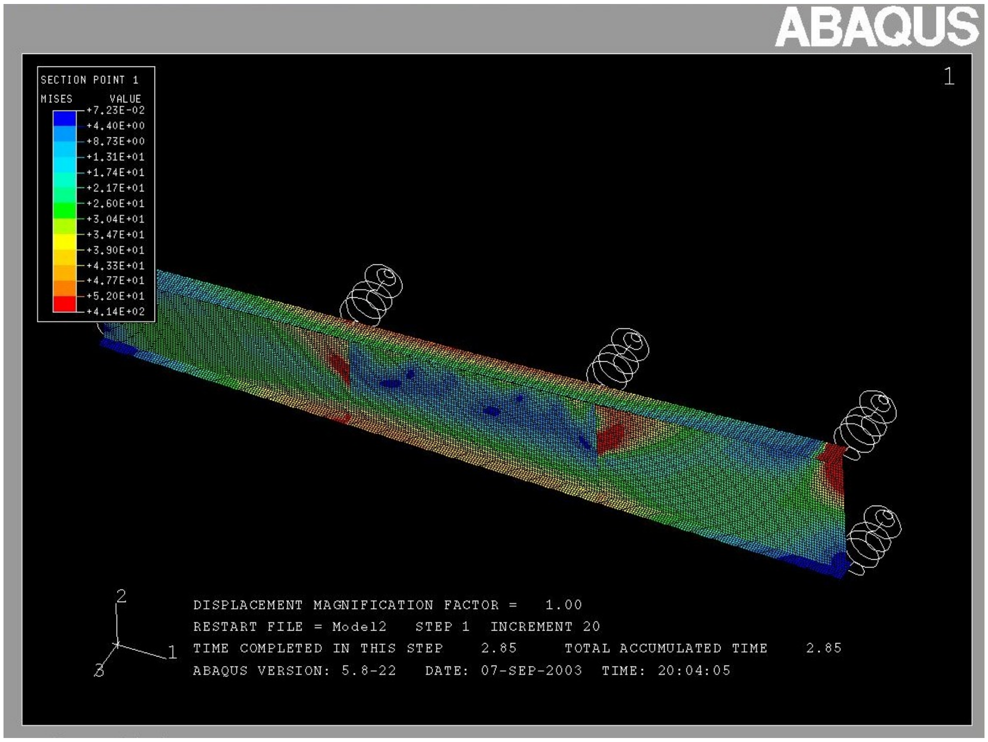

Figure 35 von Mises Stress Distribution for Sub-assemblage Beam

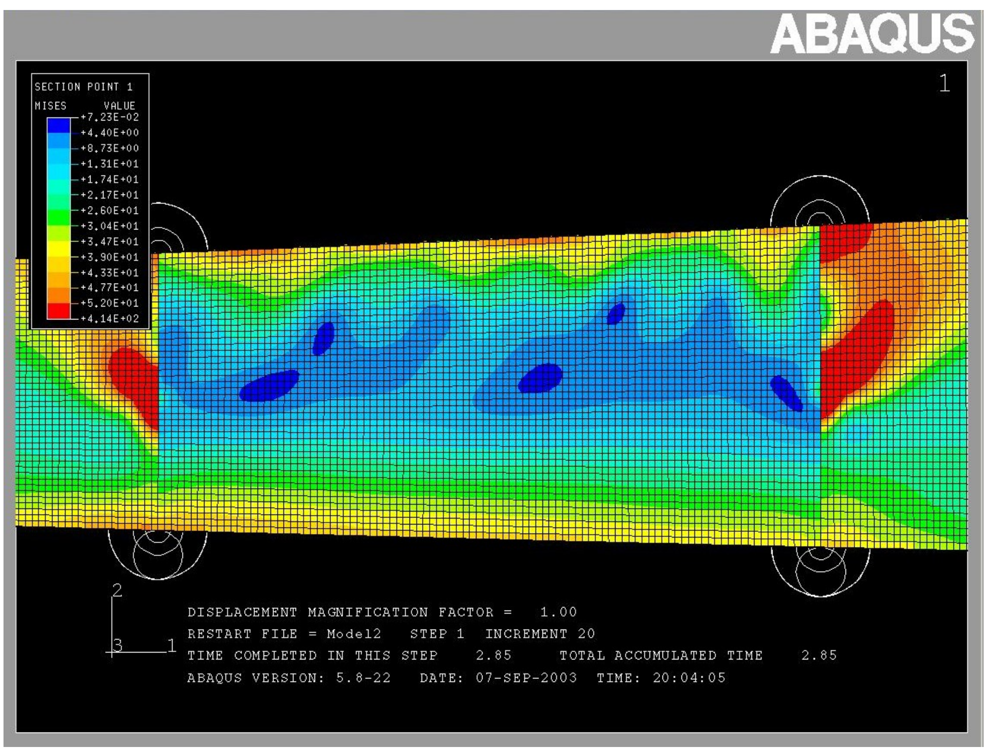

Figure 36 von Mises Stresses on Critical Section of Sub-assemblage Beam

4.0 PARAMETRIC STUDY

A parametric study is performed to determine the effects of various cross-sectional proportions and beam geometries on flexural ductility of web-tapered I-shaped beams. The web-tapered member parameters that vary in the study include the slenderness ratios, h/t_w and $b/2t_f$, the tapering ratio γ, and the unbraced lengths of the beams. Figure 37 shows the two rafter sections of the benchmark frame whose geometry serve as the points of departure in the current parametric study. The rafter section denoted by "I" is the rafter section where local buckling of the web initiated within the benchmark frame; a condition corresponding to the ultimate load of the overall gabled structure. It was this section, "I", that was considered in the sub-assemblage modeling discussed earlier. As mentioned in the earlier discussion given herein, ABAQUS SPRING1 elements were used to simulate the flexible bracing effects present at the ends of rafter section "I" in the actual benchmark frame model. The modeling techniques employed in the parametric study related to the rafter sections are similar to those used for the sub-assemblage beam, with the exception of the out-of-plane lateral bracing stiffnesses. Instead of using the lateral bracing stiffnesses consistent with those of the benchmark frame model, idealized, rigid supports replace spring elements to allow no lateral movement at the brace points. This approach is adopted in order to limit the total number of parameters being studied in this work (i.e. the effects of bracing stiffness are not considered herein). Another difference between the tested configurations of the sub-assemblage beams used in the parametric study versus those used to model the benchmark frame lies in the nature of the applied loadings. The applied loadings used in the sub-assemblages for the parametric study are constructed so as to result in the theoretical plastic cross-sectional moment, M_p, at the smaller and larger ends of the unbraced length L_b, simultaneously (see Figure 38). Initial work on the parametric studies that are part of the current research focuses on the behavior of rafter section "I".

Section "II" from Figure 37 is modeled in part 2 of the parametric study. The section "I" beam has an unbraced length of 60 inches and is modeled in the same fashion as rafter section "I". To keep the aspect ratios of the finite elements approximately one, the number of nodes is increased to 22,260 and the number of elements is increased to 21,912 in the rafter section "II" models. After the first two parts of the study are completed, sections "I" and "II" are lengthened to an unbraced length of $1.25L_b$, or 75 inches. The beam end cross-sections are held constant at their original proportions throughout any length changes. It is pointed out that as a result of this practice; subsequent length changes impact the tapering ratio, γ, for the beams. The length change is undertaken in effort to better understand the impact of cross-sectional plate slenderness ratios on beam ductility at various beam lengths. The lengthening of rafter sections "I" and "II" form the geometrical basis for the third and fourth parts of the parametric study, respectively. The 60 in. and 75 in. section "I" beams retain a positive applied moment while the 60 in. and 75 in. section "II" beams retain a negative applied moment. The positive and negative moments coincide with the positive and negative moment regions of the benchmark frame. Section "I" and "II" beams will be identified as Model-1 and Model-2, respectively hereafter.

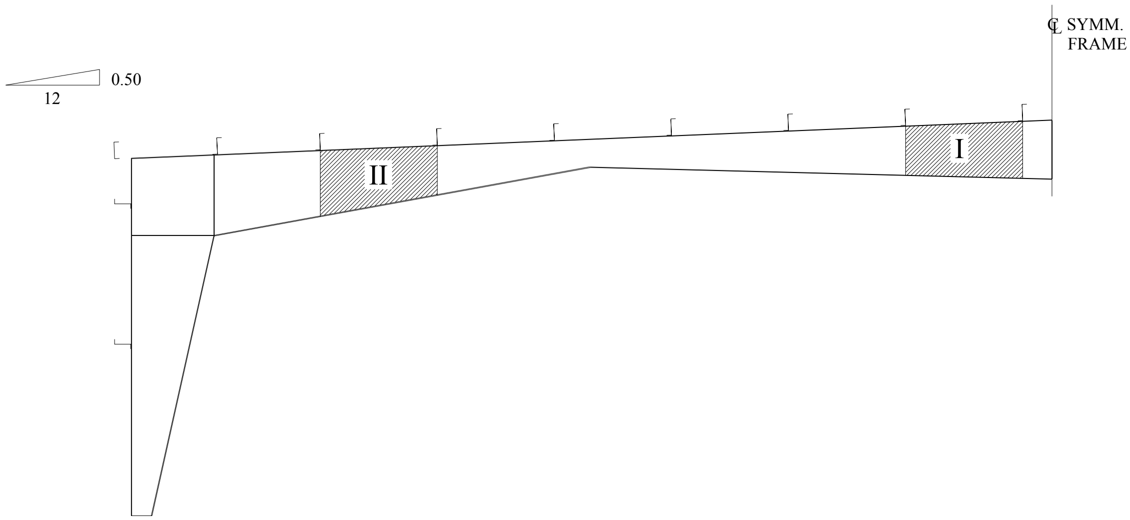

Figure 37 Modeled Sections of the Benchmark Frame

When varying the slenderness ratios h/t_w and $b/2t_f$ for each beam, oftentimes the models in ABAQUS utilize constant plate widths in effort to maintain a given flange width – to – web depth ratio and hence various plate thicknesses are used to affect slenderness change. The different plate thicknesses used in the study, presented in Table 3, include:

Table 3 Plate Thicknesses Used in Parametric Study

1/8 in.
3/16 in.
1/4 in.
5/16 in.
3/8 in.
7/16 in.
1/2 in.
9/16 in.
5/8 in.
3/4 in.
7/8 in.
1 in.
1 1/8 in.
1 1/4 in.

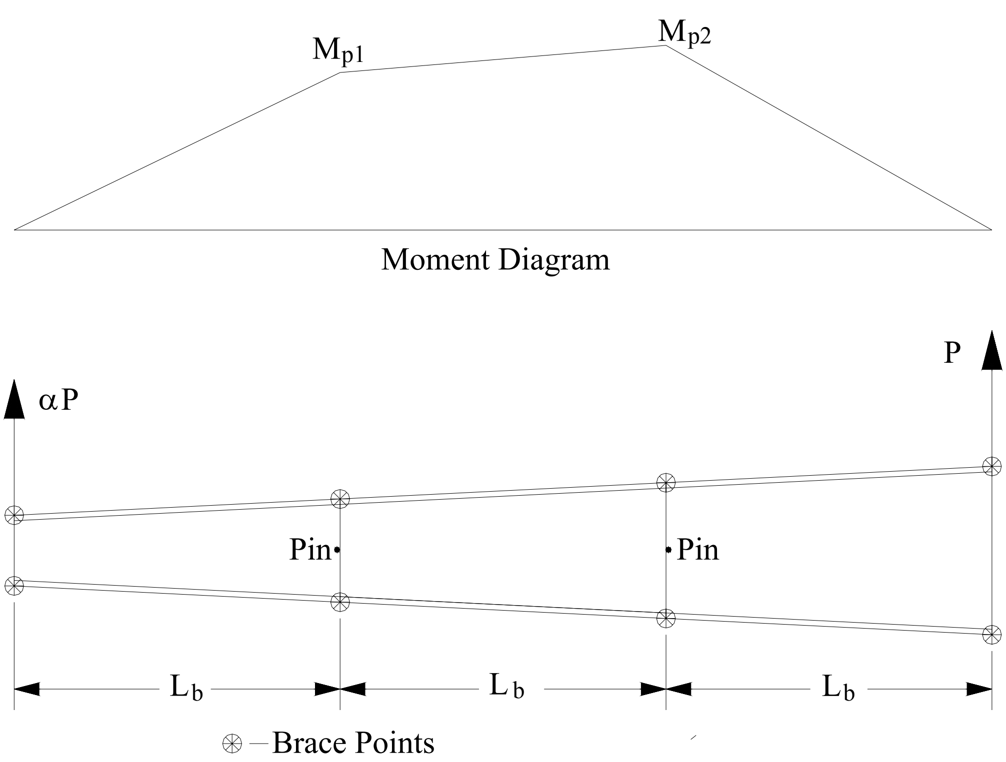

Figure 38 Applied Loadings and Moment Diagram

While it is that portions of the parametric study are carried out using constant plate widths, some variations are accommodated in this regard. Flange widths vary, to some extent, within all four parts of the parametric study. The study includes flange widths of 6 in., 8 in., 10 in., and 12 in. Appendix A presents examples of the ABAQUS input files used as part of the current research. Material properties for the parametric study beams remain the same as those used for the benchmark frame. Therefore, the limiting slenderness ratios from AISC-LRFD Table B5.1 may be expressed as follows:

For the flanges:

$$\lambda_p = 0.38\sqrt{E/F_y} = 8.67 \tag{4-1}$$

For the web:

$$\lambda_p = 3.76\sqrt{E/F_y} = 85.83 \tag{4-2}$$

4.1 PARAMETRIC STUDY RESULTS

A portion of the finite element model post-processing involves the generation of moment-rotation plots to aid in the quantification and comparison of the various parametric influences on web-tapered beam ductility. Tabulated results gleaning from this type of graphing are presented in Appendix B as results from 210 distinct parametric combinations of web-tapered beam geometries considered in the finite element modeling. From the data collected, it is observed that attainment of M_p is difficult to achieve in the case of a gradual moment gradient across the unbraced length so as to result in equal cross-sectional stresses in the end sections at ultimate. For the web-tapered I-shaped beams, an ultra-compact section ($\lambda_f << \lambda_p$, $\lambda_w << \lambda_p$) is needed to reach the plastic moment. While this was initially seen as a problem peculiar to web-tapered beams (i.e. web-tapered beams whose cross-sections easily satisfied prismatic member compactness criteria but that cannot attain M_p), it was later learned that prismatic beam suffer from the same "short coming" under the action of a constant moment loading. Experimental results by Adams, Lay, and Galambos (1965) showed prismatic I-shaped beams loaded with a constant moment not reaching the plastic moment M_p despite the fact that the members easily satisfied the compactness requirements from Table B5.1 in the Specification. The experimental results of the tests by Adams et al. are presented in Figure 39. The material used in these experiments was ASTM A441 (F_y = 50 ksi) steel. Once again it is pointed out that the beam section tested in this experimental program, the 10WF25, is considered to be a compact section, yet the rotation capacity, R, equals zero since M_p was not attained in several of the tests. As observed from Appendix B, web-tapered beams with similar L/r_y, λ_f, and λ_w values as utilized in these experimental tests, also reach similar M/M_p values as those observed in the prismatic members.

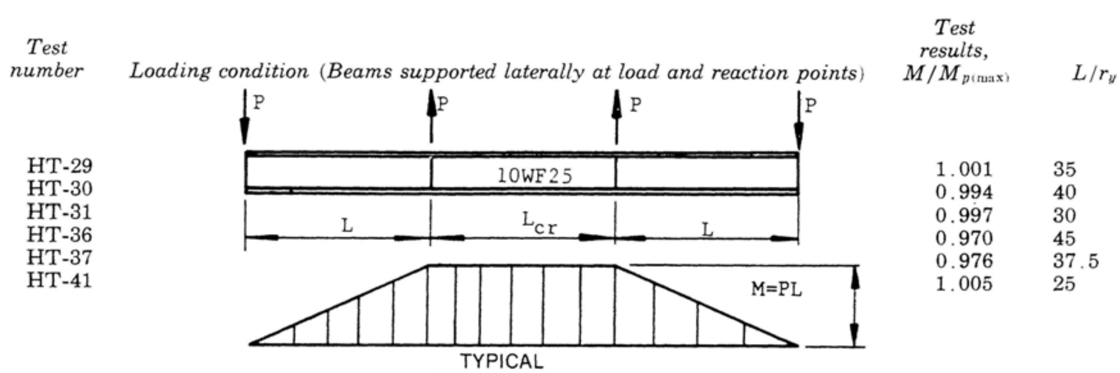

Figure 39 Experimental Results of Prismatic Members Failing to Reach M_p in a Constant Moment Loading Condition (Adams et al. 1965)

Other experimental results that show difficulty prismatic I-beams have in reaching the plastic moment, M_p, under uniform moment loadings include McDermott (1969) and Frost and Schilling (1964). McDermott (1969) presented results of beams with A514 steel needing a slenderness ratio $b/2t_f$ of the compression flange to be approximately 6 or less to obtain the full plastic moment. These results were for extremely low L/r_y values (<8). For L/r_y values in the range of 20 to 25, a slenderness ratio of the compression flange must be approximately 5 or less to obtain M_p. The limiting slenderness ratio for an A514 Grade B steel (F_y = 100 ksi) compression flange is $\lambda_f = 6.47$ according to the current Table B5.1 requirements in the current Specification. Research by Frost and Schilling (1964) indicated that a prismatic hybrid beam subjected to a uniform moment loading had difficulty reaching the plastic moment M_p for compact sections as well. The limiting slenderness ratio for the case of the USS "T-1" type A constructional alloy steel (F_y = 100 ksi) hybrid beam compression flange utilized in Frost and Schilling's work is $\lambda_f = 6.47$. Each test specimen had a $b/2t_f$ value below 4 for the compression flange; an ultra-compact condition.

Comparing the AISC-LRFD moment capacity of the web-tapered beams vs. the moment capacity obtained utilizing ABAQUS indicates that the design provisions in Appendix F are accurate for beams with slenderness ratios close to the limits specified in Table B5.1. However, almost every beam modeled in ABAQUS has a moment capacity predicted by AISC-LRFD of M_y since $0.6F_y$, from equation (1-23), nearly always controls. This is the case for beams with geometries similar to the beams modeled. Beams with larger length – to – depth ratios would use different design provisions. For ultra-compact sections, AISC-LRFD Appendix F is markedly conservative: the ratio of the ultimate moment capacity predicted by ABAQUS to the ultimate moment capacity predicted by AISC-LRFD could be as high as 1.29 (as seen in

Appendix B). For slender sections, Appendix F is slightly unconservative: the ratio of the ultimate moment capacity predicted by ABAQUS to the ultimate moment capacity predicted by AISC-LRFD could be as low as 0.949 (see Appendix B).

The general behavior of the web-tapered beams subjected to a moment gradient, equal to M_p at the beam ends, is similar to the behavior of the prismatic beams with a uniform moment across the unbraced length. Beams with lower beam slenderness ratios (i.e. L_b / r_y) fail due to local buckling while beams with higher beam slenderness ratios fail due to lateral-torsional buckling. During the parametric study of the 60-inch beams, it is discovered that the 6-inch flange width beams could only obtain the plastic moment M_p with compression flange $b/2t_f$ values of 3.0 or less. However, beams with an 8-inch flange width could reach M_p at much higher slenderness ratios, $b/2t_f$ approximately 6.4 or less. The 6-inch and 8-inch wide flange beams tend to fail due to lateral-torsional buckling, especially with sections that are considered ultra-compact according to AISC-LRFD Specification Table B5.1. The 10-inch and 12-inch flange width beams could reach M_p with $b/2t_f$ ratios as high as 6.67 and 6.86, respectively. The wider flange beams tend to fail due to local buckling, especially with sections considered non-compact according to AISC-LRFD Specification Table B5.1. The 75-inch beams exhibit lesser moment capacity as compared with shorter beams possessing the same cross-sectional slenderness ratios. The rotation capacity also decreases with increasing member length in identical cross-sections reaching M_p when considering 60-inch and 75-inch beams. Table 4 shows this trend for the modeled web-tapered beams. Appendix B shows additional cross-sections that result in similar behaviors at different unbraced lengths. The length – to – depth ratios for the beams modeled in the parametric study are all between two and three.

An interesting footnote to the results from the parametric study relates to the flatness of the overall moment – rotation response of the web-tapered members considered herein. It is noticed that if the geometry of a given beam is such that it could simultaneously attain the full plastic capacity at its ends a rotation capacity of three is also always attained. In other words, attainment of M_p equates with compactness in the beam population studied.

Table 4 Rotation Capacities for the Cross-Section: b = 10 in., t_f = 1.0 in., t_w = 0.25 in.

Model	Lb (in.)	$b/2t_f$	h/t_w	M_p(kip-in)	M_u(kip-in)	R
Model-1 End 1	60	5.00	96.48	16333	16496	2.82
Model-1 End 2	60	5.00	112.56	19362	19556	3.81
Model-1 End 1	75	5.00	96.48	16333	16333	2.20
Model-1 End 2	75	5.00	112.56	19362	19362	2.17

Appendix B compares each web-tapered beam with the limiting unbraced length L_p for prismatic members, as specified in the AISC-LRFD as equation (F1-4). The value for the plastic design for prismatic members L_{pd} is also listed in Appendix B. For prismatic, I-shaped members the limiting unbraced length is determined by the following equation:

$$L_p = 1.76 r_y \sqrt{\frac{E}{F_{yf}}} \tag{4-3}$$

The results from the beams that reached M_p are plotted in three-dimensional space. The rotation capacity R is plotted vs. the plate slenderness ratios h/t_w and $b/2t_f$. Figure 40 and Figure 41 present the h/t_w vs. R and $b/2t_f$ vs. R plots, respectively. The R value plotted is taken to be the average of the rotation capacity values calculated for the two ends of the web-tapered beams. In addition, the slenderness ratio h/t_w used in Figure 40 is the average value for the two ends of the beam. For an economical design of a web-tapered I-shaped beam, the slenderness ratios should be approximately 4.5 or greater and 50 or greater for the $b/2t_f$ and h/t_w values, respectively. Therefore, a three-dimensional surface plot may be placed under the data points representing beams that reached M_p in an "economical design space". The equation that best fits under the data points shown in Figures 40 and 41 is presented as equation (4-4). This equation is only valid for λ_w values between 50 and 100 and λ_f values between 4.5 and 7.

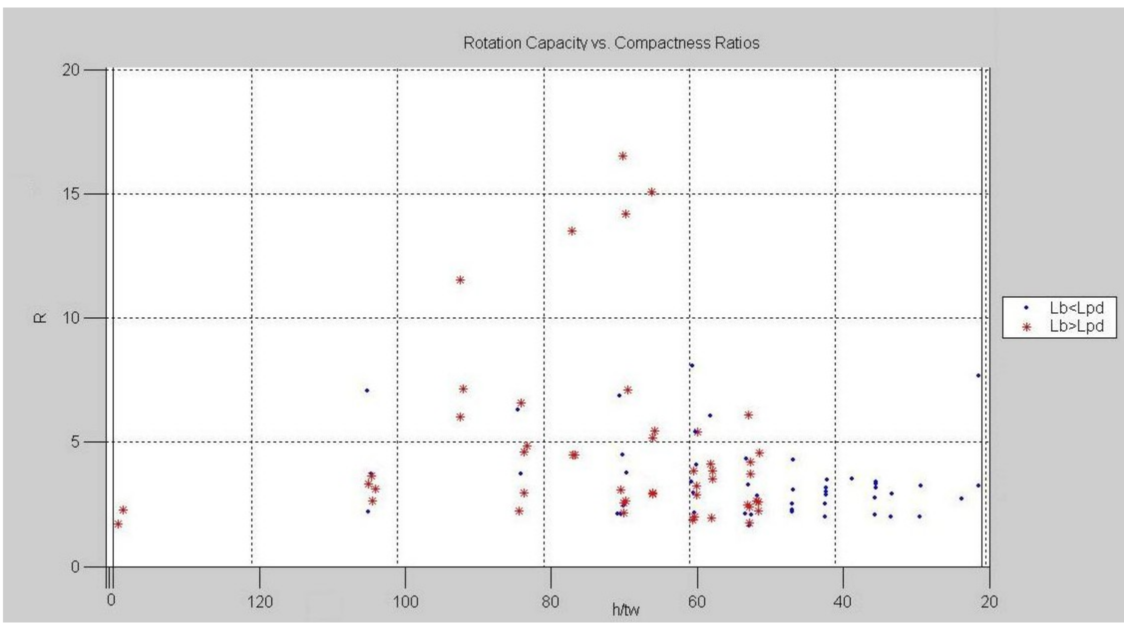

Figure 40 Slenderness Ratio h/t_w vs. Rotation Capacity R

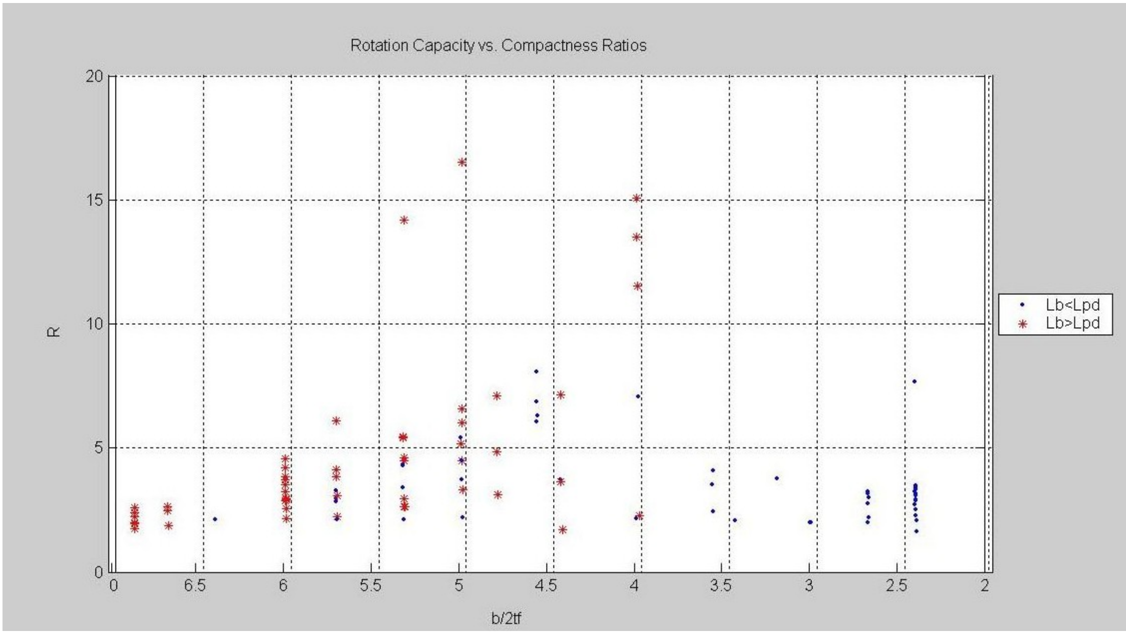

Figure 41 Slenderness Ratio b/2t_f vs. Rotation Capacity R

$$R_{surf} = \frac{\lambda_w \lambda_f}{\sqrt{(\lambda_w - 38)^2 (\lambda_f - 3.5)^2}} \tag{4-4}$$

4.2 OBSERVATIONS OF VON MISES STRESSES IN WEB-TAPERED BEAMS

The von Mises stress distribution in the web-tapered beams varied with the slenderness ratios used for the cross-sections. Only the outermost fibers of a non-compact web yields before the beam begins to unload. Figure 42 shows the von Mises stresses in a web-tapered beam with an extremely slender web at the maximum obtained moment. A greater portion of a web considered compact by AISC-LRFD Table B5.1 yields prior to unloading. Figure 43 is an illustration of a beam with a compact web and the von Mises stress distribution at the maximum loading calculated by ABAQUS.

As stated previously, the 6-inch and 8-inch wide flange beams fail due to lateral-torsional buckling, especially with sections that are considered ultra-compact according to AISC-LRFD Specification Table B5.1. Figure 44 is an illustration of a Model-2, 60-inch beam that moves laterally at the beam mid-span in the compression zone. This particular beam has a 6-inch wide flange with a $b/2t_f$ value of 2.4. The contour lines represent lateral movement with a maximum lateral displacement of approximately 1.08 inches. Figure 45 is an illustration of the von Mises stress distribution at the same load increment as displayed in Figure 44.

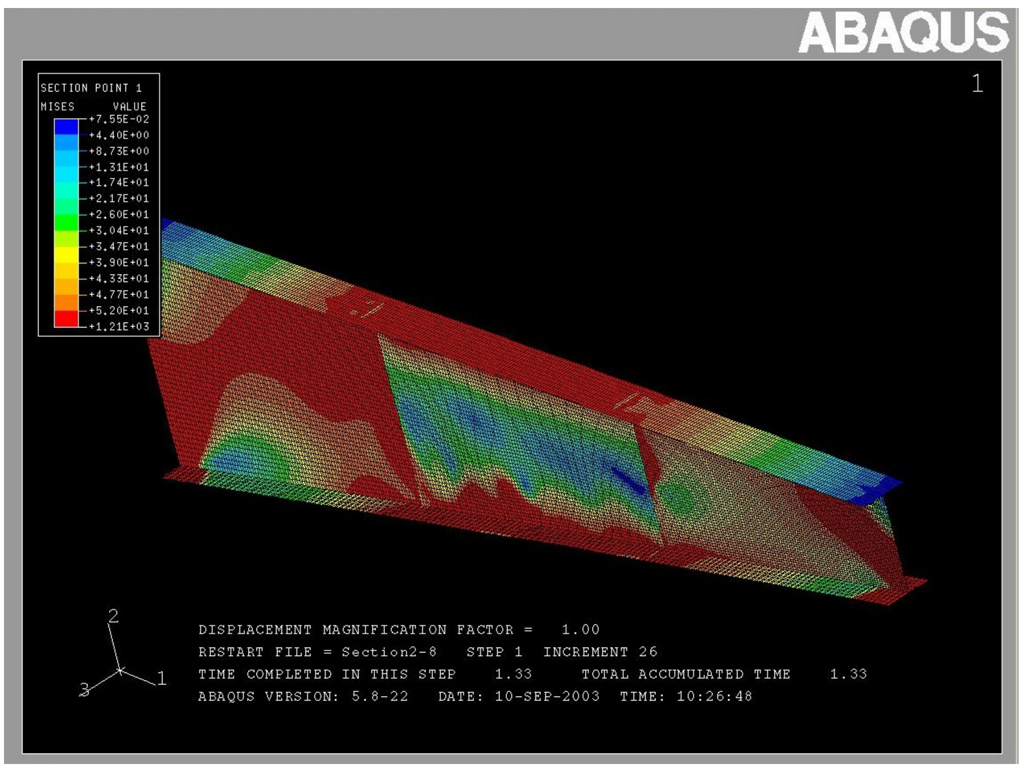

Figure 42 von Mises Stress Distribution Across a Slender Web (avg. h/t_w = 155.8)

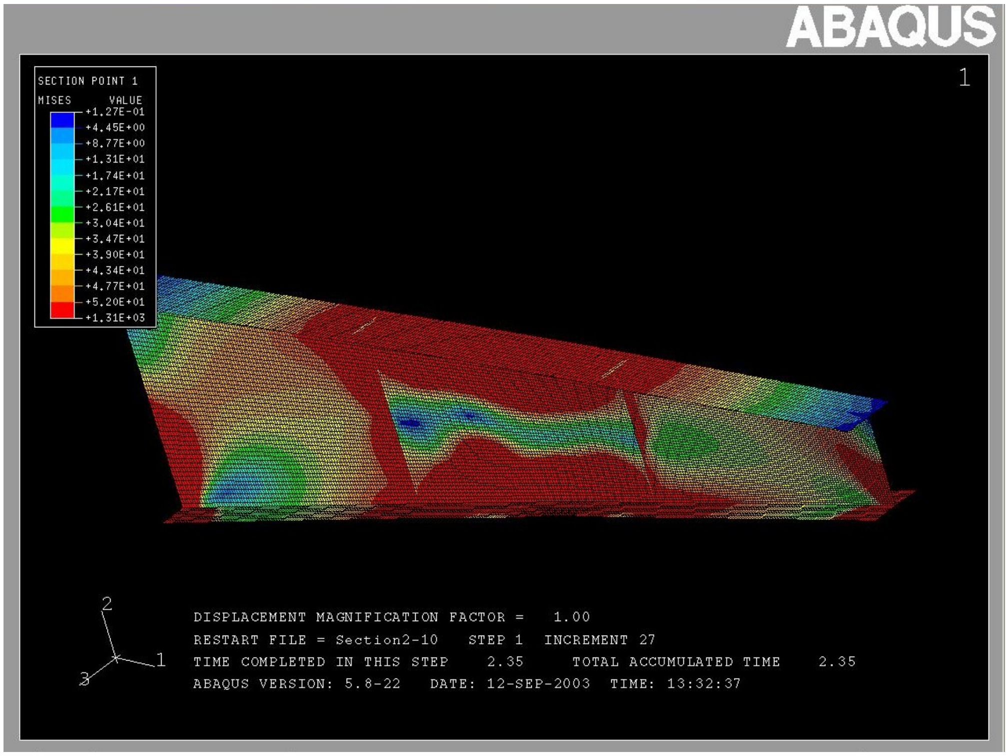

Figure 43 von Mises Stress Distribution Across a Compact Web (avg. $h/t_w = 51.5$)

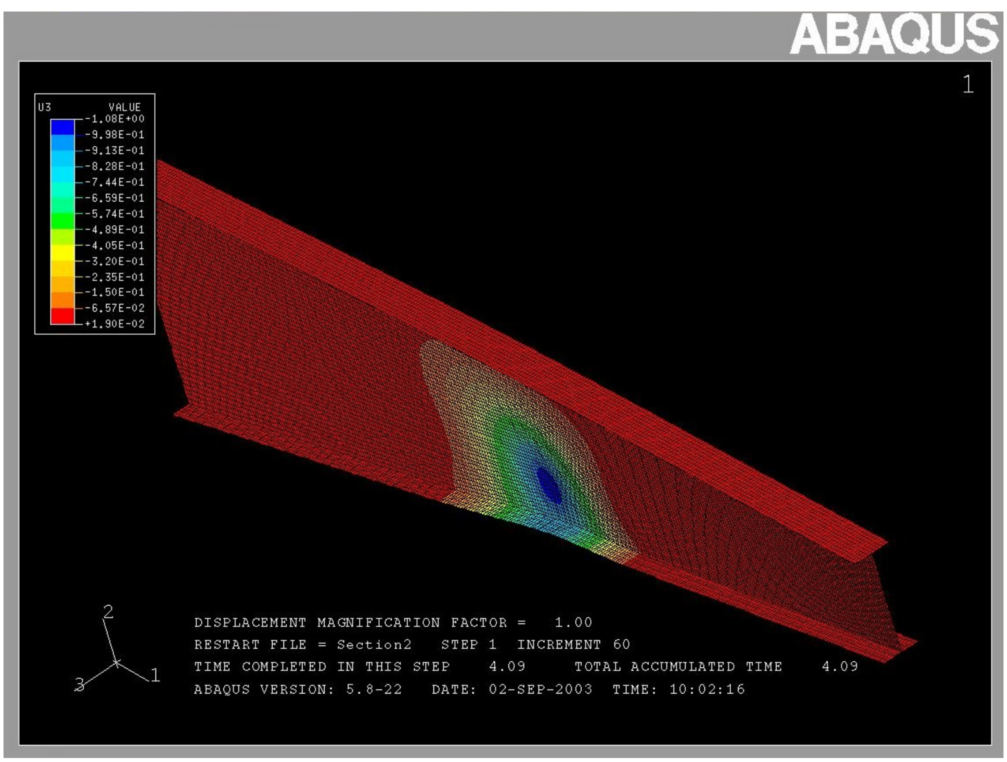

Figure 44 Lateral Displacement of a 6-inch Wide Flange Beam

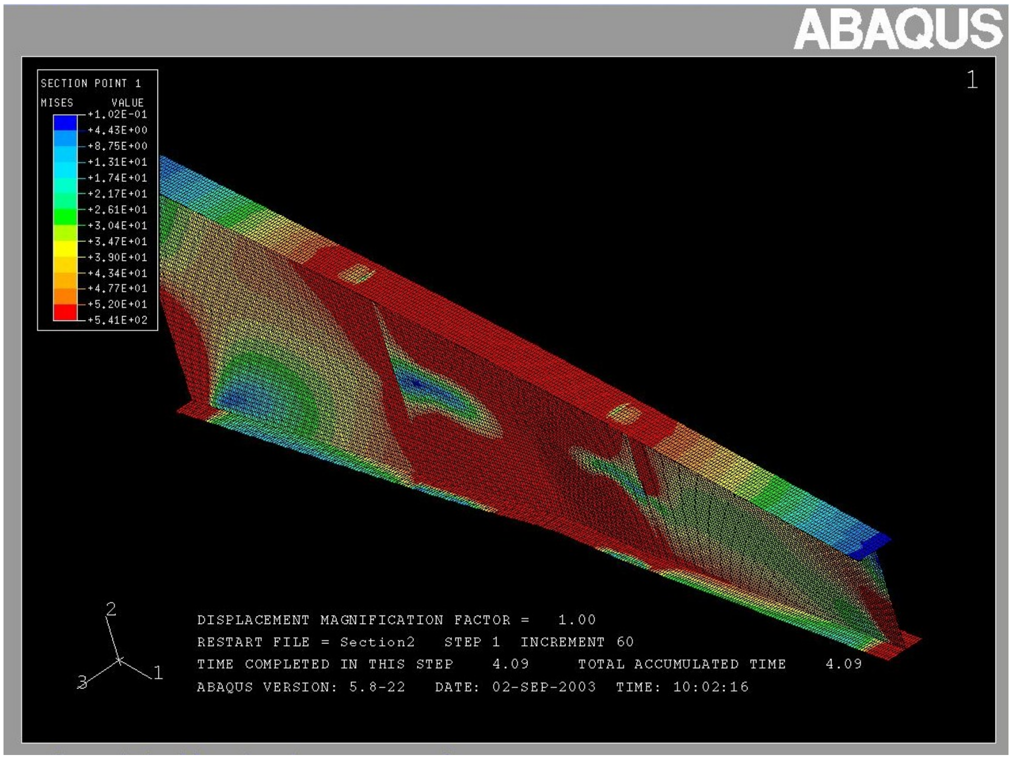

Figure 45 von Mises Stress Distribution of a 6-inch Wide Flange Beam

Also stated previously, beams possessing wider flanges tend to fail due to local buckling, especially with sections considered non-compact according to Specification Table B5.1. Figure 46 depicts a Model-1, 75-inch beam with a 12-inch wide flange. The contours in this figure show the displacements in the vertical direction. The compression flange has moved out of plane at the maximum load increment as illustrated in Figure 46. The maximum displacement at the point of unloading is approximately 0.46 inches. The slenderness ratio $b/2t_f$ for this beam is 12.0. In addition to the flange local buckling for this particular beam, the web has moved approximately 0.23 inches out of plane at the maximum load increment as shown in Figure 47, indicating web local buckling. Figure 48 is an illustration of the von Mises stress distribution at the same load increment as displayed in Figures 46 and 47.

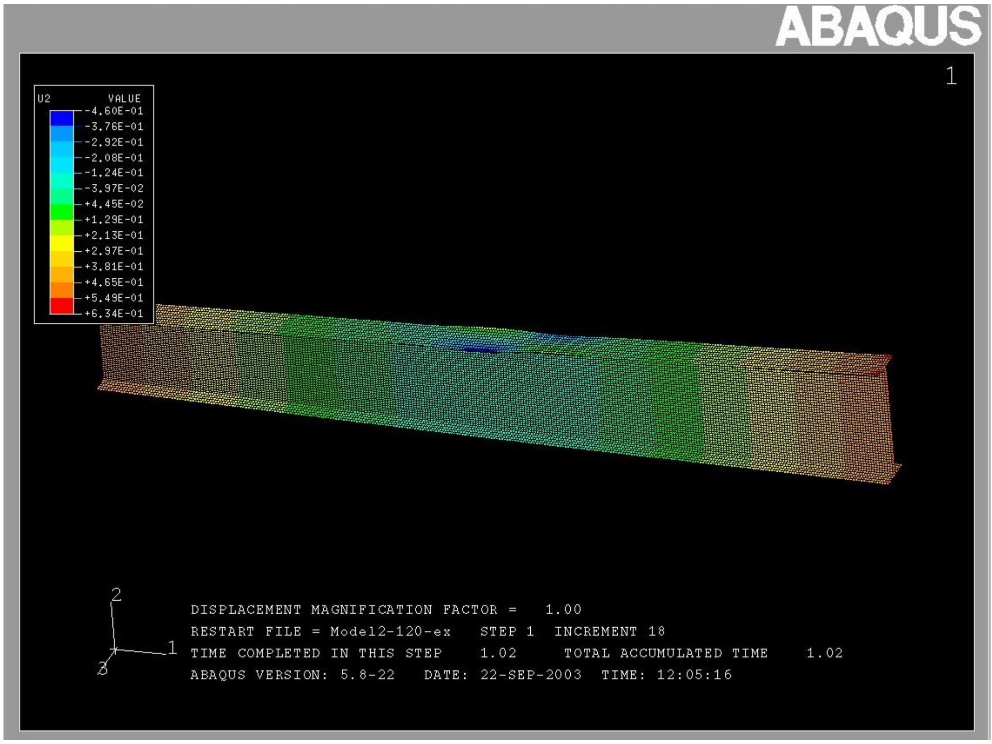

Figure 46 Flange Local Buckle of a 12-inch Wide Flange Beam

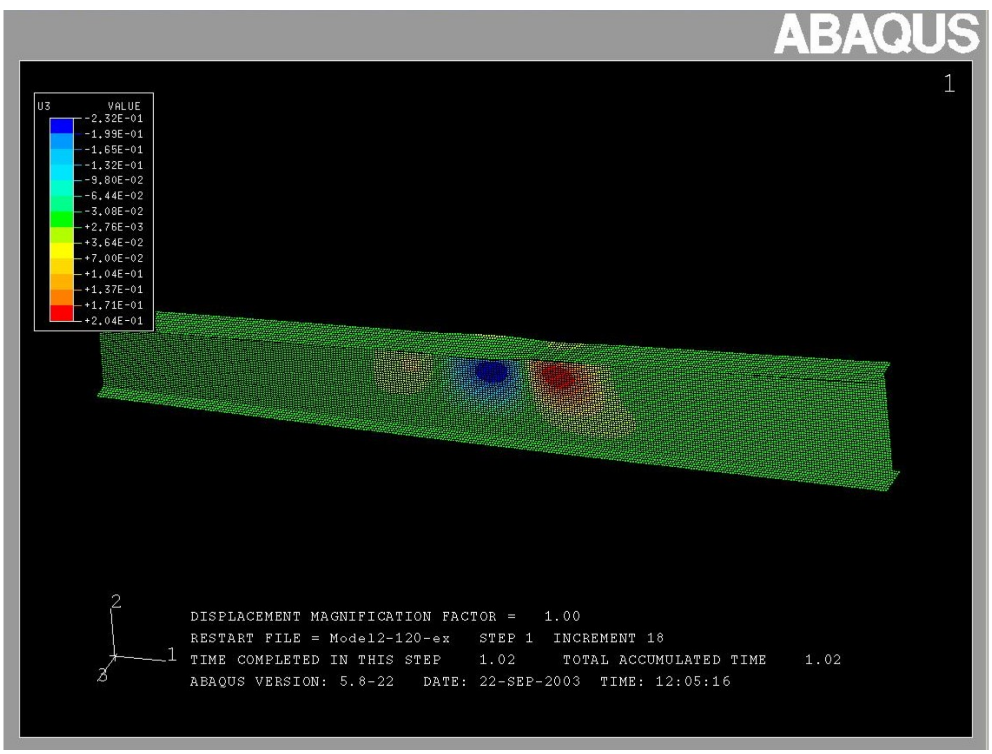

Figure 47 Local Web Buckle

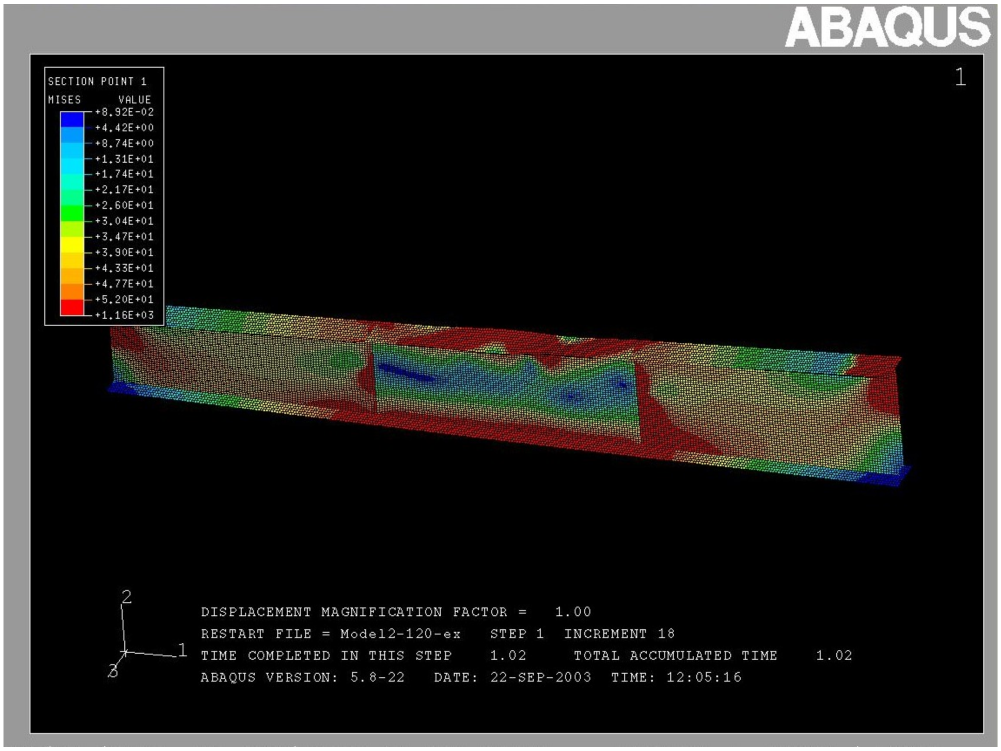

Figure 48 von Mises Stresses for a 12-inch Wide Flange Beam

5.0 CONCLUSIONS

Based on the results obtained from the current parametric study, it can be concluded that several variables affect the behavior of web-tapered I-shaped beams at ultimate: the flange width, flange thickness, web thickness, unbraced length, tapering angle, and the depth of the end sections. Overall, the behavior of gently tapered I-shaped beams is very similar to that of prismatic beams similarly loaded in that the attainment of M_p with compact cross-sections can be problematic at times. However, as a direct result of the flatness in the moment-rotation response of web-tapered beams, attainment of M_p by the beam always resulted in the manifestation of compact behavior. Unfortunately, this study appears to show that limiting cross-sectional plate slenderness ratios specified in AISC-LRFD Table B5.1 were insufficient for guaranteeing compact beam behavior in adequately braced web-tapered I-shaped beams. In other words, to obtain a rotation capacity of three, the sections studied herein oftentimes needed to be proportioned in such a way that their cross-sections would be considered ultra-compact. However, it is also noted that tests reported on in the archival literature that focused on prismatic I-beams loaded in a similar fashion to the web-tapered beams studied here, displayed a similar trend in compactness (i.e. compact cross-sections did not always yield beams that were able to attain M_p in spite of being adequately braced).

In addition, from Appendix B of this report, it can be concluded that the AISC-LRFD Appendix F design provisions accurately predict the moment capacity for beams with slenderness ratios close to the limiting values set by Table B5.1. The design equations are conservative for ultra-compact section and unconservative for slender sections. The plastic design limit L_{pd} for doubly-symmetric prismatic beams does not seem to be valid for doubly symmetric web-tapered I-shaped beams based on the three-dimensional plots illustrated in Section 4.1 of this report. Modeled beams may or may not reach M_p, irrespective of satisfying the limit, L_{pd}.

5.1 RECOMMENDATIONS

Further research must be performed to develop design equations for slender web-tapered members since they are not currently covered in the Specification. In addition, beams of different geometries must be investigated to test the validity of AISC-LRFD equations (A-F3-4) and (A-F3-5) which are presented in this report as equations (1-23) and (1-24), respectively. Provisions for strength as well as new limiting ratios, such as L_{pd}, could be developed with the help of additional research. To develop the slender section provisions, more finite element modeling must be completed with beams of larger length-to-depth ratios. In addition, the effect of different tapering angles needs to be investigated, especially the angle of the compression flange, to study the effect of the sloping flange bi-moment on the buckling response. Possibly, the new design provisions developed may be extended to larger tapering angles. Research must be performed on singly symmetric web-tapered I-shaped beams, i.e. beams with different flange thicknesses, to assist in the design of the most economical low-rise metal buildings possible. With the assistance of new design provisions, the low-rise metal building industry may be able to design more economical and efficient structures.

APPENDICES

APPENDIX A

ABAQUS INPUT FILES

Example input files used in the finite element modeling in ABAQUS are presented in this appendix. The input files presented are consistent with what is employed in the parametric study. The first section, A1, is the imperfection file for the 60-inch model-1 web-tapered I-beam. The second section, A2, is an example of an actual input file for the 60-inch model-1 web-tapered beam used for the parametric study. The file shown in Appendix A2 is very similar to the file for the sub-assemblage beam model. The only change that is made to the file is commenting out the spring elements and spring stiffnesses. The model shown in Appendix A2 is a beam with 6-inch wide flanges, $t_f = 0.375$ in., and $t_w = 0.1875$ in. The model-2 imperfection file for the 75-inch web-tapered I-shaped beam is presented in Appendix A3. An example of an input file for the 75-inch model-2 web-tapered I-shaped beam is shown in A4. The model shown in Appendix A4 is a beam with 8-inch wide flanges, $t_f = 1.125$ in., and $t_w = 0.625$ in. These input files are changed slightly for each model studied in ABAQUS. The plate thicknesses varied for each input file and the applied loads changed so that the new loads create the plastic moment M_p for the new end beam sections.

APPENDIX A1

```
*HEADING
      Model #1
      Web tapered Beam
      Lb=60 in.

*NODE
1,0,25.66,0
101,60,28.16,0
201,120,30.66,0
301,180,33.16,0
1506,0,25.66,3
1606,60,28.16,3
1706,120,30.66,3
1806,180,33.16,3
3011,0,25.66,6
3111,60,28.16,6
3211,120,30.66,6
3311,180,33.16,6
3312,0,4.56,0
3412,60,3.04,0
3512,120,1.52,0
3612,180,0,0
4817,0,4.56,3
4917,60,3.04,3
5017,120,1.52,3
5117,180,0,3
6322,0,4.56,6
6422,60,3.04,6
6522,120,1.52,6
6622,180,0,6
6623,0,5.03,3
6723,60,3.59,3
6823,120,2.16,3
6923,180,0.74,3
19566,0,25.19,3
19666,60,27.61,3
19766,120,30.02,3
19866,180,32.42,3
*NGEN,NSET=TOPFLLT1
1,101,1
*NGEN,NSET=TOPFLLT2
101,201,1
*NGEN,NSET=TOPFLLT3
201,301,1
*NGEN,NSET=TOPINT1
1506,1606,1
*NGEN,NSET=TOPINT2
1606,1706,1
*NGEN,NSET=TOPINT3
1706,1806,1
*NGEN,NSET=TOPFLRT1
3011,3111,1
*NGEN,NSET=TOPFLRT2
3111,3211,1
*NGEN,NSET=TOPFLRT3
3211,3311,1
```

```
*NGEN,NSET=BOTFLLT1
3312,3412,1
*NGEN,NSET=BOTFLLT2
3412,3512,1
*NGEN,NSET=BOTFLLT3
3512,3612,1
*NGEN,NSET=BOTINT1
4817,4917,1
*NGEN,NSET=BOTINT2
4917,5017,1
*NGEN,NSET=BOTINT3
5017,5117,1
*NGEN,NSET=BOTFLRT1
6322,6422,1
*NGEN,NSET=BOTFLRT2
6422,6522,1
*NGEN,NSET=BOTFLRT3
6522,6622,1
*NGEN,NSET=BOTWEB1
6623,6723,1
*NGEN,NSET=BOTWEB2
6723,6823,1
*NGEN,NSET=BOTWEB3
6823,6923,1
*NGEN,NSET=TOPWEB1
19566,19666,1
*NGEN,NSET=TOPWEB2
19666,19766,1
*NGEN,NSET=TOPWEB3
19766,19866,1
*NFILL,NSET=TLFLANGE1
TOPFLLT1,TOPINT1,5,301
*NFILL,NSET=TLFLANGE2
TOPFLLT2,TOPINT2,5,301
*NFILL,NSET=TLFLANGE3
TOPFLLT3,TOPINT3,5,301
*NFILL,NSET=TRFLANGE1
TOPINT1,TOPFLRT1,5,301
*NFILL,NSET=TRFLANGE2
TOPINT2,TOPFLRT2,5,301
*NFILL,NSET=TRFLANGE3
TOPINT3,TOPFLRT3,5,301
*NFILL,NSET=BLFLANGE1
BOTFLLT1,BOTINT1,5,301
*NFILL,NSET=BLFLANGE2
BOTFLLT2,BOTINT2,5,301
*NFILL,NSET=BLFLANGE3
BOTFLLT3,BOTINT3,5,301
*NFILL,NSET=BRFLANGE1
BOTINT1,BOTFLRT1,5,301
*NFILL,NSET=BRFLANGE2
BOTINT2,BOTFLRT2,5,301
*NFILL,NSET=BRFLANGE3
BOTINT3,BOTFLRT3,5,301
*NFILL,NSET=WEB1
BOTWEB1,TOPWEB1,43,301
*NFILL,NSET=WEB2
BOTWEB2,TOPWEB2,43,301
```

```
*NFILL,NSET=WEB3
BOTWEB3,TOPWEB3,43,301
*NSET,NSET=PINNED
13344
*NSET,NSET=PINNED
13446
*NSET,NSET=LATERSUP,GENERATE
6623,19566,12943
6923,19866,12943
*ELEMENT,TYPE=S4R
1,1,302,303,2
*ELGEN,ELSET=TFLANGE1
1,100,1,1,10,301,300
*ELEMENT,TYPE=S4R
101,101,402,403,102
*ELGEN,ELSET=TFLANGE2
101,100,1,1,10,301,300
*ELEMENT,TYPE=S4R
201,201,502,503,202
*ELGEN,ELSET=TFLANGE3
201,100,1,1,10,301,300
*ELEMENT,TYPE=S4R
3001,3312,3613,3614,3313
*ELGEN,ELSET=BFLANGE1
3001,100,1,1,10,301,300
*ELEMENT,TYPE=S4R
3101,3412,3713,3714,3413
*ELGEN,ELSET=BFLANGE2
3101,100,1,1,10,301,300
*ELEMENT,TYPE=S4R
3201,3512,3813,3814,3513
*ELGEN,ELSET=BFLANGE3
3201,100,1,1,10,301,300
*ELEMENT,TYPE=S4R
6001,6623,6624,6925,6924
*ELGEN,ELSET=WEB1
6001,100,1,1,43,301,300
*ELEMENT,TYPE=S4R
6101,6723,6724,7025,7024
*ELGEN,ELSET=WEB2
6101,100,1,1,43,301,300
*ELEMENT,TYPE=S4R
6201,6823,6824,7125,7124
*ELGEN,ELSET=WEB3
6201,100,1,1,43,301,300
*ELEMENT,TYPE=S4R
18901,4817,4818,6624,6623
*ELGEN,ELSET=BSTITCH1
18901,100,1,1
*ELEMENT,TYPE=S4R
19001,4917,4918,6724,6723
*ELGEN,ELSET=BSTITCH2
19001,100,1,1
*ELEMENT,TYPE=S4R
19101,5017,5018,6824,6823
*ELGEN,ELSET=BSTITCH3
19101,100,1,1
*ELEMENT,TYPE=S4R
```

```
19201,1506,19566,19567,1507
*ELGEN,ELSET=TSTITCH1
19201,100,1,1
*ELEMENT,TYPE=S4R
19301,1606,19666,19667,1607
*ELGEN,ELSET=TSTITCH2
19301,100,1,1
*ELEMENT,TYPE=S4R
19401,1706,19766,19767,1707
*ELGEN,ELSET=TSTITCH3
19401,100,1,1
**ELEMENT,TYPE=SPRING1,ELSET=BRACE1
**19501,1606
**19502,4917
**ELEMENT,TYPE=SPRING1,ELSET=BRACE2
**19503,1706
**19504,5017
**SPRING, ELSET=BRACE1
**3
**0.6892
**SPRING, ELSET=BRACE2
**3
**0.5125
*SHELL SECTION,MATERIAL=RIGID,ELSET=BFLANGE1
0.34375
*SHELL SECTION,MATERIAL=STEEL1,ELSET=BFLANGE2
0.34375
*SHELL SECTION,MATERIAL=RIGID,ELSET=BFLANGE3
0.34375
*SHELL SECTION,MATERIAL=RIGID,ELSET=TFLANGE1
0.34375
*SHELL SECTION,MATERIAL=STEEL1,ELSET=TFLANGE2
0.25
*SHELL SECTION,MATERIAL=RIGID,ELSET=TFLANGE3
0.34375
*SHELL SECTION,MATERIAL=RIGID,ELSET=WEB1
0.125
*SHELL SECTION,MATERIAL=STEEL1,ELSET=WEB2
0.125
*SHELL SECTION,MATERIAL=RIGID,ELSET=WEB3
0.125
*SHELL SECTION,MATERIAL=RIGID,ELSET=BSTITCH1
0.125
*SHELL SECTION,MATERIAL=STEEL1,ELSET=BSTITCH2
0.125
*SHELL SECTION,MATERIAL=RIGID,ELSET=BSTITCH3
0.125
*SHELL SECTION,MATERIAL=RIGID,ELSET=TSTITCH1
0.125
*SHELL SECTION,MATERIAL=STEEL1,ELSET=TSTITCH2
0.125
*SHELL SECTION,MATERIAL=RIGID,ELSET=TSTITCH3
0.125
*MATERIAL,NAME=RIGID
*ELASTIC
2.9E5,0.3
*MATERIAL,NAME=STEEL1
*ELASTIC
```

```
29600,0.3
*PLASTIC
56.8,0
61.62,0.024
76.13,0.0557
80.9,0.24
*BOUNDARY
PINNED,1,3
LATERSUP,3
*STEP
*BUCKLE
3,,20,80
*CLOAD
1,2,3.2527
302,2,3.2527
603,2,3.2527
904,2,3.2527
1205,2,3.2527
1506,2,3.2527
1807,2,3.2527
2108,2,3.2527
2409,2,3.2527
2710,2,3.2527
3011,2,3.2527
301,2,3.38
602,2,3.38
903,2,3.38
1204,2,3.38
1505,2,3.38
1806,2,3.38
2107,2,3.38
2408,2,3.38
2709,2,3.38
3010,2,3.38
3311,2,3.38
*RESTART,WRITE,FREQUENCY=1
*ELPRINT,FREQUENCY=0
*NODE PRINT,FREQUENCY=1
CF
*NODE FILE,LAST MODE=1,GLOBAL=YES
U
*END STEP
```

APPENDIX A2

```
*HEADING
      Model #1
      Web tapered Beam
      Lb=60 in.

*NODE
1,0,25.66,0
101,60,28.16,0
201,120,30.66,0
301,180,33.16,0
1506,0,25.66,3
1606,60,28.16,3
1706,120,30.66,3
1806,180,33.16,3
3011,0,25.66,6
3111,60,28.16,6
3211,120,30.66,6
3311,180,33.16,6
3312,0,4.56,0
3412,60,3.04,0
3512,120,1.52,0
3612,180,0,0
4817,0,4.56,3
4917,60,3.04,3
5017,120,1.52,3
5117,180,0,3
6322,0,4.56,6
6422,60,3.04,6
6522,120,1.52,6
6622,180,0,6
6623,0,5.03,3
6723,60,3.59,3
6823,120,2.16,3
6923,180,0.74,3
19566,0,25.19,3
19666,60,27.61,3
19766,120,30.02,3
19866,180,32.42,3
*NGEN,NSET=TOPFLLT1
1,101,1
*NGEN,NSET=TOPFLLT2
101,201,1
*NGEN,NSET=TOPFLLT3
201,301,1
*NGEN,NSET=TOPINT1
1506,1606,1
*NGEN,NSET=TOPINT2
1606,1706,1
*NGEN,NSET=TOPINT3
1706,1806,1
*NGEN,NSET=TOPFLRT1
3011,3111,1
*NGEN,NSET=TOPFLRT2
3111,3211,1
*NGEN,NSET=TOPFLRT3
3211,3311,1
```

```
*NGEN,NSET=BOTFLLT1
3312,3412,1
*NGEN,NSET=BOTFLLT2
3412,3512,1
*NGEN,NSET=BOTFLLT3
3512,3612,1
*NGEN,NSET=BOTINT1
4817,4917,1
*NGEN,NSET=BOTINT2
4917,5017,1
*NGEN,NSET=BOTINT3
5017,5117,1
*NGEN,NSET=BOTFLRT1
6322,6422,1
*NGEN,NSET=BOTFLRT2
6422,6522,1
*NGEN,NSET=BOTFLRT3
6522,6622,1
*NGEN,NSET=BOTWEB1
6623,6723,1
*NGEN,NSET=BOTWEB2
6723,6823,1
*NGEN,NSET=BOTWEB3
6823,6923,1
*NGEN,NSET=TOPWEB1
19566,19666,1
*NGEN,NSET=TOPWEB2
19666,19766,1
*NGEN,NSET=TOPWEB3
19766,19866,1
*NFILL,NSET=TLFLANGE1
TOPFLLT1,TOPINT1,5,301
*NFILL,NSET=TLFLANGE2
TOPFLLT2,TOPINT2,5,301
*NFILL,NSET=TLFLANGE3
TOPFLLT3,TOPINT3,5,301
*NFILL,NSET=TRFLANGE1
TOPINT1,TOPFLRT1,5,301
*NFILL,NSET=TRFLANGE2
TOPINT2,TOPFLRT2,5,301
*NFILL,NSET=TRFLANGE3
TOPINT3,TOPFLRT3,5,301
*NFILL,NSET=BLFLANGE1
BOTFLLT1,BOTINT1,5,301
*NFILL,NSET=BLFLANGE2
BOTFLLT2,BOTINT2,5,301
*NFILL,NSET=BLFLANGE3
BOTFLLT3,BOTINT3,5,301
*NFILL,NSET=BRFLANGE1
BOTINT1,BOTFLRT1,5,301
*NFILL,NSET=BRFLANGE2
BOTINT2,BOTFLRT2,5,301
*NFILL,NSET=BRFLANGE3
BOTINT3,BOTFLRT3,5,301
*NFILL,NSET=WEB1
BOTWEB1,TOPWEB1,43,301
*NFILL,NSET=WEB2
BOTWEB2,TOPWEB2,43,301
```

```
*NFILL,NSET=WEB3
BOTWEB3,TOPWEB3,43,301
*NSET,NSET=PINNED
13344
*NSET,NSET=PINNED
13446
*NSET,NSET=LATERSUP
1506
1606
1706
1806
4817
4917
5017
5117
*ELEMENT,TYPE=S4R
1,1,302,303,2
*ELGEN,ELSET=TFLANGE1
1,100,1,1,10,301,300
*ELEMENT,TYPE=S4R
101,101,402,403,102
*ELGEN,ELSET=TFLANGE2
101,100,1,1,10,301,300
*ELEMENT,TYPE=S4R
201,201,502,503,202
*ELGEN,ELSET=TFLANGE3
201,100,1,1,10,301,300
*ELEMENT,TYPE=S4R
3001,3312,3613,3614,3313
*ELGEN,ELSET=BFLANGE1
3001,100,1,1,10,301,300
*ELEMENT,TYPE=S4R
3101,3412,3713,3714,3413
*ELGEN,ELSET=BFLANGE2
3101,100,1,1,10,301,300
*ELEMENT,TYPE=S4R
3201,3512,3813,3814,3513
*ELGEN,ELSET=BFLANGE3
3201,100,1,1,10,301,300
*ELEMENT,TYPE=S4R
6001,6623,6624,6925,6924
*ELGEN,ELSET=WEB1
6001,100,1,1,43,301,300
*ELEMENT,TYPE=S4R
6101,6723,6724,7025,7024
*ELGEN,ELSET=WEB2
6101,100,1,1,43,301,300
*ELEMENT,TYPE=S4R
6201,6823,6824,7125,7124
*ELGEN,ELSET=WEB3
6201,100,1,1,43,301,300
*ELEMENT,TYPE=S4R
18901,4817,4818,6624,6623
*ELGEN,ELSET=BSTITCH1
18901,100,1,1
*ELEMENT,TYPE=S4R
19001,4917,4918,6724,6723
*ELGEN,ELSET=BSTITCH2
```

```
19001,100,1,1
*ELEMENT,TYPE=S4R
19101,5017,5018,6824,6823
*ELGEN,ELSET=BSTITCH3
19101,100,1,1
*ELEMENT,TYPE=S4R
19201,1506,19566,19567,1507
*ELGEN,ELSET=TSTITCH1
19201,100,1,1
*ELEMENT,TYPE=S4R
19301,1606,19666,19667,1607
*ELGEN,ELSET=TSTITCH2
19301,100,1,1
*ELEMENT,TYPE=S4R
19401,1706,19766,19767,1707
*ELGEN,ELSET=TSTITCH3
19401,100,1,1
**ELEMENT,TYPE=SPRING1,ELSET=BRACE1
**19501,1606
**19502,4917
**ELEMENT,TYPE=SPRING1,ELSET=BRACE2
**19503,1706
**19504,5017
**ELEMENT,TYPE=SPRING1,ELSET=BRACE3
**19505,1506
**19506,4817
**19507,1806
**19508,5117
**SPRING, ELSET=BRACE1
**3
**0.6892
**SPRING, ELSET=BRACE2
**3
**0.5125
**SPRING, ELSET=BRACE3
**3
**0.5125
*SHELL SECTION,MATERIAL=RIGID,ELSET=BFLANGE1
0.375
*SHELL SECTION,MATERIAL=STEEL1,ELSET=BFLANGE2
0.375
*SHELL SECTION,MATERIAL=RIGID,ELSET=BFLANGE3
0.375
*SHELL SECTION,MATERIAL=RIGID,ELSET=TFLANGE1
0.375
*SHELL SECTION,MATERIAL=STEEL1,ELSET=TFLANGE2
0.375
*SHELL SECTION,MATERIAL=RIGID,ELSET=TFLANGE3
0.375
*SHELL SECTION,MATERIAL=RIGID,ELSET=WEB1
0.1875
*SHELL SECTION,MATERIAL=STEEL1,ELSET=WEB2
0.1875
*SHELL SECTION,MATERIAL=RIGID,ELSET=WEB3
0.1875
*SHELL SECTION,MATERIAL=RIGID,ELSET=BSTITCH1
0.1875
*SHELL SECTION,MATERIAL=STEEL1,ELSET=BSTITCH2
```

```
0.1875
*SHELL SECTION,MATERIAL=RIGID,ELSET=BSTITCH3
0.1875
*SHELL SECTION,MATERIAL=RIGID,ELSET=TSTITCH1
0.1875
*SHELL SECTION,MATERIAL=STEEL1,ELSET=TSTITCH2
0.1875
*SHELL SECTION,MATERIAL=RIGID,ELSET=TSTITCH3
0.1875
*MATERIAL,NAME=RIGID
*ELASTIC
2.9E5,0.3
*MATERIAL,NAME=STEEL1
*ELASTIC
29600,0.3
*PLASTIC
56.8,0
61.62,0.024
76.13,0.0557
80.9,0.24
*BOUNDARY
PINNED,1,3
LATERSUP,3
*IMPERFECTION,FILE=Model2_imp,STEP=1
1,0.12
*STEP,NLGEOM,INC=50
*STATIC,RIKS
0.001,1.0,0.0000000000001
*CLOAD
1,2,7.33427
302,2,7.33427
603,2,7.33427
904,2,7.33427
1205,2,7.33427
1506,2,7.33427
1807,2,7.33427
2108,2,7.33427
2409,2,7.33427
2710,2,7.33427
3011,2,7.33427
301,2,8.98046
602,2,8.98046
903,2,8.98046
1204,2,8.98046
1505,2,8.98046
1806,2,8.98046
2107,2,8.98046
2408,2,8.98046
2709,2,8.98046
3010,2,8.98046
3311,2,8.98046
*RESTART,WRITE,FREQUENCY=1
*ELPRINT,FREQUENCY=0
*NODE PRINT,FREQUENCY=1
CF
*END STEP
```

APPENDIX A3

```
*HEADING
      Model #2
      Web tapered Beam
      Lb=75 in.

*NODE
1,0,42.3721,0
101,75,44.8721,0
201,150,47.3721,0
301,225,49.8721,0
1506,0,42.3721,4
1606,75,44.8721,4
1706,150,47.3721,4
1806,225,49.8721,4
3011,0,42.3721,8
3111,75,44.8721,8
3211,150,47.3721,8
3311,225,49.8721,8
3312,0,0,0
3412,75,10.9375,0
3512,150,21.875,0
3612,225,32.8125,0
4817,0,0,4
4917,75,10.9375,4
5017,150,21.875,4
5117,225,32.8125,4
6322,0,0,8
6422,75,10.9375,8
6522,150,21.875,8
6622,225,32.8125,8
6623,0,0.8647,4
6723,75,11.63,4
6823,150,22.3953,4
6923,225,33.1607,4
20770,0,41.5074,4
20870,75,44.1796,4
20970,150,46.8518,4
21070,225,49.5239,4
*NGEN,NSET=TOPFLLT1
1,101,1
*NGEN,NSET=TOPFLLT2
101,201,1
*NGEN,NSET=TOPFLLT3
201,301,1
*NGEN,NSET=TOPINT1
1506,1606,1
*NGEN,NSET=TOPINT2
1606,1706,1
*NGEN,NSET=TOPINT3
1706,1806,1
*NGEN,NSET=TOPFLRT1
3011,3111,1
*NGEN,NSET=TOPFLRT2
3111,3211,1
*NGEN,NSET=TOPFLRT3
3211,3311,1
```

```
*NGEN,NSET=BOTFLLT1
3312,3412,1
*NGEN,NSET=BOTFLLT2
3412,3512,1
*NGEN,NSET=BOTFLLT3
3512,3612,1
*NGEN,NSET=BOTINT1
4817,4917,1
*NGEN,NSET=BOTINT2
4917,5017,1
*NGEN,NSET=BOTINT3
5017,5117,1
*NGEN,NSET=BOTFLRT1
6322,6422,1
*NGEN,NSET=BOTFLRT2
6422,6522,1
*NGEN,NSET=BOTFLRT3
6522,6622,1
*NGEN,NSET=BOTWEB1
6623,6723,1
*NGEN,NSET=BOTWEB2
6723,6823,1
*NGEN,NSET=BOTWEB3
6823,6923,1
*NGEN,NSET=TOPWEB1
20770,20870,1
*NGEN,NSET=TOPWEB2
20870,20970,1
*NGEN,NSET=TOPWEB3
20970,21070,1
*NFILL,NSET=TLFLANGE1
TOPFLLT1,TOPINT1,5,301
*NFILL,NSET=TLFLANGE2
TOPFLLT2,TOPINT2,5,301
*NFILL,NSET=TLFLANGE3
TOPFLLT3,TOPINT3,5,301
*NFILL,NSET=TRFLANGE1
TOPINT1,TOPFLRT1,5,301
*NFILL,NSET=TRFLANGE2
TOPINT2,TOPFLRT2,5,301
*NFILL,NSET=TRFLANGE3
TOPINT3,TOPFLRT3,5,301
*NFILL,NSET=BLFLANGE1
BOTFLLT1,BOTINT1,5,301
*NFILL,NSET=BLFLANGE2
BOTFLLT2,BOTINT2,5,301
*NFILL,NSET=BLFLANGE3
BOTFLLT3,BOTINT3,5,301
*NFILL,NSET=BRFLANGE1
BOTINT1,BOTFLRT1,5,301
*NFILL,NSET=BRFLANGE2
BOTINT2,BOTFLRT2,5,301
*NFILL,NSET=BRFLANGE3
BOTINT3,BOTFLRT3,5,301
*NFILL,NSET=WEB1
BOTWEB1,TOPWEB1,47,301
*NFILL,NSET=WEB2
BOTWEB2,TOPWEB2,47,301
```

```
*NFILL,NSET=WEB3
BOTWEB3,TOPWEB3,47,301
*NSET,NSET=PINNED
13645
*NSET,NSET=PINNED
13747
*NSET,NSET=LATERSUP
1506
1606
1706
1806
4817
4917
5017
5117
*ELEMENT,TYPE=S4R
1,1,302,303,2
*ELGEN,ELSET=TFLANGE1
1,100,1,1,10,301,300
*ELEMENT,TYPE=S4R
101,101,402,403,102
*ELGEN,ELSET=TFLANGE2
101,100,1,1,10,301,300
*ELEMENT,TYPE=S4R
201,201,502,503,202
*ELGEN,ELSET=TFLANGE3
201,100,1,1,10,301,300
*ELEMENT,TYPE=S4R
3001,3312,3613,3614,3313
*ELGEN,ELSET=BFLANGE1
3001,100,1,1,10,301,300
*ELEMENT,TYPE=S4R
3101,3412,3713,3714,3413
*ELGEN,ELSET=BFLANGE2
3101,100,1,1,10,301,300
*ELEMENT,TYPE=S4R
3201,3512,3813,3814,3513
*ELGEN,ELSET=BFLANGE3
3201,100,1,1,10,301,300
*ELEMENT,TYPE=S4R
6001,6623,6624,6925,6924
*ELGEN,ELSET=WEB1
6001,100,1,1,47,301,300
*ELEMENT,TYPE=S4R
6101,6723,6724,7025,7024
*ELGEN,ELSET=WEB2
6101,100,1,1,47,301,300
*ELEMENT,TYPE=S4R
6201,6823,6824,7125,7124
*ELGEN,ELSET=WEB3
6201,100,1,1,47,301,300
*ELEMENT,TYPE=S4R
20101,4817,4818,6624,6623
*ELGEN,ELSET=BSTITCH1
20101,100,1,1
*ELEMENT,TYPE=S4R
20201,4917,4918,6724,6723
*ELGEN,ELSET=BSTITCH2
```

```
20201,100,1,1
*ELEMENT,TYPE=S4R
20301,5017,5018,6824,6823
*ELGEN,ELSET=BSTITCH3
20301,100,1,1
*ELEMENT,TYPE=S4R
20401,1506,20770,20771,1507
*ELGEN,ELSET=TSTITCH1
20401,100,1,1
*ELEMENT,TYPE=S4R
20501,1606,20870,20871,1607
*ELGEN,ELSET=TSTITCH2
20501,100,1,1
*ELEMENT,TYPE=S4R
20601,1706,20970,20971,1707
*ELGEN,ELSET=TSTITCH3
20601,100,1,1
**ELEMENT,TYPE=SPRING1,ELSET=BRACE1
**20701,1606
**20702,4917
**ELEMENT,TYPE=SPRING1,ELSET=BRACE2
**20703,1706
**20704,5017
**SPRING, ELSET=BRACE1
**3
**0.6472
**SPRING, ELSET=BRACE2
**3
**0.6892
*SHELL SECTION,MATERIAL=RIGID,ELSET=BFLANGE1
0.34375
*SHELL SECTION,MATERIAL=STEEL1,ELSET=BFLANGE2
0.172
*SHELL SECTION,MATERIAL=RIGID,ELSET=BFLANGE3
0.34375
*SHELL SECTION,MATERIAL=RIGID,ELSET=TFLANGE1
0.34375
*SHELL SECTION,MATERIAL=STEEL1,ELSET=TFLANGE2
0.34375
*SHELL SECTION,MATERIAL=RIGID,ELSET=TFLANGE3
0.34375
*SHELL SECTION,MATERIAL=RIGID,ELSET=WEB1
0.125
*SHELL SECTION,MATERIAL=STEEL1,ELSET=WEB2
0.125
*SHELL SECTION,MATERIAL=RIGID,ELSET=WEB3
0.125
*SHELL SECTION,MATERIAL=RIGID,ELSET=BSTITCH1
0.125
*SHELL SECTION,MATERIAL=STEEL1,ELSET=BSTITCH2
0.125
*SHELL SECTION,MATERIAL=RIGID,ELSET=BSTITCH3
0.125
*SHELL SECTION,MATERIAL=RIGID,ELSET=TSTITCH1
0.125
*SHELL SECTION,MATERIAL=STEEL1,ELSET=TSTITCH2
0.125
*SHELL SECTION,MATERIAL=RIGID,ELSET=TSTITCH3
```

```
0.125
*MATERIAL,NAME=RIGID
*ELASTIC
2.9E5,0.3
*MATERIAL,NAME=STEEL1
*ELASTIC
29600,0.3
*PLASTIC
56.8,0
61.62,0.024
76.13,0.0557
80.9,0.24
*BOUNDARY
PINNED,1,3
LATERSUP,3
*STEP
*BUCKLE
3,,20,80
*CLOAD
3312,2,-.32527
3613,2,-.32527
3914,2,-.32527
4215,2,-.32527
4516,2,-.32527
4817,2,-.32527
5118,2,-.32527
5419,2,-.32527
5720,2,-.32527
6021,2,-.32527
6322,2,-.32527
3612,2,-.338
3913,2,-.338
4214,2,-.338
4515,2,-.338
4816,2,-.338
5117,2,-.338
5418,2,-.338
5719,2,-.338
6020,2,-.338
6321,2,-.338
6622,2,-.338
*RESTART,WRITE,FREQUENCY=1
*ELPRINT,FREQUENCY=0
*NODE PRINT,FREQUENCY=1
CF
*NODE FILE,LAST MODE=1,GLOBAL=YES
U
*END STEP
```

APPENDIX A4

```
*HEADING
      Model #2
      Web tapered Beam
      Lb=75 in.

*NODE
1,0,42.3721,0
101,75,44.8721,0
201,150,47.3721,0
301,225,49.8721,0
1506,0,42.3721,4
1606,75,44.8721,4
1706,150,47.3721,4
1806,225,49.8721,4
3011,0,42.3721,8
3111,75,44.8721,8
3211,150,47.3721,8
3311,225,49.8721,8
3312,0,0,0
3412,75,10.9375,0
3512,150,21.875,0
3612,225,32.8125,0
4817,0,0,4
4917,75,10.9375,4
5017,150,21.875,4
5117,225,32.8125,4
6322,0,0,8
6422,75,10.9375,8
6522,150,21.875,8
6622,225,32.8125,8
6623,0,0.8647,4
6723,75,11.63,4
6823,150,22.3953,4
6923,225,33.1607,4
20770,0,41.5074,4
20870,75,44.1796,4
20970,150,46.8518,4
21070,225,49.5239,4
*NGEN,NSET=TOPFLLT1
1,101,1
*NGEN,NSET=TOPFLLT2
101,201,1
*NGEN,NSET=TOPFLLT3
201,301,1
*NGEN,NSET=TOPINT1
1506,1606,1
*NGEN,NSET=TOPINT2
1606,1706,1
*NGEN,NSET=TOPINT3
1706,1806,1
*NGEN,NSET=TOPFLRT1
3011,3111,1
*NGEN,NSET=TOPFLRT2
3111,3211,1
*NGEN,NSET=TOPFLRT3
3211,3311,1
```

```
*NGEN,NSET=BOTFLLT1
3312,3412,1
*NGEN,NSET=BOTFLLT2
3412,3512,1
*NGEN,NSET=BOTFLLT3
3512,3612,1
*NGEN,NSET=BOTINT1
4817,4917,1
*NGEN,NSET=BOTINT2
4917,5017,1
*NGEN,NSET=BOTINT3
5017,5117,1
*NGEN,NSET=BOTFLRT1
6322,6422,1
*NGEN,NSET=BOTFLRT2
6422,6522,1
*NGEN,NSET=BOTFLRT3
6522,6622,1
*NGEN,NSET=BOTWEB1
6623,6723,1
*NGEN,NSET=BOTWEB2
6723,6823,1
*NGEN,NSET=BOTWEB3
6823,6923,1
*NGEN,NSET=TOPWEB1
20770,20870,1
*NGEN,NSET=TOPWEB2
20870,20970,1
*NGEN,NSET=TOPWEB3
20970,21070,1
*NFILL,NSET=TLFLANGE1
TOPFLLT1,TOPINT1,5,301
*NFILL,NSET=TLFLANGE2
TOPFLLT2,TOPINT2,5,301
*NFILL,NSET=TLFLANGE3
TOPFLLT3,TOPINT3,5,301
*NFILL,NSET=TRFLANGE1
TOPINT1,TOPFLRT1,5,301
*NFILL,NSET=TRFLANGE2
TOPINT2,TOPFLRT2,5,301
*NFILL,NSET=TRFLANGE3
TOPINT3,TOPFLRT3,5,301
*NFILL,NSET=BLFLANGE1
BOTFLLT1,BOTINT1,5,301
*NFILL,NSET=BLFLANGE2
BOTFLLT2,BOTINT2,5,301
*NFILL,NSET=BLFLANGE3
BOTFLLT3,BOTINT3,5,301
*NFILL,NSET=BRFLANGE1
BOTINT1,BOTFLRT1,5,301
*NFILL,NSET=BRFLANGE2
BOTINT2,BOTFLRT2,5,301
*NFILL,NSET=BRFLANGE3
BOTINT3,BOTFLRT3,5,301
*NFILL,NSET=WEB1
BOTWEB1,TOPWEB1,47,301
*NFILL,NSET=WEB2
BOTWEB2,TOPWEB2,47,301
```

```
*NFILL,NSET=WEB3
BOTWEB3,TOPWEB3,47,301
*NSET,NSET=PINNED
13645
*NSET,NSET=PINNED
13747
*NSET,NSET=LATERSUP
1506
1606
1706
1806
4817
4917
5017
5117
*ELEMENT,TYPE=S4R
1,1,302,303,2
*ELGEN,ELSET=TFLANGE1
1,100,1,1,10,301,300
*ELEMENT,TYPE=S4R
101,101,402,403,102
*ELGEN,ELSET=TFLANGE2
101,100,1,1,10,301,300
*ELEMENT,TYPE=S4R
201,201,502,503,202
*ELGEN,ELSET=TFLANGE3
201,100,1,1,10,301,300
*ELEMENT,TYPE=S4R
3001,3312,3613,3614,3313
*ELGEN,ELSET=BFLANGE1
3001,100,1,1,10,301,300
*ELEMENT,TYPE=S4R
3101,3412,3713,3714,3413
*ELGEN,ELSET=BFLANGE2
3101,100,1,1,10,301,300
*ELEMENT,TYPE=S4R
3201,3512,3813,3814,3513
*ELGEN,ELSET=BFLANGE3
3201,100,1,1,10,301,300
*ELEMENT,TYPE=S4R
6001,6623,6624,6925,6924
*ELGEN,ELSET=WEB1
6001,100,1,1,47,301,300
*ELEMENT,TYPE=S4R
6101,6723,6724,7025,7024
*ELGEN,ELSET=WEB2
6101,100,1,1,47,301,300
*ELEMENT,TYPE=S4R
6201,6823,6824,7125,7124
*ELGEN,ELSET=WEB3
6201,100,1,1,47,301,300
*ELEMENT,TYPE=S4R
20101,4817,4818,6624,6623
*ELGEN,ELSET=BSTITCH1
20101,100,1,1
*ELEMENT,TYPE=S4R
20201,4917,4918,6724,6723
*ELGEN,ELSET=BSTITCH2
```

```
20201,100,1,1
*ELEMENT,TYPE=S4R
20301,5017,5018,6824,6823
*ELGEN,ELSET=BSTITCH3
20301,100,1,1
*ELEMENT,TYPE=S4R
20401,1506,20770,20771,1507
*ELGEN,ELSET=TSTITCH1
20401,100,1,1
*ELEMENT,TYPE=S4R
20501,1606,20870,20871,1607
*ELGEN,ELSET=TSTITCH2
20501,100,1,1
*ELEMENT,TYPE=S4R
20601,1706,20970,20971,1707
*ELGEN,ELSET=TSTITCH3
20601,100,1,1
**ELEMENT,TYPE=SPRING1,ELSET=BRACE1
**20701,1606
**20702,4917
**ELEMENT,TYPE=SPRING1,ELSET=BRACE2
**20703,1706
**20704,5017
**SPRING, ELSET=BRACE1
**3
**0.6472
**SPRING, ELSET=BRACE2
**3
**0.6892
*SHELL SECTION,MATERIAL=RIGID,ELSET=BFLANGE1
1.125
*SHELL SECTION,MATERIAL=STEEL1,ELSET=BFLANGE2
1.125
*SHELL SECTION,MATERIAL=RIGID,ELSET=BFLANGE3
1.125
*SHELL SECTION,MATERIAL=RIGID,ELSET=TFLANGE1
1.125
*SHELL SECTION,MATERIAL=STEEL1,ELSET=TFLANGE2
1.125
*SHELL SECTION,MATERIAL=RIGID,ELSET=TFLANGE3
1.125
*SHELL SECTION,MATERIAL=RIGID,ELSET=WEB1
0.625
*SHELL SECTION,MATERIAL=STEEL1,ELSET=WEB2
0.625
*SHELL SECTION,MATERIAL=RIGID,ELSET=WEB3
0.625
*SHELL SECTION,MATERIAL=RIGID,ELSET=BSTITCH1
0.625
*SHELL SECTION,MATERIAL=STEEL1,ELSET=BSTITCH2
0.625
*SHELL SECTION,MATERIAL=RIGID,ELSET=BSTITCH3
0.625
*SHELL SECTION,MATERIAL=RIGID,ELSET=TSTITCH1
0.625
*SHELL SECTION,MATERIAL=STEEL1,ELSET=TSTITCH2
0.625
*SHELL SECTION,MATERIAL=RIGID,ELSET=TSTITCH3
```

```
0.625
*MATERIAL,NAME=RIGID
*ELASTIC
2.9E5,0.3
*MATERIAL,NAME=STEEL1
*ELASTIC
29600,0.3
*PLASTIC
56.8,0
61.62,0.024
76.13,0.0557
80.9,0.24
*BOUNDARY
PINNED,1,3
LATERSUP,3
*IMPERFECTION,FILE=Section2-8-ex_imp,STEP=1
1,0.15
*STEP,NLGEOM,INC=150
*STATIC,RIKS
0.001,1.0,0.0000000000001
*CLOAD
3312,2,-32.60732
3613,2,-32.60732
3914,2,-32.60732
4215,2,-32.60732
4516,2,-32.60732
4817,2,-32.60732
5118,2,-32.60732
5419,2,-32.60732
5720,2,-32.60732
6021,2,-32.60732
6322,2,-32.60732
3612,2,-22.18892
3913,2,-22.18892
4214,2,-22.18892
4515,2,-22.18892
4816,2,-22.18892
5117,2,-22.18892
5418,2,-22.18892
5719,2,-22.18892
6020,2,-22.18892
6321,2,-22.18892
6622,2,-22.18892
*RESTART,WRITE,FREQUENCY=1
*ELPRINT,FREQUENCY=0
*NODE PRINT,FREQUENCY=1
CF
*END STEP
```

APPENDIX B

PARAMETRIC STUDY RESULTS

The results of the parametric study are presented in this appendix. Appendix B1 presents the results from the Model-1, 60-inch finite element modeled beams. Appendix B2 includes the Model-2, 60-inch beam results. The 75-inch Model-1 and Model-2 data are shown as Appendix B3 and Appendix B4, respectively. The cross-section information is given for both ends of the web-tapered beam, where End 1 is the shallow end of the beam and End 2 is the deep end of the beam. Appendix B utilizes the following notation throughout its entirety.

Notation:

Model1 End 1 = Shallow End of the 60-inch Model-1 beam

Model1 End 2 = Deep End of the 60-inch Model-1 beam

Model2 End 1 = Shallow End of the 60-inch Model-2 beam

Model2 End 2 = Deep End of the 60-inch Model-2 beam

Model1-ex End 1 = Shallow End of the 75-inch Model-1 beam

Model1-ex End 2 = Deep End of the 75-inch Model-1 beam

Model2-ex End 1 = Shallow End of the 75-inch Model-2 beam

Model2-ex End 2 = Deep End of the 75-inch Model-2 beam

t_{f1} = compression flange thickness (in.)

t_{f2} = tension flange thickness (in.)

b_{f1} = compression flange width (in.)

b_{f2} = tension flange width (in.)

t_w = web thickness (in.)

d_w = depth of web (in.)

M_p = plastic moment = F_yZ (kip-in.)

θ_p = theoretical rotation at which M_p is achieved (rad.)

L_b = unbraced length of beam (in.)

r_y = radius of gyration taken about the y-axis (in.)

m(top) = slope of the top of the beam (in./in.)

m(bot) = slope of the bottom of the beam (in./in.)

$M_{(aisc)}$ = moment capacity calculated by ASIC-LRFD Specification Appendix F (kip-in.)

$M_{u(abaqus)}$ = moment capacity determined by ABAQUS (kip-in.)

M_y = moment at which the outermost fiber of the beam begins to yield = F_yS_x (kip-in.)

α = ratio of M_p applied to the shallow to M_p applied the deep end of the beam

L_p = limiting unbraced length for prismatic I-shaped beams (in.)

L_{pd} = limiting unbraced length for plastic analysis of prismatic I-shaped beams (in.)

R = rotation capacity

APPENDIX B1

Table B1 Model-1 L_b = 60 in. Parametric Study Results

E	Fy
29600	56.8

End 1 = Shallow End
End 2 = Deep End

DESCRIPTION	tf1	bf1	tf2	bf2	tw	dw	Mp(in kips)	θ p	Comp. bf1/2tf1	h/tw	Tension bf2/2tf2	Web λ p	Flanges λ p	Lb/ry	m(top)	m(bot)	M(aisc)	Mu(abaqus)	My	Mu/My	Mu/Mp	Mu/M(aisc)	α	Lp	Lpd	R
Model1 End 1	1.25	6	1.25	6	1.25	23.87	20814.66	0.00557	2.40	19.10	2.40	85.83	8.67	57.46	0.0417	-0.0253	17116.81	21647.25	17116.81	1.2647	1.0400	1.2647	0.7938	41.95	32.47	7.8654
Model1 End 2	1.25	6	1.25	6	1.25	27.89	26220.51	0.00488	2.40	22.31	2.40	85.83	8.67	60.20	0.0417	-0.0253	21230.99	27269.34	21230.99	1.2844	1.0400	1.2844		40.05	30.99	7.4881
Model1 End 1	1.25	6	1	6	0.75	23.995	15725.58	0.00534	2.40	31.99	3.00	85.83	8.67	52.37	0.0417	-0.0253	13497.76	15882.83	13497.76	1.1767	1.0100	1.1767	0.8067	46.03	35.04	3.3737
Model1 End 2	1.25	6	1	6	0.75	28.015	19493.55	0.00467	2.40	37.35	3.00	85.83	8.67	54.73	0.0417	-0.0253	16487.92	19688.48	16487.92	1.1941	1.0100	1.1941		44.05	33.53	3.2825
Model1 End 1	1.25	6	0.875	6	0.75	24.058	15175.91	0.00538	2.40	32.08	3.43	85.83	8.67	53.25	0.0417	-0.0253	12934.35	15327.67	12934.35	1.1850	1.0100	1.1850	0.8045	45.27	34.56	3.4340
Model1 End 2	1.25	6	0.875	6	0.75	28.078	18863.61	0.00470	2.40	37.44	3.43	85.83	8.67	55.69	0.0417	-0.0253	15841.15	19052.25	15841.15	1.2027	1.0100	1.2027		43.28	33.04	3.3487
Model1 End 1	1.25	6	1.25	6	0.625	23.87	15757.89	0.00519	2.40	38.19	2.40	85.83	8.67	48.66	0.0417	-0.0253	13913.38	15915.47	13913.38	1.1439	1.0100	1.1439	0.8157	49.54	37.27	3.5355
Model1 End 2	1.25	6	1.25	6	0.625	27.89	19317.08	0.00454	2.40	44.62	2.40	85.83	8.67	50.62	0.0417	-0.0253	16826.12	19510.25	16826.12	1.1595	1.0100	1.1595		47.62	35.83	3.4400
Model1 End 1	1.25	6	1.125	6	0.625	23.933	15237.90	0.00522	2.40	38.29	2.67	85.83	8.67	49.31	0.0417	-0.0253	13390.01	15390.28	13390.01	1.1494	1.0100	1.1494	0.8142	48.88	36.85	3.2091
Model1 End 2	1.25	6	1.125	6	0.625	27.953	18715.92	0.00456	2.40	44.72	2.67	85.83	8.67	51.34	0.0417	-0.0253	16220.91	18903.08	16220.91	1.1654	1.0100	1.1654		46.95	35.40	3.1356
Model1 End 1	1.25	6	1	6	0.625	23.995	14695.08	0.00525	2.40	38.39	3.00	85.83	8.67	50.03	0.0417	-0.0253	12841.10	14842.03	12841.10	1.1558	1.0100	1.1558	0.8122	48.19	36.42	2.9059
Model1 End 2	1.25	6	1	6	0.625	28.015	18091.94	0.00459	2.40	44.82	3.00	85.83	8.67	52.14	0.0417	-0.0253	15588.48	18272.86	15588.48	1.1722	1.0100	1.1722		46.24	34.95	2.8530
Model1 End 1	1.25	6	0.875	6	0.625	24.058	14129.44	0.00528	2.40	38.49	3.43	85.83	8.67	50.81	0.0417	-0.0253	12264.65	14270.73	12264.65	1.1636	1.0100	1.1636	0.8099	47.44	35.96	2.5505
Model1 End 2	1.25	6	0.875	6	0.625	28.078	17445.13	0.00462	2.40	44.92	3.43	85.83	8.67	53.01	0.0417	-0.0253	14926.87	17619.58	14926.87	1.1804	1.0100	1.1804		45.48	34.48	2.5146
Model1 End 1	1.25	6	1.25	6	0.5625	23.87	15252.21	0.00514	2.40	42.44	2.40	85.83	8.67	47.50	0.0417	-0.0253	13593.04	15404.74	13593.04	1.1333	1.0100	1.1333	0.8188	50.75	38.03	3.1182
Model1 End 2	1.25	6	1.25	6	0.5625	27.89	18626.73	0.00449	2.40	49.58	2.40	85.83	8.67	49.32	0.0417	-0.0253	16385.64	18813.00	16385.64	1.1481	1.0100	1.1481		48.88	36.62	3.0522
Model1 End 1	1.25	6	1.125	6	0.5625	23.933	14728.15	0.00517	2.40	42.55	2.67	85.83	8.67	48.11	0.0417	-0.0253	13066.33	14875.43	13066.33	1.1385	1.0100	1.1385	0.8173	50.11	37.62	2.5551
Model1 End 2	1.25	6	1.125	6	0.5625	27.953	18021.06	0.00451	2.40	49.69	2.67	85.83	8.67	50.00	0.0417	-0.0253	15776.53	18201.27	15776.53	1.1537	1.0100	1.1537		48.21	36.20	2.5130
Model1 End 1	1.25	6	1	6	0.5625	23.995	14178.42	0.00519	2.40	42.66	3.00	85.83	8.67	48.77	0.0417	-0.0253	12512.29	14178.42	12512.29	1.1332	1.0000	1.1332	0.8153	49.43	37.20	2.2801
Model1 End 2	1.25	6	1	6	0.5625	28.015	17389.71	0.00454	2.40	49.80	3.00	85.83	8.67	50.74	0.0417	-0.0253	15138.16	17389.71	15138.16	1.1487	1.0000	1.1487		47.51	35.76	2.2488
Model1 End 1	1.25	6	1.25	6	0.5	23.87	14746.54	0.00509	2.40	47.74	2.40	85.83	8.67	46.29	0.0417	-0.0253	13272.69	14746.54	13272.69	1.1110	1.0000	1.1110	0.8222	52.07	38.85	2.0711
Model1 End 2	1.25	6	1.25	6	0.5	27.89	17936.39	0.00444	2.40	55.78	2.40	85.83	8.67	47.97	0.0417	-0.0253	15945.15	17936.39	15945.15	1.1249	1.0000	1.1249		50.26	37.49	2.0404
Model1 End 1	1.25	6	1	6	0.5	23.995	13660.33	0.00514	2.40	47.99	3.00	85.83	8.67	47.46	0.0417	-0.0253	12183.07	13660.33	12183.07	1.1213	1.0000	1.1213	0.8187	50.79	38.07	1.6552
Model1 End 2	1.25	6	1	6	0.5	28.015	16686.07	0.00449	2.40	56.03	3.00	85.83	8.67	49.27	0.0417	-0.0253	14687.36	16686.07	14687.36	1.1361	1.0000	1.1361		48.93	36.67	1.6346
Model1 End 1	1.125	6	1	6	0.75	24.058	15250.46	0.00537	2.67	32.08	3.00	85.83	8.67	53.25	0.0417	-0.0253	13025.41	15402.97	13025.41	1.1825	1.0100	1.1825	0.8053	45.27	34.53	3.1959
Model1 End 2	1.125	6	1	6	0.75	28.078	18938.16	0.00470	2.67	37.44	3.00	85.83	8.67	55.69	0.0417	-0.0253	15937.41	19127.54	15937.41	1.2002	1.0100	1.2002		43.28	33.01	3.1295
Model1 End 1	1.125	6	0.875	6	0.75	24.12	14719.52	0.00540	2.67	32.16	3.43	85.83	8.67	54.22	0.0417	-0.0253	12484.98	14866.71	12484.98	1.1908	1.0100	1.1908	0.8032	44.46	34.00	2.7703
Model1 End 2	1.125	6	0.875	6	0.75	28.14	18326.94	0.00473	2.67	37.52	3.43	85.83	8.67	56.76	0.0417	-0.0253	15314.92	18510.21	15314.92	1.2086	1.0100	1.2086		42.47	32.48	2.7234
Model1 End 1	1.125	6	1.125	6	0.625	23.995	14740.88	0.00524	2.67	38.39	2.67	85.83	8.67	50.03	0.0417	-0.0253	12891.46	14888.29	12891.46	1.1549	1.0100	1.1549	0.8127	48.19	36.40	3.0198
Model1 End 2	1.125	6	1.125	6	0.625	28.015	18137.73	0.00458	2.67	44.82	2.67	85.83	8.67	52.14	0.0417	-0.0253	15642.19	18319.11	15642.19	1.1711	1.0100	1.1711		46.24	34.92	2.9756
Model1 End 1	1.125	6	1.125	6	0.5625	23.995	14229.89	0.00519	2.67	42.66	2.67	85.83	8.67	48.77	0.0417	-0.0253	12566.06	14229.89	12566.06	1.1324	1.0000	1.1324	0.8159	49.43	37.18	2.2084
Model1 End 2	1.125	6	1.125	6	0.5625	28.015	17441.19	0.00453	2.67	49.80	2.67	85.83	8.67	50.74	0.0417	-0.0253	15195.75	17441.19	15195.75	1.1478	1.0000	1.1478		47.51	35.74	2.1893
Model1 End 1	1	6	1	6	0.625	24.12	13724.14	0.00530	3.00	38.59	3.00	85.83	8.67	51.68	0.0417	-0.0253	11870.55	13724.14	11870.55	1.1562	1.0000	1.1562	0.8093	46.64	35.39	1.9989
Model1 End 2	1	6	1	6	0.625	28.14	16958.67	0.00463	3.00	45.02	3.00	85.83	8.67	53.97	0.0417	-0.0253	14459.20	16958.67	14459.20	1.1729	1.0000	1.1729		44.67	33.89	1.9879
Model1 End 1	1	6	1	6	0.5625	24.12	13207.82	0.00525	3.00	42.88	3.00	85.83	8.67	50.31	0.0417	-0.0253	11540.04	13194.61	11540.04	1.1434	0.9990	1.1434	0.8125	47.91	36.20	0
Model1 End 2	1	6	1	6	0.5625	28.14	16255.89	0.00459	3.00	50.03	3.00	85.83	8.67	52.45	0.0417	-0.0253	14006.76	16239.63	14006.76	1.1594	0.9990	1.1594		45.96	34.73	0
Model1 End 1	0.875	6	0.875	6	0.75	24.245	13751.07	0.00547	3.43	32.33	3.43	85.83	8.67	56.50	0.0417	-0.0253	11521.96	13751.07	11521.96	1.1935	1.0000	1.1935	0.7996	42.67	32.78	2.0826
Model1 End 2	0.875	6	0.875	6	0.75	28.265	17197.94	0.00479	3.43	37.69	3.43	85.83	8.67	59.26	0.0417	-0.0253	14194.10	17197.94	14194.10	1.2116	1.0000	1.2116		40.68	31.25	2.0702
Model1 End 1	1	8	1	8	0.25	24.12	13479.83	0.00485	4.00	96.48	4.00	85.83	8.67	30.48	0.0417	-0.0253	12742.61	13614.63	12742.61	1.0684	1.0100	1.0684	0.8397	79.09	57.63	7.8614
Model1 End 2	1	8	1	8	0.25	28.14	16052.32	0.00421	4.00	112.56	4.00	85.83	8.67	31.17	0.0417	-0.0253	15056.17	16212.84	15056.17	1.0768	1.0100	1.0768		77.35	56.36	6.2699
Model1 End 1	1.125	10	1.125	10	0.25	23.995	18095.63	0.00478	4.44	95.98	4.44	85.83	8.67	23.39	0.0417	-0.0253	17364.02	18457.54	17364.02	1.0630	1.0200	1.0630	0.8453	103.06	74.53	3.1946
Model1 End 2	1.125	10	1.125	10	0.25	28.015	21406.64	0.00414	4.44	112.06	4.44	85.83	8.67	23.80	0.0417	-0.0253	20415.46	21834.78	20415.46	1.0695	1.0200	1.0695		101.30	73.25	4.0552
Model1 End 1	0.875	8	0.875	8	0.4375	24.245	13639.54	0.00507	4.57	55.42	4.57	85.83	8.67	34.41	0.0417	-0.0253	12341.50	13912.33	12341.50	1.1273	1.0200	1.1273	0.8242	70.07	52.13	8.9029
Model1 End 2	0.875	8	0.875	8	0.4375	28.265	16549.29	0.00442	4.57	64.61	4.57	85.83	8.67	35.61	0.0417	-0.0253	14799.01	16880.28	14799.01	1.1406	1.0200	1.1406		67.70	50.37	7.2771
Model1 End 1	0.875	8	0.875	8	0.375	24.245	13117.85	0.00501	4.57	64.65	4.57	85.83	8.67	33.34	0.0417	-0.0253	12005.82	13249.03	12005.82	1.1036	1.0100	1.1036	0.8281	72.30	53.51	7.5913
Model1 End 2	0.875	8	0.875	8	0.375	28.265	15840.26	0.00436	4.57	75.37	4.57	85.83	8.67	34.41	0.0417	-0.0253	14340.52	15998.66	14340.52	1.1156	1.0100	1.1156		70.06	51.85	6.1609
Model1 End 1	0.875	8	0.875	8	0.3125	24.245	12596.16	0.00495	4.57	77.58	4.57	85.83	8.67	32.24	0.0417	-0.0253	11670.15	12722.12	11670.15	1.0901	1.0100	1.0901	0.8325	74.77	55.02	6.9402
Model1 End 2	0.875	8	0.875	8	0.3125	28.265	15131.23	0.00431	4.57	90.45	4.57	85.83	8.67	33.16	0.0417	-0.0253	13882.02	15282.54	13882.02	1.1009	1.0100	1.1009		72.69	53.49	5.6978
Model1 End 1	0.875	8	0.875	8	0.25	24.245	12074.47	0.00488	4.57	96.98	4.57	85.83	8.67	31.09	0.0417	-0.0253	11334.47	12062.40	11334.47	1.0642	0.9990	1.0642	0.8372	77.53	56.69	0
Model1 End 2	0.875	8	0.875	8	0.25	28.265	14422.20	0.00425	4.57	113.06	4.57	85.83	8.67	31.86	0.0417	-0.0253	13423.53	14407.77	13423.53	1.0733	0.9990	1.0733		75.66	55.32	0
Model1 End 1	1	10	1	10	0.4375	24.12	17882.43	0.00494	5.00	55.13	5.00	85.83	8.67	25.68	0.0417	-0.0253	16589.29	18418.91	16589.29	1.1103	1.0300	1.1103	0.8329	93.89	69.05	30.1394
Model1 End 2	1	10	1	10	0.4375	28.14	21470.95	0.00430	5.00	64.32	5.00	85.83	8.67	26.40	0.0417	-0.0253	19725.09	22115.08	19725.09	1.1212	1.0300	1.1212		91.30	67.15	20.5839
Model1 End 1	1	10	1	10	0.375	24.12	17366.11	0.00490	5.00	64.32	5.00	85.83	8.67	25.04	0.0417	-0.0253	16258.78	17887.09	16258.78	1.1001	1.0300	1.1001	0.8362	96.27	70.49	18.9001
Model1 End 2	1	10	1	10	0.375	28.14	20768.17	0.00426	5.00	75.04	5.00	85.83	8.67	25.68	0.0417	-0.0253	19272.65	21391.22	19272.65	1.1099	1.0300	1.1099		93.87	68.73	14.1353
Model1 End 1	1	10	1	10	0.3125	24.12	16849.78	0.00485	5.00	77.18	5.00	85.83	8.67	24.38	0.0417	-0.0253	15928.27	17186.78	15928.27	1.0790	1.0200	1.0790	0.8397	98.86	72.04	5.7369
Model1 End 2	1	10	1	10	0.3125	28.14	20065.40	0.00421	5.00	90.05	5.00	85.83	8.67	24.93	0.0417	-0.0253	18820.21	20466.70	18820.21	1.0875	1.0200	1.0875		96.68	70.45	7.4041
Model1 End 1	1	10	1	10	0.25	24.12	16333.46	0.00480	5.00	96.48	5.00	85.83	8.67	23.71	0.0417	-0.0253	15597.75	16496.79	15597.75	1.0576	1.0100	1.0576	0.8436	101.67	73.71	2.8281
Model1 End 2	1	10	1	10	0.25	28.14	19362.62	0.00417	5.00	112.56	5.00	85.83	8.67	24.16	0.0417	-0.0253	18367.77	19556.25	18367.77	1.0647	1.0100	1.0647		99.77	72.32	3.8104
Model1 End 1	0.75	8	0.75	8	0.5	24.37	12777.56	0.00519	5.33	48.74	5.33	85.83	8.67	36.81	0.0417	-0.0253	11290.62	12905.34	11290.62	1.1430	1.0100	1.1430	0.8163	65.49	49.23	4.7504
Model1 End 2	0.75	8	0.75	8	0.5	28.39	15653.46	0.00453	5.33	56.78	5.33	85.83	8.67	38.30	0.0417	-0.0253	13649.94	15809.99	13649.94	1.1582	1.0100	1.1582		62.95	47.32	3.8961
Model1 End 1	0.75	8	0.75	8	0.4375	24.37	12250.48	0.00513	5.33	55.70	5.33	85.83	8.67	35.66	0.0417	-0.0253	10949.72	12250.48	10949.72	1.1188	1.0000	1.1188	0.8201	67.61	50.58	3.7101
Model1 End 2	0.75	8	0.75	8	0.4375	28.39	14938.14	0.00448	5.33	64.89	5.33	85.83	8.67	37.01	0.0417	-0.0253	13185.34	14938.14	13185.34	1.1329	1.0000	1.1329		65.14	48.73	3.0947

Table B1 Continued

	E	Fy																								
	29600	56.8				End 1 = Shallow End End 2 = Deep End			Comp.		Tension	Web	Flanges													
DESCRIPTION	tf1	bf1	tf2	bf2	tw	dw	Mp(in kips)	θ p	bf1/2tf1	h/tw	bf2/2tf2	λ p	λ p	Lb/ry	m(top)	m(bot)	M(aisc)	Mu(abaqus)	My	Mu/My	Mu/Mp	Mu/M(aisc)	α	Lp	Lpd	R
Model1 End 1	1.125	12	1.125	12	0.375	23.995	22327.94	0.00482	5.33	63.99	5.33	85.83	8.67	20.00	0.0417	-0.0253	21227.30	22997.78	21227.30	1.0834	1.0300	1.0834	0.8418	120.56	87.60	13.7
Model1 End 2	1.125	12	1.125	12	0.375	28.015	26523.83	0.00419	5.33	74.71	5.33	85.83	8.67	20.41	0.0417	-0.0253	25034.27	27319.54	25034.27	1.0913	1.0300	1.0913		118.11	85.83	14.66
Model1 End 1	0.75	8	0.75	8	0.375	24.37	11723.40	0.00506	5.33	64.99	5.33	85.83	8.67	34.45	0.0417	-0.0253	10608.83	11723.40	10608.83	1.1051	1.0000	1.1051	0.8243	69.97	52.05	2.275
Model1 End 2	0.75	8	0.75	8	0.375	28.39	14222.82	0.00442	5.33	75.71	5.33	85.83	8.67	35.66	0.0417	-0.0253	12720.73	14222.82	12720.73	1.1181	1.0000	1.1181		67.61	50.30	1.957
Model1 End 1	1.125	12	1.125	12	0.3125	23.995	21816.95	0.00478	5.33	76.78	5.33	85.83	8.67	19.58	0.0417	-0.0253	20901.90	22253.29	20901.90	1.0647	1.0200	1.0647	0.8447	123.14	89.12	4.133
Model1 End 2	1.125	12	1.125	12	0.3125	28.015	25827.28	0.00415	5.33	89.65	5.33	85.83	8.67	19.93	0.0417	-0.0253	24587.83	26343.83	24587.83	1.0714	1.0200	1.0714		120.96	87.55	5.067
Model1 End 1	1.125	12	1.125	12	0.25	23.995	21305.96	0.00475	5.33	95.98	5.33	85.83	8.67	19.15	0.0417	-0.0253	20576.50	21519.02	20576.50	1.0458	1.0100	1.0458	0.8478	125.90	90.74	2.3850
Model1 End 2	1.125	12	1.125	12	0.25	28.015	25130.73	0.00411	5.33	112.06	5.33	85.83	8.67	19.44	0.0417	-0.0253	24141.40	25382.04	24141.40	1.0514	1.0100	1.0514		124.03	89.39	2.872
Model1 End 1	0.875	10	0.875	10	0.5	24.245	16658.16	0.00503	5.71	48.49	5.71	85.83	8.67	27.02	0.0417	-0.0253	15175.12	17157.91	15175.12	1.1307	1.0300	1.1307	0.8265	89.22	66.18	6.747
Model1 End 2	0.875	10	0.875	10	0.5	28.265	20154.84	0.00439	5.71	56.53	5.71	85.83	8.67	27.92	0.0417	-0.0253	18154.89	20759.49	18154.89	1.1435	1.0300	1.1435		86.35	64.05	5.4240
Model1 End 1	0.875	10	0.875	10	0.4375	24.245	16136.47	0.00498	5.71	55.42	5.71	85.83	8.67	26.33	0.0417	-0.0253	14839.44	16459.20	14839.44	1.1092	1.0200	1.1092	0.8298	91.57	67.62	3.588
Model1 End 2	0.875	10	0.875	10	0.4375	28.265	19445.81	0.00434	5.71	64.61	5.71	85.83	8.67	27.13	0.0417	-0.0253	17696.40	19834.73	17696.40	1.1208	1.0200	1.1208		88.84	65.61	4.12
Model1 End 1	0.875	10	0.875	10	0.375	24.245	15614.78	0.00493	5.71	64.65	5.71	85.83	8.67	25.61	0.0417	-0.0253	14503.76	15770.93	14503.76	1.0874	1.0100	1.0874	0.8334	94.12	69.18	2.855
Model1 End 2	0.875	10	0.875	10	0.375	28.265	18736.78	0.00429	5.71	75.37	5.71	85.83	8.67	26.33	0.0417	-0.0253	17237.90	18924.14	17237.90	1.0978	1.0100	1.0978		91.57	67.30	3.288
Model1 End 1	0.875	10	0.875	10	0.3125	24.245	15093.09	0.00488	5.71	77.58	5.71	85.83	8.67	24.88	0.0417	-0.0253	14168.08	15244.02	14168.08	1.0759	1.0100	1.0759	0.8372	96.91	70.86	2.062
Model1 End 2	0.875	10	0.875	10	0.3125	28.265	18027.74	0.00425	5.71	90.45	5.71	85.83	8.67	25.49	0.0417	-0.0253	16779.41	18208.02	16779.41	1.0851	1.0100	1.0851		94.57	69.15	2.403
Model1 End 1	1	12	1	12	0.5	24.12	21252.39	0.00493	6.00	48.24	6.00	85.83	8.67	21.22	0.0417	-0.0253	19774.95	21889.96	19774.95	1.1070	1.0300	1.1070	0.8339	113.59	83.42	3.866
Model1 End 2	1	12	1	12	0.5	28.14	25484.03	0.00429	6.00	56.28	6.00	85.83	8.67	21.80	0.0417	-0.0253	23489.13	26248.55	23489.13	1.1175	1.0300	1.1175		110.56	81.20	4.534
Model1 End 1	0.5	6	0.5	6	0.5	24.62	8584.07	0.00555	6.00	49.24	6.00	85.83	8.67	60.09	0.0417	-0.0253	7092.99	8242.77	7092.99	1.1621	0.9602	1.1621	0.7956	40.12	30.98	0
Model1 End 2	0.5	6	0.5	6	0.5	28.64	10789.23	0.00485	6.00	57.28	6.00	85.83	8.67	63.23	0.0417	-0.0253	8781.84	10342.99	8781.84	1.1778	0.9586	1.1778		38.13	29.44	0
Model1 End 1	1	12	1	12	0.4375	24.12	20736.07	0.00489	6.00	55.13	6.00	85.83	8.67	20.78	0.0417	-0.0253	19444.43	21150.79	19444.43	1.0878	1.0200	1.0878	0.8368	116.03	84.89	3.0270
Model1 End 2	1	12	1	12	0.4375	28.14	24781.25	0.00425	6.00	64.32	6.00	85.83	8.67	21.30	0.0417	-0.0253	23036.69	25276.88	23036.69	1.0972	1.0200	1.0972		113.19	82.81	3.46
Model1 End 1	0.5	6	0.5	6	0.4375	24.62	8046.12	0.00547	6.00	56.27	6.00	85.83	8.67	57.64	0.0417	-0.0253	6741.49	7675.76	6741.49	1.1386	0.9540	1.1386	0.7997	41.82	32.12	0
Model1 End 2	0.5	6	0.5	6	0.4375	28.64	10061.26	0.00479	6.00	65.46	6.00	85.83	8.67	60.54	0.0417	-0.0253	8304.85	9582.64	8304.85	1.1539	0.9524	1.1539		39.82	30.59	0
Model1 End 1	1	12	1	12	0.375	24.12	20219.74	0.00485	6.00	64.32	6.00	85.83	8.67	20.32	0.0417	-0.0253	19113.92	20624.14	19113.92	1.0790	1.0200	1.0790	0.8397	118.63	86.45	2.41
Model1 End 2	1	12	1	12	0.375	28.14	24078.48	0.00421	6.00	75.04	6.00	85.83	8.67	20.78	0.0417	-0.0253	22584.25	24560.05	22584.25	1.0875	1.0200	1.0875		116.02	84.54	2.679
Model1 End 1	0.5	6	0.5	6	0.375	24.62	7508.17	0.00539	6.00	65.65	6.00	85.83	8.67	55.03	0.0417	-0.0253	6390.00	7123.00	6390.00	1.1147	0.9487	1.1147	0.8045	43.81	33.44	0
Model1 End 2	0.5	6	0.5	6	0.375	28.64	9333.29	0.00471	6.00	76.37	6.00	85.83	8.67	57.66	0.0417	-0.0253	7827.87	8840.49	7827.87	1.1294	0.9472	1.1294		41.81	31.92	0
Model1 End 1	0.625	8	0.625	8	0.5	24.495	11394.12	0.00527	6.40	48.99	6.40	85.83	8.67	38.66	0.0417	-0.0253	9904.91	11394.12	9904.91	1.1503	1.0000	1.1503	0.8110	62.36	47.20	2.305
Model1 End 2	0.625	8	0.625	8	0.5	28.515	14048.81	0.00461	6.40	57.03	6.40	85.83	8.67	40.35	0.0417	-0.0253	12043.18	14048.81	12043.18	1.1665	1.0000	1.1665		59.74	45.22	1.946
Model1 End 1	0.625	8	0.625	8	0.4375	24.495	10861.61	0.00521	6.40	55.99	6.40	85.83	8.67	37.33	0.0417	-0.0253	9558.74	10807.30	9558.74	1.1306	0.9950	1.1306	0.8150	64.57	48.62	0
Model1 End 2	0.625	8	0.625	8	0.4375	28.515	13327.18	0.00455	6.40	65.18	6.40	85.83	8.67	38.88	0.0417	-0.0253	11572.41	13260.54	11572.41	1.1459	0.9950	1.1459		62.01	46.70	0
Model1 End 1	0.75	10	0.75	10	0.5	24.37	14917.79	0.00509	6.67	48.74	6.67	85.83	8.67	27.95	0.0417	-0.0253	13431.48	15216.14	13431.48	1.1329	1.0200	1.1329	0.8225	86.24	64.30	2.289
Model1 End 2	0.75	10	0.75	10	0.5	28.39	18136.18	0.00444	6.67	56.78	6.67	85.83	8.67	28.96	0.0417	-0.0253	16133.22	18498.91	16133.22	1.1466	1.0200	1.1466		83.23	62.06	2.697
Model1 End 1	0.75	10	0.75	10	0.4375	24.37	14390.70	0.00504	6.67	55.70	6.67	85.83	8.67	27.17	0.0417	-0.0253	13090.58	14534.61	13090.58	1.1103	1.0100	1.1103	0.8261	88.73	65.86	1.737
Model1 End 2	0.75	10	0.75	10	0.4375	28.39	17420.87	0.00439	6.67	64.89	6.67	85.83	8.67	28.08	0.0417	-0.0253	15668.61	17595.07	15668.61	1.1230	1.0100	1.1230		85.85	63.72	1.969
Model1 End 1	0.875	12	0.875	12	0.5	24.245	19155.09	0.00497	6.86	48.49	6.86	85.83	8.67	21.74	0.0417	-0.0253	17673.06	19538.19	17673.06	1.1055	1.0200	1.1055	0.8310	110.88	81.75	2.262
Model1 End 2	0.875	12	0.875	12	0.5	28.265	23051.36	0.00433	6.86	56.53	6.86	85.83	8.67	22.39	0.0417	-0.0253	21052.28	23512.39	21052.28	1.1169	1.0200	1.1169		107.67	79.39	2.522
Model1 End 1	0.875	12	0.875	12	0.4375	24.245	18633.40	0.00493	6.86	55.42	6.86	85.83	8.67	21.24	0.0417	-0.0253	17337.38	18819.73	17337.38	1.0855	1.0100	1.0855	0.8340	113.48	83.34	1.89
Model1 End 2	0.875	12	0.875	12	0.4375	28.265	22342.33	0.00429	6.86	64.61	6.86	85.83	8.67	21.82	0.0417	-0.0253	20593.78	22565.75	20593.78	1.0958	1.0100	1.0958		110.46	81.12	2.08
Model1 End 1	0.4375	6	0.4375	6	0.1875	24.6825	5367.46	0.00512	6.86	131.64	6.86	85.83	8.67	47.50	0.0417	-0.0253	4808.31	4975.63	4808.31	1.0348	0.9270	1.0348	0.8209	50.75	37.93	0
Model1 End 2	0.4375	6	0.4375	6	0.1875	28.7025	6538.23	0.00447	6.86	153.08	6.86	85.83	8.67	49.27	0.0417	-0.0253	5785.45	6060.94	5785.45	1.0476	0.9270	1.0476		48.93	36.56	0
Model1 End 1	0.5	8	0.5	8	0.3125	24.62	8397.03	0.00516	8.00	78.78	8.00	85.83	8.67	36.36	0.0417	-0.0253	7465.50	8027.56	7465.50	1.0753	0.9560	1.0753	0.8184	66.30	49.70	0
Model1 End 2	0.5	8	0.5	8	0.3125	28.64	10260.47	0.00450	8.00	91.65	8.00	85.83	8.67	37.79	0.0417	-0.0253	9006.19	9809.01	9006.19	1.0891	0.9560	1.0891		63.80	47.83	0
Model1 End 1	0.375	6	0.375	6	0.25	24.745	5384.05	0.00532	8.00	98.98	8.00	85.83	8.67	53.32	0.0417	-0.0253	4638.09	4872.57	4638.09	1.0506	0.9050	1.0506	0.8082	45.21	34.35	0
Model1 End 2	0.375	6	0.375	6	0.25	28.765	6661.45	0.00465	8.00	115.06	8.00	85.83	8.67	55.76	0.0417	-0.0253	5657.34	6028.61	5657.34	1.0656	0.9050	1.0656		43.23	32.85	0
Model1 End 1	0.375	6	0.375	6	0.1875	24.745	4840.62	0.00518	8.00	131.97	8.00	85.83	8.67	49.34	0.0417	-0.0253	4281.21	4356.56	4281.21	1.0176	0.9000	1.0176	0.8167	48.85	36.71	0
Model1 End 2	0.375	6	0.375	6	0.1875	28.765	5927.11	0.00453	8.00	153.41	8.00	85.83	8.67	51.33	0.0417	-0.0253	5174.08	5334.40	5174.08	1.0310	0.9000	1.0310		46.96	35.29	0
Model1 End 1	0.5625	10	0.5625	10	0.3125	24.5575	10701.97	0.00502	8.89	78.58	8.89	85.83	8.67	26.95	0.0417	-0.0253	9771.32	10273.89	9771.32	1.0514	0.9600	1.0514	0.8274	89.46	66.27	0
Model1 End 2	0.5625	10	0.5625	10	0.3125	28.5775	12934.22	0.00438	8.89	91.45	8.89	85.83	8.67	27.83	0.0417	-0.0253	11680.74	12416.85	11680.74	1.0630	0.9600	1.0630		86.63	64.18	0
Model1 End 1	0.4375	8	0.4375	8	0.25	24.6825	7156.61	0.00512	9.14	98.73	9.14	85.83	8.67	35.62	0.0417	-0.0253	6411.08	6619.86	6411.08	1.0326	0.9250	1.0326	0.8209	67.67	50.57	0
Model1 End 2	0.4375	8	0.4375	8	0.25	28.7025	8717.64	0.00447	9.14	114.81	9.14	85.83	8.67	36.95	0.0417	-0.0253	7713.93	8063.82	7713.93	1.0454	0.9250	1.0454		65.23	48.74	0
Model1 End 1	0.625	12	0.625	12	0.3125	24.495	13363.64	0.00493	9.60	78.38	9.60	85.83	8.67	21.28	0.0417	-0.0253	12434.18	12815.73	12434.18	1.0307	0.9590	1.0307	0.8341	113.27	83.17	0
Model1 End 2	0.625	12	0.625	12	0.3125	28.515	16021.79	0.00429	9.60	91.25	9.60	85.83	8.67	21.86	0.0417	-0.0253	14769.39	15364.90	14769.39	1.0403	0.9590	1.0403		110.26	80.96	0
Model1 End 1	0.3125	6	0.3125	6	0.25	24.8075	4859.99	0.00541	9.60	99.23	9.60	85.83	8.67	56.35	0.0417	-0.0253	4113.77	4247.63	4113.77	1.0325	0.8740	1.0325	0.8028	42.78	32.73	0
Model1 End 2	0.3125	6	0.3125	6	0.25	28.8275	6053.55	0.00474	9.60	115.31	9.60	85.83	8.67	59.11	0.0417	-0.0253	5049.20	5290.80	5049.20	1.0479	0.8740	1.0479		40.78	31.20	0
Model1 End 1	0.5	10	0.5	10	0.25	24.62	9285.89	0.00498	10.00	98.48	10.00	85.83	8.67	26.41	0.0417	-0.0253	8541.01	8645.17	8541.01	1.0122	0.9310	1.0122	0.8300	91.27	67.38	0
Model1 End 2	0.5	10	0.5	10	0.25	28.64	11187.65	0.00434	10.00	114.56	10.00	85.83	8.67	27.22	0.0417	-0.0253	10184.52	10415.70	10184.52	1.0227	0.9310	1.0227		88.56	65.38	0
Model1 End 1	0.5	10	0.5	10	0.1875	24.62	8747.94	0.00490	10.00	131.31	10.00	85.83	8.67	25.13	0.0417	-0.0253	8189.51	8109.34	8189.51	0.9902	0.9270	0.9902	0.8363	95.94	70.23	0
Model1 End 2	0.5	10	0.5	10	0.1875	28.64	10459.67	0.00426	10.00	152.75	10.00	85.83	8.67	25.77	0.0417	-0.0253	9707.53	9696.12	9707.53	0.9988	0.9270	0.9988		93.56	68.49	0
Model1 End 1	0.5625	12	0.5625	12	0.25	24.5575	11771.91	0.00489	10.67	98.23	10.67	85.83	8.67	20.89	0.0417	-0.0253	11027.93	11006.74	11027.93	0.9981	0.9350	0.9981	0.8366	115.40	84.45	0
Model1 End 2	0.5625	12	0.5625	12	0.25	28.5775	14071.47	0.00425	10.67	114.31	10.67	85.83	8.67	21.42	0.0417	-0.0253	13069.15	13156.82	13069.15	1.0067	0.9350	1.0067		112.56	82.37	0
Model1 End 1	0.375	8	0.375	8	0.25	24.745	6454.17	0.00518	10.67	98.98	10.67	85.83	8.67	37.01	0.0417	-0.0253	5708.28	5744.21	5708.28	1.0063	0.8900	1.0063	0.8167	65.14	48.95	0
Model1 End 2	0.375	8	0.375	8	0.25	28.765	7902.82	0.00453	10.67	115.06	10.67	85.83	8.67	38.50	0.0417	-0.0253	6898.77	7033.51	6898.77	1.0195	0.8900	1.0195		62.61	47.05	0

Table B1 Continued

	E	Fy																									
	29600	56.8				End 1 = Shallow End End 2 = Deep End			Comp.		Tension	Web	Flanges														
DESCRIPTION	tf1	bf1	tf2	bf2	tw	dw	Mp(in kips)	θ p	bf1/2tf1	h/tw	bf2/2tf2	λ p	λ p	Lb/ry	m(top)	m(bot)	M(aisc)	Mu(abaqus)	My	Mu/My	Mu/Mp	Mu/M(aisc)	α	Lp	Lpd	R
Model1 End 1	0.5625	12	0.5625	12	0.1875	24.5575	11236.68	0.00482	10.67	130.97	10.67	85.83	8.67	20.06	0.0417	-0.0253	10679.10	10472.59	10679.10	0.9807	0.9320	0.9807	0.8419	120.19	87.32	0
Model1 End 2	0.5625	12	0.5625	12	0.1875	28.5775	13346.67	0.00419	10.67	152.41	10.67	85.83	8.67	20.47	0.0417	-0.0253	12595.28	12439.10	12595.28	0.9876	0.9320	0.9876		117.76	85.56	0
Model1 End 1	0.375	8	0.375	8	0.1875	24.745	5910.74	0.00506	10.67	131.97	10.67	85.83	8.67	34.59	0.0417	-0.0253	5351.40	5248.73	5351.40	0.9808	0.8880	0.9808	0.8245	69.69	51.83	0
Model1 End 2	0.375	8	0.375	8	0.1875	28.765	7168.48	0.00441	10.67	153.41	10.67	85.83	8.67	35.79	0.0417	-0.0253	6415.51	6365.61	6415.51	0.9922	0.8880	0.9922		67.35	50.09	0
Model1 End 1	0.4375	10	0.4375	10	0.25	24.6825	8405.07	0.00503	11.43	98.73	11.43	85.83	8.67	27.14	0.0417	-0.0253	7659.67	7589.78	7659.67	0.9909	0.9030	0.9909	0.8268	88.84	65.87	0
Model1 End 2	0.4375	10	0.4375	10	0.25	28.7025	10165.90	0.00438	11.43	114.81	11.43	85.83	8.67	28.03	0.0417	-0.0253	9162.30	9179.81	9162.30	1.0019	0.9030	1.0019		85.99	63.76	0
Model1 End 1	0.5	12	0.5	12	0.25	24.62	10712.71	0.00493	12.00	98.48	12.00	85.83	8.67	21.30	0.0417	-0.0253	9968.01	9737.85	9968.01	0.9769	0.9090	0.9769	0.8341	113.17	83.09	0
Model1 End 2	0.5	12	0.5	12	0.25	28.64	12842.80	0.00429	12.00	114.56	12.00	85.83	8.67	21.88	0.0417	-0.0253	11839.83	11674.10	11839.83	0.9860	0.9090	0.9860		110.16	80.88	0

APPENDIX B2

Table B2 Model-2 L_b = 60 in. Parametric Study Results

E	Fy
29600	56.8

End 1 = Shallow End
End 2 = Deep End

DESCRIPTION	tf1	bf1	tf2	bf2	tw	dw	Mp(in kips)	θ p	Comp. bf1/2tf1	h/tw	Tension bf2/2tf2	Web λ p	Flanges λ p	Lb/ry	m(top)	m(bot)	M(aisc)	Mu(abaqus)	My	Mu/My	Mu/Mp	Mu/M(aisc)	α	Lp	Lpd	R
Model2 End 1	1.25	6	1.25	6	0.875	24.247	18166.69	0.00529	2.40	27.71	2.40	85.83	8.67	53.03	0.0417	0.1823	15501.67	18166.69	15501.67	1.1719	1.0000	1.1719	0.6551	45.45	41.39	3.2310
Model2 End 2	1.25	6	1.25	6	0.875	32.685	27729.56	0.00409	2.40	37.35	2.40	85.83	8.67	57.90	0.0417	0.1823	22985.67	27729.56	22985.67	1.2064	1.0000	1.2064		41.64	37.92	2.5934
Model2 End 1	1.25	6	1.25	6	0.75	24.247	17123.13	0.00521	2.40	32.33	2.40	85.83	8.67	51.04	0.0417	0.1823	14840.07	17106.01	14840.07	1.1527	0.9990	1.1527	0.6628	47.23	42.65	0
Model2 End 2	1.25	6	1.25	6	0.75	32.685	25833.35	0.00403	2.40	43.58	2.40	85.83	8.67	55.52	0.0417	0.1823	21768.10	25807.52	21768.10	1.1856	0.9990	1.1856		43.42	39.21	0
Model2 End 1	1.25	6	1.25	6	0.625	24.247	16079.57	0.00512	2.40	38.80	2.40	85.83	8.67	48.85	0.0417	0.1823	14178.47	15967.01	14178.47	1.1261	0.9930	1.1261	0.6717	49.35	44.13	0
Model2 End 2	1.25	6	1.25	6	0.625	32.685	23937.15	0.00395	2.40	52.30	2.40	85.83	8.67	52.85	0.0417	0.1823	20550.53	23769.59	20550.53	1.1566	0.9930	1.1566		45.61	40.79	0
Model2 End 1	1.25	6	1.25	6	0.5625	24.247	15557.79	0.00507	2.40	43.11	2.40	85.83	8.67	47.68	0.0417	0.1823	13847.67	15417.77	13847.67	1.1134	0.9910	1.1134	0.6767	50.56	44.97	0
Model2 End 2	1.25	6	1.25	6	0.5625	32.685	22989.05	0.00391	2.40	58.11	2.40	85.83	8.67	51.40	0.0417	0.1823	19941.74	22782.15	19941.74	1.1424	0.9910	1.1424		46.90	41.71	0
Model2 End 1	1.25	6	1.25	6	0.5	24.247	15036.01	0.00502	2.40	48.49	2.40	85.83	8.67	46.45	0.0417	0.1823	13516.87	14840.54	13516.87	1.0979	0.9870	1.0979	0.6822	51.90	45.88	0
Model2 End 2	1.25	6	1.25	6	0.5	32.685	22040.95	0.00387	2.40	65.37	2.40	85.83	8.67	49.89	0.0417	0.1823	19332.96	21754.42	19332.96	1.1253	0.9870	1.1253		48.32	42.72	0
Model2 End 1	1.125	6	1.125	6	1	24.372	18210.38	0.00543	2.67	24.37	2.67	85.83	8.67	56.62	0.0417	0.1823	15157.01	18210.38	15157.01	1.2014	1.0000	1.2014	0.6436	42.58	39.26	3.6147
Model2 End 2	1.125	6	1.125	6	1	32.81	28296.40	0.00420	2.67	32.81	2.67	85.83	8.67	62.10	0.0417	0.1823	22868.04	28296.40	22868.04	1.2374	1.0000	1.2374		38.82	35.80	2.8871
Model2 End 1	1.125	6	1.125	6	0.875	24.372	17156.03	0.00535	2.67	27.85	2.67	85.83	8.67	54.73	0.0417	0.1823	14485.13	17156.03	14485.13	1.1844	1.0000	1.1844	0.6502	44.05	40.33	2.2109
Model2 End 2	1.125	6	1.125	6	0.875	32.81	26385.66	0.00414	2.67	37.50	2.67	85.83	8.67	59.91	0.0417	0.1823	21636.44	26385.66	21636.44	1.2195	1.0000	1.2195		40.24	36.84	1.7871
Model2 End 1	1.125	6	1.125	6	0.75	24.372	16101.68	0.00526	2.67	32.50	2.67	85.83	8.67	52.60	0.0417	0.1823	13813.24	16021.17	13813.24	1.1598	0.9950	1.1598	0.6579	45.83	41.61	0
Model2 End 2	1.125	6	1.125	6	0.75	32.81	24474.93	0.00407	2.67	43.75	2.67	85.83	8.67	57.39	0.0417	0.1823	20404.85	24352.55	20404.85	1.1935	0.9950	1.1935		42.01	38.14	0
Model2 End 1	1	6	1	6	1	24.497	17210.94	0.00549	3.00	24.50	3.00	85.83	8.67	58.77	0.0417	0.1823	14152.08	17210.94	14152.08	1.2161	1.0000	1.2161	0.6382	41.02	38.04	2.2013
Model2 End 2	1	6	1	6	1	32.935	26967.48	0.00425	3.00	32.93	3.00	85.83	8.67	64.62	0.0417	0.1823	21534.04	26967.48	21534.04	1.2523	1.0000	1.2523		37.31	34.60	1.7776
Model2 End 1	1	6	1	6	0.625	24.497	14015.37	0.00523	3.00	39.20	3.00	85.83	8.67	51.90	0.0417	0.1823	12105.25	13791.12	12105.25	1.1393	0.9840	1.1393	0.6614	46.45	42.01	0
Model2 End 2	1	6	1	6	0.625	32.935	21191.52	0.00404	3.00	52.70	3.00	85.83	8.67	56.56	0.0417	0.1823	17796.88	20852.45	17796.88	1.1717	0.9840	1.1717		42.62	38.55	0
Model2 End 1	1	8	1	8	0.4375	24.497	15314.05	0.00495	4.00	55.99	4.00	85.83	8.67	33.54	0.0417	0.1823	13979.79	15467.19	13979.79	1.1064	1.0100	1.1064	0.6911	71.88	62.90	16.6442
Model2 End 2	1	8	1	8	0.4375	32.935	22158.51	0.00380	4.00	75.28	4.00	85.83	8.67	35.77	0.0417	0.1823	19784.38	22380.09	19784.38	1.1312	1.0100	1.1312		67.39	58.98	13.5374
Model2 End 1	1	8	1	8	0.375	24.497	14781.46	0.00489	4.00	65.33	4.00	85.83	8.67	32.58	0.0417	0.1823	13638.65	14929.27	13638.65	1.0946	1.0100	1.0946	0.6974	74.00	64.31	14.7960
Model2 End 2	1	8	1	8	0.375	32.935	21195.85	0.00375	4.00	87.83	4.00	85.83	8.67	34.55	0.0417	0.1823	19161.52	21407.80	19161.52	1.1172	1.0100	1.1172		69.76	60.63	12.2230
Model2 End 1	1	8	1	8	0.3125	24.497	14248.86	0.00484	4.00	78.39	4.00	85.83	8.67	31.58	0.0417	0.1823	13297.51	14248.86	13297.51	1.0715	1.0000	1.0715	0.7042	76.34	65.82	12.5432
Model2 End 2	1	8	1	8	0.3125	32.935	20233.18	0.00370	4.00	105.39	4.00	85.83	8.67	33.29	0.0417	0.1823	18538.65	20233.18	18538.65	1.0914	1.0000	1.0914		72.42	62.44	10.5627
Model2 End 1	0.875	8	0.875	8	0.5	24.622	14442.01	0.00505	4.57	49.24	4.57	85.83	8.67	35.56	0.0417	0.1823	12912.72	14442.01	12912.72	1.1184	1.0000	1.1184	0.6796	67.80	60.11	6.8779
Model2 End 2	0.875	8	0.875	8	0.5	33.06	21252.25	0.00389	4.57	66.12	4.57	85.83	8.67	38.28	0.0417	0.1823	18535.23	21252.25	18535.23	1.1466	1.0000	1.1466		62.98	55.84	5.2298
Model2 End 1	0.875	8	0.875	8	0.4375	24.622	13903.96	0.00500	4.57	56.28	4.57	85.83	8.67	34.52	0.0417	0.1823	12566.34	13876.15	12566.34	1.1042	0.9980	1.1042	0.6855	69.83	61.50	0
Model2 End 2	0.875	8	0.875	8	0.4375	33.06	20282.27	0.00384	4.57	75.56	4.57	85.83	8.67	36.99	0.0417	0.1823	17905.25	20241.70	17905.25	1.1305	0.9980	1.1305		65.17	57.40	0
Model2 End 1	1	10	1	10	0.3125	24.497	17145.33	0.00478	5.00	78.39	5.00	85.83	8.67	24.44	0.0417	0.1823	16195.47	17145.33	16195.47	1.0586	1.0000	1.0586	0.7118	98.65	84.33	6.6935
Model2 End 2	1	10	1	10	0.3125	32.935	24088.16	0.00365	5.00	105.39	5.00	85.83	8.67	25.57	0.0417	0.1823	22394.74	24088.16	22394.74	1.0756	1.0000	1.0756		94.27	80.58	5.3727
Model2 End 1	1	10	1	10	0.25	24.497	16612.74	0.00473	5.00	97.99	5.00	85.83	8.67	23.75	0.0417	0.1823	15854.33	16579.51	15854.33	1.0457	0.9980	1.0457	0.7184	101.49	86.10	0
Model2 End 2	1	10	1	10	0.25	32.935	23125.49	0.00360	5.00	131.74	5.00	85.83	8.67	24.69	0.0417	0.1823	21771.88	23079.24	21771.88	1.0600	0.9980	1.0600		97.63	82.82	0
Model2 End 1	0.75	8	0.75	8	0.625	24.747	14124.63	0.00522	5.33	39.60	5.33	85.83	8.67	39.15	0.0417	0.1823	12208.81	14124.63	12208.81	1.1569	1.0000	1.1569	0.6619	61.57	55.66	4.9147
Model2 End 2	0.75	8	0.75	8	0.625	33.185	21338.22	0.00404	5.33	53.10	5.33	85.83	8.67	42.69	0.0417	0.1823	17938.33	21338.22	17938.33	1.1895	1.0000	1.1895		56.47	51.05	3.6651
Model2 End 1	0.75	8	0.75	8	0.4375	24.747	12494.06	0.00506	5.33	56.56	5.33	85.83	8.67	35.78	0.0417	0.1823	11153.74	12331.64	11153.74	1.1056	0.9870	1.1056	0.6788	67.37	59.78	0
Model2 End 2	0.75	8	0.75	8	0.4375	33.185	18406.23	0.00390	5.33	75.85	5.33	85.83	8.67	38.55	0.0417	0.1823	16026.87	18166.95	16026.87	1.1335	0.9870	1.1335		62.53	55.48	0
Model2 End 1	0.875	10	0.875	10	0.5	24.622	16976.42	0.00496	5.71	49.24	5.71	85.83	8.67	27.10	0.0417	0.1823	15448.13	17146.18	15448.13	1.1099	1.0100	1.1099	0.6894	88.94	77.99	4.4608
Model2 End 2	0.875	10	0.875	10	0.5	33.06	24625.35	0.00381	5.71	66.12	5.71	85.83	8.67	28.95	0.0417	0.1823	21909.08	24871.60	21909.08	1.1352	1.0100	1.1352		83.27	73.02	3.8172
Model2 End 1	1	12	1	12	0.5	24.497	21639.59	0.00486	6.00	48.99	6.00	85.83	8.67	21.28	0.0417	0.1823	20116.84	21855.99	20116.84	1.0865	1.0100	1.0865	0.7019	113.30	97.96	4.3118
Model2 End 2	1	12	1	12	0.5	32.935	30831.11	0.00372	6.00	65.87	6.00	85.83	8.67	22.48	0.0417	0.1823	28119.41	31139.42	28119.41	1.1074	1.0100	1.1074		107.25	92.72	3.3633
Model2 End 1	1	12	1	12	0.4375	24.497	21106.99	0.00482	6.00	55.99	6.00	85.83	8.67	20.83	0.0417	0.1823	19775.70	21318.06	19775.70	1.0780	1.0100	1.0780	0.7067	115.75	99.53	3.2228
Model2 End 2	1	12	1	12	0.4375	32.935	29868.45	0.00369	6.00	75.28	6.00	85.83	8.67	21.90	0.0417	0.1823	27496.55	30167.13	27496.55	1.0971	1.0100	1.0971		110.06	94.64	2.6819
Model2 End 1	1	12	1	12	0.25	24.497	19509.21	0.00470	6.00	97.99	6.00	85.83	8.67	19.40	0.0417	0.1823	18752.29	19333.62	18752.29	1.0310	0.9910	1.0310	0.7231	124.24	104.81	0
Model2 End 2	1	12	1	12	0.25	32.935	26980.47	0.00357	6.00	131.74	6.00	85.83	8.67	20.07	0.0417	0.1823	25627.96	26737.64	25627.96	1.0433	0.9910	1.0433		120.10	101.33	0
Model2 End 1	0.5	6	0.5	6	0.25	24.997	6562.94	0.00511	6.00	99.99	6.00	85.83	8.67	49.45	0.0417	0.1823	5795.09	6037.91	5795.09	1.0419	0.9200	1.0419	0.6731	48.75	43.53	0
Model2 End 2	0.5	6	0.5	6	0.25	33.435	9750.90	0.00394	6.00	133.74	6.00	85.83	8.67	53.52	0.0417	0.1823	8389.52	8970.83	8389.52	1.0693	0.9200	1.0693		45.04	40.22	0
Model2 End 1	0.625	8	0.625	8	0.1875	24.872	8888.26	0.00483	6.40	132.65	6.40	85.83	8.67	31.46	0.0417	0.1823	8313.76	8434.95	8313.76	1.0146	0.9490	1.0146	0.7059	76.63	65.95	0
Model2 End 2	0.625	8	0.625	8	0.1875	33.31	12591.55	0.00369	6.40	177.65	6.40	85.83	8.67	33.11	0.0417	0.1823	11571.66	11949.38	11571.66	1.0326	0.9490	1.0326		72.81	62.66	0
Model2 End 1	0.75	10	0.75	10	0.5625	24.747	15753.46	0.00507	6.67	43.99	6.67	85.83	8.67	28.82	0.0417	0.1823	14030.10	15753.46	14030.10	1.1228	1.0000	1.1228	0.6775	83.65	74.33	2.8064
Model2 End 2	0.75	10	0.75	10	0.5625	33.185	23252.12	0.00391	6.67	58.99	6.67	85.83	8.67	31.08	0.0417	0.1823	20192.88	23252.12	20192.88	1.1515	1.0000	1.1515		77.57	68.93	2.4318
Model2 End 1	0.75	10	0.75	10	0.5	24.747	15209.94	0.00502	6.67	49.49	6.67	85.83	8.67	28.05	0.0417	0.1823	13678.41	15179.52	13678.41	1.1097	0.9980	1.1097	0.6828	85.95	75.92	0
Model2 End 2	0.75	10	0.75	10	0.5	33.185	22274.79	0.00386	6.67	66.37	6.67	85.83	8.67	30.12	0.0417	0.1823	19555.72	22230.24	19555.72	1.1368	0.9980	1.1368		80.03	70.69	0
Model2 End 1	0.75	10	0.75	10	0.3125	24.747	13579.37	0.00486	6.67	79.19	6.67	85.83	8.67	25.58	0.0417	0.1823	12623.34	13267.05	12623.34	1.0510	0.9770	1.0510	0.7020	94.24	81.46	0
Model2 End 2	0.75	10	0.75	10	0.3125	33.185	19342.79	0.00372	6.67	106.19	6.67	85.83	8.67	27.02	0.0417	0.1823	17644.26	18897.91	17644.26	1.0711	0.9770	1.0711		89.21	77.12	0
Model2 End 1	0.875	12	0.875	12	0.5625	24.622	20048.87	0.00494	6.86	43.77	6.86	85.83	8.67	22.30	0.0417	0.1823	18329.92	20249.36	18329.92	1.1047	1.0100	1.1047	0.6921	108.12	94.52	2.9277
Model2 End 2	0.875	12	0.875	12	0.5625	33.06	28968.43	0.00379	6.86	58.77	6.86	85.83	8.67	23.76	0.0417	0.1823	25912.91	29258.12	25912.91	1.1291	1.0100	1.1291		101.46	88.70	2.2931
Model2 End 1	0.875	12	0.875	12	0.5	24.622	19510.83	0.00490	6.86	49.24	6.86	85.83	8.67	21.80	0.0417	0.1823	17983.54	19510.83	17983.54	1.0849	1.0000	1.0849	0.6969	110.56	96.14	2.1310
Model2 End 2	0.875	12	0.875	12	0.5	33.06	27998.45	0.00376	6.86	66.12	6.86	85.83	8.67	23.14	0.0417	0.1823	25282.93	27998.45	25282.93	1.1074	1.0000	1.1074		104.18	90.59	1.7929
Model2 End 1	0.875	12	0.875	12	0.3125	24.622	17896.70	0.00477	6.86	78.79	6.86	85.83	8.67	20.24	0.0417	0.1823	16944.38	17628.24	16944.38	1.0404	0.9850	1.0404	0.7133	119.08	101.61	0
Model2 End 2	0.875	12	0.875	12	0.3125	33.06	25088.50	0.00364	6.86	105.79	6.86	85.83	8.67	21.15	0.0417	0.1823	23392.98	24712.18	23392.98	1.0564	0.9850	1.0564		113.96	97.24	0

Table B2 Continued

E	Fy
29600	56.8

End 1 = Shallow End
End 2 = Deep End

									Comp.		Tension	Web	Flanges												
DESCRIPTION	tf1	bf1	tf2	bf2	tw	dw	Mp(in kips)	θ p	bf1/2tf1	h/tw	bf2/2tf2	λ p	λ p	Lb/ry	m(top)	m(bot)	M(aisc)	Mu(abaqus)	My	Mu/My	Mu/Mp	Mu/M(aisc)	α	Lp	Lpd	R
Model2 End 1	0.4375	6	0.4375	6	0.25	25.0596	6030.96	0.00517	6.86	100.24	6.86	85.83	8.67	51.25	0.0417	0.1823	5262.72	5433.89	5262.72	1.0325	0.9010	1.0325	0.6669	47.04	42.29	0
Model2 End 2	0.4375	6	0.4375	6	0.25	33.4971	9042.95	0.00399	6.86	133.99	6.86	85.83	8.67	55.73	0.0417	0.1823	7681.22	8147.69	7681.22	1.0607	0.9010	1.0607		43.26	38.89	0
Model2 End 1	0.5625	8	0.5625	8	0.1875	24.9346	8172.43	0.00486	7.11	132.98	7.11	85.83	8.67	32.02	0.0417	0.1823	7597.35	7649.39	7597.35	1.0069	0.9360	1.0069	0.7022	75.28	65.07	0
Model2 End 2	0.5625	8	0.5625	8	0.1875	33.3721	11638.90	0.00372	7.11	177.98	7.11	85.83	8.67	33.82	0.0417	0.1823	10618.52	10894.01	10618.52	1.0259	0.9360	1.0259		71.28	61.60	0
Model2 End 1	0.75	12	0.75	12	0.5625	24.7471	17925.81	0.00500	8.00	43.99	8.00	85.83	8.67	23.05	0.0417	0.1823	16203.08	17818.26	16203.08	1.0997	0.9940	1.0997	0.6857	104.60	92.11	0
Model2 End 2	0.75	12	0.75	12	0.5625	33.1846	26143.34	0.00384	8.00	58.99	8.00	85.83	8.67	24.69	0.0417	0.1823	23084.57	25986.48	23084.57	1.1257	0.9940	1.1257		97.63	85.97	0
Model2 End 1	0.75	12	0.75	12	0.5	24.7471	17382.29	0.00495	8.00	49.49	8.00	85.83	8.67	22.49	0.0417	0.1823	15851.39	17173.70	15851.39	1.0834	0.9880	1.0834	0.6907	107.21	93.87	0
Model2 End 2	0.75	12	0.75	12	0.5	33.1846	25166.01	0.00380	8.00	66.37	8.00	85.83	8.67	23.99	0.0417	0.1823	22447.42	24864.02	22447.42	1.1077	0.9880	1.1077		100.48	87.98	0
Model2 End 1	0.625	10	0.625	10	0.375	24.8721	12345.63	0.00498	8.00	66.33	8.00	85.83	8.67	27.45	0.0417	0.1823	11195.56	11938.22	11195.56	1.0663	0.9670	1.0663	0.6876	87.82	77.16	0
Model2 End 2	0.625	10	0.625	10	0.375	33.3096	17955.03	0.00383	8.00	88.83	8.00	85.83	8.67	29.37	0.0417	0.1823	15914.43	17362.51	15914.43	1.0910	0.9670	1.0910		82.08	72.13	0
Model2 End 1	0.75	12	0.75	12	0.3125	24.7471	15751.73	0.00481	8.00	79.19	8.00	85.83	8.67	20.71	0.0417	0.1823	14796.32	15263.42	14796.32	1.0316	0.9690	1.0316	0.7085	116.42	99.90	0
Model2 End 2	0.75	12	0.75	12	0.3125	33.1846	22234.02	0.00367	8.00	106.19	8.00	85.83	8.67	21.74	0.0417	0.1823	20535.96	21544.77	20535.96	1.0491	0.9690	1.0491		110.88	95.15	0
Model2 End 1	0.5	8	0.5	8	0.25	24.9971	8011.18	0.00499	8.00	99.99	8.00	85.83	8.67	34.66	0.0417	0.1823	7243.51	7410.34	7243.51	1.0230	0.9250	1.0230	0.6860	69.55	61.22	0
Model2 End 2	0.5	8	0.5	8	0.25	33.4346	11678.39	0.00384	8.00	133.74	8.00	85.83	8.67	37.13	0.0417	0.1823	10317.15	10802.51	10317.15	1.0470	0.9250	1.0470		64.92	57.15	0
Model2 End 1	0.5	8	0.5	8	0.1875	24.9971	7456.62	0.00489	8.00	133.32	8.00	85.83	8.67	32.71	0.0417	0.1823	6881.05	6867.54	6881.05	0.9980	0.9210	0.9980	0.6978	73.69	64.01	0
Model2 End 2	0.5	8	0.5	8	0.1875	33.4346	10686.28	0.00375	8.00	178.32	8.00	85.83	8.67	34.69	0.0417	0.1823	9665.49	9842.06	9665.49	1.0183	0.9210	1.0183		69.49	60.36	0
Model2 End 1	0.625	12	0.625	12	0.375	24.8721	14155.92	0.00491	9.60	66.33	9.60	85.83	8.67	22.05	0.0417	0.1823	13006.21	13448.13	13006.21	1.0340	0.9500	1.0340	0.6951	109.32	95.25	0
Model2 End 2	0.625	12	0.625	12	0.375	33.3096	20364.38	0.00377	9.60	88.83	9.60	85.83	8.67	23.44	0.0417	0.1823	18324.06	19346.16	18324.06	1.0558	0.9500	1.0558		102.85	89.61	0
Model2 End 1	0.5	10	0.5	10	0.25	24.9971	9459.41	0.00491	10.00	99.99	10.00	85.83	8.67	26.49	0.0417	0.1823	8691.93	8655.36	8691.93	0.9958	0.9150	0.9958	0.6952	91.00	79.28	0
Model2 End 2	0.5	10	0.5	10	0.25	33.4346	13605.87	0.00377	10.00	133.74	10.00	85.83	8.67	28.15	0.0417	0.1823	12244.77	12449.37	12244.77	1.0167	0.9150	1.0167		85.62	74.59	0
Model2 End 1	0.5	10	0.5	10	0.1875	24.9971	8904.85	0.00483	10.00	133.32	10.00	85.83	8.67	25.19	0.0417	0.1823	8329.47	8156.85	8329.47	0.9793	0.9160	0.9793	0.7060	95.71	82.36	0
Model2 End 2	0.5	10	0.5	10	0.1875	33.4346	12613.76	0.00369	10.00	178.32	10.00	85.83	8.67	26.51	0.0417	0.1823	11593.11	11554.21	11593.11	0.9966	0.9160	0.9966		90.94	78.26	0
Model2 End 1	0.5625	12	0.5625	12	0.3125	24.9346	12534.53	0.00489	10.67	79.79	10.67	85.83	8.67	21.75	0.0417	0.1823	11575.89	11569.37	11575.89	0.9994	0.9230	0.9994	0.6982	110.85	96.24	0
Model2 End 2	0.5625	12	0.5625	12	0.3125	33.3721	17952.56	0.00375	10.67	106.79	10.67	85.83	8.67	23.05	0.0417	0.1823	16251.79	16570.21	16251.79	1.0196	0.9230	1.0196		104.57	90.79	0
Model2 End 1	0.5625	12	0.5625	12	0.1875	24.9346	11430.96	0.00475	10.67	132.98	10.67	85.83	8.67	20.10	0.0417	0.1823	10856.41	10390.74	10856.41	0.9571	0.9090	0.9571	0.7155	119.96	102.10	0
Model2 End 2	0.5625	12	0.5625	12	0.1875	33.3721	15975.74	0.00362	10.67	177.98	10.67	85.83	8.67	20.95	0.0417	0.1823	14955.76	14521.95	14955.76	0.9710	0.9090	0.9710		115.05	97.93	0
Model2 End 1	0.5	12	0.5	12	0.25	24.9971	10907.65	0.00486	12.00	99.99	12.00	85.83	8.67	21.36	0.0417	0.1823	10140.35	9740.53	10140.35	0.9606	0.8930	0.9606	0.7022	112.87	97.55	0
Model2 End 2	0.5	12	0.5	12	0.25	33.4346	15533.36	0.00372	12.00	133.74	12.00	85.83	8.67	22.56	0.0417	0.1823	14172.40	13871.29	14172.40	0.9788	0.8930	0.9788		106.87	92.36	0

APPENDIX B3

Table B3 Model-1 L_b = 75 in. Parametric Study Results

E	Fy
29600	56.8

End 1 = Shallow End
End 2 = Deep End

DESCRIPTION	tf1	bf1	tf2	bf2	tw	dw	Mp(in kips)	θ p	Comp. bf1/2tf1	h/tw	Tension bf2/2tf2	Web λ p	Flanges λ p	Lb/ry	m(top)	m(bot)	M(aisc)	Mu(abaqus)	My	Mu/My	Mu/Mp	Mu/M(aisc)	α	Lp	Lpd	R
Model1-ex End 1	1.25	6	1.25	6	1.25	23.87	20814.66	0.00697	2.40	19.10	2.40	85.83	8.67	71.83	0.0333	-0.0203	16450.81	21022.81	17116.81	1.2282	1.0100	1.2779	0.7938	41.95	32.47	3.1754
Model1-ex End 2	1.25	6	1.25	6	1.25	27.89	26220.51	0.00610	2.40	22.31	2.40	85.83	8.67	75.24	0.0333	-0.0203	20404.92	26482.72	21230.99	1.2474	1.0100	1.2979		40.05	30.99	3.3471
Model1-ex End 1	1.25	6	1.25	6	1.125	23.87	19803.31	0.00689	2.40	21.22	2.40	85.83	8.67	70.16	0.0333	-0.0203	15896.13	20199.37	16476.12	1.2260	1.0200	1.2707	0.7972	42.95	33.10	2.6569
Model1-ex End 2	1.25	6	1.25	6	1.125	27.89	24839.83	0.00603	2.40	24.79	2.40	85.83	8.67	73.48	0.0333	-0.0203	19633.66	25336.62	20350.02	1.2450	1.0200	1.2905		41.01	31.60	2.8109
Model1-ex End 1	1.25	6	1.25	6	0.625	23.87	15757.89	0.00649	2.40	38.19	2.40	85.83	8.67	60.83	0.0333	-0.0203	13669.32	15663.34	13913.38	1.1258	0.9940	1.1459	0.8157	49.54	37.27	0
Model1-ex End 2	1.25	6	1.25	6	0.625	27.89	19317.08	0.00567	2.40	44.62	2.40	85.83	8.67	63.27	0.0333	-0.0203	16530.97	19201.17	16826.12	1.1412	0.9940	1.1615		47.62	35.83	0
Model1-ex End 1	1.25	6	1.25	6	0.5625	23.87	15252.21	0.00643	2.40	42.44	2.40	85.83	8.67	59.38	0.0333	-0.0203	13388.25	15130.20	13593.04	1.1131	0.9920	1.1301	0.8188	50.75	38.03	0
Model1-ex End 2	1.25	6	1.25	6	0.5625	27.89	18626.73	0.00561	2.40	49.58	2.40	85.83	8.67	61.65	0.0333	-0.0203	16138.78	18477.72	16385.64	1.1277	0.9920	1.1449		48.88	36.62	0
Model1-ex End 1	1.125	6	1.125	6	0.625	23.995	14740.88	0.00655	2.67	38.39	2.67	85.83	8.67	62.54	0.0333	-0.0203	12597.71	14593.47	12891.46	1.1320	0.9900	1.1584	0.8127	48.19	36.40	0
Model1-ex End 2	1.125	6	1.125	6	0.625	28.015	18137.73	0.00573	2.67	44.82	2.67	85.83	8.67	65.17	0.0333	-0.0203	15285.75	17956.36	15642.19	1.1479	0.9900	1.1747		46.24	34.92	0
Model1-ex End 1	1.125	6	1.125	6	0.5625	23.995	14229.89	0.00649	2.67	42.66	2.67	85.83	8.67	60.97	0.0333	-0.0203	12315.92	14116.05	12566.06	1.1233	0.9920	1.1462	0.8159	49.43	37.18	0
Model1-ex End 2	1.125	6	1.125	6	0.5625	28.015	17441.19	0.00567	2.67	49.80	2.67	85.83	8.67	63.42	0.0333	-0.0203	14893.27	17301.66	15195.75	1.1386	0.9920	1.1617		47.51	35.74	0
Model1-ex End 1	1.25	8	1.25	8	0.375	23.87	17302.22	0.00612	3.20	63.65	3.20	85.83	8.67	39.05	0.0333	-0.0203	16201.99	17302.22	16201.99	1.0679	1.0000	1.0679	0.8361	77.16	56.50	3.8397
Model1-ex End 2	1.25	8	1.25	8	0.375	27.89	20693.58	0.00532	3.20	74.37	3.20	85.83	8.67	40.05	0.0333	-0.0203	19204.59	20693.58	19204.59	1.0775	1.0000	1.0775		75.23	55.09	3.6964
Model1-ex End 1	1.125	8	1.125	8	0.4375	23.995	16418.25	0.00622	3.56	54.85	3.56	85.83	8.67	40.83	0.0333	-0.0203	15127.74	16418.25	15127.74	1.0853	1.0000	1.0853	0.8304	73.81	54.46	4.2023
Model1-ex End 2	1.125	8	1.125	8	0.4375	28.015	19772.19	0.00542	3.56	64.03	3.56	85.83	8.67	42.06	0.0333	-0.0203	18028.82	19772.19	18028.82	1.0967	1.0000	1.0967		71.64	52.86	3.9581
Model1-ex End 1	1.125	8	1.125	8	0.375	23.995	15907.27	0.00616	3.56	63.99	3.56	85.83	8.67	39.75	0.0333	-0.0203	14802.34	15907.27	14802.34	1.0746	1.0000	1.0746	0.8339	75.80	55.67	2.4319
Model1-ex End 2	1.125	8	1.125	8	0.375	28.015	19075.64	0.00536	3.56	74.71	3.56	85.83	8.67	40.84	0.0333	-0.0203	17582.39	19075.64	17582.39	1.0849	1.0000	1.0849		73.78	54.19	2.4523
Model1-ex End 1	1	8	1	8	0.4375	24.12	15028.80	0.00627	4.00	55.13	4.00	85.83	8.67	41.80	0.0333	-0.0203	13734.15	15028.80	13734.15	1.0943	1.0000	1.0943	0.8275	72.10	53.40	2.1174
Model1-ex End 2	1	8	1	8	0.4375	28.14	18160.64	0.00546	4.00	64.32	4.00	85.83	8.67	43.15	0.0333	-0.0203	16413.49	18160.64	16413.49	1.1064	1.0000	1.1064		69.83	51.73	2.1628
Model1-ex End 1	1	8	1	8	0.25	24.12	13479.83	0.00606	4.00	96.48	4.00	85.83	8.67	38.10	0.0333	-0.0203	12742.61	13358.51	12742.61	1.0483	0.9910	1.0483	0.8397	79.09	57.63	0
Model1-ex End 2	1	8	1	8	0.25	28.14	16052.32	0.00527	4.00	112.56	4.00	85.83	8.67	38.96	0.0333	-0.0203	15056.17	15907.85	15056.17	1.0566	0.9910	1.0566		77.35	56.36	0
Model1-ex End 1	1.25	10	1.25	10	0.1875	23.87	19352.23	0.00589	4.00	127.31	4.00	85.83	8.67	28.21	0.0333	-0.0203	18810.95	19352.23	18810.95	1.0288	1.0000	1.0288	0.8503	106.82	76.73	2.3194
Model1-ex End 2	1.25	10	1.25	10	0.1875	27.89	22760.43	0.00510	4.00	148.75	4.00	85.83	8.67	28.57	0.0333	-0.0203	22023.55	22760.43	22023.55	1.0335	1.0000	1.0335		105.48	75.77	2.2074
Model1-ex End 1	1.125	10	1.125	10	0.25	23.995	18095.63	0.00597	4.44	95.98	4.44	85.83	8.67	29.24	0.0333	-0.0203	17364.02	18276.58	17364.02	1.0526	1.0100	1.0526	0.8453	103.06	74.53	3.8924
Model1-ex End 2	1.125	10	1.125	10	0.25	28.015	21406.64	0.00518	4.44	112.06	4.44	85.83	8.67	29.75	0.0333	-0.0203	20415.46	21620.71	20415.46	1.0590	1.0100	1.0590		101.30	73.25	3.5885
Model1-ex End 1	1.125	10	1.125	10	0.1875	23.995	17584.64	0.00591	4.44	127.97	4.44	85.83	8.67	28.46	0.0333	-0.0203	17038.62	17584.64	17038.62	1.0320	1.0000	1.0320	0.8491	105.88	76.18	1.7571
Model1-ex End 2	1.125	10	1.125	10	0.1875	28.015	20710.10	0.00512	4.44	149.41	4.44	85.83	8.67	28.85	0.0333	-0.0203	19969.02	20710.10	19969.02	1.0371	1.0000	1.0371		104.44	75.14	1.6561
Model1-ex End 1	0.875	8	0.875	8	0.4375	24.245	13639.54	0.00633	4.57	55.42	4.57	85.83	8.67	43.01	0.0333	-0.0203	12341.50	13584.99	12341.50	1.1008	0.9960	1.1008	0.8242	70.07	52.13	0
Model1-ex End 2	0.875	8	0.875	8	0.4375	28.265	16549.29	0.00552	4.57	64.61	4.57	85.83	8.67	44.51	0.0333	-0.0203	14799.01	16483.10	14799.01	1.1138	0.9960	1.1138		67.70	50.37	0
Model1-ex End 1	0.875	8	0.875	8	0.375	24.245	13117.85	0.00626	4.57	64.65	4.57	85.83	8.67	41.68	0.0333	-0.0203	12005.82	13012.91	12005.82	1.0839	0.9920	1.0839	0.8281	72.30	53.51	0
Model1-ex End 2	0.875	8	0.875	8	0.375	28.265	15840.26	0.00546	4.57	75.37	4.57	85.83	8.67	43.01	0.0333	-0.0203	14340.52	15713.54	14340.52	1.0957	0.9920	1.0957		70.06	51.85	0
Model1-ex End 1	0.875	8	0.875	8	0.3125	24.245	12596.16	0.00618	4.57	77.58	4.57	85.83	8.67	40.30	0.0333	-0.0203	11670.15	12457.61	11670.15	1.0675	0.9890	1.0675	0.8325	74.77	55.02	0
Model1-ex End 2	0.875	8	0.875	8	0.3125	28.265	15131.23	0.00538	4.57	90.45	4.57	85.83	8.67	41.45	0.0333	-0.0203	13882.02	14964.78	13882.02	1.0780	0.9890	1.0780		72.69	53.49	0
Model1-ex End 1	1.25	12	1.25	12	0.375	23.87	24436.30	0.00600	4.80	63.65	4.80	85.83	8.67	24.67	0.0333	-0.0203	23341.96	25169.39	23341.96	1.0783	1.0300	1.0783	0.8435	122.16	88.56	7.5762
Model1-ex End 2	1.25	12	1.25	12	0.375	27.89	28969.34	0.00521	4.80	74.37	4.80	85.83	8.67	25.14	0.0333	-0.0203	27485.43	29838.42	27485.43	1.0856	1.0300	1.0856		119.87	86.90	6.6175
Model1-ex End 1	1.25	12	1.25	12	0.3125	23.87	23930.62	0.00596	4.80	76.38	4.80	85.83	8.67	24.19	0.0333	-0.0203	23021.62	24409.24	23021.62	1.0603	1.0200	1.0603	0.8462	124.56	89.97	5.1872
Model1-ex End 2	1.25	12	1.25	12	0.3125	27.89	28279.00	0.00516	4.80	89.25	4.80	85.83	8.67	24.59	0.0333	-0.0203	27044.94	28844.58	27044.94	1.0665	1.0200	1.0665		122.53	88.50	4.5250
Model1-ex End 1	1.25	12	1.25	12	0.25	23.87	23424.95	0.00591	4.80	95.48	4.80	85.83	8.67	23.71	0.0333	-0.0203	22701.28	23659.20	22701.28	1.0422	1.0100	1.0422	0.8491	127.12	91.46	3.3584
Model1-ex End 2	1.25	12	1.25	12	0.25	27.89	27588.65	0.00512	4.80	111.56	4.80	85.83	8.67	24.03	0.0333	-0.0203	26604.46	27864.54	26604.46	1.0474	1.0100	1.0474		125.38	90.21	2.8948
Model1-ex End 1	1	10	1	10	0.4375	24.12	17882.43	0.00618	5.00	55.13	5.00	85.83	8.67	32.10	0.0333	-0.0203	16589.29	18240.08	16589.29	1.0995	1.0200	1.0995	0.8329	93.89	69.05	5.5453
Model1-ex End 2	1	10	1	10	0.4375	28.14	21470.95	0.00538	5.00	64.32	5.00	85.83	8.67	33.00	0.0333	-0.0203	19725.09	21900.37	19725.09	1.1103	1.0200	1.1103		91.30	67.15	5.2790
Model1-ex End 1	1	10	1	10	0.375	24.12	17366.11	0.00612	5.00	64.32	5.00	85.83	8.67	31.30	0.0333	-0.0203	16258.78	17539.77	16258.78	1.0788	1.0100	1.0788	0.8362	96.27	70.49	4.5812
Model1-ex End 2	1	10	1	10	0.375	28.14	20768.17	0.00532	5.00	75.04	5.00	85.83	8.67	32.10	0.0333	-0.0203	19272.65	20975.85	19272.65	1.0884	1.0100	1.0884		93.87	68.73	4.3887
Model1-ex End 1	1	10	1	10	0.3125	24.12	16849.78	0.00606	5.00	77.18	5.00	85.83	8.67	30.48	0.0333	-0.0203	15928.27	17018.28	15928.27	1.0684	1.0100	1.0684	0.8397	98.86	72.04	3.7859
Model1-ex End 2	1	10	1	10	0.3125	28.14	20065.40	0.00527	5.00	90.05	5.00	85.83	8.67	31.17	0.0333	-0.0203	18820.21	20266.05	18820.21	1.0768	1.0100	1.0768		96.68	70.45	3.6647
Model1-ex End 1	1	10	1	10	0.25	24.12	16333.46	0.00600	5.00	96.48	5.00	85.83	8.67	29.64	0.0333	-0.0203	15597.75	16333.46	15597.75	1.0472	1.0000	1.0472	0.8436	101.67	73.71	2.2029
Model1-ex End 2	1	10	1	10	0.25	28.14	19362.62	0.00521	5.00	112.56	5.00	85.83	8.67	30.20	0.0333	-0.0203	18367.77	19362.62	18367.77	1.0542	1.0000	1.0542		99.77	72.32	2.1780
Model1-ex End 1	1.125	12	1.125	12	0.4375	23.995	22838.93	0.00607	5.33	54.85	5.33	85.83	8.67	25.51	0.0333	-0.0203	21552.71	23295.70	21552.71	1.0809	1.0200	1.0809	0.8390	118.13	86.16	5.7141
Model1-ex End 2	1.125	12	1.125	12	0.4375	28.015	27220.37	0.00528	5.33	64.03	5.33	85.83	8.67	26.10	0.0333	-0.0203	25480.71	27764.78	25480.71	1.0896	1.0200	1.0896		115.46	84.21	5.0992
Model1-ex End 1	0.75	8	0.75	8	0.4375	24.37	12250.48	0.00641	5.33	55.70	5.33	85.83	8.67	44.57	0.0333	-0.0203	10949.72	12115.73	10949.72	1.1065	0.9890	1.1065	0.8201	67.61	50.58	0
Model1-ex End 2	0.75	8	0.75	8	0.4375	28.39	14938.14	0.00560	5.33	64.89	5.33	85.83	8.67	46.26	0.0333	-0.0203	13185.34	14773.82	13185.34	1.1205	0.9890	1.1205		65.14	48.73	0
Model1-ex End 1	1.125	12	1.125	12	0.375	23.995	22327.94	0.00603	5.33	63.99	5.33	85.83	8.67	25.00	0.0333	-0.0203	21227.30	22551.22	21227.30	1.0624	1.0100	1.0624	0.8418	120.56	87.60	2.3851
Model1-ex End 2	1.125	12	1.125	12	0.375	28.015	26523.83	0.00523	5.33	74.71	5.33	85.83	8.67	25.51	0.0333	-0.0203	25034.27	26789.06	25034.27	1.0701	1.0100	1.0701		118.11	85.83	2.8717
Model1-ex End 1	1.125	12	1.125	12	0.3125	23.995	21816.95	0.00598	5.33	76.78	5.33	85.83	8.67	24.47	0.0333	-0.0203	20901.90	22035.12	20901.90	1.0542	1.0100	1.0542	0.8447	123.14	89.12	3.1021
Model1-ex End 2	1.125	12	1.125	12	0.3125	28.015	25827.28	0.00519	5.33	89.65	5.33	85.83	8.67	24.91	0.0333	-0.0203	24587.83	26085.55	24587.83	1.0609	1.0100	1.0609		120.96	87.55	2.7893
Model1-ex End 1	0.875	10	0.875	10	0.5	24.245	16658.16	0.00629	5.71	48.49	5.71	85.83	8.67	33.77	0.0333	-0.0203	15175.12	16824.74	15175.12	1.1087	1.0100	1.1087	0.8265	89.22	66.18	3.5289
Model1-ex End 2	0.875	10	0.875	10	0.5	28.265	20154.84	0.00548	5.71	56.53	5.71	85.83	8.67	34.89	0.0333	-0.0203	18154.89	20356.39	18154.89	1.1213	1.0100	1.1213		86.35	64.05	3.0620
Model1-ex End 1	0.875	10	0.875	10	0.4375	24.245	16136.47	0.00623	5.71	55.42	5.71	85.83	8.67	32.91	0.0333	-0.0203	14839.44	16297.84	14839.44	1.0983	1.0100	1.0983	0.8298	91.57	67.62	2.9783
Model1-ex End 2	0.875	10	0.875	10	0.4375	28.265	19445.81	0.00543	5.71	64.61	5.71	85.83	8.67	33.92	0.0333	-0.0203	17696.40	19640.27	17696.40	1.1098	1.0100	1.1098		88.84	65.61	2.9345
Model1-ex End 1	0.875	10	0.875	10	0.375	24.245	15614.78	0.00617	5.71	64.65	5.71	85.83	8.67	32.01	0.0333	-0.0203	14503.76	15614.78	14503.76	1.0766	1.0000	1.0766	0.8334	94.12	69.18	2.1209
Model1-ex End 2	0.875	10	0.875	10	0.375	28.265	18736.78	0.00537	5.71	75.37	5.71	85.83	8.67	32.91	0.0333	-0.0203	17237.90	18736.78	17237.90	1.0870	1.0000	1.0870		91.57	67.30	2.1323

Table B3 Continued

E	Fy
29600	56.8

End 1 = Shallow End
End 2 = Deep End

DESCRIPTION	tf1	bf1	tf2	bf2	tw	dw	Mp(in kips)	θ p	Comp. bf1/2tf1	h/tw	Tension bf2/2tf2	Web λ p	Flanges λ p	Lb/ry	m(top)	m(bot)	M(aisc)	Mu(abaqus)	My	Mu/My	Mu/Mp	Mu/M(aisc)	α	Lp	Lpd	R
Model1-ex End 1	1	12	1	12	0.5	24.12	21252.39	0.00616	6.00	48.24	6.00	85.83	8.67	26.53	0.0333	-0.0203	19774.95	21677.44	19774.95	1.0962	1.0200	1.0962	0.8339	113.59	83.42	3.9110
Model1-ex End 2	1	12	1	12	0.5	28.14	25484.03	0.00536	6.00	56.28	6.00	85.83	8.67	27.25	0.0333	-0.0203	23489.13	25993.71	23489.13	1.1066	1.0200	1.1066		110.56	81.20	3.5599
Model1-ex End 1	1	12	1	12	0.4375	24.12	20736.07	0.00611	6.00	55.13	6.00	85.83	8.67	25.97	0.0333	-0.0203	19444.43	21150.79	19444.43	1.0878	1.0200	1.0878	0.8368	116.03	84.89	2.981
Model1-ex End 2	1	12	1	12	0.4375	28.14	24781.25	0.00531	6.00	64.32	6.00	85.83	8.67	26.62	0.0333	-0.0203	23036.69	25276.88	23036.69	1.0972	1.0200	1.0972		113.19	82.81	2.743
Model1-ex End 1	1	12	1	12	0.375	24.12	20219.74	0.00606	6.00	64.32	6.00	85.83	8.67	25.40	0.0333	-0.0203	19113.92	20421.94	19113.92	1.0684	1.0100	1.0684	0.8397	118.63	86.45	2.2152
Model1-ex End 2	1	12	1	12	0.375	28.14	24078.48	0.00527	6.00	75.04	6.00	85.83	8.67	25.97	0.0333	-0.0203	22584.25	24319.26	22584.25	1.0768	1.0100	1.0768		116.02	84.54	2.0798
Model1-ex End 1	0.875	12	0.875	12	0.5	24.245	19155.09	0.00621	6.86	48.49	6.86	85.83	8.67	27.18	0.0333	-0.0203	17673.06	19346.64	17673.06	1.0947	1.0100	1.0947	0.8310	110.88	81.75	1.8158
Model1-ex End 2	0.875	12	0.875	12	0.5	28.265	23051.36	0.00541	6.86	56.53	6.86	85.83	8.67	27.99	0.0333	-0.0203	21052.28	23281.87	21052.28	1.1059	1.0100	1.1059		107.67	79.39	1.7048
Model1-ex End 1	0.4375	6	0.4375	6	0.1875	24.6825	5367.46	0.00640	6.86	131.64	6.86	85.83	8.67	59.37	0.0333	-0.0203	4691.40	4938.06	4808.31	1.0270	0.9200	1.0526	0.8209	50.75	37.93	0
Model1-ex End 2	0.4375	6	0.4375	6	0.1875	28.7025	6538.23	0.00558	6.86	153.08	6.86	85.83	8.67	61.59	0.0333	-0.0203	5644.77	6015.17	5785.45	1.0397	0.9200	1.0656		48.93	36.56	0
Model1-ex End 1	0.5	8	0.5	8	0.3125	24.62	8397.03	0.00644	8.00	78.78	8.00	85.83	8.67	45.45	0.0333	-0.0203	7465.50	7935.19	7465.50	1.0629	0.9450	1.0629	0.8184	66.30	49.70	0
Model1-ex End 2	0.5	8	0.5	8	0.3125	28.64	10260.47	0.00563	8.00	91.65	8.00	85.83	8.67	47.23	0.0333	-0.0203	9006.19	9696.14	9006.19	1.0766	0.9450	1.0766		63.80	47.83	0
Model1-ex End 1	0.375	6	0.375	6	0.25	24.745	5384.05	0.00665	8.00	98.98	8.00	85.83	8.67	66.65	0.0333	-0.0203	4448.75	4834.88	4638.09	1.0424	0.8980	1.0868	0.8082	45.21	34.35	0
Model1-ex End 2	0.375	6	0.375	6	0.25	28.765	6661.45	0.00582	8.00	115.06	8.00	85.83	8.67	69.70	0.0333	-0.0203	5426.39	5981.98	5657.34	1.0574	0.8980	1.1024		43.23	32.85	0
Model1-ex End 1	0.375	6	0.375	6	0.1875	24.745	4840.62	0.00648	8.00	131.97	8.00	85.83	8.67	61.68	0.0333	-0.0203	4154.73	4342.04	4281.21	1.0142	0.8970	1.0451	0.8167	48.85	36.71	0
Model1-ex End 2	0.375	6	0.375	6	0.1875	28.765	5927.11	0.00566	8.00	153.41	8.00	85.83	8.67	64.17	0.0333	-0.0203	5021.22	5316.62	5174.08	1.0275	0.8970	1.0588		46.96	35.29	0
Model1-ex End 1	0.3125	6	0.3125	6	0.25	24.8075	4859.99	0.00677	9.60	99.23	9.60	85.83	8.67	70.44	0.0333	-0.0203	3906.36	4213.61	4113.77	1.0243	0.8670	1.0787	0.8028	42.78	32.73	0
Model1-ex End 2	0.3125	6	0.3125	6	0.25	28.8275	6053.55	0.00592	9.60	115.31	9.60	85.83	8.67	73.89	0.0333	-0.0203	4794.61	5248.43	5049.20	1.0395	0.8670	1.0947		40.78	31.20	0
Model1-ex End 1	0.5	10	0.5	10	0.25	24.62	9285.89	0.00623	10.00	98.48	10.00	85.83	8.67	33.02	0.0333	-0.0203	8541.01	8505.88	8541.01	0.9959	0.9160	0.9959	0.8300	91.27	67.38	0
Model1-ex End 2	0.5	10	0.5	10	0.25	28.64	11187.65	0.00543	10.00	114.56	10.00	85.83	8.67	34.03	0.0333	-0.0203	10184.52	10247.88	10184.52	1.0062	0.9160	1.0062		88.56	65.38	0
Model1-ex End 1	0.5	10	0.5	10	0.1875	24.62	8747.94	0.00612	10.00	131.31	10.00	85.83	8.67	31.41	0.0333	-0.0203	8189.51	8021.86	8189.51	0.9795	0.9170	0.9795	0.8363	95.94	70.23	0
Model1-ex End 2	0.5	10	0.5	10	0.1875	28.64	10459.67	0.00532	10.00	152.75	10.00	85.83	8.67	32.21	0.0333	-0.0203	9707.53	9591.52	9707.53	0.9880	0.9170	0.9880		93.56	68.49	0
Model1-ex End 1	0.5625	12	0.5625	12	0.25	24.5575	11771.91	0.00612	10.67	98.23	10.67	85.83	8.67	26.11	0.0333	-0.0203	11027.93	10841.93	11027.93	0.9831	0.9210	0.9831	0.8366	115.40	84.45	0
Model1-ex End 2	0.5625	12	0.5625	12	0.25	28.5775	14071.47	0.00532	10.67	114.31	10.67	85.83	8.67	26.77	0.0333	-0.0203	13069.15	12959.82	13069.15	0.9916	0.9210	0.9916		112.56	82.37	0
Model1-ex End 1	0.375	8	0.375	8	0.25	24.745	6454.17	0.00648	10.67	98.98	10.67	85.83	8.67	46.26	0.0333	-0.0203	5890.62	5686.12	5708.28	0.9961	0.8810	0.9653	0.8167	65.14	48.95	0
Model1-ex End 2	0.375	8	0.375	8	0.25	28.765	7902.82	0.00566	10.67	115.06	10.67	85.83	8.67	48.13	0.0333	-0.0203	7119.14	6962.38	6898.77	1.0092	0.8810	0.9780		62.61	47.05	0
Model1-ex End 1	0.5625	12	0.5625	12	0.1875	24.5575	11236.68	0.00603	10.67	130.97	10.67	85.83	8.67	25.07	0.0333	-0.0203	10679.10	10326.51	10679.10	0.9670	0.9190	0.9670	0.8419	120.19	87.32	0
Model1-ex End 2	0.5625	12	0.5625	12	0.1875	28.5775	13346.67	0.00523	10.67	152.41	10.67	85.83	8.67	25.59	0.0333	-0.0203	12595.28	12265.59	12595.28	0.9738	0.9190	0.9738		117.76	85.56	0
Model1-ex End 1	0.375	8	0.375	8	0.1875	24.745	5910.74	0.00633	10.67	131.97	10.67	85.83	8.67	43.24	0.0333	-0.0203	5351.40	5171.89	5351.40	0.9665	0.8750	0.9665	0.8245	69.69	51.83	0
Model1-ex End 2	0.375	8	0.375	8	0.1875	28.765	7168.48	0.00552	10.67	153.41	10.67	85.83	8.67	44.74	0.0333	-0.0203	6415.51	6272.42	6415.51	0.9777	0.8750	0.9777		67.35	50.09	0
Model1-ex End 1	0.4375	10	0.4375	10	0.25	24.6825	8405.07	0.00629	11.43	98.73	11.43	85.83	8.67	33.92	0.0333	-0.0203	7659.67	7480.51	7659.67	0.9766	0.8900	0.9766	0.8268	88.84	65.87	0
Model1-ex End 2	0.4375	10	0.4375	10	0.25	28.7025	10165.90	0.00548	11.43	114.81	11.43	85.83	8.67	35.04	0.0333	-0.0203	9162.30	9047.65	9162.30	0.9875	0.8900	0.9875		85.99	63.76	0
Model1-ex End 1	0.5	12	0.5	12	0.25	24.62	10712.71	0.00616	12.00	98.48	12.00	85.83	8.67	26.63	0.0333	-0.0203	9968.01	9598.59	9968.01	0.9629	0.8960	0.9629	0.8341	113.17	83.09	0
Model1-ex End 2	0.5	12	0.5	12	0.25	28.64	12842.80	0.00536	12.00	114.56	12.00	85.83	8.67	27.35	0.0333	-0.0203	11839.83	11507.15	11839.83	0.9719	0.8960	0.9719		110.16	80.88	0

APPENDIX B4

Table B4 Model-2 L_b = 75 in. Parametric Study Results

E = 29600, Fy = 56.8

End 1 = Shallow End
End 2 = Deep End

DESCRIPTION	tf1	bf1	tf2	bf2	tw	dw	Mp(in kips)	θ p	Comp. bf1/2tf1	h/tw	Tension bf2/2tf2	Web λ p	Flanges λ p	Lb/ry	m(top)	m(bot)	M(aisc)	Mu(abaqus)	My	Mu/My	Mu/Mp	Mu/M(aisc)	α	Lp	Lpd	R
Model2-ex End 1	1.25	6	1.25	6	1.125	24.247	20253.82	0.00679	2.40	21.55	2.40	85.83	8.67	70.48	0.0333	0.1458	16283.93	20031.02	16824.87	1.1906	0.9890	1.2301	0.6425	42.76	39.47	0
Model2-ex End 2	1.25	6	1.25	6	1.125	32.685	31521.96	0.00526	2.40	29.05	2.40	85.83	8.67	77.19	0.0333	0.1458	24603.50	31175.22	25420.81	1.2264	0.9890	1.2671		39.04	36.04	0
Model2-ex End 1	1.125	8	1.125	8	0.75	24.372	19360.21	0.00640	3.56	32.50	3.56	85.83	8.67	45.90	0.0333	0.1458	17073.89	19360.21	17073.89	1.1339	1.0000	1.1339	0.6720	65.65	58.69	3.6140
Model2-ex End 2	1.125	8	1.125	8	0.75	32.81	28811.77	0.00494	3.56	43.75	3.56	85.83	8.67	49.67	0.0333	0.1458	24743.28	28811.77	24743.28	1.1644	1.0000	1.1644		60.67	54.24	3.4260
Model2-ex End 1	1.125	8	1.125	8	0.625	24.372	18305.86	0.00630	3.56	39.00	3.56	85.83	8.67	44.01	0.0333	0.1458	16402.00	18269.25	16402.00	1.1138	0.9980	1.1138	0.6805	68.46	60.64	0
Model2-ex End 2	1.125	8	1.125	8	0.625	32.81	26901.04	0.00485	3.56	52.50	3.56	85.83	8.67	47.34	0.0333	0.1458	23511.69	26847.24	23511.69	1.1419	0.9980	1.1419		63.66	56.38	0
Model2-ex End 1	1	8	1	8	0.625	24.497	16911.84	0.00636	4.00	39.20	4.00	85.83	8.67	45.30	0.0333	0.1458	15003.20	16793.46	15003.20	1.1193	0.9930	1.1193	0.6752	66.52	59.26	0
Model2-ex End 2	1	8	1	8	0.625	32.935	25046.49	0.00491	4.00	52.70	4.00	85.83	8.67	48.92	0.0333	0.1458	21652.96	24871.16	21652.96	1.1486	0.9930	1.1486		61.60	54.88	0
Model2-ex End 1	1	8	1	8	0.4375	24.497	15314.05	0.00618	4.00	55.99	4.00	85.83	8.67	41.92	0.0333	0.1458	13979.79	15084.34	13979.79	1.0790	0.9850	1.0790	0.6911	71.88	62.90	0
Model2-ex End 2	1	8	1	8	0.4375	32.935	22158.51	0.00475	4.00	75.28	4.00	85.83	8.67	44.71	0.0333	0.1458	19784.38	21826.13	19784.38	1.1032	0.9850	1.1032		67.39	58.98	0
Model2-ex End 1	1	8	1	8	0.375	24.497	14781.46	0.00612	4.00	65.33	4.00	85.83	8.67	40.72	0.0333	0.1458	13638.65	14515.39	13638.65	1.0643	0.9820	1.0643	0.6974	74.00	64.31	0
Model2-ex End 2	1	8	1	8	0.375	32.935	21195.85	0.00469	4.00	87.83	4.00	85.83	8.67	43.19	0.0333	0.1458	19161.52	20814.32	19161.52	1.0863	0.9820	1.0863		69.76	60.63	0
Model2-ex End 1	1.125	10	1.125	10	0.3125	24.372	18928.52	0.00594	4.44	77.99	4.44	85.83	8.67	30.05	0.0333	0.1458	17982.93	18928.52	17982.93	1.0526	1.0000	1.0526	0.7153	100.27	85.36	6.9061
Model2-ex End 2	1.125	10	1.125	10	0.3125	32.81	26461.04	0.00453	4.44	104.99	4.44	85.83	8.67	31.34	0.0333	0.1458	24771.14	26461.04	24771.14	1.0682	1.0000	1.0682		96.15	81.86	7.3674
Model2-ex End 1	1.125	10	1.125	10	0.25	24.372	18401.34	0.00589	4.44	97.49	4.44	85.83	8.67	29.29	0.0333	0.1458	17646.99	18309.34	17646.99	1.0375	0.9950	1.0375	0.7215	102.89	86.97	0
Model2-ex End 2	1.125	10	1.125	10	0.25	32.81	25505.68	0.00448	4.44	131.24	4.44	85.83	8.67	30.35	0.0333	0.1458	24155.34	25378.15	24155.34	1.0506	0.9950	1.0506		99.30	83.94	0
Model2-ex End 1	0.875	8	0.875	8	0.25	24.622	12289.83	0.00602	4.57	98.49	4.57	85.83	8.67	38.96	0.0333	0.1458	11527.17	11970.29	11527.17	1.0384	0.9740	1.0384	0.7074	77.35	66.45	0
Model2-ex End 2	0.875	8	0.875	8	0.25	33.06	17372.32	0.00460	4.57	132.24	4.57	85.83	8.67	40.94	0.0333	0.1458	16015.31	16920.64	16015.31	1.0565	0.9740	1.0565		73.60	63.23	0
Model2-ex End 1	0.625	6	0.625	6	0.3125	24.872	8176.01	0.00639	4.80	79.59	4.80	85.83	8.67	61.70	0.0333	0.1458	7076.81	7538.29	7217.20	1.0445	0.9220	1.0652	0.6728	48.83	43.62	0
Model2-ex End 2	0.625	6	0.625	6	0.3125	33.31	12151.61	0.00493	4.80	106.59	4.80	85.83	8.67	66.79	0.0333	0.1458	10247.51	11203.78	10450.79	1.0721	0.9220	1.0933		45.12	40.30	0
Model2-ex End 1	1	10	1	10	0.4375	24.497	18210.52	0.00609	5.00	55.99	5.00	85.83	8.67	32.18	0.0333	0.1458	16877.75	18210.52	16877.75	1.0790	1.0000	1.0790	0.7000	93.64	81.12	5.1532
Model2-ex End 2	1	10	1	10	0.4375	32.935	26013.48	0.00467	5.00	75.28	5.00	85.83	8.67	34.05	0.0333	0.1458	23640.46	26013.48	23640.46	1.1004	1.0000	1.1004		88.49	76.66	5.2063
Model2-ex End 1	1	10	1	10	0.375	24.497	17677.93	0.00603	5.00	65.33	5.00	85.83	8.67	31.38	0.0333	0.1458	16536.61	17677.93	16536.61	1.0690	1.0000	1.0690	0.7057	96.04	82.68	4.4096
Model2-ex End 2	1	10	1	10	0.375	32.935	25050.82	0.00462	5.00	87.83	5.00	85.83	8.67	33.03	0.0333	0.1458	23017.60	25050.82	23017.60	1.0883	1.0000	1.0883		91.23	78.54	4.5609
Model2-ex End 1	1	10	1	10	0.3125	24.497	17145.33	0.00598	5.00	78.39	5.00	85.83	8.67	30.55	0.0333	0.1458	16195.47	17076.75	16195.47	1.0544	0.9960	1.0544	0.7118	98.65	84.33	0
Model2-ex End 2	1	10	1	10	0.3125	32.935	24088.16	0.00456	5.00	105.39	5.00	85.83	8.67	31.97	0.0333	0.1458	22394.74	23991.80	22394.74	1.0713	0.9960	1.0713		94.27	80.58	0
Model2-ex End 1	1.125	12	1.125	12	0.4375	24.372	23241.40	0.00599	5.33	55.71	5.33	85.83	8.67	25.56	0.0333	0.1458	21915.46	23473.81	21915.46	1.0711	1.0100	1.0711	0.7106	117.87	100.90	5.2225
Model2-ex End 2	1.125	12	1.125	12	0.4375	32.81	32708.62	0.00457	5.33	74.99	5.33	85.83	8.67	26.79	0.0333	0.1458	30341.16	33035.71	30341.16	1.0888	1.0100	1.0888		112.50	96.30	5.6594
Model2-ex End 1	1.125	12	1.125	12	0.375	24.372	22714.22	0.00594	5.33	64.99	5.33	85.83	8.67	25.04	0.0333	0.1458	21579.52	22941.36	21579.52	1.0631	1.0100	1.0631	0.7153	120.32	102.43	4.2176
Model2-ex End 2	1.125	12	1.125	12	0.375	32.81	31753.25	0.00453	5.33	87.49	5.33	85.83	8.67	26.12	0.0333	0.1458	29725.36	32070.79	29725.36	1.0789	1.0100	1.0789		115.38	98.23	4.7234
Model2-ex End 1	0.875	10	0.875	10	0.5625	24.622	17514.46	0.00626	5.71	43.77	5.71	85.83	8.67	34.73	0.0333	0.1458	15794.52	17514.46	15794.52	1.1089	1.0000	1.1089	0.6843	86.76	76.52	2.8529
Model2-ex End 2	0.875	10	0.875	10	0.5625	33.06	25595.33	0.00482	5.71	58.77	5.71	85.83	8.67	37.25	0.0333	0.1458	22539.06	25595.33	22539.06	1.1356	1.0000	1.1356		80.89	71.34	2.8085
Model2-ex End 1	0.875	10	0.875	10	0.5	24.622	16976.42	0.00620	5.71	49.24	5.71	85.83	8.67	33.88	0.0333	0.1458	15448.13	16942.47	15448.13	1.0967	0.9980	1.0967	0.6894	88.94	77.99	0
Model2-ex End 2	0.875	10	0.875	10	0.5	33.06	24625.35	0.00477	5.71	66.12	5.71	85.83	8.67	36.19	0.0333	0.1458	21909.08	24576.10	21909.08	1.1217	0.9980	1.1217		83.27	73.02	0
Model2-ex End 1	0.875	10	0.875	10	0.3125	24.622	15362.28	0.00602	5.71	78.79	5.71	85.83	8.67	31.17	0.0333	0.1458	14408.97	15193.30	14408.97	1.0544	0.9890	1.0544	0.7074	96.68	83.06	0
Model2-ex End 2	0.875	10	0.875	10	0.3125	33.06	21715.40	0.00460	5.71	105.79	5.71	85.83	8.67	32.75	0.0333	0.1458	20019.14	21476.54	20019.14	1.0728	0.9890	1.0728		92.00	79.03	0
Model2-ex End 1	1	12	1	12	0.5625	24.497	22172.19	0.00612	6.00	43.55	6.00	85.83	8.67	27.15	0.0333	0.1458	20457.98	22393.91	20457.98	1.0946	1.0100	1.0946	0.6974	111.00	96.46	4.4626
Model2-ex End 2	1	12	1	12	0.5625	32.935	31793.77	0.00469	6.00	58.55	6.00	85.83	8.67	28.80	0.0333	0.1458	28742.27	32111.71	28742.27	1.1172	1.0100	1.1172		104.65	90.94	4.6650
Model2-ex End 1	1	12	1	12	0.5	24.497	21639.59	0.00607	6.00	48.99	6.00	85.83	8.67	26.60	0.0333	0.1458	20116.84	21855.99	20116.84	1.0865	1.0100	1.0865	0.7019	113.30	97.96	3.4583
Model2-ex End 2	1	12	1	12	0.5	32.935	30831.11	0.00465	6.00	65.87	6.00	85.83	8.67	28.10	0.0333	0.1458	28119.41	31139.42	28119.41	1.1074	1.0100	1.1074		107.25	92.72	3.5953
Model2-ex End 1	1	12	1	12	0.4375	24.497	21106.99	0.00602	6.00	55.99	6.00	85.83	8.67	26.03	0.0333	0.1458	19775.70	21318.06	19775.70	1.0780	1.0100	1.0780	0.7067	115.75	99.53	2.8870
Model2-ex End 2	1	12	1	12	0.4375	32.935	29868.45	0.00461	6.00	75.28	6.00	85.83	8.67	27.38	0.0333	0.1458	27496.55	30167.13	27496.55	1.0971	1.0100	1.0971		110.06	94.64	2.9810
Model2-ex End 1	0.5	6	0.5	6	0.375	24.997	7672.06	0.00664	6.00	66.66	6.00	85.83	8.67	69.10	0.0333	0.1458	6288.98	6920.20	6520.00	1.0614	0.9020	1.1004	0.6538	43.61	39.77	0
Model2-ex End 2	0.5	6	0.5	6	0.375	33.435	11735.13	0.00513	6.00	89.16	6.00	85.83	8.67	75.80	0.0333	0.1458	9349.41	10585.08	9692.85	1.0921	0.9020	1.1322		39.75	36.25	0
Model2-ex End 1	0.5	6	0.5	6	0.25	24.997	6562.94	0.00639	6.00	99.99	6.00	85.83	8.67	61.81	0.0333	0.1458	5678.51	5946.02	5795.09	1.0260	0.9060	1.0471	0.6731	48.75	43.53	0
Model2-ex End 2	0.5	6	0.5	6	0.25	33.435	9750.90	0.00493	6.00	133.74	6.00	85.83	8.67	66.90	0.0333	0.1458	8220.76	8834.32	8389.52	1.0530	0.9060	1.0746		45.04	40.22	0
Model2-ex End 1	0.5	6	0.5	6	0.1875	24.997	6008.38	0.00624	6.00	133.32	6.00	85.83	8.67	57.77	0.0333	0.1458	5364.94	5467.63	5432.63	1.0064	0.9100	1.0191	0.6860	52.16	45.92	0
Model2-ex End 2	0.5	6	0.5	6	0.1875	33.435	8758.79	0.00480	6.00	178.32	6.00	85.83	8.67	61.89	0.0333	0.1458	7641.44	7970.50	7737.86	1.0301	0.9100	1.0431		48.69	42.86	0
Model2-ex End 1	0.875	12	0.875	12	0.5625	24.622	20048.87	0.00617	6.86	43.77	6.86	85.83	8.67	27.87	0.0333	0.1458	18329.92	20048.87	18329.92	1.0938	1.0000	1.0938	0.6921	108.12	94.52	2.2471
Model2-ex End 2	0.875	12	0.875	12	0.5625	33.06	28968.43	0.00474	6.86	58.77	6.86	85.83	8.67	29.70	0.0333	0.1458	25912.91	28968.43	25912.91	1.1179	1.0000	1.1179		101.46	88.70	2.2419
Model2-ex End 1	0.4375	6	0.4375	6	0.375	25.06	7145.63	0.00673	6.86	66.83	6.86	85.83	8.67	72.08	0.0333	0.1458	5738.44	6366.76	5993.08	1.0624	0.8910	1.1095	0.6476	41.81	38.38	0
Model2-ex End 2	0.4375	6	0.4375	6	0.375	33.497	11034.60	0.00520	6.86	89.33	6.86	85.83	8.67	79.39	0.0333	0.1458	8609.81	9831.82	8991.87	1.0934	0.8910	1.1419		37.96	34.85	0
Model2-ex End 1	0.875	12	0.875	12	0.3125	24.622	17896.70	0.00596	6.86	78.79	6.86	85.83	8.67	25.30	0.0333	0.1458	16944.38	17592.45	16944.38	1.0382	0.9830	1.0382	0.7133	119.08	101.61	0
Model2-ex End 2	0.875	12	0.875	12	0.3125	33.06	25088.50	0.00455	6.86	105.79	6.86	85.83	8.67	26.44	0.0333	0.1458	23392.98	24662.00	23392.98	1.0542	0.9830	1.0542		113.96	97.24	0
Model2-ex End 1	0.4375	6	0.4375	6	0.3125	25.06	6588.29	0.00661	6.86	80.19	6.86	85.83	8.67	68.21	0.0333	0.1458	5438.44	5850.41	5627.90	1.0395	0.8880	1.0758	0.6563	44.18	40.18	0
Model2-ex End 2	0.4375	6	0.4375	6	0.3125	33.497	10038.77	0.00511	6.86	107.19	6.86	85.83	8.67	74.72	0.0333	0.1458	8055.91	8914.43	8336.55	1.0693	0.8880	1.1066		40.33	36.68	0
Model2-ex End 1	0.4375	6	0.4375	6	0.1875	25.06	5473.62	0.00631	6.86	133.65	6.86	85.83	8.67	59.58	0.0333	0.1458	4819.30	4882.47	4897.54	0.9969	0.8920	1.0131	0.6802	50.57	44.81	0
Model2-ex End 2	0.4375	6	0.4375	6	0.1875	33.497	8047.12	0.00486	6.86	178.65	6.86	85.83	8.67	64.14	0.0333	0.1458	6913.67	7178.03	7025.90	1.0217	0.8920	1.0382		46.98	41.63	0
Model2-ex End 1	0.5	8	0.5	8	0.3125	24.997	8565.74	0.00636	8.00	79.99	8.00	85.83	8.67	45.62	0.0333	0.1458	7605.96	7957.57	7605.96	1.0462	0.9290	1.0462	0.6760	66.05	58.79	0
Model2-ex End 2	0.5	8	0.5	8	0.3125	33.435	12670.50	0.00490	8.00	106.99	8.00	85.83	8.67	49.27	0.0333	0.1458	10968.81	11770.89	10968.81	1.0731	0.9290	1.0731		61.16	54.44	0
Model2-ex End 1	0.375	6	0.375	6	0.25	25.122	5499.01	0.00656	8.00	100.49	8.00	85.83	8.67	66.94	0.0333	0.1458	4583.59	4767.64	4730.45	1.0079	0.8670	1.0402	0.6597	45.01	40.79	0
Model2-ex End 2	0.375	6	0.375	6	0.25	33.56	8335.02	0.00507	8.00	134.24	8.00	85.83	8.67	73.17	0.0333	0.1458	6756.54	7226.46	6973.01	1.0363	0.8670	1.0696		41.18	37.32	0

Table B4 Continued

E	Fy
29600	56.8

End 1 = Shallow End
End 2 = Deep End

DESCRIPTION	tf1	bf1	tf2	bf2	tw	dw	Mp(in kips)	θ p	Comp. bf1/2tf1	h/tw	Tension bf2/2tf2	Web λ p	Flanges λ p
Model2-ex End 1	0.5	8	0.5	8	0.1875	24.9971	7456.62	0.00612	8.00	133.32	8.00	85.83	8.67
Model2-ex End 2	0.5	8	0.5	8	0.1875	33.4346	10686.28	0.00469	8.00	178.32	8.00	85.83	8.67
Model2-ex End 1	0.375	6	0.375	6	0.1875	25.1221	4938.89	0.00639	8.00	133.98	8.00	85.83	8.67
Model2-ex End 2	0.375	6	0.375	6	0.1875	33.5596	7335.47	0.00493	8.00	178.98	8.00	85.83	8.67
Model2-ex End 1	0.5625	10	0.5625	10	0.1875	24.9346	9801.69	0.00600	8.89	132.98	8.89	85.83	8.67
Model2-ex End 2	0.5625	10	0.5625	10	0.1875	33.3721	13807.32	0.00458	8.89	177.98	8.89	85.83	8.67
Model2-ex End 1	0.4375	8	0.4375	8	0.25	25.0596	7298.17	0.00631	9.14	100.24	9.14	85.83	8.67
Model2-ex End 2	0.4375	8	0.4375	8	0.25	33.4971	10729.50	0.00486	9.14	133.99	9.14	85.83	8.67
Model2-ex End 1	0.4375	8	0.4375	8	0.1875	25.0596	6740.83	0.00617	9.14	133.65	9.14	85.83	8.67
Model2-ex End 2	0.4375	8	0.4375	8	0.1875	33.4971	9733.67	0.00474	9.14	178.65	9.14	85.83	8.67
Model2-ex End 1	0.625	12	0.625	12	0.3125	24.8721	13606.90	0.00607	9.60	79.59	9.60	85.83	8.67
Model2-ex End 2	0.625	12	0.625	12	0.3125	33.3096	19379.68	0.00465	9.60	106.59	9.60	85.83	8.67
Model2-ex End 1	0.5	10	0.5	10	0.3125	24.9971	10013.97	0.00624	10.00	79.99	10.00	85.83	8.67
Model2-ex End 2	0.5	10	0.5	10	0.3125	33.4346	14597.99	0.00480	10.00	106.99	10.00	85.83	8.67
Model2-ex End 1	0.5	10	0.5	10	0.25	24.9971	9459.41	0.00614	10.00	99.99	10.00	85.83	8.67
Model2-ex End 2	0.5	10	0.5	10	0.25	33.4346	13605.87	0.00471	10.00	133.74	10.00	85.83	8.67
Model2-ex End 1	0.375	8	0.375	8	0.1875	25.1221	6025.06	0.00624	10.67	133.98	10.67	85.83	8.67
Model2-ex End 2	0.375	8	0.375	8	0.1875	33.5596	8781.09	0.00480	10.67	178.98	10.67	85.83	8.67
Model2-ex End 1	0.5	12	0.5	12	0.25	24.9971	10907.65	0.00607	12.00	99.99	12.00	85.83	8.67
Model2-ex End 2	0.5	12	0.5	12	0.25	33.4346	15533.36	0.00465	12.00	133.74	12.00	85.83	8.67

DESCRIPTION	Lb/ry	m(top)	m(bot)	M(aisc)	Mu(abaqus)	My	Mu/My	Mu/Mp	Mu/M(aisc)	α	Lp	Lpd	R
Model2-ex End 1	40.89	0.0333	0.1458	6881.05	6852.63	6881.05	0.9959	0.9190	0.9959	0.6978	73.69	64.01	0
Model2-ex End 2	43.36	0.0333	0.1458	9665.49	9820.69	9665.49	1.0161	0.9190	1.0161		69.49	60.36	0
Model2-ex End 1	61.92	0.0333	0.1458	4272.54	4272.14	4362.53	0.9793	0.8650	0.9999	0.6733	48.67	43.45	0
Model2-ex End 2	67.01	0.0333	0.1458	6183.77	6345.18	6314.02	1.0049	0.8650	1.0261		44.97	40.14	0
Model2-ex End 1	30.91	0.0333	0.1458	9226.88	9174.38	9226.88	0.9943	0.9360	0.9943	0.7099	97.49	83.52	0
Model2-ex End 2	32.41	0.0333	0.1458	12787.14	12923.65	12787.14	1.0107	0.9360	1.0107		92.98	79.66	0
Model2-ex End 1	44.69	0.0333	0.1458	6530.05	6561.05	6530.05	1.0047	0.8990	1.0047	0.6802	67.43	59.74	0
Model2-ex End 2	48.10	0.0333	0.1458	9367.87	9645.82	9367.87	1.0297	0.8990	1.0297		62.65	55.50	0
Model2-ex End 1	41.98	0.0333	0.1458	6164.87	6033.04	6164.87	0.9786	0.8950	0.9786	0.6925	71.79	62.73	0
Model2-ex End 2	44.72	0.0333	0.1458	8712.54	8711.64	8712.54	0.9999	0.8950	0.9999		67.38	58.88	0
Model2-ex End 1	26.67	0.0333	0.1458	12649.17	12749.66	12649.17	1.0079	0.9370	1.0079	0.7021	112.98	97.65	0
Model2-ex End 2	28.17	0.0333	0.1458	17679.68	18158.76	17679.68	1.0271	0.9370	1.0271		106.96	92.45	0
Model2-ex End 1	34.66	0.0333	0.1458	9054.38	9212.85	9054.38	1.0175	0.9200	1.0175	0.6860	86.94	76.53	0
Model2-ex End 2	37.13	0.0333	0.1458	12896.44	13430.15	12896.44	1.0414	0.9200	1.0414		81.15	71.43	0
Model2-ex End 1	33.11	0.0333	0.1458	8691.93	8645.90	8691.93	0.9947	0.9140	0.9947	0.6952	91.00	79.28	0
Model2-ex End 2	35.19	0.0333	0.1458	12244.77	12435.77	12244.77	1.0156	0.9140	1.0156		85.62	74.59	0
Model2-ex End 1	43.38	0.0333	0.1458	5448.78	5169.50	5448.78	0.9487	0.8580	0.9487	0.6861	69.46	61.13	0
Model2-ex End 2	46.47	0.0333	0.1458	7759.69	7534.17	7759.69	0.9709	0.8580	0.9709		64.84	57.07	0
Model2-ex End 1	26.70	0.0333	0.1458	10140.35	9653.27	10140.35	0.9520	0.8850	0.9520	0.7022	112.87	97.55	0
Model2-ex End 2	28.20	0.0333	0.1458	14172.40	13747.02	14172.40	0.9700	0.8850	0.9700		106.87	92.36	0

APPENDIX C

ROTATION CAPACITIES FOR PARAMETRIC STUDY

Appendix C illustrates 64 rotation capacity plots of beams that reached the plastic moment M_p and that are considered to have economical cross-sections. The slenderness ratios for the flanges and web for each of the beams are approximately 4.5 or greater and 50 or greater, respectively. Not every beam shown in Appendix C obtains a rotation capacity of three. However, as indicated by the moment vs. rotation plots, the web-tapered beams rotate markedly before unloading occurs, similar to prismatic members. The analysis data and numerical results of each beam are found in Appendix B.

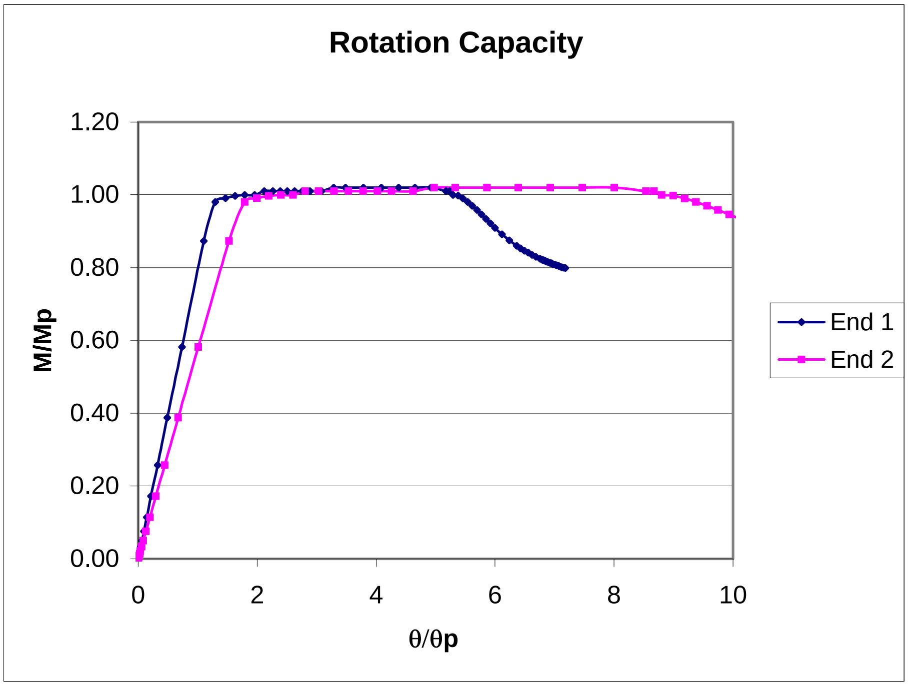

Figure C1 Model-1, L_b=60 in., t_f=1.125 in., t_w=0.25 in., b_f=10 in.

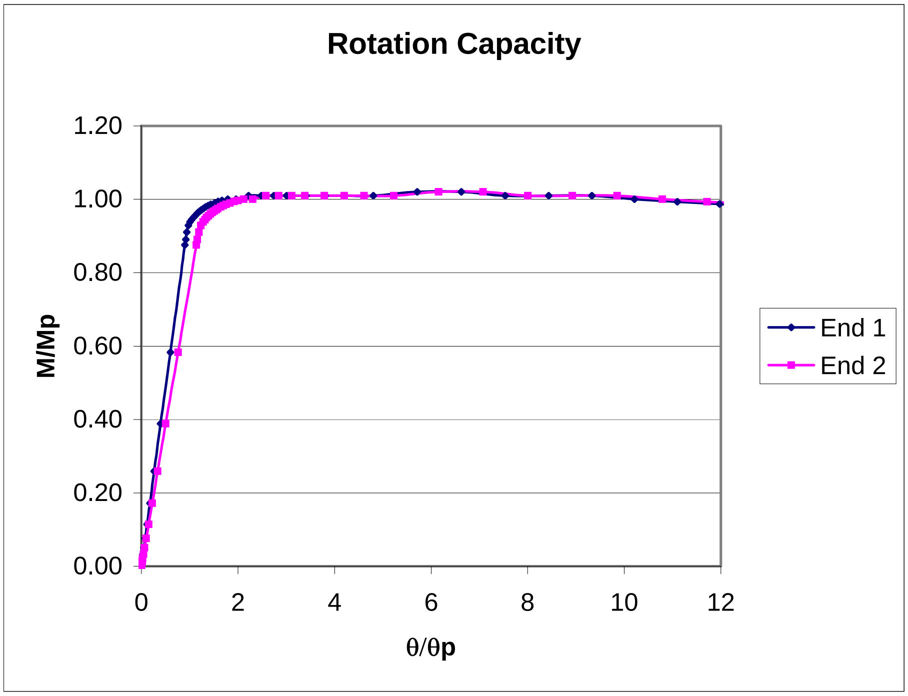

Figure C2 Model-1, L_b=60 in., t_f=0.875 in., t_w=0.4375 in., b_f=8 in.

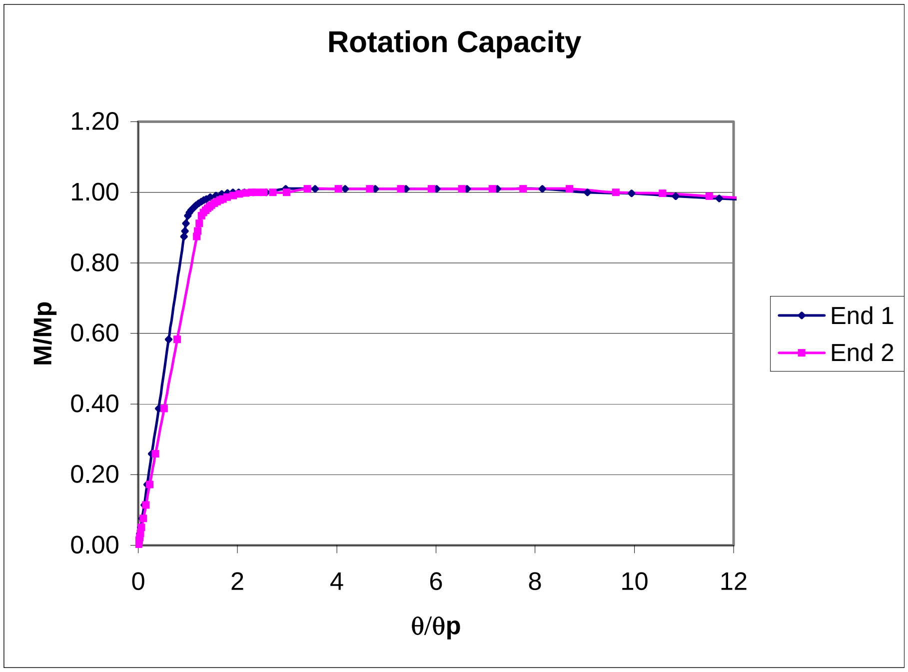

Figure C3 Model-1, L_b=60 in., t_f=0.875 in., t_w=0.375 in., b_f=8 in.

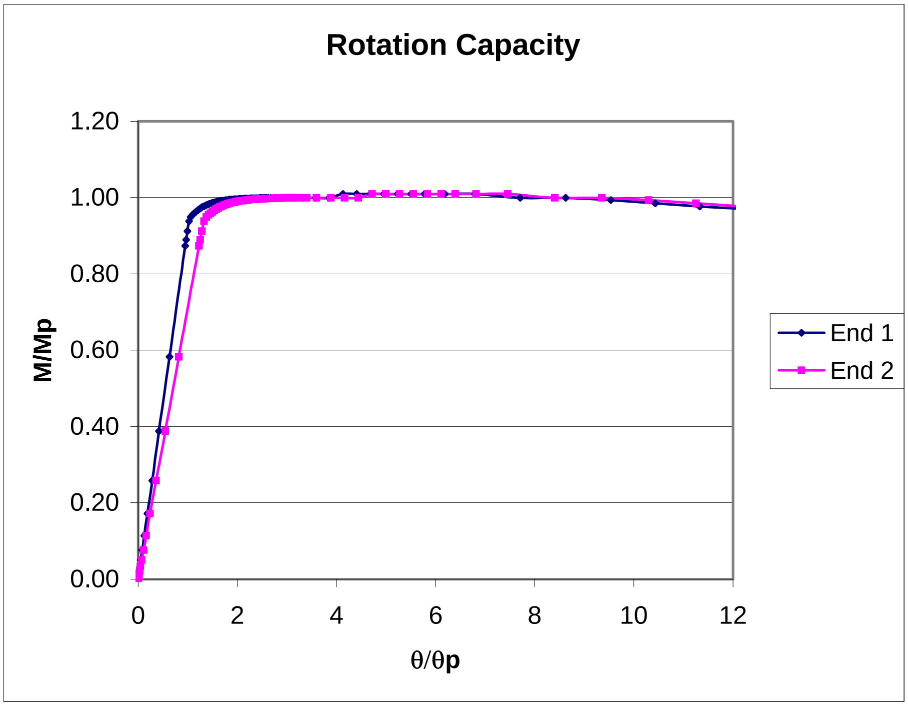

Figure C4 Model-1, L_b=60 in., t_f=0.875 in., t_w=0.3125 in., b_f=8 in.

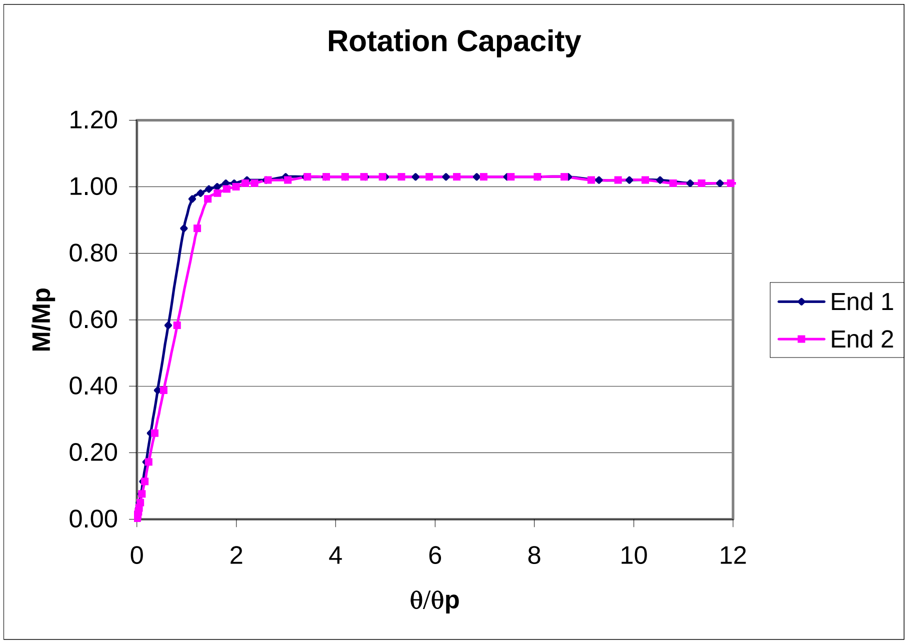

Figure C5 Model-1, L_b=60 in., t_f=1.0 in., t_w=0.4375 in., b_f=10 in.

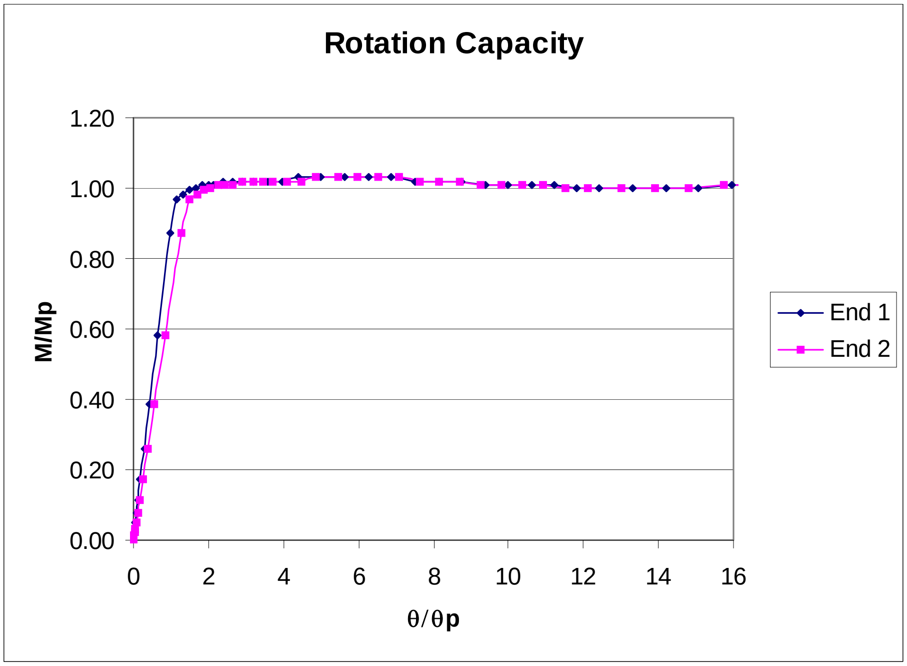

Figure C6 Model-1, L_b=60 in., t_f=1.0 in., t_w=0.375 in., b_f=10 in.

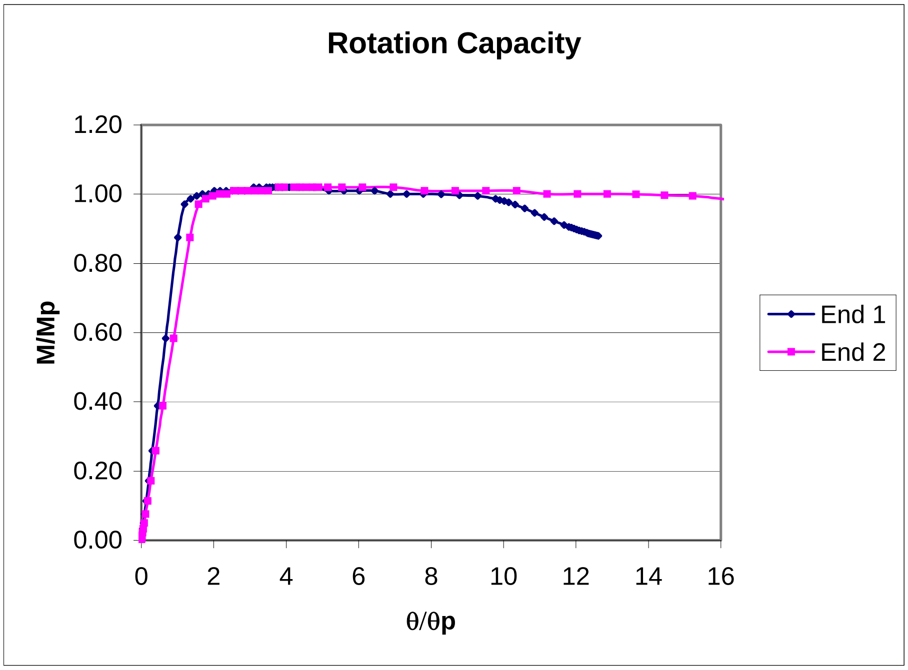

Figure C7 Model-1, L_b=60 in., t_f=1.0 in., t_w=0.3125 in., b_f=10 in.

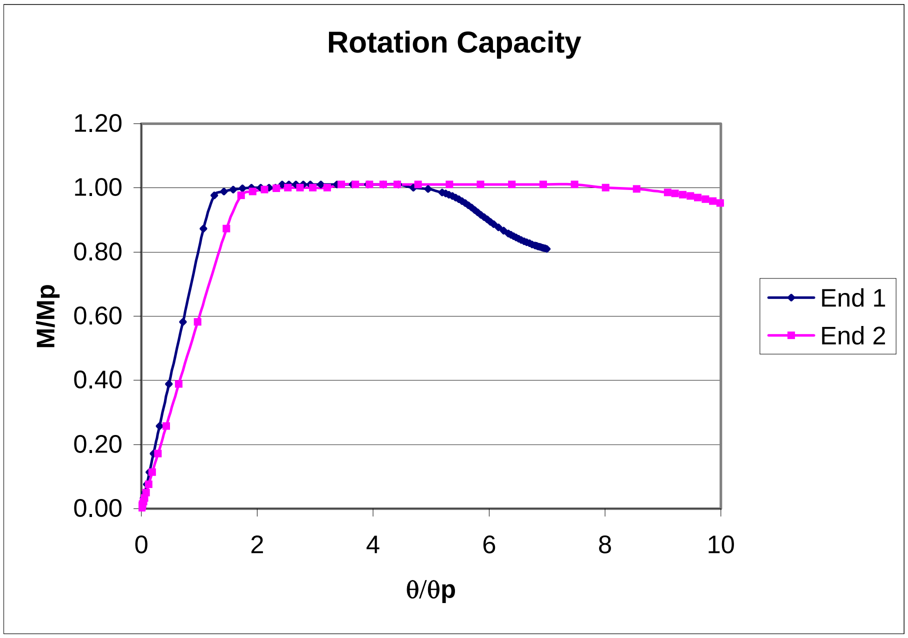

Figure C8 Model-1, L_b=60 in., t_f=1.0 in., t_w=0.25 in., b_f=10 in.

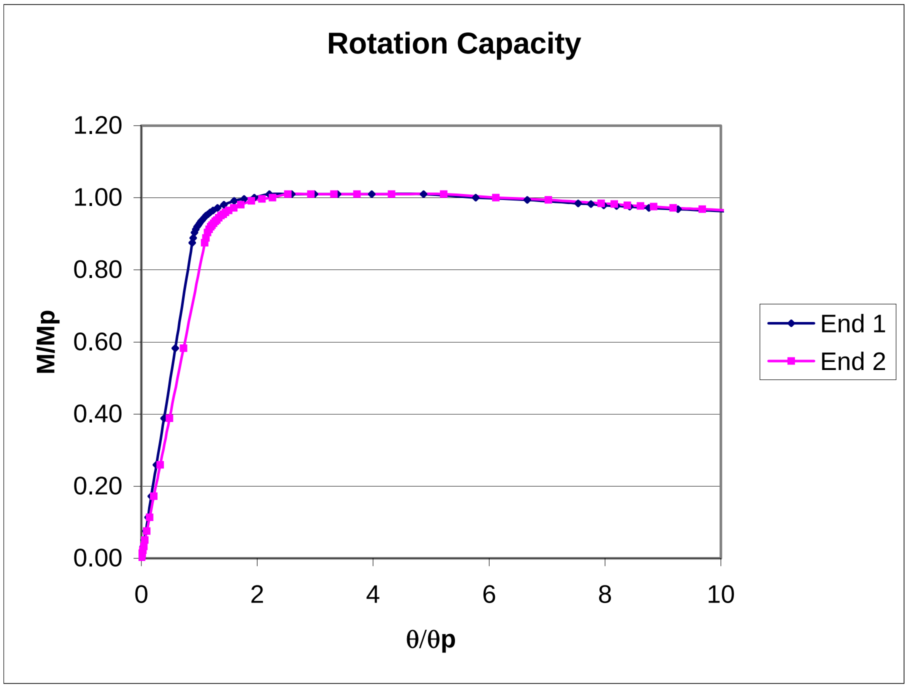

Figure C9 Model-1, L_b=60 in., t_f=0.75 in., t_w=0.5 in., b_f=8 in.

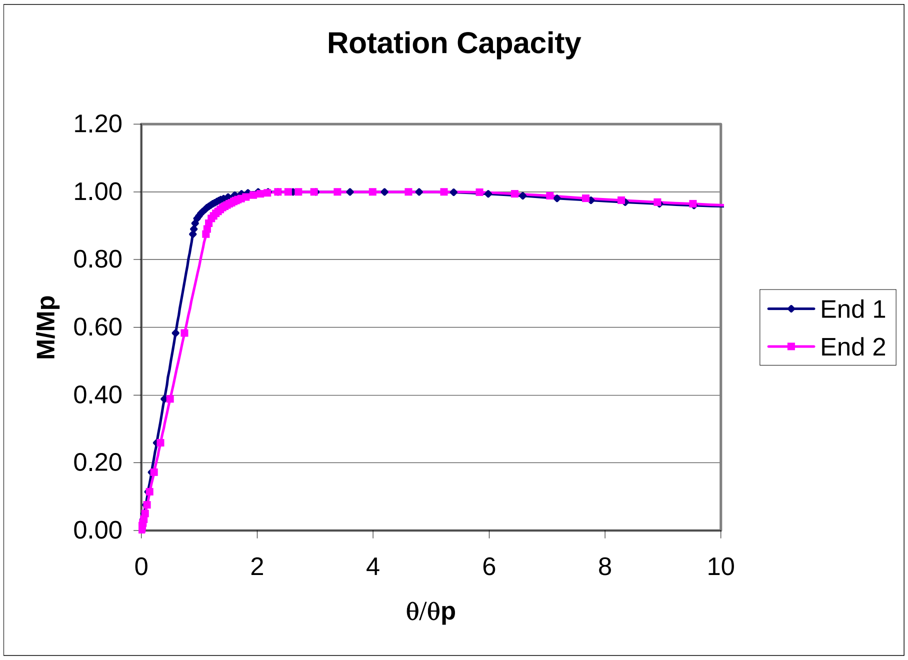

Figure C10 Model-1, L_b=60 in., t_f=0.75 in., t_w=0.4375 in., b_f=8 in.

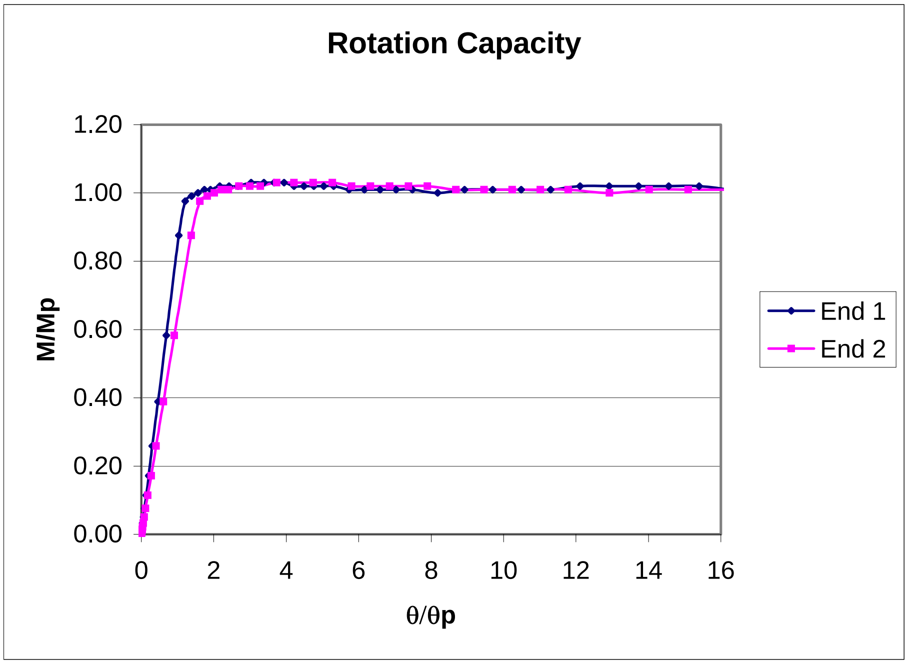

Figure C11 Model-1, L_b=60 in., t_f=1.125 in., t_w=0.375 in., b_f=12 in.

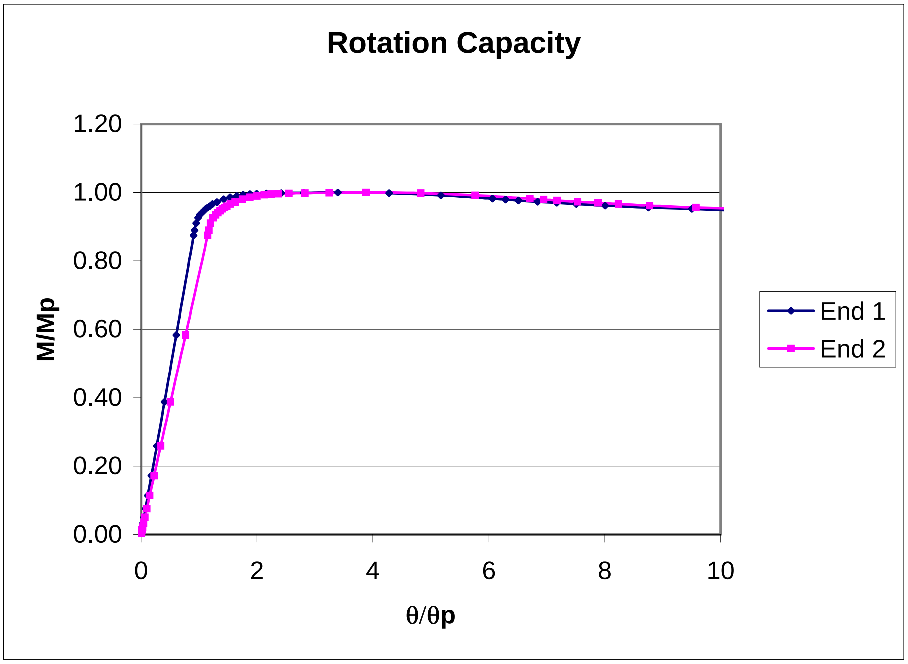

Figure C12 Model-1, L_b=60 in., t_f=0.75 in., t_w=0.375 in., b_f=8 in.

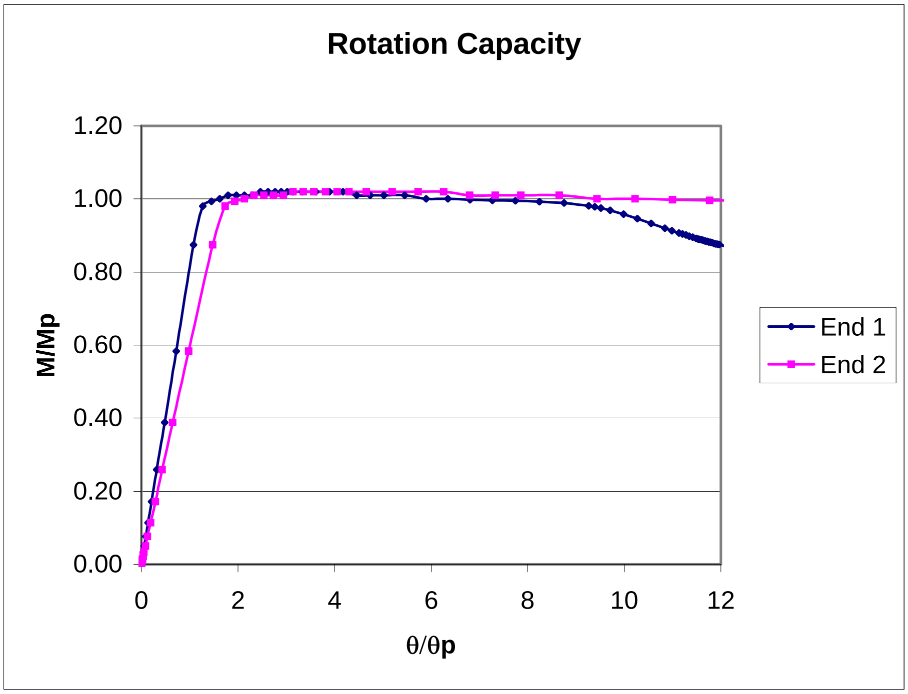

Figure C13 Model-1, L_b=60 in., t_f=1.125 in., t_w=0.3125 in., b_f=12 in.

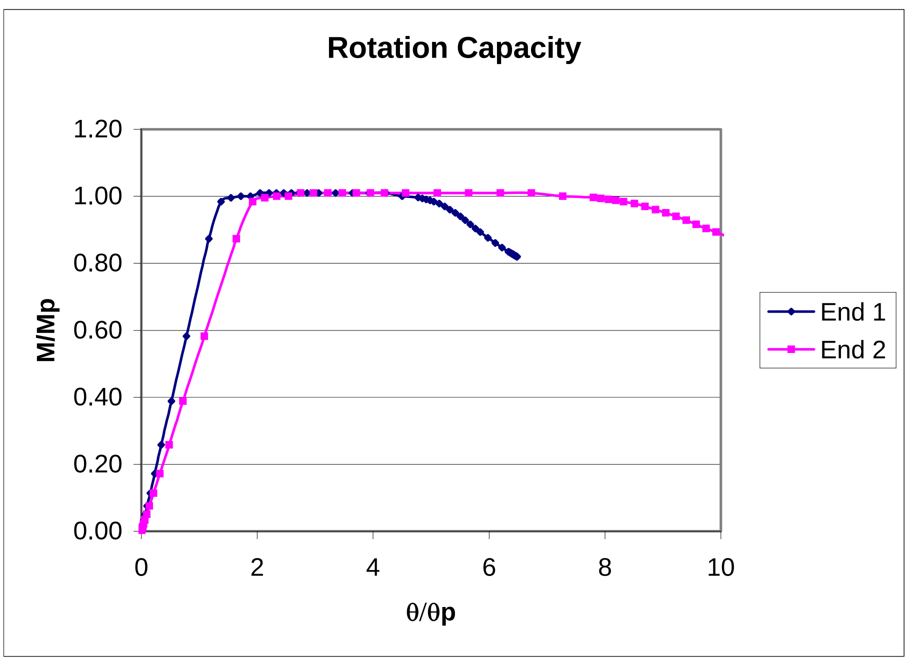

Figure C14 Model-1, L_b=60 in., t_f=1.125 in., t_w=0.25 in., b_f=12 in.

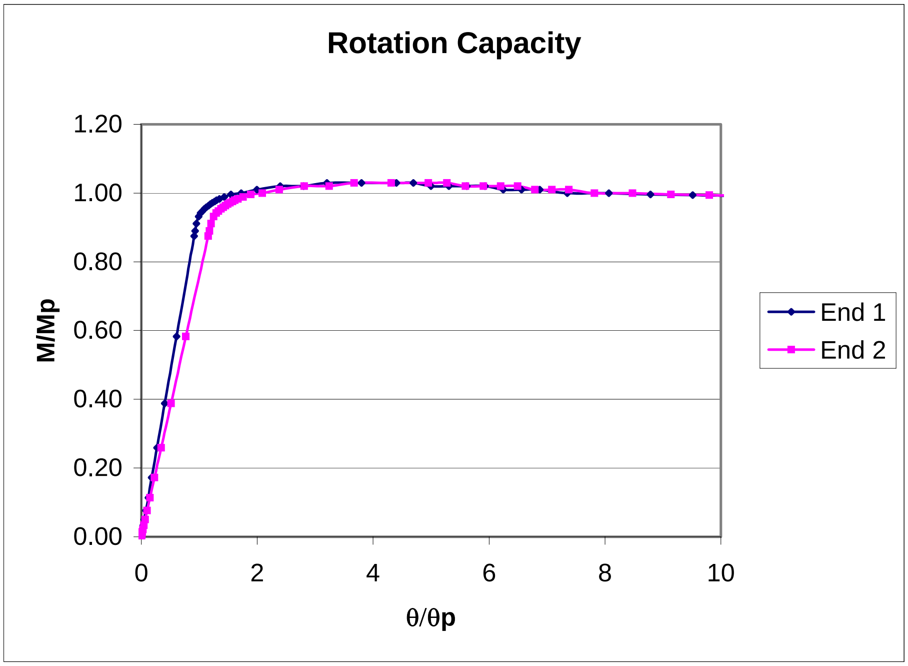

Figure C15 Model-1, L_b=60 in., t_f=0.875 in., t_w=0.5 in., b_f=10 in.

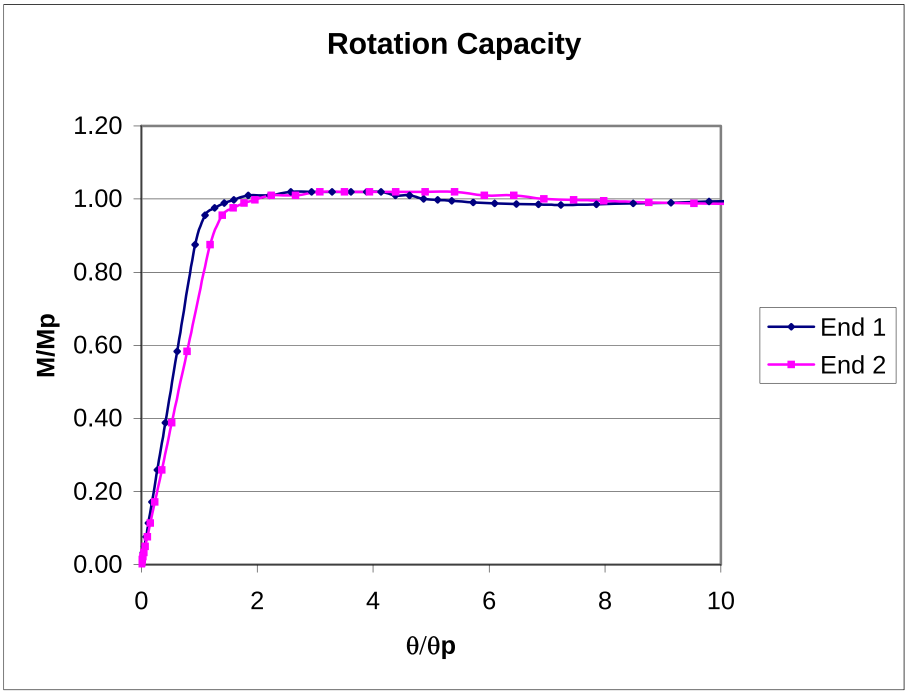

Figure C16 Model-1, L_b=60 in., t_f=0.875 in., t_w=0.4375 in., b_f=10 in.

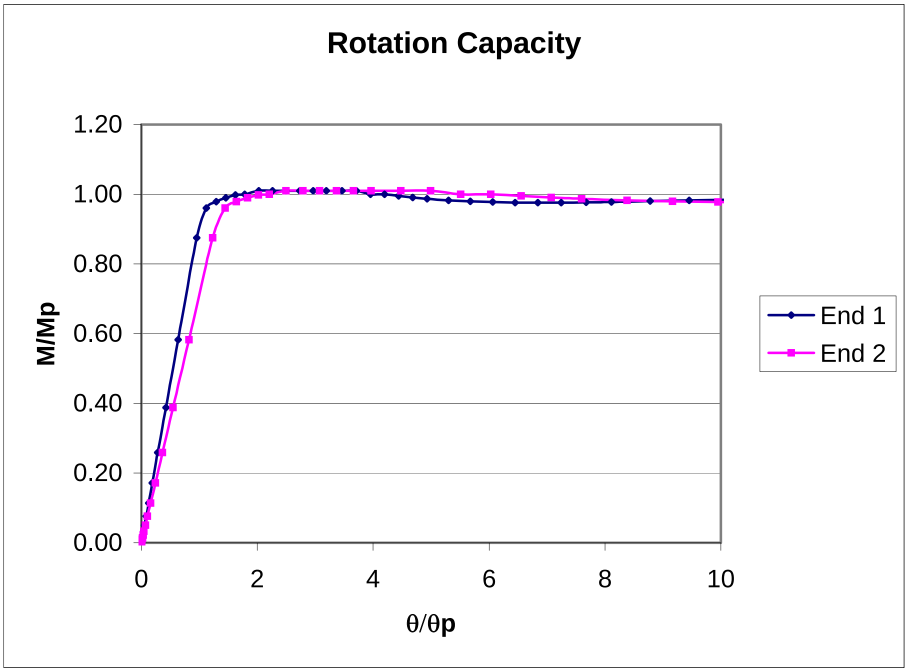

Figure C17 Model-1, L_b=60 in., t_f=0.875 in., t_w=0.375 in., b_f=10 in.

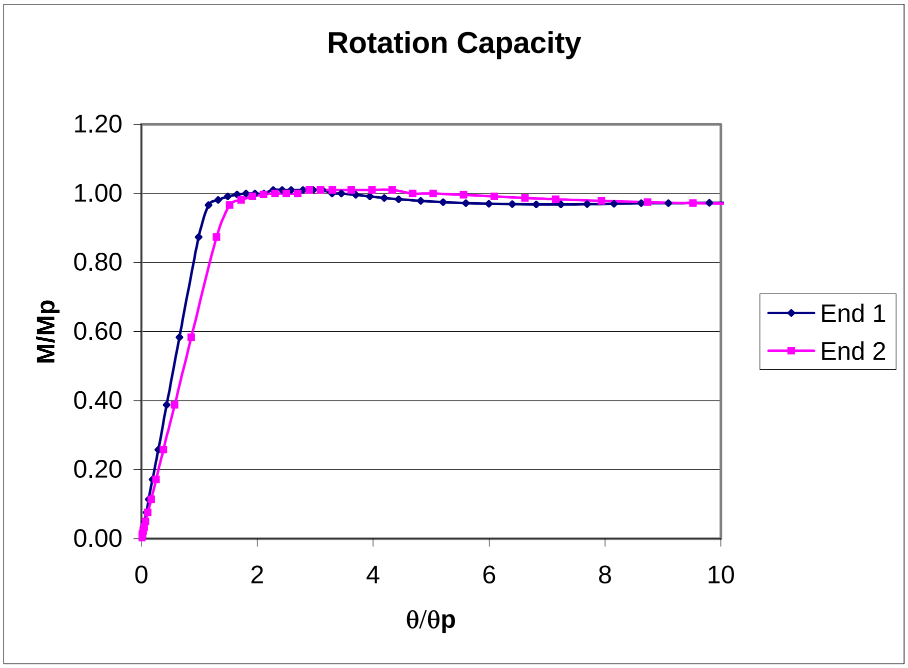

Figure C18 Model-1, L_b=60 in., t_f=0.875 in., t_w=0.3125 in., b_f=10 in.

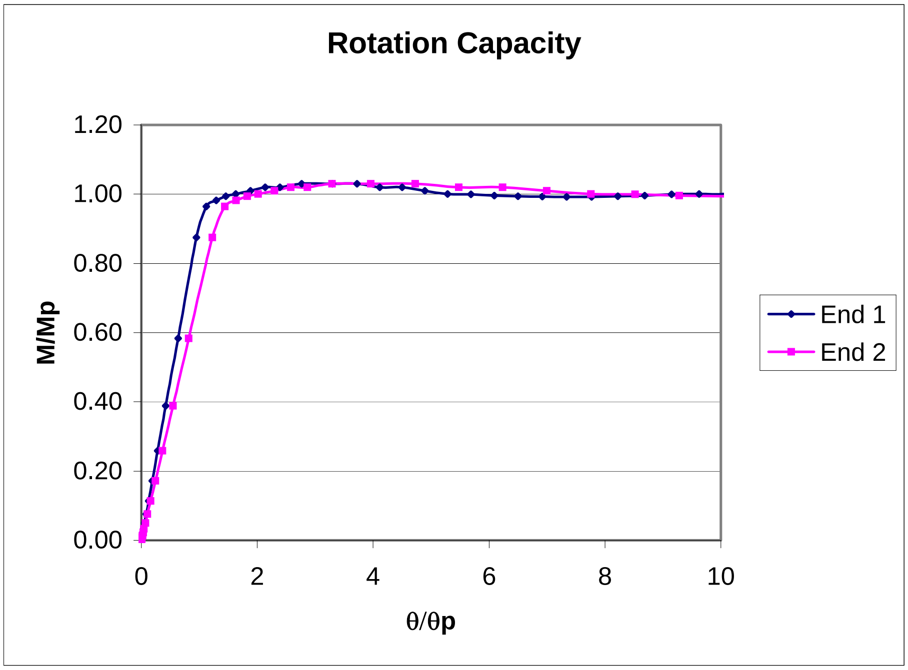

Figure C19 Model-1, L_b=60 in., t_f=1.0 in., t_w=0.5 in., b_f=12 in.

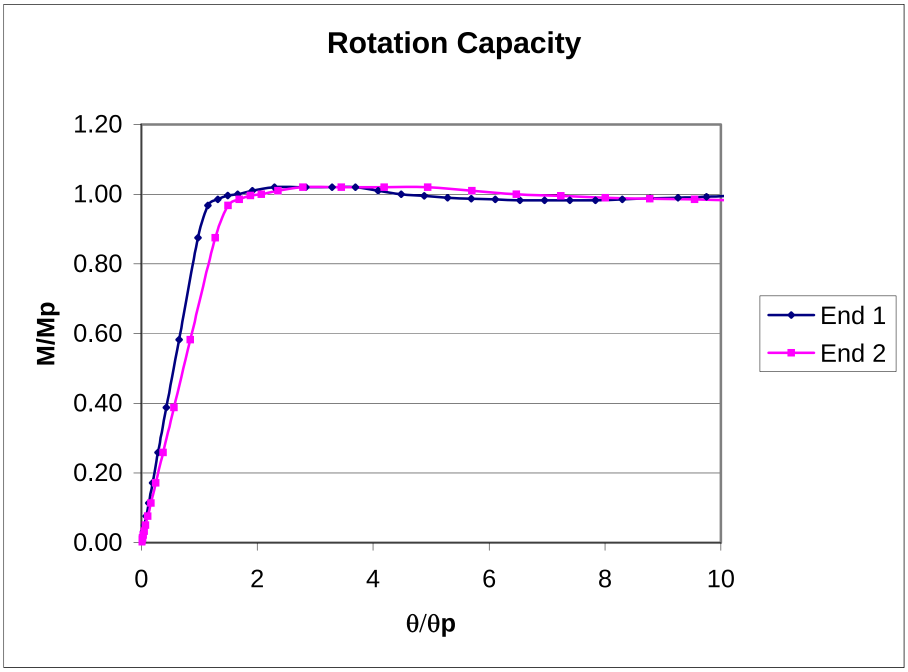

Figure C20 Model-1, L_b=60 in., t_f=1.0 in., t_w=0.4375 in., b_f=12 in.

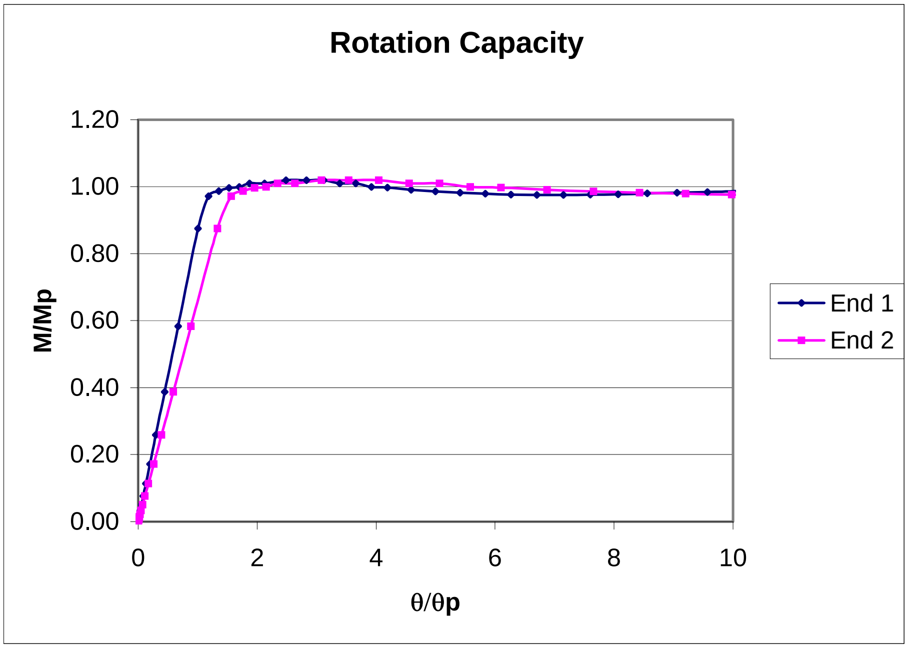

Figure C21 Model-1, L_b=60 in., t_f=1.0 in., t_w=0.375 in., b_f=12 in.

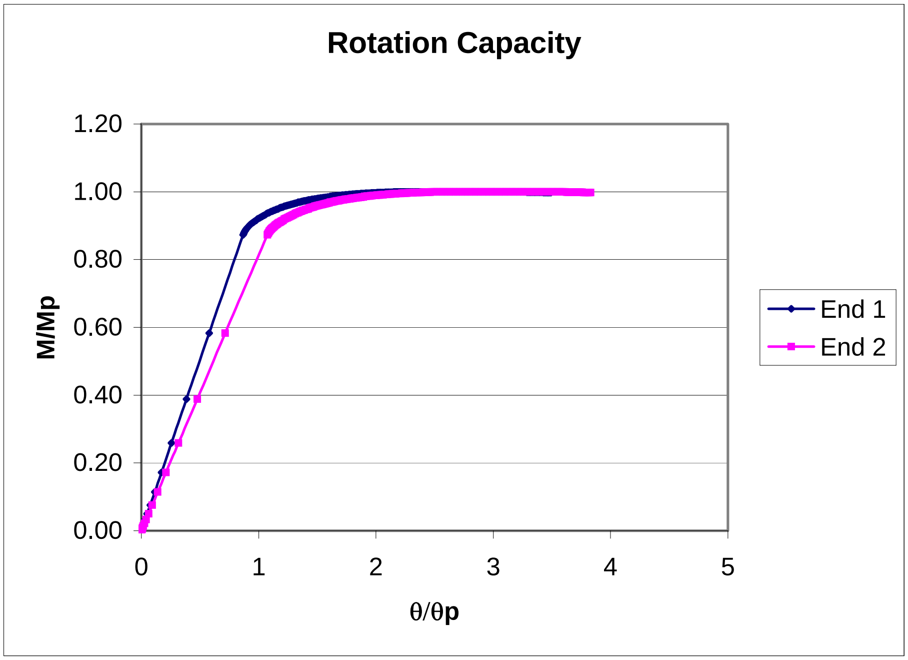

Figure C22 Model-1, L_b=60 in., t_f=0.625 in., t_w=0.5 in., b_f=8 in.

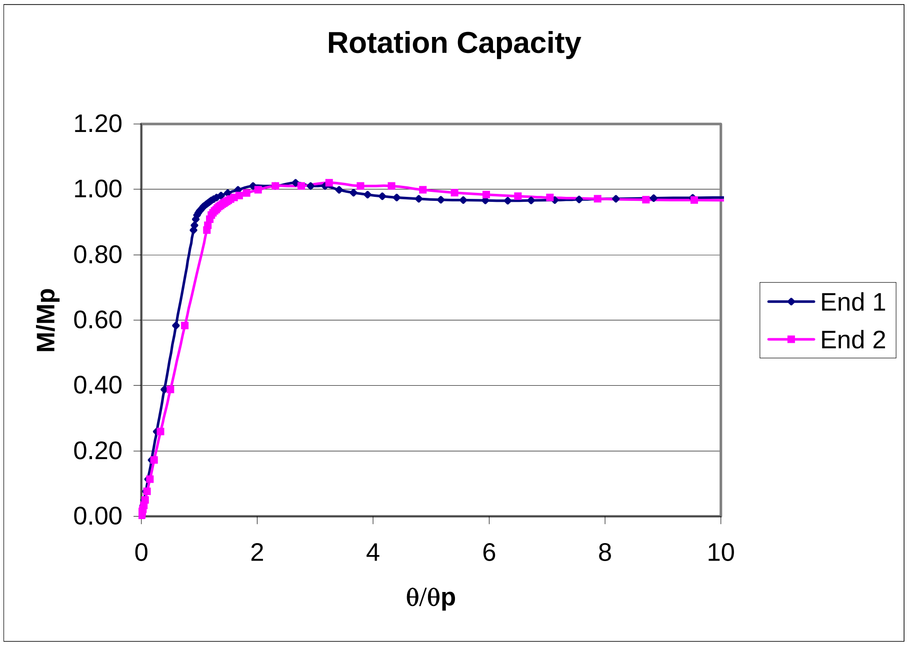

Figure C23 Model-1, L_b=60 in., t_f=0.75 in., t_w=0.5 in., b_f=10 in.

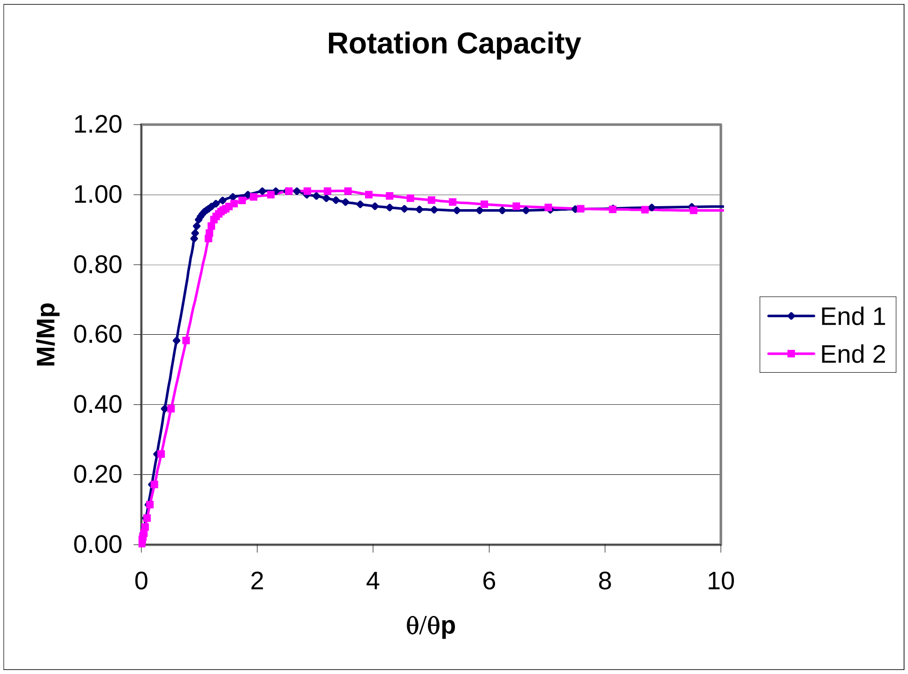

Figure C24 Model-1, L_b=60 in., t_f=0.75 in., t_w=0.4375 in., b_f=10 in.

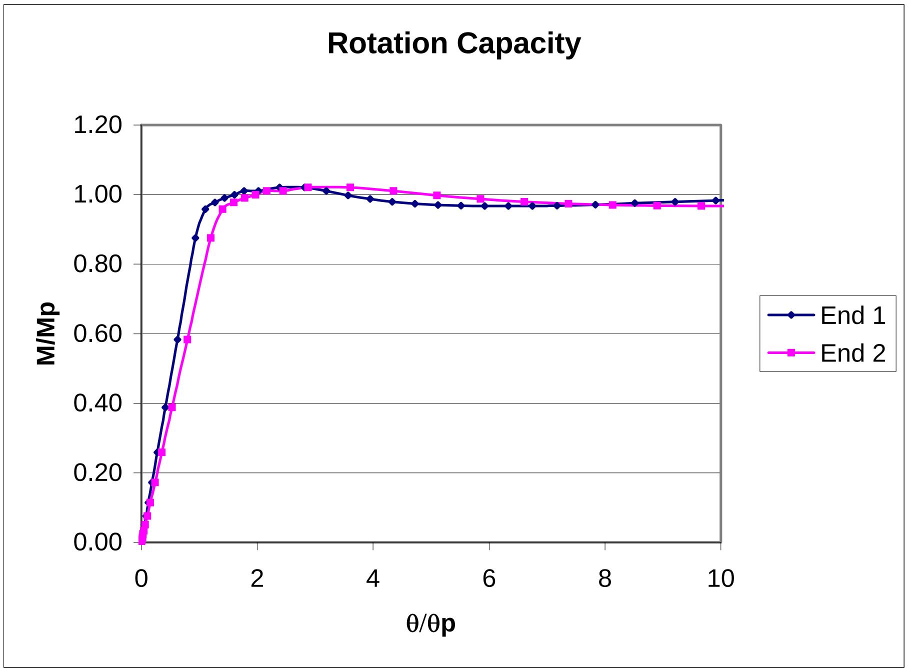

Figure C25 Model-1, L_b=60 in., t_f=0.875 in., t_w=0.5 in., b_f=12 in.

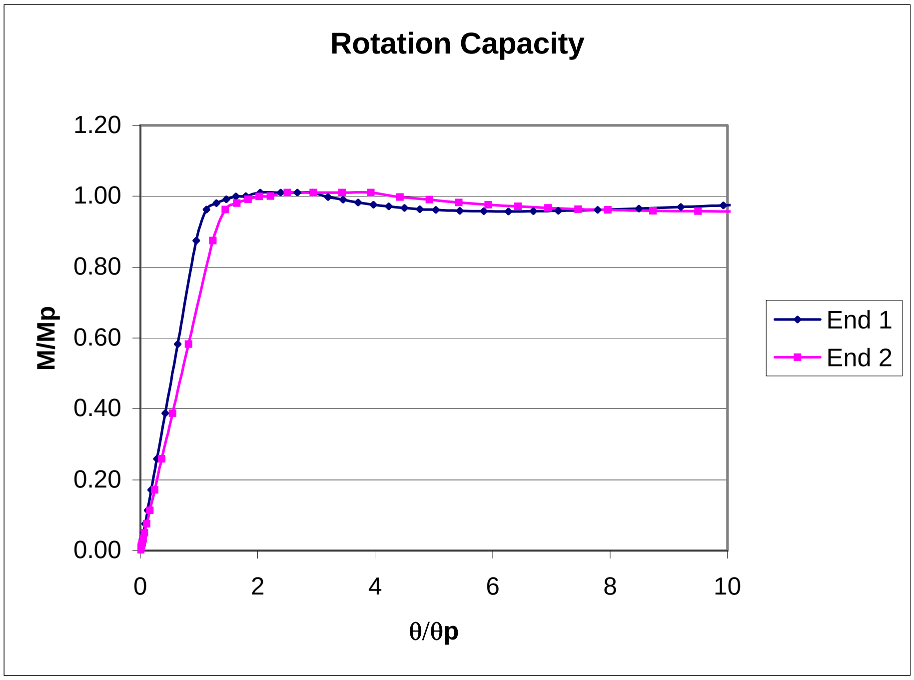

Figure C26 Model-1, L_b=60 in., t_f=0.875 in., t_w=0.4375 in., b_f=12 in.

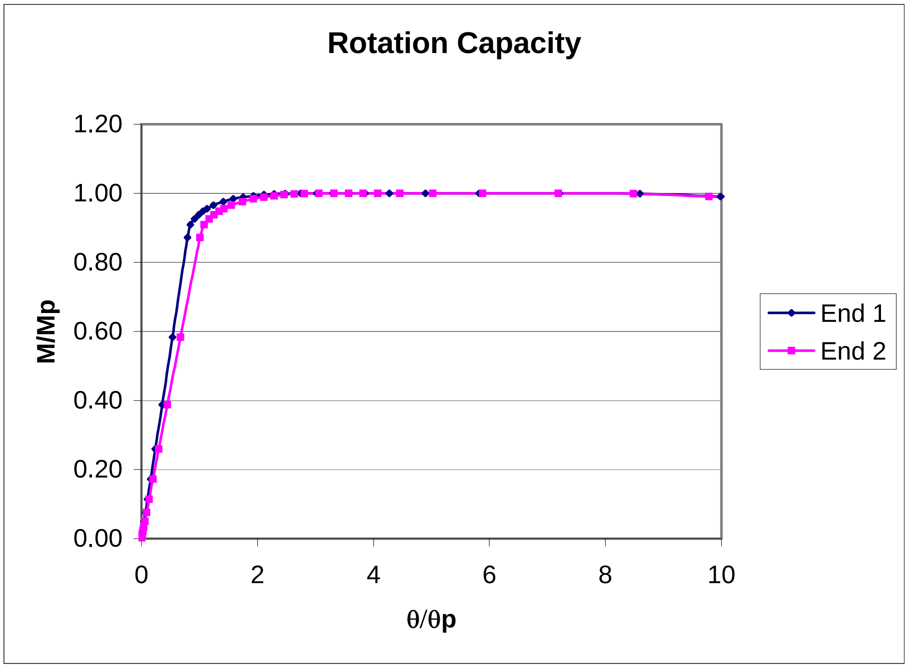

Figure C27 Model-2, L_b=60 in., t_f=0.875 in., t_w=0.5 in., b_f=8 in.

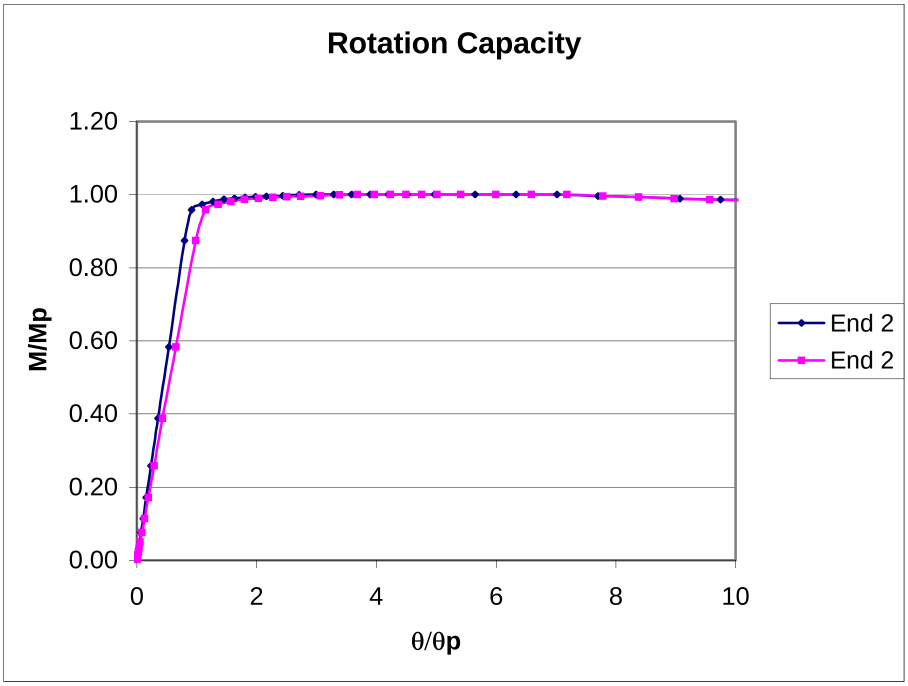

Figure C28 Model-2, L_b=60 in., t_f=1.0 in., t_w=0.3125 in., b_f=10 in.

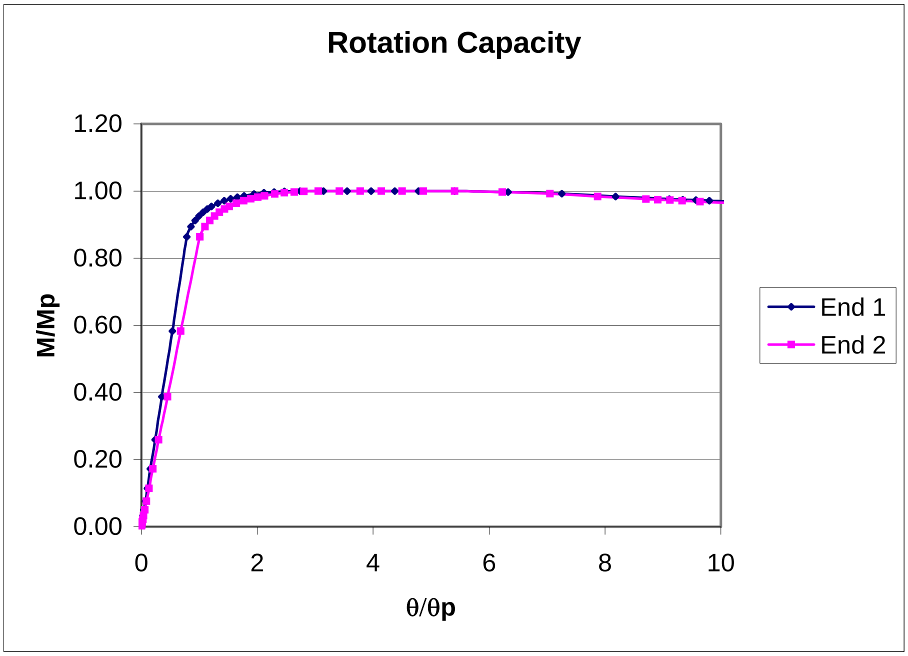

Figure C29 Model-2, L_b=60 in., t_f=0.75 in., t_w=0.625 in., b_f=8 in.

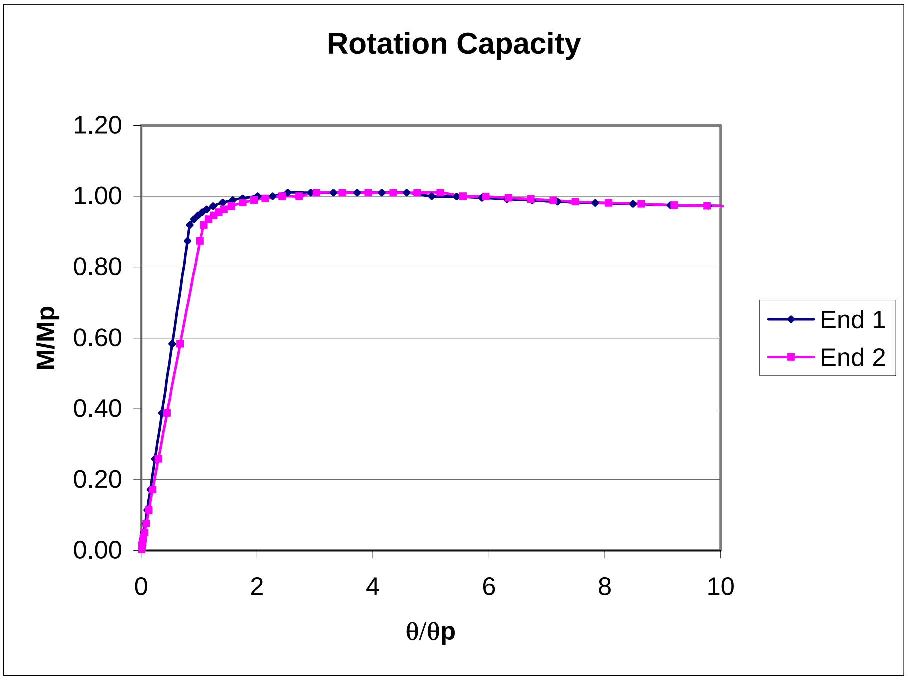

Figure C30 Model-2, L_b=60 in., t_f=0.875 in., t_w=0.5 in., b_f=10 in.

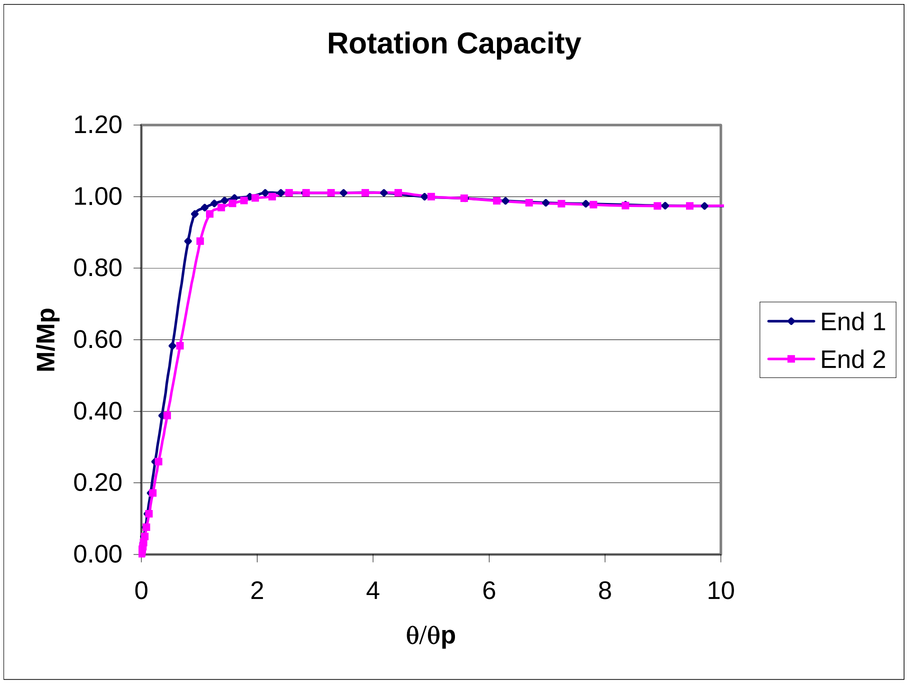

Figure C31 Model-2, L_b=60 in., t_f=1.0 in., t_w=0.5 in., b_f=12 in.

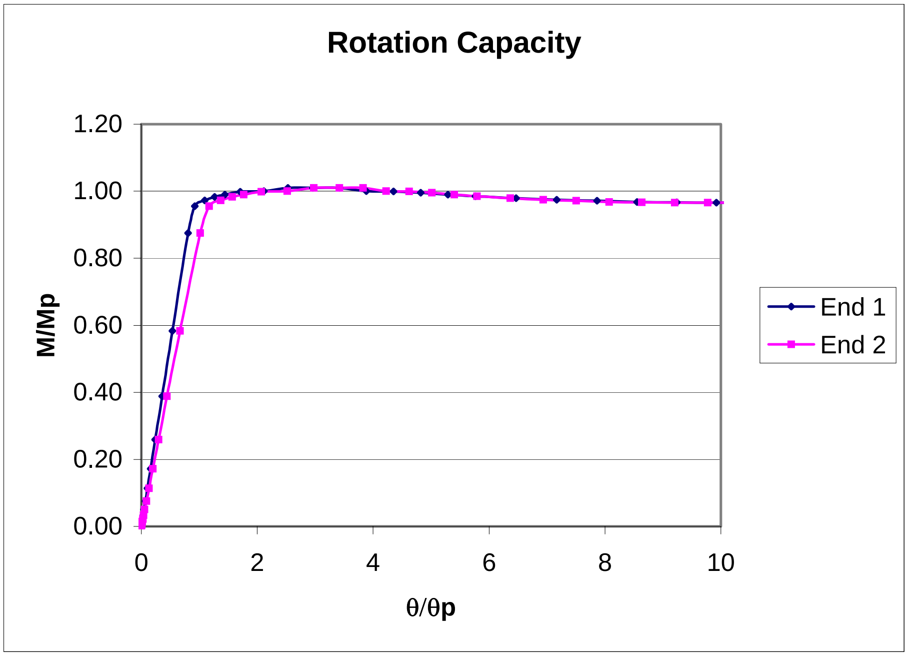

Figure C32 Model-2, L_b=60 in., t_f=1.0 in., t_w=0.4375 in., b_f=12 in.

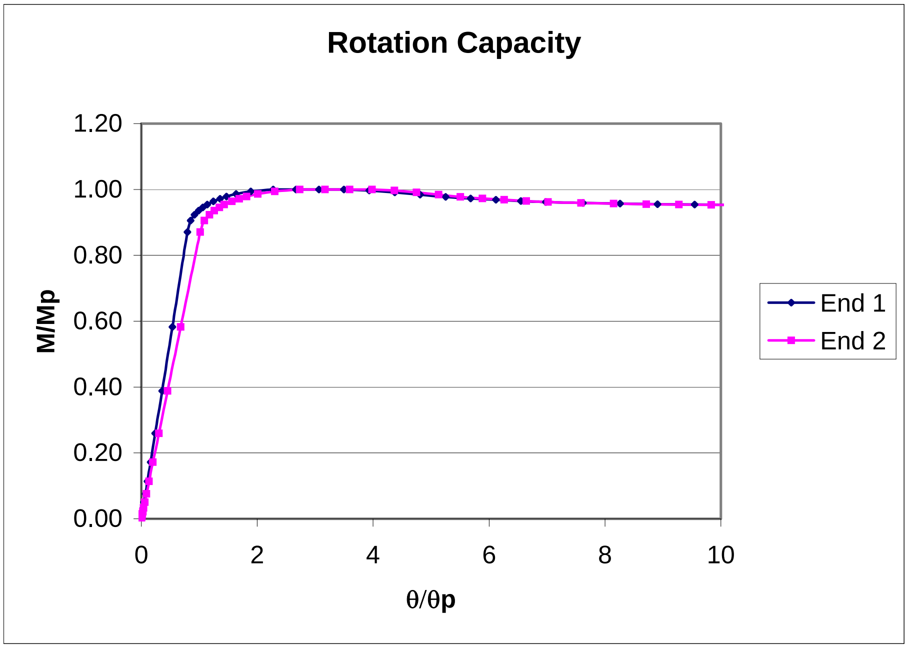

Figure C33 Model-2, L_b=60 in., t_f=0.75 in., t_w=0.5625 in., b_f=10 in.

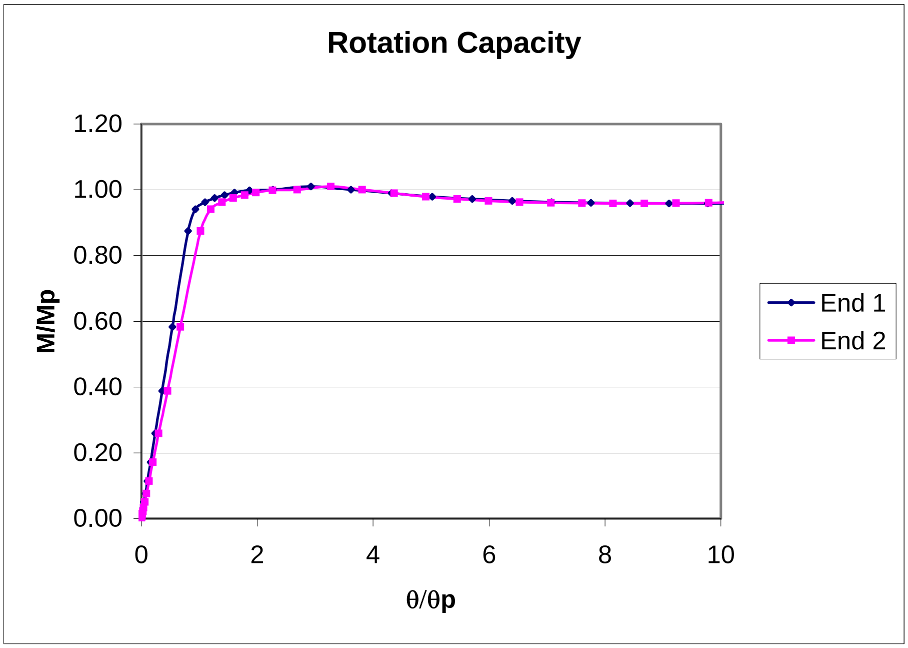

Figure C34 Model-2, L_b=60 in., t_f=0.875 in., t_w=0.5625 in., b_f=12 in.

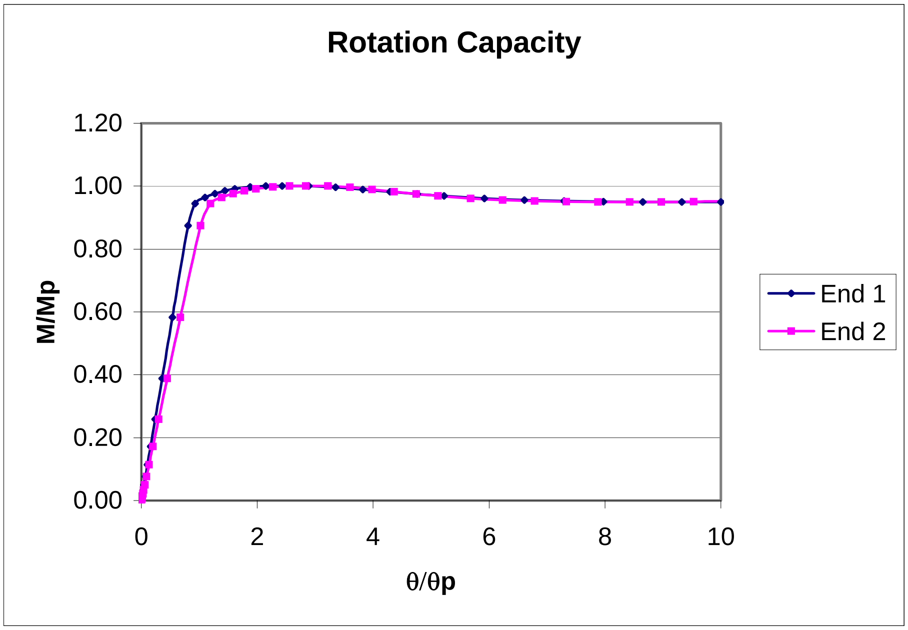

Figure C35 Model-2, L_b=60 in., t_f=0.875 in., t_w=0.5 in., b_f=12 in.

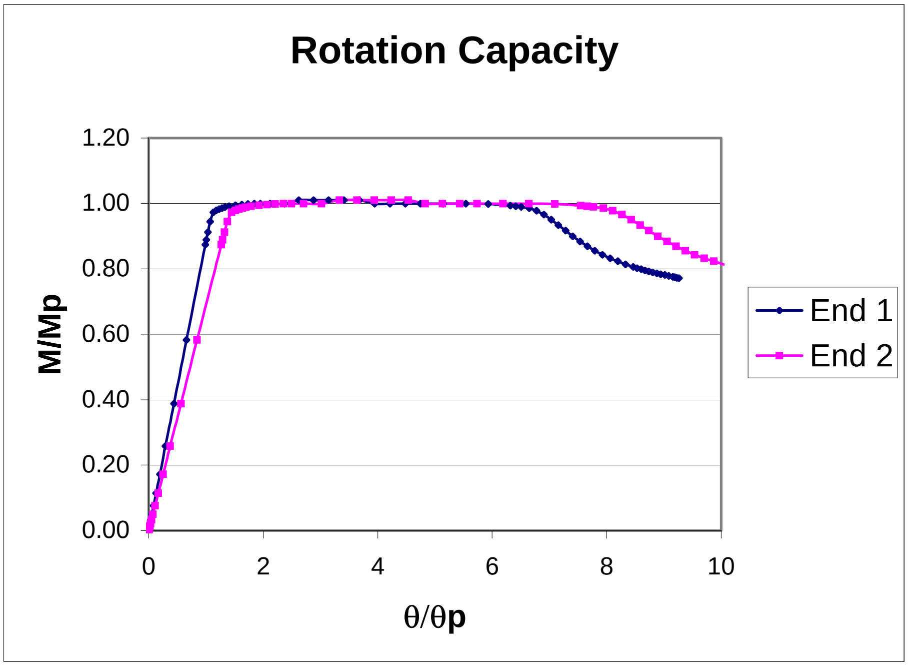

Figure C36 Model-1, L_b=75 in., t_f=1.125 in., t_w=0.25 in., b_f=10 in.

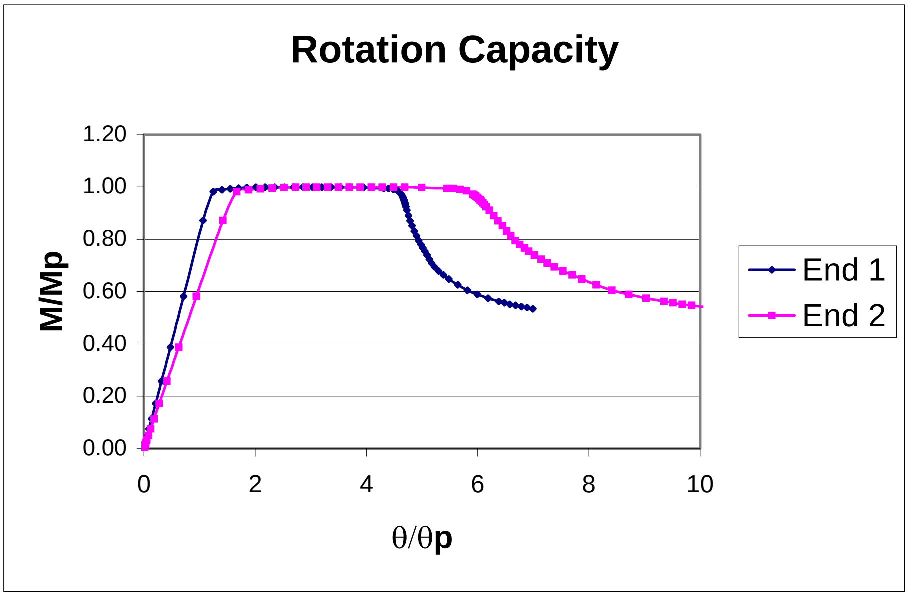

Figure C37 Model-1, L_b=75 in., t_f=1.125 in., t_w=0.1875 in., b_f=10 in.

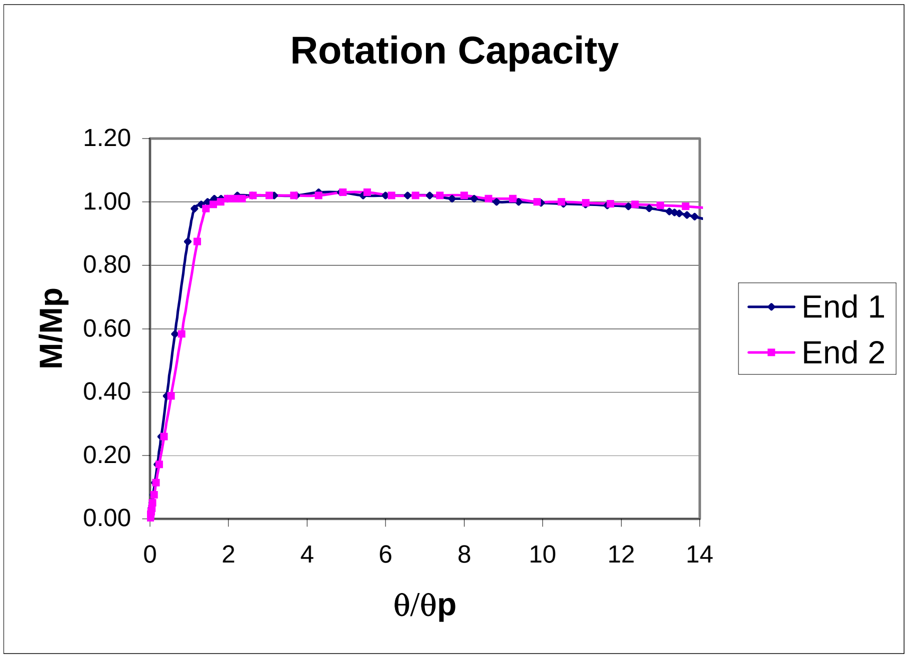

Figure C38 Model-1, L_b=75 in., t_f=1.25 in., t_w=0.375 in., b_f=12 in.

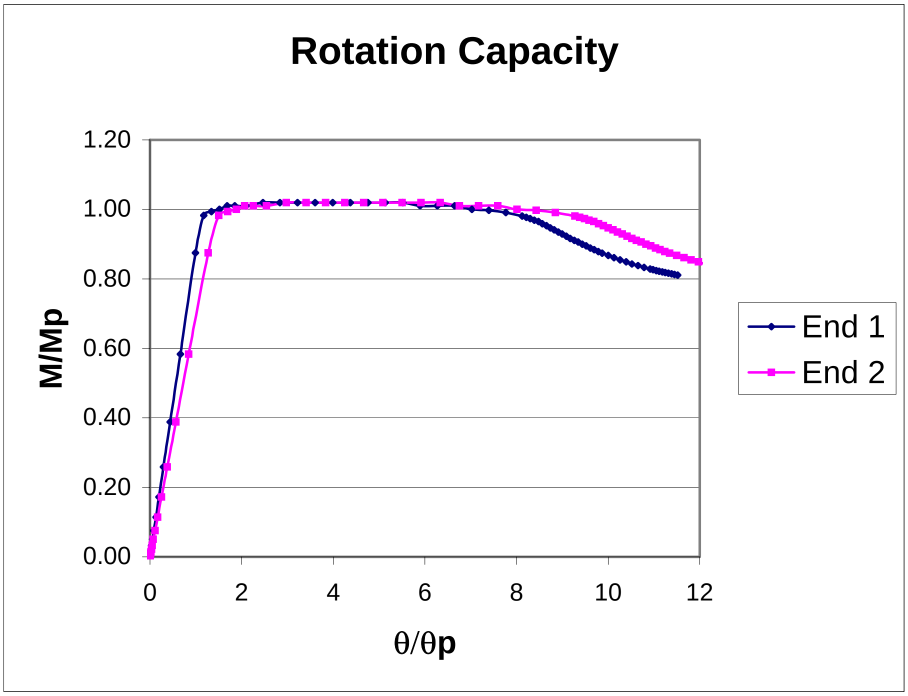

Figure C39 Model-1, L_b=75 in., t_f=1.25 in., t_w=0.3125 in., b_f=12 in.

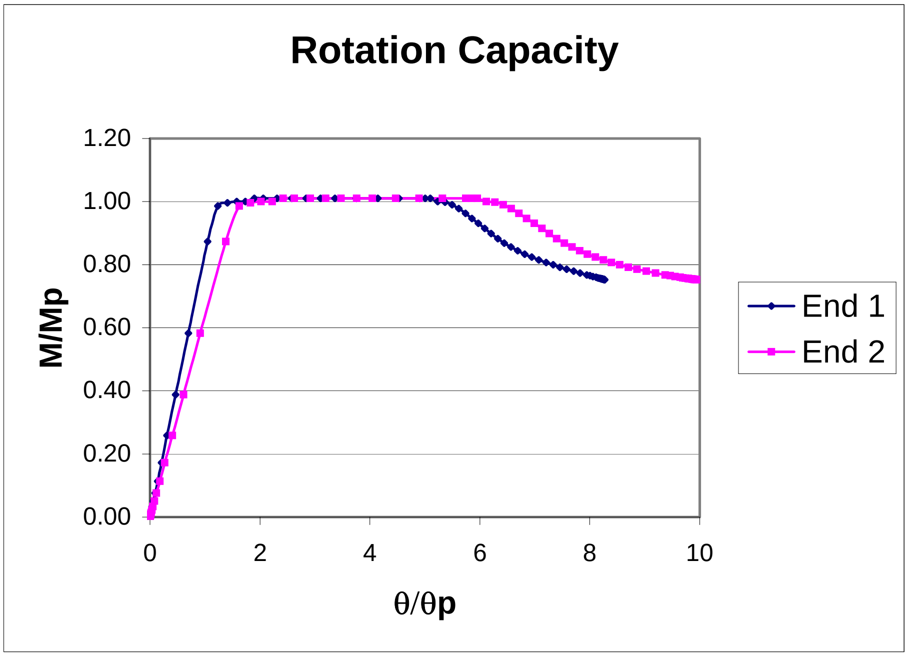

Figure C40 Model-1, L_b=75 in., t_f=1.25 in., t_w=0.25 in., b_f=12 in.

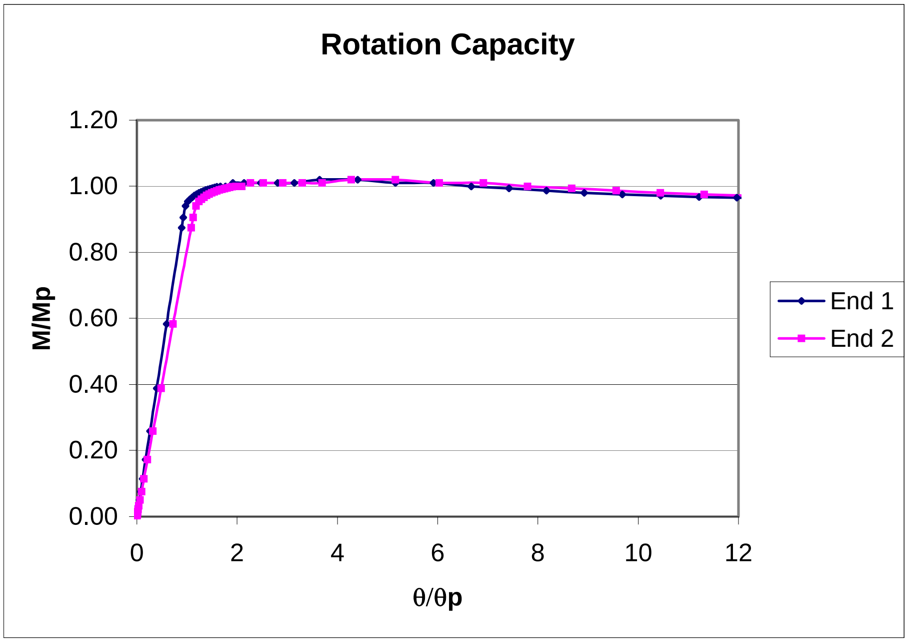

Figure C41 Model-1, L_b=75 in., t_f=1.0 in., t_w=0.4375 in., b_f=10 in.

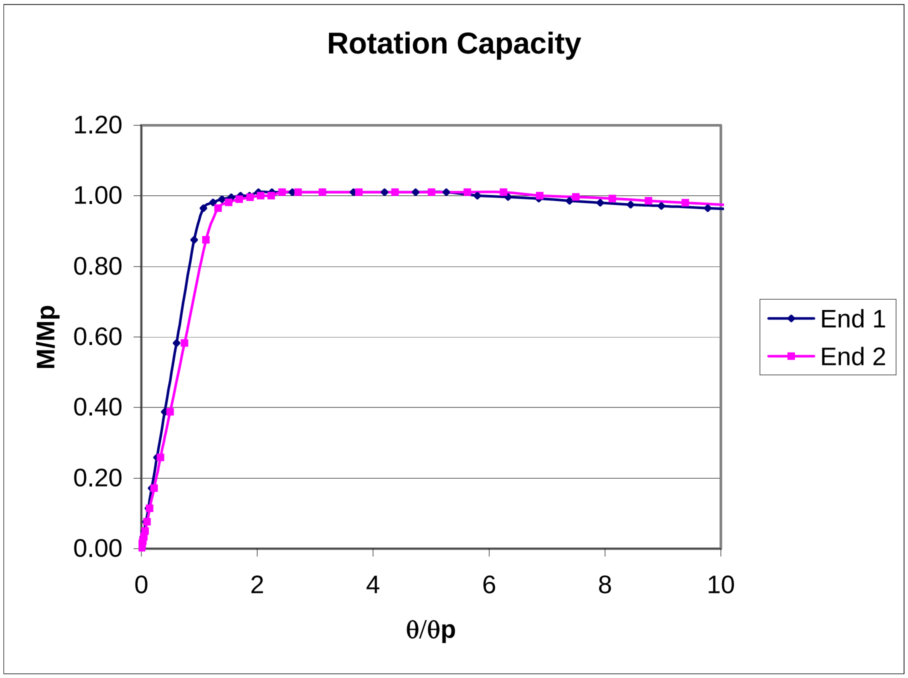

Figure C42 Model-1, L_b=75 in., t_f=1.0 in., t_w=0.375 in., b_f=10 in.

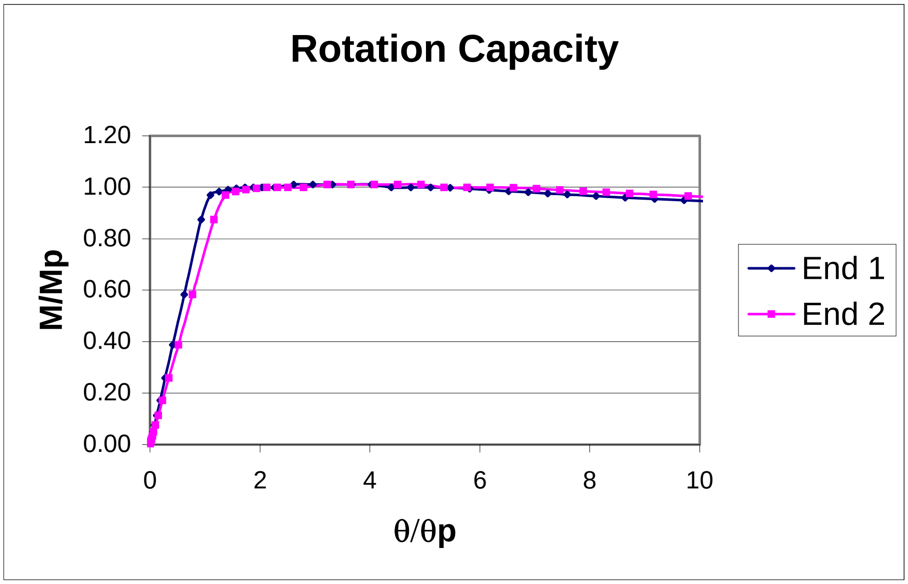

Figure C43 Model-1, L_b=75 in., t_f=1.0 in., t_w=0.3125 in., b_f=10 in.

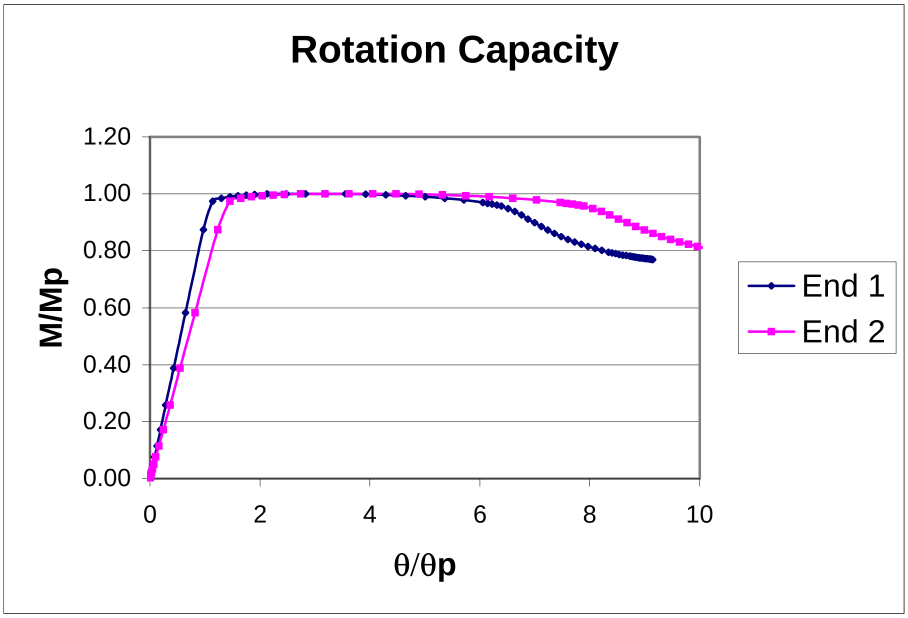

Figure C44 Model-1, L_b=75 in., t_f=1.0 in., t_w=0.25 in., b_f=10 in.

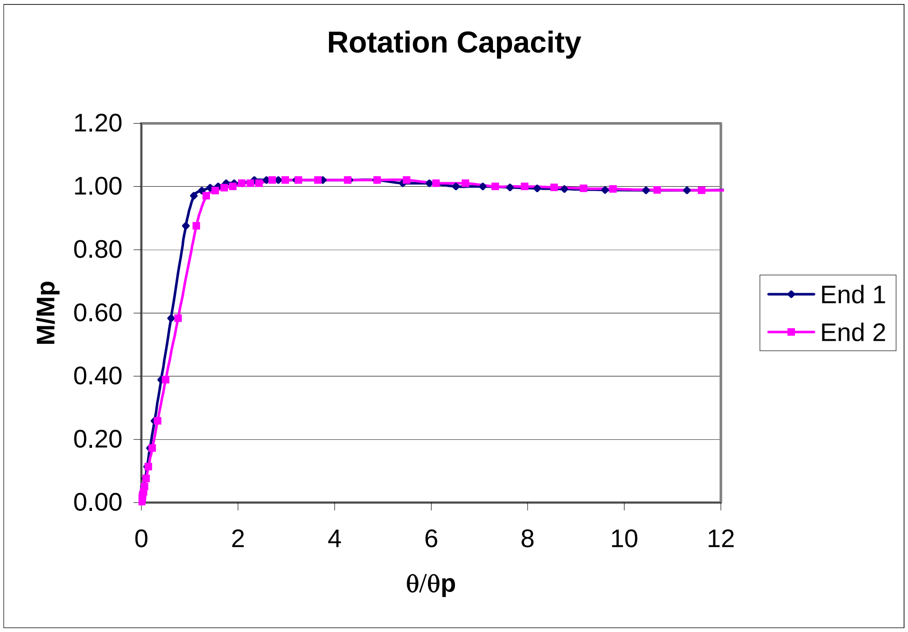

Figure C45 Model-1, L_b=75 in., t_f=1.125 in., t_w=0.4375 in., b_f=12 in.

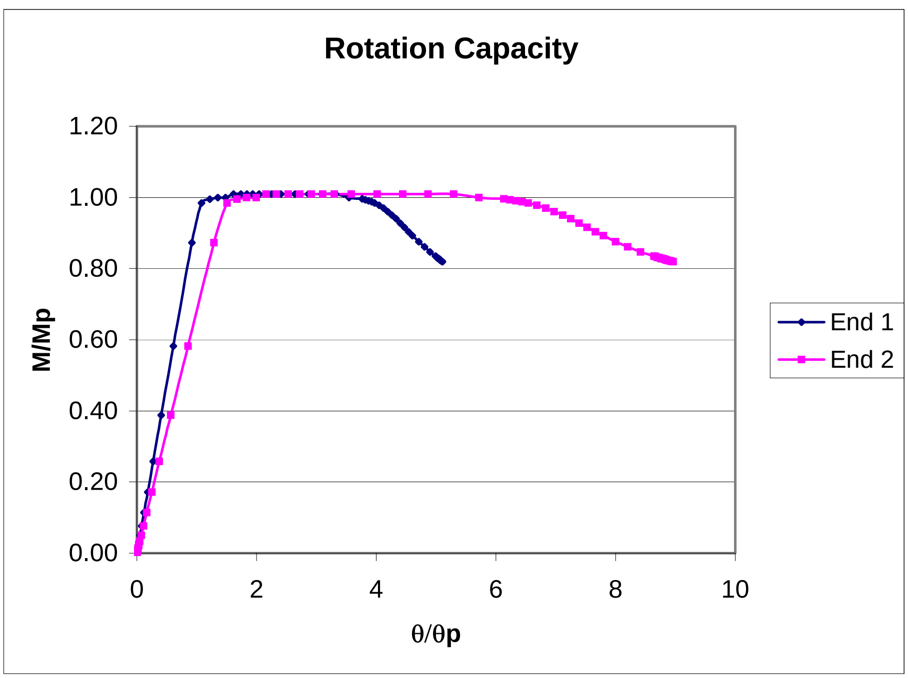

Figure C46 Model-1, L_b=75 in., t_f=1.125 in., t_w=0.375 in., b_f=12 in.

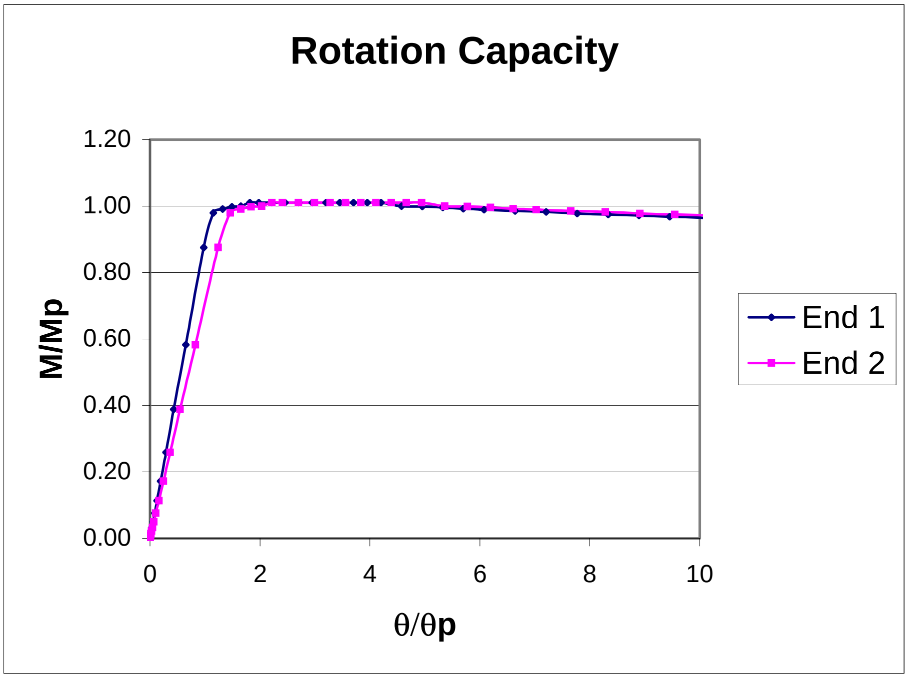

Figure C47 Model-1, L_b=75 in., t_f=1.125 in., t_w=0.3125 in., b_f=12 in.

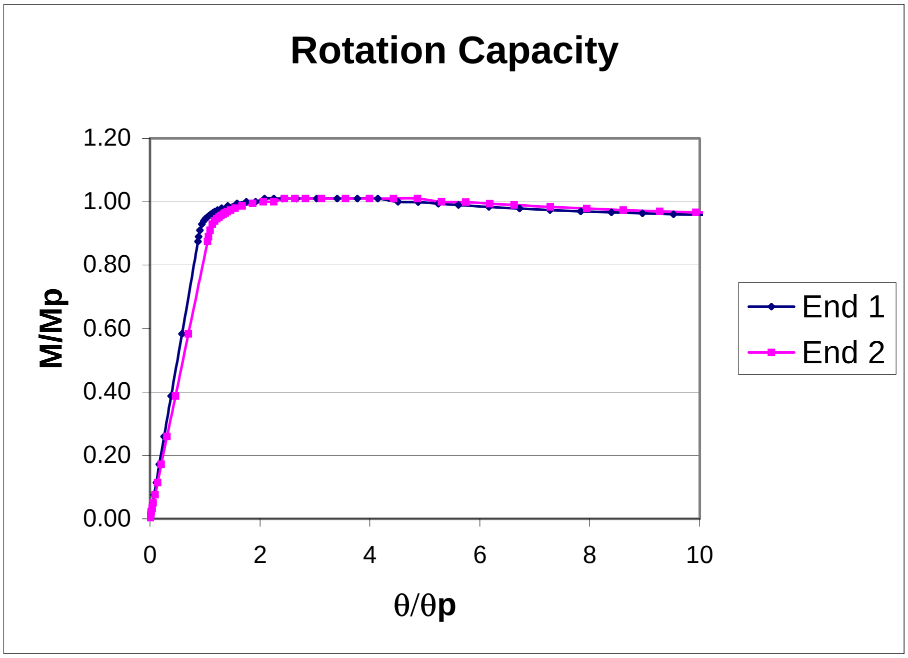

Figure C48 Model-1, L_b=75 in., t_f=0.875 in., t_w=0.5 in., b_f=10 in.

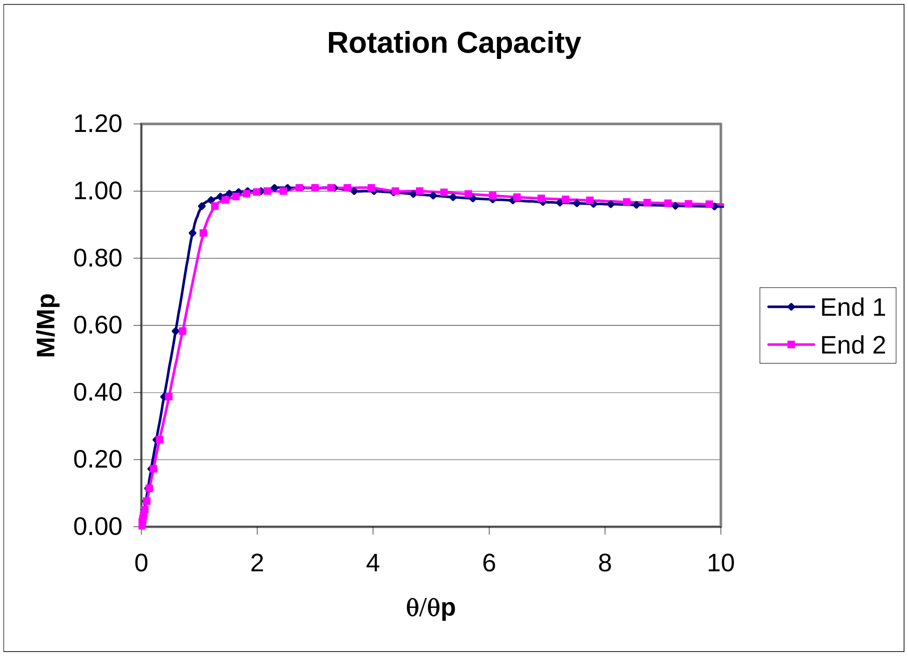

Figure C49 Model-1, L_b=75 in., t_f=0.875 in., t_w=0.4375 in., b_f=10 in.

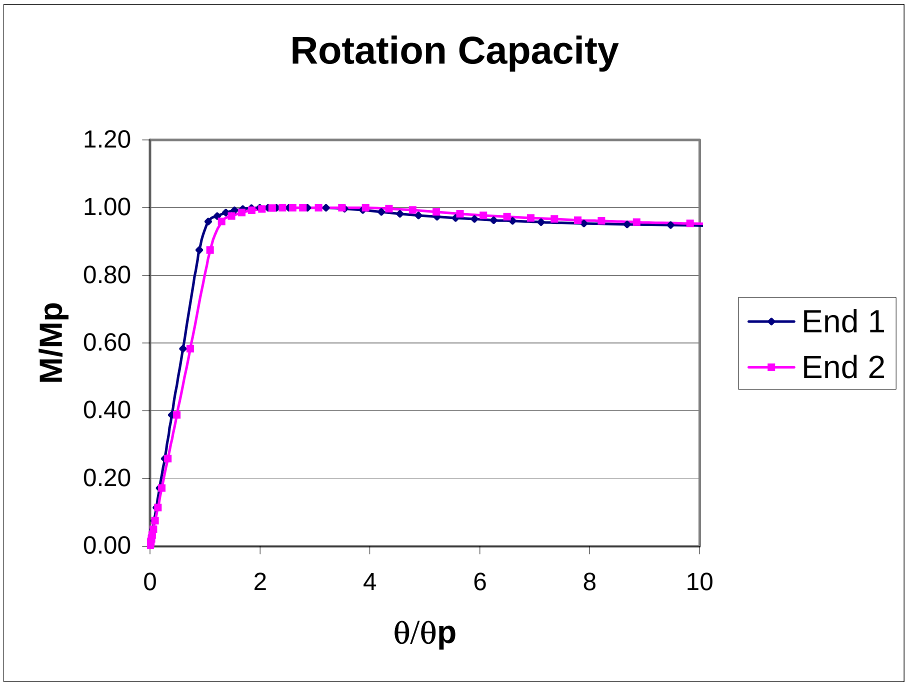

Figure C50 Model-1, L_b=75 in., t_f=0.875 in., t_w=0.375 in., b_f=10 in.

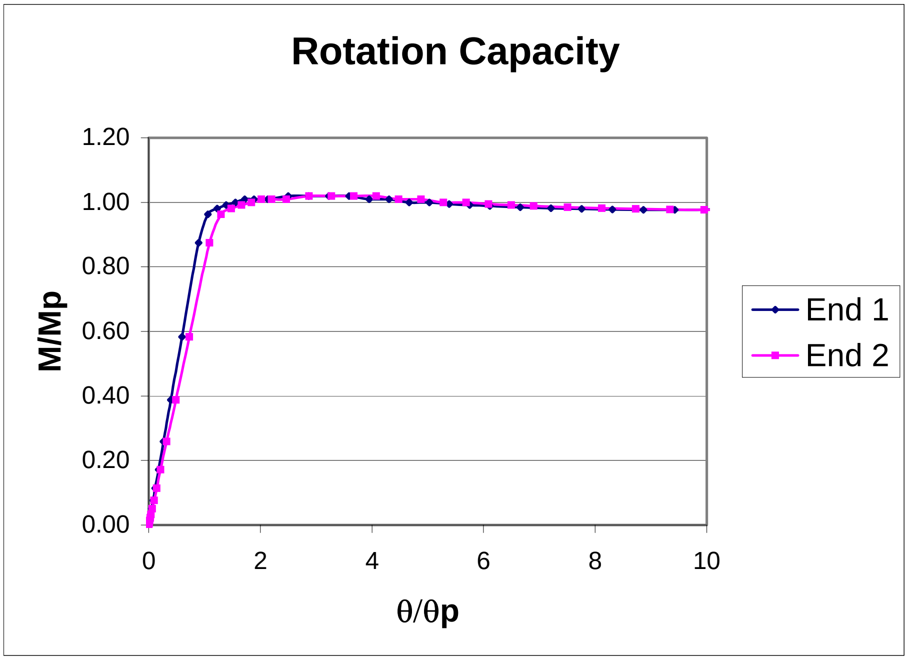

Figure C51 Model-1, L_b=75 in., t_f=1.0 in., t_w=0.5 in., b_f=12 in.

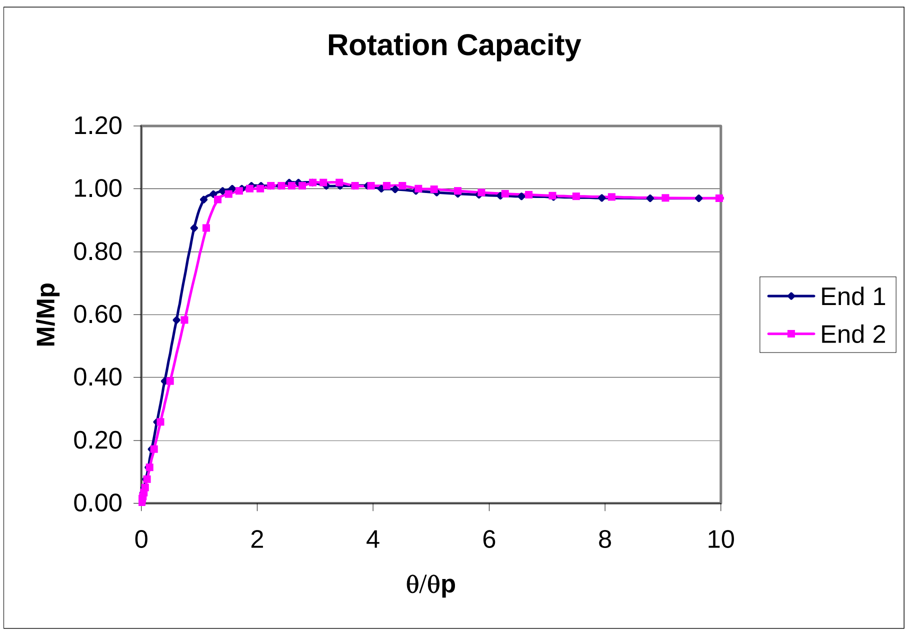

Figure C52 Model-1, L_b=75 in., t_f=1.0 in., t_w=0.4375 in., b_f=12 in.

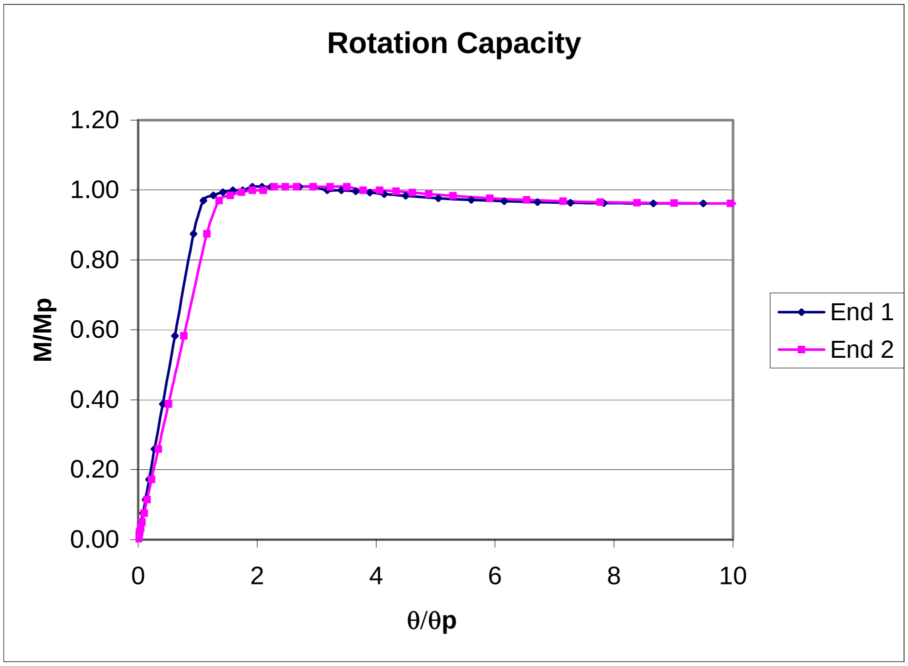

Figure C53 Model-1, L_b=75 in., t_f=1.0 in., t_w=0.375 in., b_f=12 in.

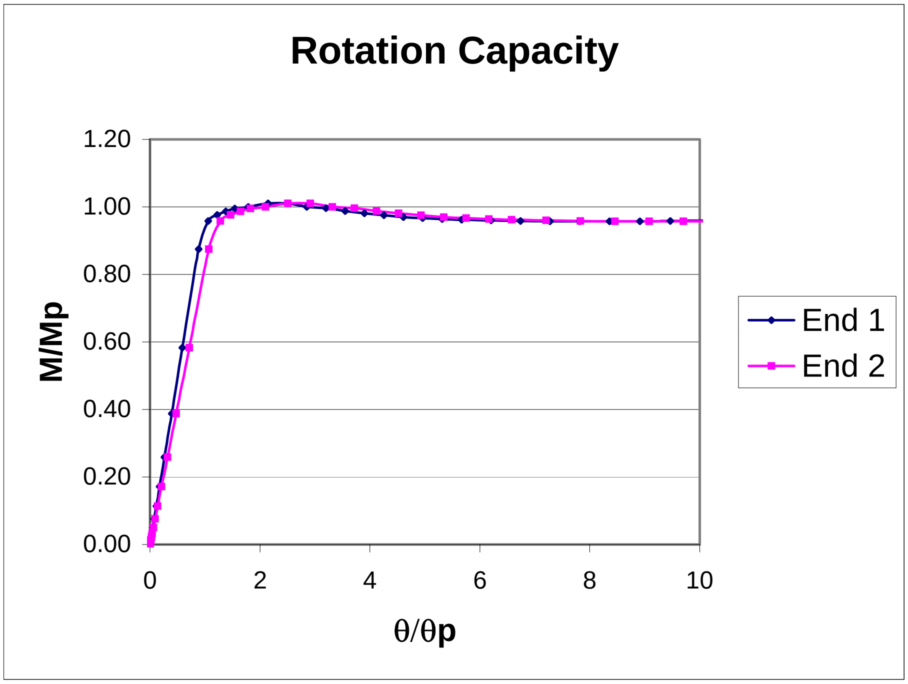

Figure C54 Model-1, L_b=75 in., t_f=0.875 in., t_w=0.5 in., b_f=12 in.

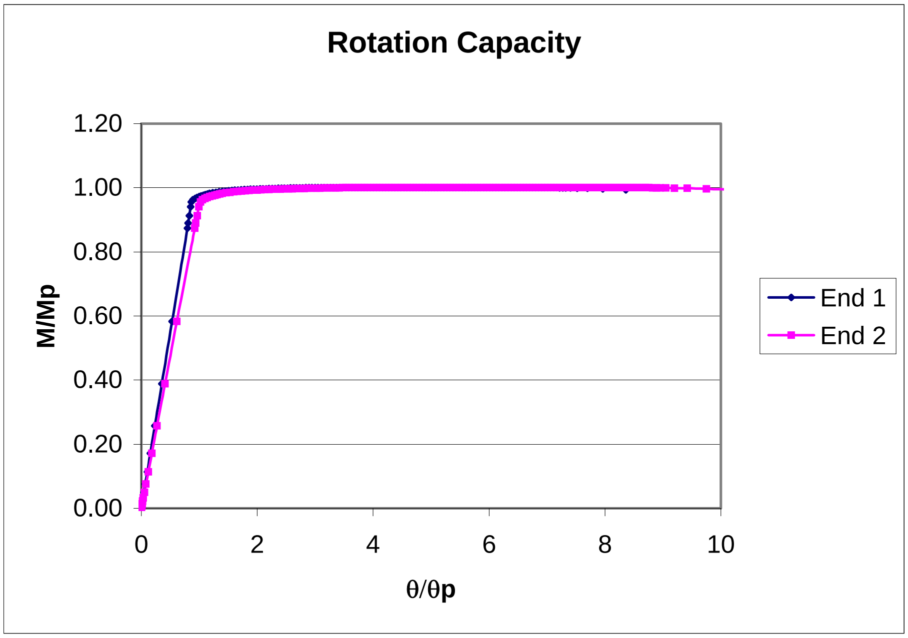

Figure C55 Model-2, L_b=75 in., t_f=1.125 in., t_w=0.3125 in., b_f=10 in.

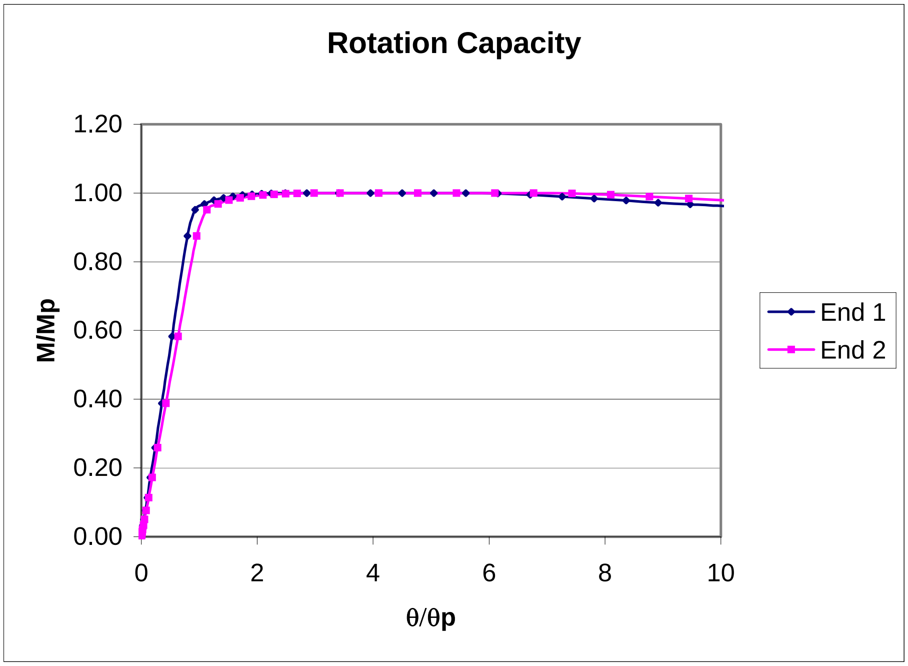

Figure C56 Model-2, L_b=75 in., t_f=1.0 in., t_w=0.4375 in., b_f=10 in.

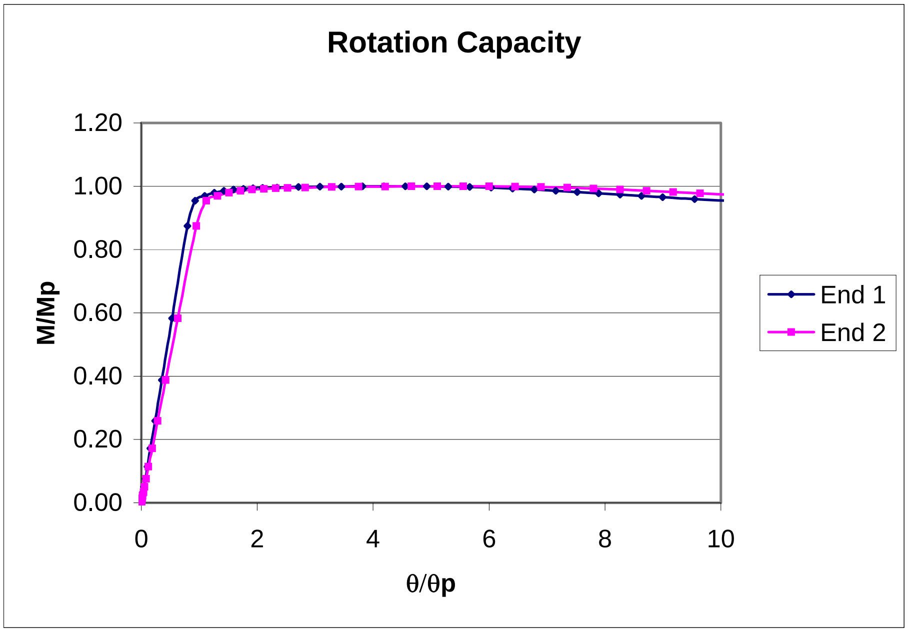

Figure C57 Model-2, L_b=75 in., t_f=1.0 in., t_w=0.375 in., b_f=10 in.

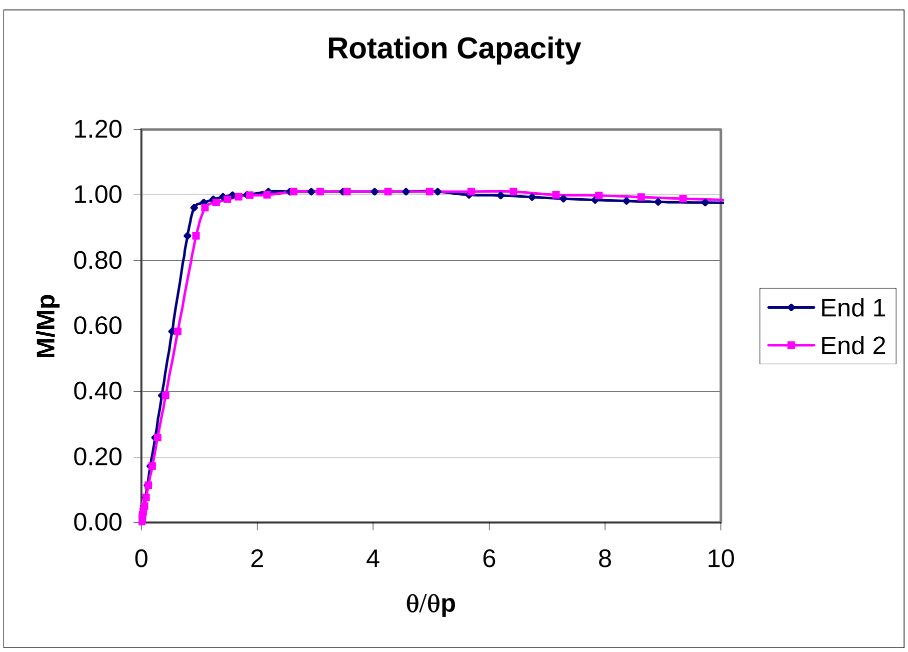

Figure C58 Model-2, L_b=75 in., t_f=1.125 in., t_w=0.4375 in., b_f=12 in.

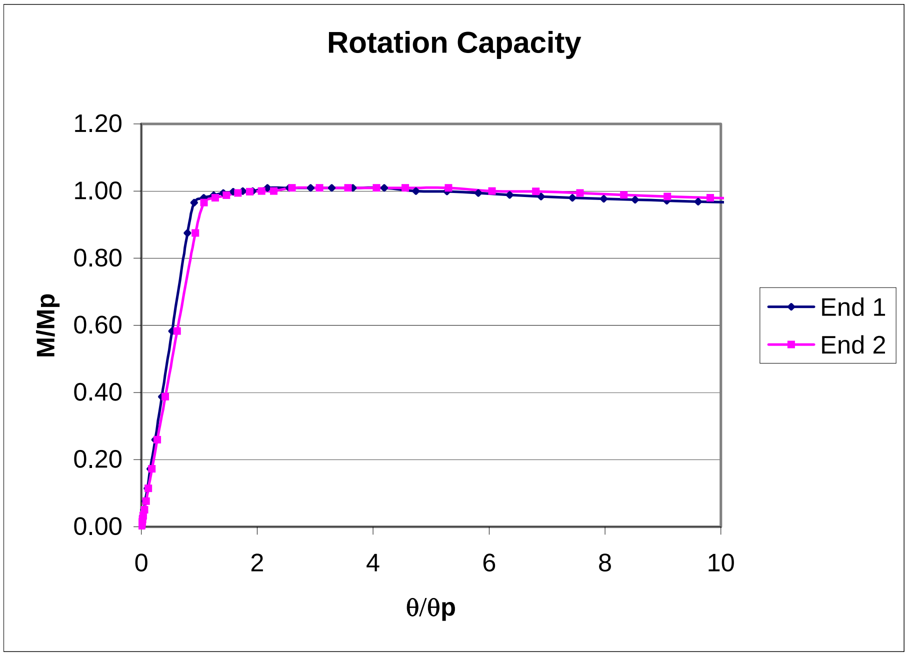

Figure C59 Model-2, L_b=75 in., t_f=1.125 in., t_w=0.375 in., b_f=12 in.

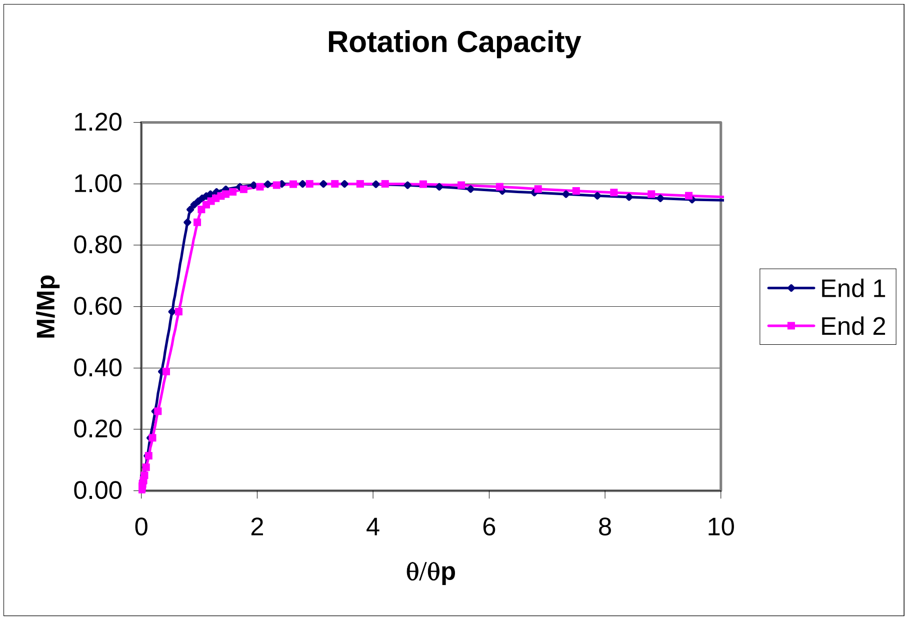

Figure C60 Model-2, L_b=75 in., t_f=0.875 in., t_w=0.5625 in., b_f=10 in.

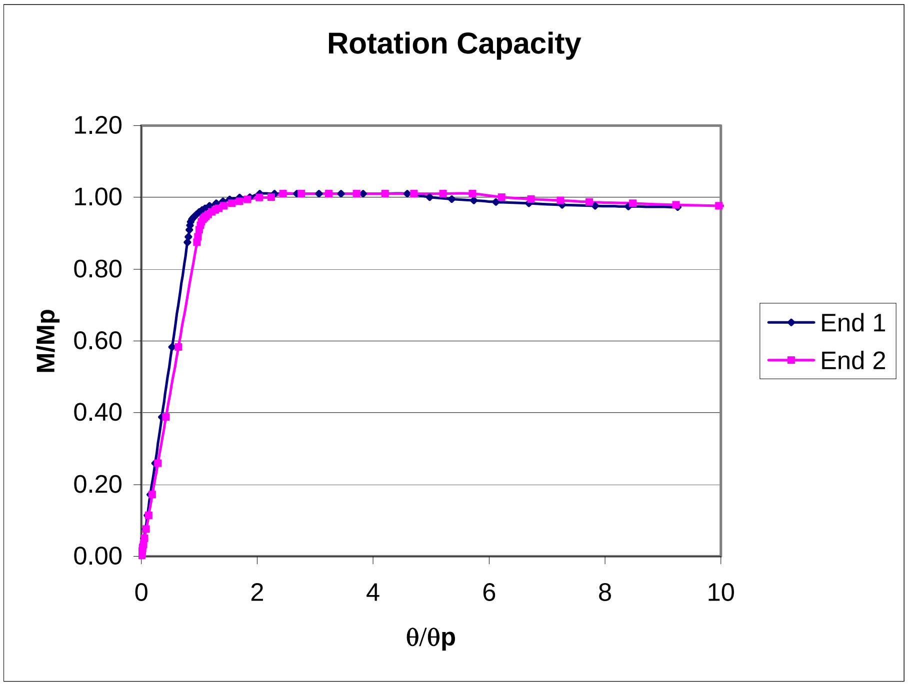

Figure C61 Model-2, L_b=75 in., t_f=1.0 in., t_w=0.5625 in., b_f=12 in.

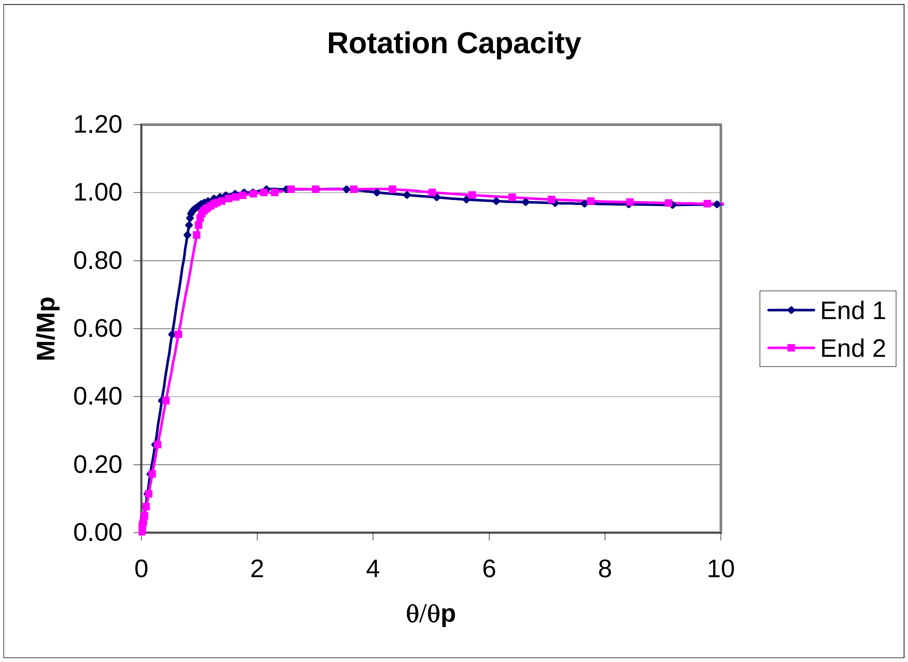

Figure C62 Model-2, L_b=75 in., t_f=1.0 in., t_w=0.5 in., b_f=12 in.

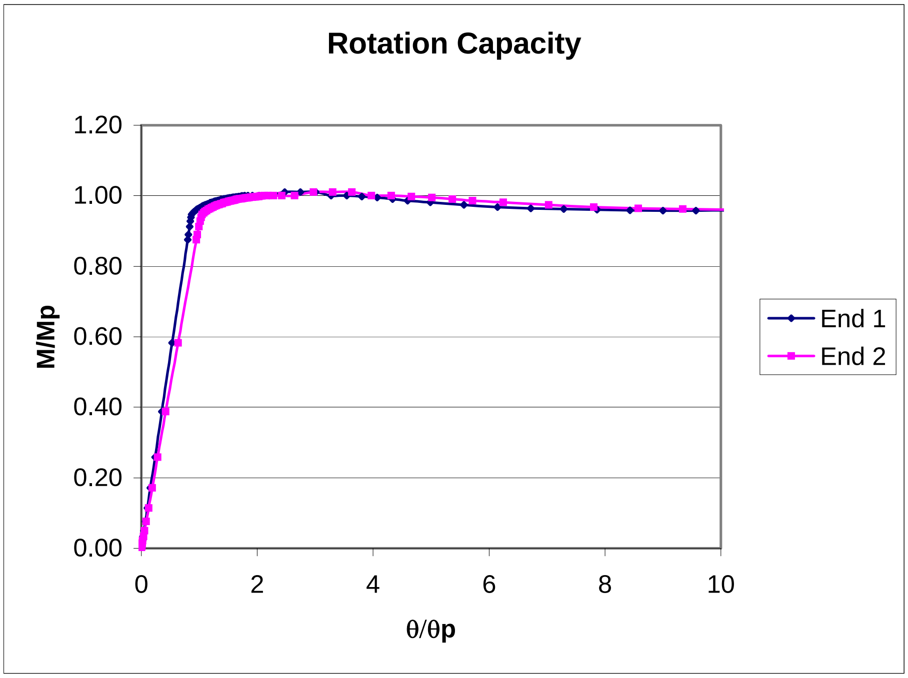

Figure C63 Model-2, L_b=75 in., t_f=1.0 in., t_w=0.4375 in., b_f=12 in.

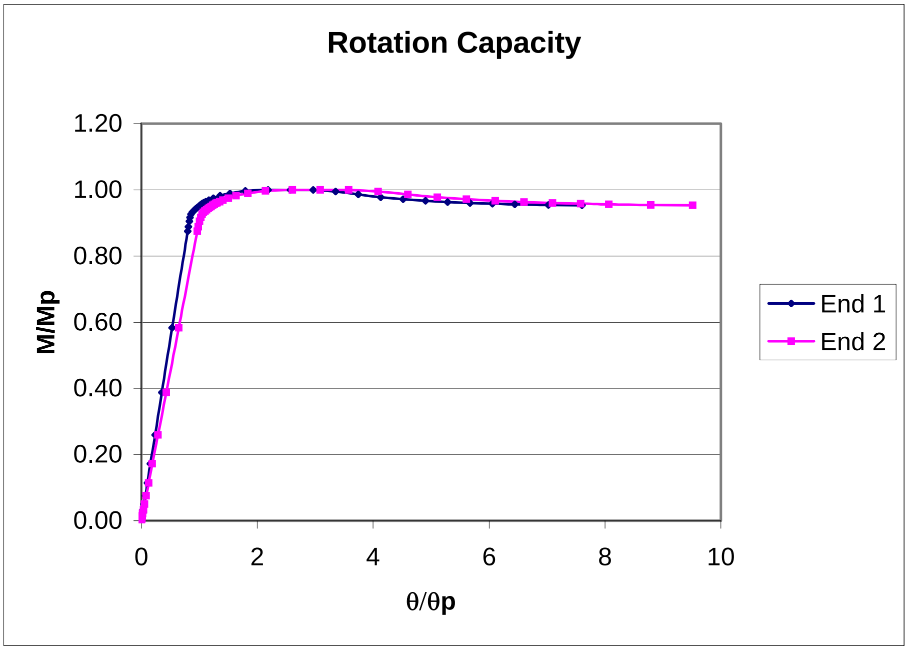

Figure C64 Model-2, L_b=75 in., t_f=0.875 in., t_w=0.5625 in., b_f=12 in.

BIBLIOGRAPHY

BIBLIOGRAPHY

1. ABAQUS, (2001) *ABAQUS Standard User's Manual*, Version 5.8, Volumes 1 to 3, Hibbit, Karlsson & Sorensen, Inc., Pawtucket, Rhode Island, USA.

2. ABAQUS, (2001) *ABAQUS Theory Manual*, Version 5.8, Hibbit, Karlsson & Sorensen, Inc., Pawtucket, Rhode Island, USA.

3. Adams, P.F., Lay, M.G., Galambos, T.V. (1965) "Experiments on High Strength Steel Members," *WRC Bulletin*, No. 110, Welding Research Council, New York, New York, pp.1-16.

4. American Institute of Steel Construction (AISC), (1999) *Load and Resistance Factor Design (LRFD) Specification for Structural Steel Buildings*, Chicago, Illinois.

5. ASCE, (1971) *Plastic Design in Steel, A Guide and Commentary*, American Society of Civil Engineers, New York, New York, p. 80.

6. Boley, B.A. (1963) "On the Accuracy of the Bernoulli-Euler Theory for Beams of Variable Section," *Journal of Applied Mechanics*, Vol. 30, pp. 373-378.

7. Boresi, A.P., Schmidt R.J., Sidebottom O.M. (1993) *Advanced Mechanics of Materials*, Fifth Edition, John Wiley & Sons, Inc.

8. Clough, R.W. (1965) "The Finite Element Method in Structural Mechanics," *Stress Analysis: Recent Development in Numerical and Experimental Methods*, John Wiley & Sons Ltd., pp. 85-119.

9. Davis, B.D. (1996) "LRFD Evaluation of Full-Scale Metal Building Rigid Frame Tests," *M.S. Thesis*, Charles Via Department of Civil Engineering, Virginia Polytechnic Institute and State University, Blacksburg, Virginia.

10. Earls, C.J. (1995) "On the Use of Nonlinear Finite Element Analysis Techniques to Model Structural Steel Angle Response," *Ph.D. Dissertation*, University of Minnesota, Minneapolis, Minnesota.

11. Earls, C.J., Shah, B.J. (2002) High Performance Steel Bridge Girder Compactness, *Journal of Constructional Steel Research,* Elsevier Science Ltd., Great Britain, Vol. 58, pp. 859-880.

12. Frost, R.W. and Schilling, C.G. (1964) "Behavior of Hybrid Beams Subjected to Static Loads," *Journal of the Structural Division*, ASCE, Vol. 90, No. ST3, June, pp. 55-88.

13. Lee, G.C., Ketter, R.L., Hsu, T.L. (1981) *Design of Single Story Rigid Frames*, Metal Building Manufacturers Association, Cleveland, Ohio.

14. Lee, G.C., Morrell, M.L., Ketter, R.L. (1972) "Design of Tapered Members," *WRC Bulletin*, No. 173, Welding Research Council, New York, New York, June.

15. Logan, D.L. (2001) *A First Course in the Finite Element Method Using Algor*, Second Edition, Brooks/Cole, Pacific Grove, California.

16. MBMA (1996) *Low-Rise Building Systems Manual*, Metal Building Manufacturers Association, Cleveland, Ohio.

17. McDermott, J.F. (1969) "Plastic Bending of A514 Steel Beams," *Journal of the Structural Division*, ASCE, Vol. 95, No. ST9, September, pp. 1851-1871.

18. Morrell, M.L., Lee, G.C. (1974) "Allowable Stress for Web-Tapered Beams with Lateral Restraints," *WRC Bulletin*, No. 192, Welding Research Council, New York, New York, February.

19. Polyzois, D., Raftoyiannis, I.G. (1998) "Lateral-Torsional Stability of Steel Web-Tapered I-Beams," *Journal of Structural Engineering*, ASCE, Vol. 124, No. 10, October, pp. 1208-1216.

20. Prawel, S.P., Morrell, M.L., Lee, G.C. (1974) "Bending and Buckling Strength of Tapered Structural Members," *Welding Research Journal Supplement*, Vol. 53, February, pp. 75-84.

21. Riks, E. (1972) "The Application of Newton's Method to the Problem of Elastic Stability," *Journal of Applied Mechanics*, Vol. 39, pp. 1060-1066.

22. Riks, E. (1979) "An Incremental Approach to the Solution of Snapping and Buckling Problems," *International Journal of Solids and Structures*, Vol. 15, pp. 529-551.

23. Salmon, C.G., Johnson, J.E. (1996) *Steel Structures, Design and Behavior*, Fourth Edition, HarperCollins College Publishers, New York, New York.

24. Sathyamoorthy, M. (1998) *Nonlinear Analysis of Structures*, CRC Press LLC, Boca Raton, Florida.

25. Sumner III, E.A. (1995) "Experimental and Analytical Investigation of the LRFD Strength of Tapered Members," *M.S. Thesis*, Charles Via Department of Civil Engineering, Virginia Polytechnic Institute and State University, Blacksburg, Virginia.

26. Winter, G. (1960) “Lateral Bracing of Columns and Beams,” *Transactions*, ASCE, Vol. 125, pp. 807-845.

27. Yura, J.A., Galambos, T.V., Ravindra, M.K. (1978) “The Bending Resistance of Steel Beams,” *Journal of the Structural Division*, ASCE, Vol. 104, No. ST9, September, pp. 1355-1369.